

**Evaluation and Performance of a Tannin-based Polymer
as a Coagulant in Water Treatment**

by

GANG FANG

B.Sc. (Hons), M.Sc.

Imperial College London

Department of Civil and Environmental Engineering,

Thesis Submitted for the Degree of Doctor of Philosophy

November 2007

ABSTRACT

In drinking water treatment, there is growing interest in the application of natural cationic polymers that provide an alternate means to achieve enhanced coagulation. A review of the relevant literature concerning the coagulation mechanisms and action of polymer is presented with particular reference to the polymer character, such as polymer type, charge density and molecular weight. In addition, basic knowledge of a novel coagulant, a tannin-based modified polymer, is described.

A full characterization of the tannin-based polymer (TBP) has been undertaken to provide an unambiguous description of the polymer, or monomer, structure. Some specialised newer analytical techniques in combination with several old classical techniques for polymer examination have been used to determine the chemical nature of the TBP, including its dissociation and precipitation behaviour, molecular weight, charge density, charge variability with pH, elemental content, functional group and chemical bonding, etc. The overall assessment of TBP indicated that it can be classified as a medium molecular weight polymer with a non-quaternized amine group and a charge density that varies with pH and time.

The fundamental coagulation mechanisms and stoichiometry of suspended solid/dissolved organic matter with TBP have been investigated through laboratory experiments. Suspensions of kaolin clay and humic acid have been flocculated in a Gator jar using TBP as a sole primary coagulant. Using online analysis by Photometric Dispersion Analyzer (PDA), the relative floc size was indicated by a Flocculation Index (FI) during the coagulation process and the optimal concentration of coagulants was determined in overall terms by NPDOC, turbidity, colour, UV/Vis absorbance and Floc volume. Under given conditions the optimum dose of TBP corresponded to that required for maximum a

Flocculation Index (FI). The optimum dose of TBP was found to depend on the charge density of TBP and hence on the pH values of the solution. At neutral and acid condition, quantitative evidence of a stoichiometric relationship between TBP dosages with the concentrations of model impurity was illustrated. Complicating effects were present at higher pH values. The coagulation behaviour of TBP was generally in agreement with the coagulation mechanisms widely observed, and typical, of cationic polymers. It was evident that the coagulation performance and kinetics of TBP was also influenced by other factors, such as the velocity gradient, ageing of polyelectrolyte and reactor design. For comparative purposes, alum and a commonly used synthetic cationic polymer (polyDADMAC) were also assessed in this study as coagulants.

The potential benefits to improving coagulation performance through the combination of TBP with alum as a dual primary coagulant have been investigated. Coagulation experiments using different model waters were carried out under conditions designed to optimize the maximization of flocculation. A full matrix of coagulation tests demonstrated that a unique optimal dosage of combined alum and cationic TBP exists at a given pH and component concentration. In this case, a significant reduction of alum with an improvement of coagulation efficiency was achieved. An approach to minimize the residual soluble TBP in treated waters and increase the floc settling by attaching the TBP to an inert solid (fine sand) has been attempted. The coagulation performance using this particle suspension ('solid bound TBP') as coagulant was found to be inferior with a high shear rate in accordance with the floc strength interpretations of TBP. Additional tests with raw waters were carried out to confirm the validity of the findings from the model water experiments using TBP and the alum/TBP combinations as primary coagulants.

In the light of these studies, the relative importance of TBP's chemical properties, especially molecular weight, charge density and solubility, as crucial

parameters of coagulation mechanism is discussed. Furthermore, approaches to improve flocculation performance with either partial replacement of inorganic coagulant or the combination with microsand are suggested and analysed.

DECLARATION

The work presented in this thesis is my own except where otherwise acknowledged.

----- Gang Fang

ACKNOWLEDGEMENTS

I am entirely grateful to my supervisor, Professor Nigel Graham, for giving me the opportunity to start on this PhD project, and for his continued guidance, support and help throughout the whole course of this research. Without these none of this project would have been possible.

Special thanks must be made to Dr. Geoff Fowler from Department of Civil and Environmental Engineering of Imperial College London and Mr. Mark Watts from WRc, for their valuable advice, assistance and encouragement during these years. Both of them devoted a great deal of their time in discussing the progress of my work. Thanks also to Dr. Alan Herod and Mr. Trevor Morgan from Department of Chemical Engineering and Chemical Technology of Imperial College London, and Dr. Joachim Steinke and Mr. Chris Drake from Department of Chemistry of Imperial College London with regard to the study of the molecular weight of TBP.

Many thanks to some of my friends at Imperial College London, Mr. John Hughes, Mr. Bo Ning, Mr. Xingwei Zhu, Mr. Hao Wang, Dr. Karl Smith and Mr. Andrew Ireson, for their assistance with the writing of this thesis. And also thanks to Mr. Khoi Tran for his assistance with some of picture and diagrams in this thesis.

My deep gratitude must go to my dear and beautiful wife Ting Miao, for her fully support, understanding and confidence in me. Thank you very much for everything.

I specially thank my parents and my wife's parents for their unlimited support for my studying and taking care of my little son when I am absent.

Finally, the financial support of Tanac SA, Brazil, and the Universities UK Overseas Research Students Award Scheme are most gratefully acknowledged.

CONTENTS

ABSTRACT	2
DECLARATION	5
ACKNOWLEDGEMENTS	6
CONTENTS	8
LIST OF TABLES	12
LIST OF FIGURES	16
LIST OF PRINCIPAL SYMBOLS AND ABBREVIATIONS	23
1. OVERVIEW	25
2. INTRODUCTION	28
2.1 Introduction	28
2.2 Characterisation of Cationic Polymer as Coagulant	29
2.2.1 Molecular Weight and Charge Density of Cationic Polymer	30
2.2.2 Types and Structure of Cationic Polymer.....	33
2.2.2.1 Synthetic Polymer	33
2.2.2.2 Natural Polymer	36
2.3 Coagulation Action of Cationic Polymer	38
2.3.1 Colloid Stability	39
2.3.2 Coagulation Mechanisms of Cationic Polymer.....	40
2.3.2.1 Charge Neutralization	41
2.3.2.2 Polymer Bridging	43
2.4 Flocculation Behaviour of Cationic Polymer	47
2.4.1 Polymer Selection	47
2.4.2 Coagulation Performance.....	48
2.4.3 Interaction with Dissolved Organic Matter	52
2.4.4 Monitoring System.....	54
2.5 Application of Cationic Polymer in Water Treatment	58
2.5.1 Primary Coagulant Used in Drinking Water Treatment	59
2.5.2 Polymer Toxicity and Residual Polymer.....	64
2.5.3 Costs.....	66
2.6 Modified Tannin-based Polymer (TBP) as Coagulant	67
2.7 Summary	70
3. OBJECTIVES OF STUDY	73
4. MATERIALS AND METHODS	76
4.1 Introduction	76
4.2 Cogulants	77
4.2.1 Tannin-based Polymer.....	77
4.2.2 PolyDADMAC.....	78
4.2.3 Alum.....	79
4.2.4 Tanfloc SL.....	79
4.3 Reagents and Chemicals	79
4.4 Model Water and Surface Water Sample	81

4.4.1 Model Water with Kaolin Suspension.....	81
4.4.2 Model Water with Humic Acid	82
4.4.3 Simulated Water with Kaolin Suspension and Humic Acid.....	83
4.4.4 Raw Surface Water.....	84
4.5 Analysis Methods.....	85
4.5.1 Polymer Characterisation	85
4.5.1.1 Dissociation, Precipitation and UV Absorbance Analysis.....	85
4.5.1.2 Charge Density Analysis	86
4.5.1.3 Functional Group and Chemical Bond Analysis	87
4.5.1.4 Element Content Analysis	89
4.5.1.5 Molecular Weight Analysis	91
4.5.2 Coagulation Experiments	92
4.5.2.1 Photometric Dispersion Analyser.....	92
4.5.2.2 Gator Jar.....	93
4.5.2.3 Coagulation Process	94
4.5.2.4 Analysis of Water Quality	98
4.5.3 Residual Tannin Measurement	100
5. RESULTS: CHARACTERISATION OF TBP.....	104
5.1 Introduction.....	104
5.2 Characterisations of TBP	105
5.2.1 Dissociation, Precipitation and UV Absorbance of TBP.....	105
5.2.1.1 Dissociation of TBP in Solution.....	106
5.2.1.2 Solubility of TBP in Solution	107
5.2.1.3 UV/visible Light Absorbance.....	108
5.2.2 Variation of Charge Density with pH and Time	110
5.2.3 Elemental Content Analysis	112
5.2.4 Chemical Functional Group/Bond Analysis.....	112
5.2.4.1 Analysis of FT-IR Spectra	113
5.2.4.2 Analysis of ¹ H NMR Spectra	114
5.2.5 Analysis of Molecular Weight.....	116
5.2.5.1 Molecular Weight Determined by SEC.....	116
5.2.5.2 Molecular Weight Determined by Light Scattering	117
5.3 Discussion.....	118
6. RESULTS: COAGULATION ACTION OF TBP IN MODEL WATER.....	122
6.1 Introduction	122
6.2 Coagulation Mechanisms Using TBP as Sole Coagulant.....	124
6.2.1 Coagulation of Kaolin Suspensions	124
6.2.2 TBP Precipitation Measured by PDA.....	129
6.2.3 Coagulation of Humic Acid Solutions	130
6.3 Coagulation Stoichiometry using TBP as Sole Coagulant	137
6.3.1 Coagulation Stoichiometry in Kaolin Suspension.....	137
6.3.2 Coagulation Stoichiometry with Humic Acid Solution.....	144
6.4 Influence of Conditions on Coagulation Performance.....	147
6.4.1 Variation of Coagulation with Ageing Time of TBP	147

6.4.2	Variation of Coagulation with Mixing Speed.....	152
6.4.3	Variation of Coagulation with Reactor.....	153
6.5	Coagulation Effectiveness in Comparison with Other Coagulant	154
6.6	Floc Strength of TBP.....	158
6.6.1	The Effect of Rapid Mixing on Floc Re-formation.....	158
6.6.2	Floc Strength of TBP in Comparison with Other Coagulants	162
6.7	Discussion.....	166
7.	RESULTS: IMPROVEMENT OF TBP COAGULATION PERFORMANCE	
	USING DUAL COAGULANTS OF TBP WITH ALUM IN MODEL WATER.169	
7.1	Introduction.....	169
7.2	Coagulation Action of Dual Coagulant in 50 mg l⁻¹ Kaolin Suspension	170
7.2.1	Effect of Solution pH and Optimum Dosage of Alum	170
7.2.2	Optimum Alum-TBP Combination at pH 7.....	174
7.2.3	Optimum Alum-TBP Combination at pH 5.....	179
7.3	Coagulation Action of Dual Coagulant in Humic Acid Solution at pH6	184
7.3.1	Optimum Alum-TBP Combinations in 15 mg l ⁻¹ HA Solution	184
7.3.2	Optimum Alum-TBP Combinations in 30 mg l ⁻¹ HA Solution	194
7.3.3	Locii of the Optimal Alum-TBP Dosage Combinations	202
7.4	Discussion.....	204
8.	RESULTS: IMPROVEMENT OF TBP COAGULATION PERFORMANCE	
	USING SOLID BOUND TBP WITH MICROSAND IN MODEL WATER.....207	
8.1	Introduction.....	207
8.2	Adsorption of TBP on Sand.....	208
8.2.1	Preparation of a Solid Bound TBP	208
8.2.2	The Effect of Mixing Time to Solid Bound TBP	212
8.3	Coagulation Action of Solid Bound TBP in HA Solution.....	213
8.3.1	Coagulation Performance of Solid Bound TBP at pH 4.....	213
8.3.2	Coagulation Performance of Solid Bound TBP at pH 6.....	215
8.4	Discussion.....	217
9.	RESULTS: COAGULATION EXPERIMENTS OF RAW WATER.....219	
9.1	Introduction.....	219
9.2	Coagulation Performance of TBP in Simulated Water.....	220
9.3	Coagulation Performance of Different Coagulants with Raw Water.....	221
9.3.1	Coagulation Tests of Raw Water without pH Adjustment.....	221
9.3.2	Coagulation Tests of Raw Water with pH Adjustment at pH 6	223
9.3.2.1	Coagulation Performance of Alum.....	223
9.3.2.2	Coagulation Performance of TBP	224
9.3.2.3	Coagulation Performance of Alum/TBP Combination.....	226
9.3.2.4	Floc Strength of Alum-TBP Combination.....	232
9.4	Discussion.....	233
10.	GENERAL DISCUSSION.....	235
11.	CONCLUSIONS	251
12.	SUGGESTED FUTURE WORK.....	256
13.	REFERENCES.....	258

14. APPENDIX	283
APPENDIX I: Laboratory G Curve for Flat Paddle in 2L Gator Jar (143).....	283
APPENDIX II: The specific refractive index increment (dn/dc) of TBP.....	284
APPENDIX III: Laser Scattering Zimm Plot for TBP.....	285

LIST OF TABLES

SECTION 2		Page
Table 2.1	Charge density of some polyelectrolytes (after Bolto and Gregory (19))	32
Table 2.2	Nature and examples of typical cationic polymers (after Graham (21))	35
Table 2.3	Characteristics of chitosan samples after deacetylation (after Huang <i>et al.</i> (28))	37
Table 2.4	Coagulation performance using chitosan and alum (after Kawamura (3))	62
 SECTION 4		
Table 4.1	Variation of NPDOC and UV/Vis-absorbance (254nm and 400nm) with TBP solution concentration	78
Table 4.2	Variation of NPDOC and UV/Vis-absorbance (254nm and 400nm) with HA solution concentration	82
Table 4.3	Variation of UV/Vis-absorbance (254nm and 400nm) of HA solutions with pH (HA concentration 30mg l ⁻¹)	83
Table 4.4	Analysis of simulated water and real water used by WRc	84
Table 4.5	Analysis of an organic-rich river water at Bamford, UK	84
 SECTION 5		
Table 5.1	Insoluble materials for a range of TBP solutions with pH 6	107
Table 5.2	Insoluble materials for a range of TBP solutions with pH 7	108
Table 5.3	Insoluble materials for a range of TBP solutions with pH 8	108
Table 5.4	Insoluble materials for a range of TBP solutions with pH 9	108
Table 5.5	Results of elemental analysis of TBP product (mass %)	112
 SECTION 6		
Table 6.1	Comparison of coagulation performances of TBP (50 mg l ⁻¹ kaolin suspension) with different charge density at different pH	128

		Page
Table 6.2	NPDOC before and after coagulation with TBP dosage at pH 4 (30 mg l ⁻¹ HA)	132
Table 6.3	Absorbance at 254nm and 400nm before and after coagulation with TBP dosage at pH 4 (30 mg l ⁻¹ HA)	132
Table 6.4	NPDOC before and after coagulation with TBP dosage at pH 7 (30 mg l ⁻¹ HA)	133
Table 6.5	Absorbance at 254nm and 400nm before and after coagulation with TBP dosage at pH7 (30 mg l ⁻¹ HA)	134
Table 6.6	NPDOC before and after coagulation with TBP dosage at pH 9 (10 mg l ⁻¹ HA)	135
Table 6.7	Absorbance at 254nm and 400nm before and after coagulation with TBP dosage at pH 9 (10 mg l ⁻¹ HA)	135
Table 6.8	Variation in optimum TBP dose and coagulation performance (HA solutions) with pH	136
Table 6.9	Optimum dosage of TBP with different Kaolin concentrations at pH 4, and the corresponding peak flocculation index and turbidity reduction	139
Table 6.10	Optimum dosage of TBP with different Kaolin concentrations at pH 7, and the corresponding peak flocculation index and turbidity reduction	140
Table 6.11	Optimum dosage of TBP with different HA concentrations at pH 4, and the corresponding peak flocculation index and reduction in NPDOC and colour	145
Table 6.12	Optimum dosage of TBP with different HA concentrations at pH 7, and the corresponding peak flocculation index and reduction in NPDOC and colour	147
Table 6.13	Optimum dose of coagulants at pH 7, and NPDOC reduction (30 mg l ⁻¹ HA)	157
Table 6.14	Strength and recovery factors obtained for different coagulants (floc breakage at 300 rpm and 60 s) at pH 7 (50 mg l ⁻¹ kaolin suspension)	164
Table 6.15	Strength and recovery factors obtained for different coagulants(floc breakage at 300 rpm and 300 s) at pH 7 (50 mg l ⁻¹ kaolin suspension)	164

SECTION 7		Page
Table 7.1	Coagulation performance for the optimum dosage of TBP at each alum dose (in terms of maximum flocculation index, residual turbidity and aluminium, and Floc volume) at pH7 (50mg l ⁻¹ kaolin suspension)	179
Table 7.2	Coagulation performances for the optimum dosage of TBP at each alum dose (in terms of maximum flocculation index, residual turbidity and aluminium, and Floc volume) at pH 5 (50 mg l ⁻¹ kaolin suspension)	183
Table 7.3	Coagulation performance for the different dosage of alum at pH6 (15 mg l ⁻¹ HA)	186
Table 7.4	Coagulation performance for the optimum TBP dosage with different alum doses at pH6 (15 mg l ⁻¹ HA)	192
Table 7.5	Coagulation performance for the optimum dosage of TBP with different alum dose at pH6 (30 mg l ⁻¹ HA)	200
 SECTION 8		
Table 8.1	Residual TBP in solution after 2 min mixing with sand (20% H ₂ O ₂ solution washed, 30mg l ⁻¹ TBP)	209
Table 8.2	Residual TBP in solution after 2 min mixing with sand (5% Decon solution washed, 30mg l ⁻¹ TBP)	210
Table 8.3	Residual NPDOC in solution after 2 min mixing with sand (5% Decon solution washed, 30mg l ⁻¹ TBP)	210
Table 8.4	Residual TBP in solution after 2 min mixing with sand (5% Decon solution washed; 60mg l ⁻¹ TBP)	211
Table 8.5	Residual TBP in solution with different mixing time (5% Decon solution washed; 60 mg l ⁻¹ TBP)	212
Table 8.6	NPDOC and UV-visible light absorbance at 254nm and 400nm in filtered water at pH4(30 mg l ⁻¹ HA)	215
Table 8.7	NPDOC and UV-visible light absorbance at 254nm and 400nm in filtered water at pH6 (30mg l ⁻¹ HA)	216

SECTION 9		Page
Table 9.1	Coagulation results for the artificial water using 15 mg l ⁻¹ TBP	221
Table 9.2	Coagulation results for the real water using 15 mg l ⁻¹ TBP	221
Table 9.3	Variation of coagulation performance with TBP dosage for Bamford raw water without pH adjustment	222
Table 9.4	Variation of coagulation performance with alum dosage at pH6 (Bamford raw water)	224
Table 9.5	Variation of coagulation performance with TBP dosage at pH6 (Bamford raw water)	225
Table 9.6	Coagulation performance for the combination of TBP/Alum at pH6 (Bamford raw water)	230
Table 9.7	Variation of coagulation performance with TBP and alum doses at pH6 (Bamford raw water)	231
Table 9.8	Strength and recovery factors obtained for different coagulants(floc breakage at 300rpm for 60s) at pH6 (Bamford raw water)	233
 SECTION 10		
Table10.1	Characteristics and coagulation behaviours of TBP with kaolin	241
Table 10.2	Optimum dose of coagulants and treatment effectiveness from real water and model water	247

LIST OF FIGURES

SECTION 2	Page
Figure 2.1 Synthesis of (a) linear polyamine and (b) branched polyamine (after Choi <i>et al.</i> (23))	34
Figure 2.2 Basic structure of chitosan (deacetylation degree 100%) (after Bolto and Gregory (19))	37
Figure 2.3 The net interaction energy curve (after Ravina (42))	39
Figure 2.4 “Electrostatic patch” model for flocculation of negative particles by cationic polyelectrolytes (after Bolto and Gregory, (19))	43
Figure 2.5 Model of an adsorbed polymer chain (after Bolto and Gregory (19))	44
Figure 2.6 Chemical structure of condense-tannin	68
 SECTION 4	
Figure 4.1 Schematic of coagulation apparatus	94
Figure 4.2 Apparatus of coagulation tests	98
Figure 4.3 Absorbance at 700nm with low tannin acid concentration	102
Figure 4.4 Absorbance at 700nm with high tannin acid concentration	102
Figure 4.5 Absorbance at 700nm (10mm cell path) with whole range of tannin acid concentration	103
 SECTION 5	
Figure 5.1 TBP solution titration curve: 100ml Tannin (0.03g l^{-1}) titrated with 0.001mol l^{-1} NaOH	106
Figure 5.2 UV-Vis scan of TBP solution with a series of TBP concentrations	109
Figure 5.3 Variation of absorbance at 210nm (10mm cell path) with TBP concentrations (pH = 4, 6 and 8)	110
Figure 5.4 Charge density of TBP as a function of pH	111
Figure 5.5 Temporal variation of charge density of TBP at different pH	112
Figure 5.6 FT-IR spectra of TBP	114
Figure 5.7 FT-IR spectra of tannin extract	114
Figure 5.8 ^1H NMR spectra of TBP	115
Figure 5.9 Elution curve of TBP by size exclusion chromatography	117
Figure 5.10 The proposed basic repeating unit in TBP	120
 SECTION 6	
Figure 6.1 Flocculation index response with TBP dose at pH4 (50 mg l^{-1} kaolin suspension)	125

		Page
Figure 6.2	Flocculation index response with TBP dose at pH7 (50 mg l ⁻¹ kaolin suspension)	125
Figure 6.3	Flocculation index response with TBP dose at pH9 (50 mg l ⁻¹ kaolin suspension)	126
Figure 6.4	Residual turbidities before and after coagulation using TBP at pH 4 (50 mg l ⁻¹ kaolin suspension)	126
Figure 6.5	Residual turbidities before and after coagulation using TBP at pH 7 (50 mg l ⁻¹ kaolin suspension)	127
Figure 6.6	Residual turbidities before and after coagulation using TBP at pH 9 (50 mg l ⁻¹ kaolin suspension)	127
Figure 6.7	Comparison of the FI response between TBP precipitation in blank water and coagulation in kaolin suspension at pH 7 and pH 9	130
Figure 6.8	Flocculation index response with TBP dose at pH 4 (30 mg l ⁻¹ HA)	131
Figure 6.9	Flocculation index response with TBP dose at pH 7 (30 mg l ⁻¹ HA)	133
Figure 6.10	Flocculation index response with TBP dose at pH 9 (10 mg l ⁻¹ HA)	134
Figure 6.11	Flocculation index response with TBP dose at pH4 (25 mg l ⁻¹ kaolin suspension)	138
Figure 6.12	Flocculation index response with TBP dose at pH4 (100 mg l ⁻¹ kaolin suspension)	138
Figure 6.13	Flocculation index response with TBP dose at pH7 (25 mg l ⁻¹ kaolin suspension)	139
Figure 6.14	Flocculation index response with TBP dose at pH7 (100 mg l ⁻¹ kaolin suspension)	140
Figure 6.15	Flocculation index response with TBP dose at pH9 (50 mg l ⁻¹ kaolin suspension)	142
Figure 6.16	Flocculation index response with TBP dose at pH9 (25 mg l ⁻¹ kaolin suspension)	143
Figure 6.17	Flocculation index response with TBP dose at pH9 (12.5 mg l ⁻¹ kaolin suspension)	143
Figure 6.18	Flocculation index response with TBP dose at pH4 (15 mg l ⁻¹ HA)	144

	Page
Figure 6.19 Flocculation index response with TBP dose at pH4 (50 mg l ⁻¹ HA)	145
Figure 6.20 Flocculation index response with TBP dose at pH7 (15 mg l ⁻¹ HA)	146
Figure 6.21 Flocculation index response with TBP dose at pH7 (50 mg l ⁻¹ HA)	146
Figure 6.22 Flocculation index response for different aging periods at pH 4 (50mg l ⁻¹ kaolin suspension)	148
Figure 6.23 Flocculation index response for different aging periods at pH 7 (50mg l ⁻¹ kaolin suspension)	149
Figure 6.24 Flocculation index response for different aging periods at pH 9 (50mg l ⁻¹ kaolin suspension)	149
Figure 6.25 Flocculation index response for different aging periods at pH 4 (30 mg l ⁻¹ HA)	150
Figure 6.26 Flocculation index response for different aging periods at pH 7 (30 mg l ⁻¹ HA)	151
Figure 6.27 Flocculation index response for different aging periods at pH 9 (10 mg l ⁻¹ HA)	151
Figure 6.28 Flocculation index response for different mixing intensities at pH 4 (50mg l ⁻¹ kaolin suspension)	152
Figure 6.29 Flocculation index response for different reactors at pH 9 (50mg l ⁻¹ kaolin suspension)	153
Figure 6.30 Flocculation index response for different reactors at pH 7 (50mg l ⁻¹ kaolin suspension)	154
Figure 6.31 Flocculation index response with different coagulants at pH 7, and TBP at pH9 (50 mg l ⁻¹ kaolin suspension)	155
Figure 6.32 Residual turbidity before and after coagulation with different coagulants at pH 7 (50 mg l ⁻¹ kaolin suspension)	155
Figure 6.33 Flocculation index response with different coagulants at pH 7 (30 mg l ⁻¹ HA)	157
Figure 6.34 Monitoring of floc formation at 50 rpm (48 s ⁻¹), with varying breakage speed (200 rpm (350 s ⁻¹) to 400 rpm (950 s ⁻¹)) and re-formation at 50 rpm (48 s ⁻¹) (50 mg l ⁻¹ kaolin suspension at pH7)	159
Figure 6.35 Variation of residual turbidity before breakage and after re-formation, with velocity gradient at pH7 (50 mg l ⁻¹ kaolin suspension)	160
Figure 6.36 Monitoring of floc formation at 50 rpm (48 s ⁻¹), breakage at 300 rpm (600 s ⁻¹) for different periods and re-formation at 50 rpm (48 s ⁻¹) at pH7 (50 mg l ⁻¹ kaolin suspension)	161

		Page
Figure 6.37	Variation of residual turbidity before breakage and after re-formation, with breakage period at pH 7 (50 mg l ⁻¹ kaolin suspension)	162
Figure 6.38	Monitoring of floc formation at 50 rpm, breakage at 300 rpm for 60 s and re-formation at 50 rpm using different coagulants at pH 7 (50 mg l ⁻¹ kaolin suspension)	163
Figure 6.39	Monitoring of floc formation at 50 rpm, breakage at 300 rpm for 300 s and re-formation at 50 rpm using different coagulants at pH 7 (50 mg l ⁻¹ kaolin suspension)	164
Figure 6.40	Monitoring of floc formation, and re-formation at pH9 using TBP (50 mg l ⁻¹ kaolin suspension)	166
 SECTION 7		
Figure 7.1	Dynamic monitoring of kaolin coagulation (50 mg l ⁻¹) at pH4 using different dosages of alum	171
Figure 7.2	Dynamic monitoring of kaolin coagulation (50 mg l ⁻¹) at pH5 using different dosage of alum	172
Figure 7.3	Dynamic monitoring of kaolin coagulation (50 mg l ⁻¹) at pH7 using different dosage of alum	173
Figure 7.4	Flocculation index response with TBP dose and 3.4 mg l ⁻¹ Al ³⁺ at pH7 (50 mg l ⁻¹ kaolin suspension)	174
Figure 7.5	Flocculation index response with TBP dose and 3.0 mg l ⁻¹ Al ³⁺ at pH7 (50 mg l ⁻¹ kaolin suspension)	175
Figure 7.6	Flocculation index response with TBP dose and 2.5 mg l ⁻¹ Al ³⁺ at pH7 (50 mg l ⁻¹ kaolin suspension)	175
Figure 7.7	Flocculation index response with TBP dose and 2.0 mg l ⁻¹ Al ³⁺ at pH7 (50 mg l ⁻¹ kaolin suspension)	176
Figure 7.8	Flocculation index response with TBP dose and 1.5 mg l ⁻¹ Al ³⁺ at pH7 (50 mg l ⁻¹ kaolin suspension)	176
Figure 7.9	Flocculation index response with TBP dose and 1.0 mg l ⁻¹ Al ³⁺ at pH7 (50 mg l ⁻¹ kaolin suspension)	177
Figure 7.10	Variation of Flocculation index with alum and TBP doses at pH7 (50 mg l ⁻¹ kaolin suspension)	178
Figure 7.11	Flocculation index response with TBP dose and 0.05 mg l ⁻¹ Al ³⁺ at pH5 (50 mg l ⁻¹ kaolin suspension)	180
Figure 7.12	Flocculation index response with TBP dose and 0.1 mg l ⁻¹ Al ³⁺ at pH5 (50 mg l ⁻¹ kaolin suspension)	180
Figure 7.13	Flocculation index response with TBP dose and 0.15 mg l ⁻¹ Al ³⁺ at pH5 (50 mg l ⁻¹ kaolin suspension)	181

	Page	
Figure 7.14	Flocculation index response with TBP dose and 0.2 mg l ⁻¹ Al ³⁺ at pH5 (50 mg l ⁻¹ kaolin suspension)	181
Figure 7.15	Flocculation index with alum and TBP doses at pH 5 (50 mg l ⁻¹ kaolin suspension)	182
Figure 7.16	Locus of alum-polymer dosage combinations for 50 mg l ⁻¹ kaolin at pH5	183
Figure 7.17	Dynamic monitoring of 15 mg l ⁻¹ HA at pH 6 using different dosages of alum	185
Figure 7.18	Flocculation index response with TBP dose at pH 6 (15 mg l ⁻¹ HA)	187
Figure 7.19	Flocculation index response with Tanfloc SL dose at pH 6 (15 mg l ⁻¹ HA)	187
Figure 7.20	Flocculation index response with 1.35 mg l ⁻¹ as Al ³⁺ and different TBP dosages at pH 6 (15 mg l ⁻¹ HA)	188
Figure 7.21	Flocculation index response with 0.81 mg l ⁻¹ as Al ³⁺ and different TBP dosages at pH 6 (15 mg l ⁻¹ HA)	189
Figure 7.22	Flocculation index response with 0.135 mg l ⁻¹ as Al ³⁺ and different TBP dosages at pH 6 (15 mg l ⁻¹ HA)	189
Figure 7.23	Flocculation index response with TBP dose and different Al concentrations at pH 6 (15 mg l ⁻¹ HA)	190
Figure 7.24	Flocculation index response with different optimum coagulants at pH6 (15 mg l ⁻¹ HA)	193
Figure 7.25	Dynamic monitoring of 30 mg l ⁻¹ HA at pH 6 using different dosages of alum	195
Figure 7.26	Flocculation index response with TBP dose at pH 6 (30 mg l ⁻¹ HA)	195
Figure 7.27	Flocculation index response with Tanfloc SL dose at pH 6 (30 mg l ⁻¹ HA)	196
Figure 7.28	Flocculation index response with 2.7 mg l ⁻¹ as Al ³⁺ and different TBP doses at pH 6 (30 mg l ⁻¹ HA)	197
Figure 7.29	Flocculation index response with 1.35 mg l ⁻¹ as Al ³⁺ and different TBP doses at pH6 (30 mg l ⁻¹ HA)	197
Figure 7.30	Flocculation index response with 0.81 mg l ⁻¹ as Al ³⁺ and different TBP doses at pH6(30 mg l ⁻¹ HA)	198
Figure 7.31	Flocculation index response with 0.405 mg l ⁻¹ as Al ³⁺ and different TBP doses at pH6 (30 mg l ⁻¹ HA)	198
Figure 7.32	Flocculation index response with TBP dose and different Al concentrations at pH6 (30 mg l ⁻¹ HA)	199

		Page
Figure 7.33	Flocculation index response with different optimum coagulants at pH6 (30 mg l ⁻¹ HA)	201
Figure 7.34	Locii of alum-TBP dosage combinations for optimal coagulation performance at pH6	202
Figure 7.35	Variation of Flocculation Index and colour removal along coagulant dosage locus for 15 mg l ⁻¹ HA at pH6	203
Figure 7.36	Variation of Flocculation Index and colour removal along coagulant dosage locus for 30 mg l ⁻¹ HA at pH6	204
 SECTION 8		
Figure 8.1	Variation of the residual TBP with TBP/Sand Ratio	211
Figure 8.2	Flocculation index response with the solid bound TBP at pH4 (30 mg l ⁻¹ HA)	213
Figure 8.3	Flocculation index response with the solid bound TBP at pH6 (30mg l ⁻¹ HA)	216
 SECTION 9		
Figure 9.1	Flocculation index response with TBP dose for artificial water	220
Figure 9.2	Dynamic monitoring of raw water (Bamford, UK) using different dosage of TBP without pH adjustment	222
Figure 9.3	Dynamic monitoring of raw water at pH 6 using different doses of alum (Bamford raw water, UK)	223
Figure 9.4	Dynamic monitoring of raw water at pH 6 using different doses of TBP (Bamford raw water, UK)	225
Figure 9.5	Flocculation index response with 25 mg l ⁻¹ TBP and different Alum doses at pH6 (Bamford raw water, UK)	226
Figure 9.6	Flocculation index response with 20 mg l ⁻¹ TBP and different Alum doses at pH6 (Bamford raw water, UK)	227
Figure 9.7	Flocculation index response with 30 mg l ⁻¹ TBP and different Alum doses at pH6 (Bamford raw water, UK)	227
Figure 9.8	Locus of alum-TBP dosage combinations for optimal coagulation performance at pH6 (Bamford raw water, UK)	228
Figure 9.9	Variation of Flocculation Index and colour removal along locus line of coagulant dosage at pH6 (Bamford raw water, UK)	229
Figure 9.10	Flocculation index response with 10 mg l ⁻¹ TBP and different Alum doses at pH6 (Bamford raw water, UK)	231

		Page
Figure 9.11	Monitoring of floc formation at 50 rpm, breakage at 300 rpm for 60s and re-formation at 50 rpm using different coagulants at pH6 (Bamford raw water, UK)	232

SECTION 10

Figure 10.1	Proposed model structure for TBP	236
Figure 10.2	Locii of alum-TBP dose combinations for FI_{max} (optimum) and $0.75 FI_{max}$ with HA at two concentrations at pH6	245

LIST OF PRINCIPAL SYMBOLS AND ABBREVIATIONS

A	Titration volume for sample
Abs	Absorbance units
a_c	Fluctuating component
B	Titration used for blank
C	Floc strength co-efficient
CD	Charge density
cm	Centimetre
CPAM	Cationic polyacrylamide
d	Floc diameter
DBPs	Disinfection by-products
d_c	Average transmitted light intensity
DD	Deacetylation degree
d_g	Drain diameter
DL	Detection limit
DMA	Dimethylamine
DMAEMA	Dimethylaminoethyl methacrylate
dn/dc	Refractive index/Polymer concentration
DOC	Dissolved organic carbon
DOM	Dissolved organic matter
DS	Degrees of substitution
ECH	Epichlorohydrin
FI	Flocculation index
G	Velocity gradient
g	Gram
h	Hour
l	Litre
m	Metre
meq	Milli-equivalent weight

mV	Millivolt
ml	Millilitre
mg	Milligram
min	Minute
μm	Micrometre
μg	Microgram
mol	Mole
M	Molarity of silver nitrate
MW	Molecular weight
$\langle M \rangle_w$	Average molecular weight
NOM	Natural organic matter
NPDOC	Non-purgeable dissolved organic carbon
NTU	Nephelometric turbidity unit
nm	Nanometer
PDA	Photometric Dispersion Analyser
PDADMAC	Polydiallyldimethyl-ammonium chloride
PEO	Polyethylene oxide
ppm	Part per million
rms	Root mean square
rpm	Revolutions per minute
s	Second
SUVA	Specific UV-absorbance
T	Retention time
TBP	Tannin based polymer
TOC	Total organic carbon
UV-	Ultra-violet
Vis-	Visible
w/w	Weight per Weight
λ	Wave length
ZP	Zeta potential

1. OVERVIEW

Water production normally involves physicochemical procedures, which include processes such as the coagulation and flocculation of suspended solids and colloids, the adsorption of soluble materials on solid substrates and ion-exchange resins, oxidation to destroy organic impurities and membrane technologies (1). The primary method for the coagulation/flocculation of suspension particles and dissolved organic matter is commonly carried out with a metal salt such as alum (aluminium sulphate), or a synthetic polymer such as polyDADMAC, and much has already been done in water and wastewater treatment to optimize this process.

Employing hydrolysable metal salts (aluminium or iron salts) for coagulation is a long-standing technology, because the high valency metal ions undergoing hydrolysis reactions in aqueous solution have a higher positive charge that interacts specifically with negative colloids (clay particles and natural organic materials) and neutralize their charge, giving destabilization and coagulation. In most practical water treatment operations, metal coagulants are added at high dosages and extensive precipitation occurs. The enmeshment of particles by the precipitate is generally thought of as “sweep coagulation”. However, this method of coagulation produces large amounts of sludge (2). Organic polymers can be used as primary coagulants in the more traditional flocculation step of binding already formed small flocs into larger and stronger flocs which can tolerate the high shear forces encountered in the filtration stages (3). The larger particles formed in this way also give accelerated rates of sedimentation because the volume of sludge produced is more than halved (1). However, the long-term effects of these polymers on human health are not well understood (4).

In water treatment, cationic polymers and inorganic metal salts appear to

have complementary roles as coagulants (5). The combined use of hydrolysable metal salts (aluminium or iron salts) with polyelectrolytes is intended to maximize the benefits of both coagulants through the reduction of the inorganic coagulant dosage and the production of larger and stronger flocs. The increased use of synthetic cationic polymers (polyamine and polyDADMAC) as coagulation aids has led to a few studies (6, 7) on the effectiveness of dual coagulants. However, there is relatively little published information on coagulation performance using optimal combinations of metal salts with natural polymers in water treatment, or further on the relationship between the character of natural polymers and treatment effectiveness. Thus, there is much opportunity for improved dual coagulants that are tailor made for particular processes.

To date, the use of natural tannin-based polymers (TBP) as coagulants in water and wastewater treatment is assumed to be commercially attractive; taking into account their proven low cost and basic information of their chemistry properties from their modification process, which includes Mannich reaction and polymerization (8). However, adequate investigation has not yet been undertaken on the characterization of TBP. As a result of the incomplete understanding of the chemical structure and functional group of this polymer, classic coagulation theories may not allow prediction of the mechanism and behaviour of the TBP in either model water or raw water, hence failure to achieving improved flocculation performance.

The emphasis here is on the application of a soluble tannin-based polymer in coagulation/flocculation processes, which are followed by a separation step in the form of sedimentation or flotation, with a final polishing by filtration. Due to a lack of available information, the characterization of the modified tannin polymer has to be assessed. The originality of this thesis is to design a broad scheme for undertaking a full characterization of TBP by qualitative or/and quantitative analysis using some modern analytical techniques and older classical

techniques, hence providing an unambiguous description of the polymer, monomer, structure and other chemical properties.

The other ambition in this research is to evaluate the coagulation performance of the TBP based on clearly unveiling the relationship between the chemical properties and coagulation mechanisms of the TBP. This should yield a much clearer understanding of the reaction action between this polymer and the particle suspensions or/and dissolved organic matter during the water treatment process. When the TBP is used as a primary coagulant to partially replace alum, it is desirable to be able to determine a unique optimal dosage combination of the metal salt and the polymer. But, achieving improved performance with the reduced alum dosage and a low concentration of the residual tannin in final water is a challenge in its practical application.

In summary, this study has attempted, through laboratory investigations, to provide the basic chemistry properties of the TBP, to evaluate their relative contribution to the various coagulation mechanisms and to improve its coagulation performance in model water and surface real water.

2. INTRODUCTION

2.1 Introduction

In water purification and wastewater treatment, coagulation/flocculation is the most conventional technique in conjunction with sedimentation and filtration to remove dissolved organic matter (DOM) and suspended particles. The primary method for making colloids aggregate, coagulation, is normally carried out with metal salts such as aluminum and iron salts, and much has already been done to optimize this process. The interest in the use of polymers to partially or completely replace inorganic coagulants as primary coagulants in water industry arises from the significant inherent advantages of polymers. This is mainly based on their high treatment efficiency, small coagulant dosage requirements, the reduced voluminous sludge, facilitation of filtration, and reduced level of aluminum in treated water (1, 9). In colloid chemistry, it is common to restrict the term ‘coagulation’ to cases where the aggregates tend to be small and dense; ‘flocculation’ is then restricted to the cases where aggregates tend to be larger and more open in structure. However, in the water industry, ‘coagulation’ is used to describe the chemical destabilizing process instigated by the addition of some reagent to the colloidal system, whilst ‘flocculation’ describes the process whereby the destabilized particles join together to form large agglomerates (10).

Polymers are broadly divided into three categories based on their ionic nature: cationic, anionic and non-ionic. Principally cationic polymers are used as primary coagulants for water treatment; anionic and nonionic polymers have gained wide acceptance as flocculant aids. The water-soluble polymers with many repeating units (or monomers), usually referred to as polyelectrolytes, are either synthetic organic compounds, meaning man-made and starting from small molecules, or natural organic materials as original extracts from certain plants or animal life, or as modified derivatives by subsequent reactions.

It is well documented that both natural and synthetic cationic polymers can be used as primary coagulants in water treatment (3, 11). A number of published studies on the chemical characterization, coagulation mechanism and flocculation performance of synthetic cationic polyelectrolytes for water treatment have been carried out over the years. However, health and environmental issues of synthetic polymers still require attention (4). Possible negative consequences could arise from the reaction of synthetic polymers with other water treatment chemicals such as chlorine for example, increasing the level of disinfection by-products (1). In marked contrast, although some investigations related to the coagulation kinetics of natural polymers in model water and the use of natural polymers in the wastewater industry have been carried out, very little is currently clearly known of the fundamental mechanism of natural polymers in the coagulation process and their application in drinking water treatment. The focus in this review is on the use of cationic polyelectrolytes in the coagulation and flocculation processes. Most of classic coagulation theories are found from the studies of synthetic polyelectrolytes as coagulants. These theories provide a reference for the mechanisms of coagulation with the tannin-based polymer in later research.

2.2 Characterisation of Cationic Polymer as Coagulant

Knowledge about a polymer's molecular weight and charge density, the chemical structure of the monomer, and the active groups in the product would be a significant step toward developing a scientific method for polymer selection in water treatment. However, the chemistry of cationic polymers is more complex than that of anionic species, because there are more variable reactions for the preparation of cationic polymers, which involve free-radical addition polymerization, epoxide addition reaction, condensation reaction, and a variety of reactions on existing polymer backbones, including Mannich reactions, Hofman degradations and nucleophilic displacements (12). Cationic polymers, as

coagulants in water treatment, must be water soluble and can vary in structure (linear versus branched), composition, molecular weight and amount of charge.

2.2.1 Molecular Weight and Charge Density of Cationic Polymer

A polymer's molecular weight (MW) and charge density (CD) are the crucial parameters governing its coagulation performance. Both of these properties can be quantified and are believed to readily relate with the two well-known coagulation mechanisms, charge neutralisation and polymer bridging. Both of these will be discussed later.

The molecular weight of the polymer ranges from a few thousands to millions of grams per mole. It is widely understood that if the polymer molecular weight is sufficient, the "polymer bridging" model should apply during the flocculation process (12). By virtue of their different uses, polymers can be conveniently divided into three classes: low ($<10^5$), medium (10^5 - 10^6) and high molecular weight ($>10^6$) (12). It has previously been stated that polymers in aqueous solution always present a random coil configuration. Generally, for polymers, the size of the coil is nearly proportional to the square root of the MW (13). The molecular weight is considered to be closely associated with rheological, osmotic, and light scattering properties by some straightforward equations (14). Both light scattering and viscosity are most commonly used to determine the molecular weight based on measuring the intensity of scattering light and intrinsic viscosity of polymers in solution. However, unlike small molecules, the molecular weight of a polymer is not unique. Rather, a given polymer will have a distribution of molecular weights. The MW distribution will depend on the way that the polymer is produced. It is more proper to use the term "average molecular weight" to indicate the polymer mass. Dentel *et al.*(15) cited a simple viscosimetric method to determine the average molecular weight of acrylamide-based polymers for water treatment. Light-scattering technology has

been also undertaken by Ghosh *et al.* (16) to measure the average molecular weight of various commercial polymers used as flocculants.

The charge density of a polyelectrolyte is another important polymer property, and should be indicative of the amount of polymer charge available to affect particle destabilization via the “charge neutralisation” mechanism, hence greatly influencing the effectiveness of the coagulant. The charge density of the polymer is dependent upon the degree of ionization of the functional groups, the degree of copolymerization and the amount of substituted groups in the polymer structure (17). It is usually found that the polymer coil can be significantly expanded for polymers with high CD values, due to the appreciable repulsion between polymer segments. The CD of a polymer in solution can be determined by a procedure known as colloid titration (18), which has been presented in a procedure manual (15). Charge density can be expressed in terms of milliequivalents per gram (meq g^{-1}) if the homogeneous segments of polymers are strongly ionic and fully charged. However, for a copolymer of non-ionic and cationic monomeric species, the charge density is commonly expressed as mole per cent of charge groups. In this case, polyelectrolytes can be regarded as having, low, medium or high CD values, corresponding to the mol% of ionic groups around: 10%, 25%, and 50-100%, respectively (19). The charge density of some cationic polyelectrolytes has been determined and summarized in Table 2.1.

TABLE 2.1 Charge density of some cationic polyelectrolytes (after Bolto and Gregory (19))

Polymer	Molecular formula	CD (mol%)	CD (meq g⁻¹)
PDADMAC Poly (Diallyldimethyl ammonium Chloride)	C ₈ H ₁₆ N Cl	100	6.2
ECH/DMA (Epichlorohydrin/Dimethylamine)	C ₅ H ₁₂ ON Cl	100	7.3
CPAM (cationic polyacrylamide)	C ₈ H ₁₆ O ₂ N Cl	100	5.2
CPAM	(C ₈ H ₁₆ O ₂ NCl) _{0.5} (C ₃ H ₅ ON) _{0.5}	50	3.8
CPAM	(C ₈ H ₁₆ O ₂ NCl) _{0.25} (C ₃ H ₅ ON) _{0.75}	25	2.5
CPAM	(C ₈ H ₁₆ O ₂ NCl) _{0.1} (C ₃ H ₅ ON) _{0.9}	10	1.2
Chitosan	C ₆ H ₁₁ O ₄ N·HCl	100	5.2

2.2.2 Types and Structure of Cationic Polymer

2.2.2.1 Synthetic Polymer

There are typically two routes for the synthesis of cationic polymers, in water treatment practice, by homopolymerization with a single repeating cationic unit, and by copolymerization with a proportion of non-ionic and cationic monomers. In general, the most prominent of synthetic cationic polymers available for water treatment contains quaternary ammonium groups that have a formal positive charge irrespective of pH (19). However, there have also been commercial polyelectrolytes which consist of polyamines containing primary, secondary or tertiary amino groups, or mixtures of them. The charge density of these non-quaternary amine groups varies with pH values of solution (20). Table 2.2 details these different forms of polymers (21). The properties of polymers are obviously affected by their synthesis processes. For example, in the preparation of polyacrylamide, heterogeneous polymers are typically formed by co-polymerizing nonionic acrylamide with a particular cationic monomer, giving cationic polymers of high molecular weight (10^5 - 10^7 g mol⁻¹). However, the nonionic polyacrylamide can be post-reacted with formaldehyde and dimethylamine, a secondary amine, to give the aminomethylated polyacrylamide as a flocculant via the Mannich reaction (22). In this case, the corresponding unquaternized amine is only cationic at low or moderate pH values due to its deprotonation at increasing pH. The preparation of cationic polyamine has been thoroughly reviewed by Chio *et al.* (23). They found that the reaction of epichlorohydrin with a secondary amine such as dimethylamine produces either linear polyamine or branched polyamine with a modifier. The synthesis process is shown in Figure 2.1.

In general, quaternary ammonium polymers have a widely commercial application as flocculants, in the protonated form after the quaternization of tertiary nitrogen. Polyamine, polyacrylamide and polyDADMAC are commonly

used as primary coagulants in the total/partial replacement of conventional inorganic coagulants such as FeCl_3 and $\text{Al}_2(\text{SO}_4)_3$ (24). Mangravite (25) stated that both polyDADMAC and polyamine which contain quarternary amine groups are pH-independent in their charge density. Mangravite also found that the typical polymer dose of primary coagulants for most applications is 0.5 to 10 mg l^{-1} and 0.1 to 1.0 mg l^{-1} when applied as coagulant aids. In the UK, polyamines are more frequently used in potable water treatment than poly DADMAC (19).

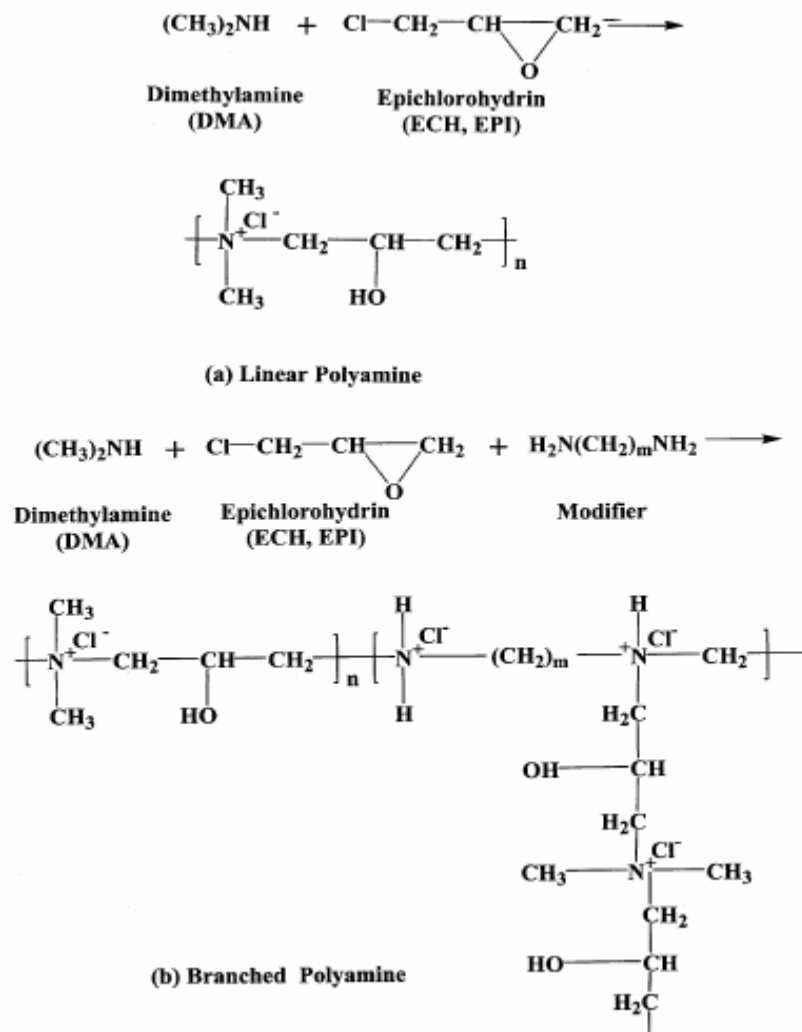


Figure 2.1 The synthesis of (a) linear polyamine and (b) branched polyamine (after Choi *et al.* (23))

2.2.2.2 Natural Polymer

There are several natural cationic polymers, which can either be extracted from certain kinds of plants and animals and have inherent cationic properties, or can be modified to yield cationic polyelectrolytes. Since natural polymers are potentially low cost and believed to be biodegradable and non-toxic, they are workable alternatives to synthetic polyelectrolytes in water and wastewater treatment (26). The most prominent of them is chitosan, a high molecular-weight linear cationic polymer with a MW value of up to 10^6 g mol⁻¹. The physico-chemical properties of chitosan are related to the presence of amine functions (acid-base properties and cationicity) which make chitosan very efficient for interacting with anionic elements in acidic solutions (4).

Chitosan is a deacetylated chitin which is considered as a 1:4 random copolymer of N-acetyl- α -D-glucosamine and α -D-glucosamine (27). Chitin with a deacetylation degree (DD) more than 50% is usually referred as chitosan. Figure 2.2 shows the composition and structure of chitosan. The molecular weight of chitosan samples is correlated with the preparative condition adopted. Table 2.3 shows the properties of chitosan samples after deacetylation (28). An important feature of chitosan is that the charge density and solubility of this material are pH-dependent. For chitosan with a degree of deacetylation above 70%, the dissociation constant pK_a can be approximately fixed to 6.3-6.4. Hence, at pH of below 5, most of the amine groups are protonated, therefore having increased charge density and can more easily attract particle anions (29). At pH6, the charge density of chitosan is found to be about 4.5 meq g⁻¹ (30).

Very good coagulation effectiveness of chitosan for high-alkalinity water at high turbidity was reported by Kawamura (3). Bolto *et al.* (31) also found that it is quite effective at natural organic matter (NOM) removal using chitosan as a coagulant, even though it would be slightly charged (17 mol %) at neutral pH

levels. In this case, Bolto believed that hydrogen bonding is dominant through the free amino groups on the polymer and hydroxyl groups on the NOM. Divakaran and Pillai (32) have studied the mechanism of kaolinite and titanium dioxide flocculation using chitosan, and observed that chitosan solution started to precipitate at pH values close to neutral.

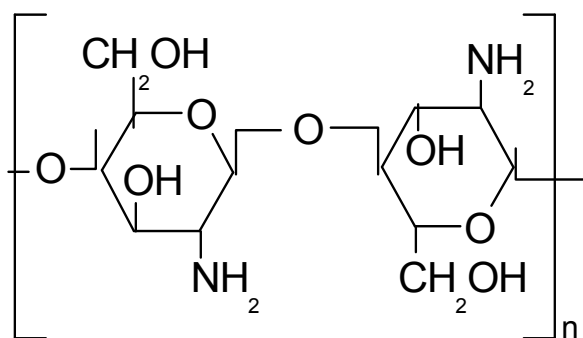


Figure 2.2 Basic structure of chitosan (DD 100%, after Bolto and Gregory (19))

TABLE 2.3 Characteristics of chitosan after deacetylation (after Huang *et al.* (28))

Sample No.	Concentration of NaOH (%)	Reaction time (min)	DD (%)	MW (10^6)
1	45	20	48	--
2	45	60	68	1.7
3	45	120	73	1.6
4	45	300	77	1.6
5	45	720	78	1.7
6	60	300	86	4.7

* DD—Deacetylation Degree

Natural starch is composed of α -D-glucose units. Cationic starch derivatives with potential use as flocculants in wastewater treatment are made from the primary OH group in alkali treated starch with N-(3-chloro-2-hydroxypropyl) trimethylammonium chloride to form the polymer, where the cationic site is attached via an ether link to the polymer chain (19). It has reported that starch derivate has a medium MW and the CD can be low or medium (1). There are two other routes to modify starch, which are the copolymerization of starch with

either 2-hydroxy-3-methacryloyloxypropyltrimethylammonium chloride or the mixture of acrylamide and the nitric acid salt of dimethylaminoethyl methacrylate (DMAEMA·HNO₃) (33), but whose products have seen limited use for water treatment, probably because of economic reasons(12). Cationically modified starch has been tested for clarifying particles (34). In the majority of systems the degrees of substitution (DS) for cationic starches are very low (< 0.1), and the aggregation of solid particles with cationic starches is believed to be a result of polymer adsorption (35). Sableviciene *et al.* (36) have concluded that the flocculation efficiency of cationic starch derivatives was dependent on the amino group types and followed the order: quarternary > tertiary > secondary > primary. Further observation has found that the flocculation efficiency increased on increasing the nitrogen content and decreasing the molecular weight of cationic starches.

Other natural polymers with cationic charge have also been studied in wastewater treatment. These include the modified natural polysaccharides, for example, grafting synthetic polymers onto amylopectin, guar gum and glycogen (37), and the modified lignin based polymer prepared by the Mannich reaction (38). The aqueous extract from macerated seeds of the horseradish tree *Moringa oleifera* has proved to be effective at removing suspended materials and generate reduced sludge volumes in comparison to alum (39). However, all of these technologies have not yet been adopted on treatment plants for sustained use.

2.3 Coagulation Action of Cationic Polymer

In addition to a fundamental understanding of the chemical properties of cationic polymers as coagulants, the other key factor to optimizing the coagulation and flocculation process is an understanding of how the individual colloids interact with each other, along with the coagulants. Therefore, in this section, the aspects of colloidal stability and destabilization, and coagulation

mechanisms of cationic polymers are reviewed.

2.3.1 Colloid Stability

The small turbidity particles in the size range from 0.01 to 5 microns present the real challenge to settle or filter since their stability or resistance to coagulation is quite strong (1). The charge carried by these colloidal particles, which are always anionic at the natural water pH, causes adjacent particles to repel each other and prevents effective agglomeration and flocculation. As a result, charged colloids tend to remain discrete and dispersed in suspension. According to the classic DLVO Theory (40, 41), the stability of colloidal particles is dominated by the balance between two opposing forces: electrostatic repulsion and van der Waals attraction when particles approach each other. The DLVO theory quantifies particle stability in terms of energy change when particles approach one other. The net interaction energy is determined by the summation of the van der Waals attraction and the electrostatic repulsion energies in terms of interparticle distance, and is shown in Figure 2.3. In order for aggregation to occur, two particles on a collision course must have sufficient kinetic energy (due to their speed and mass) to overcome the energy barrier.

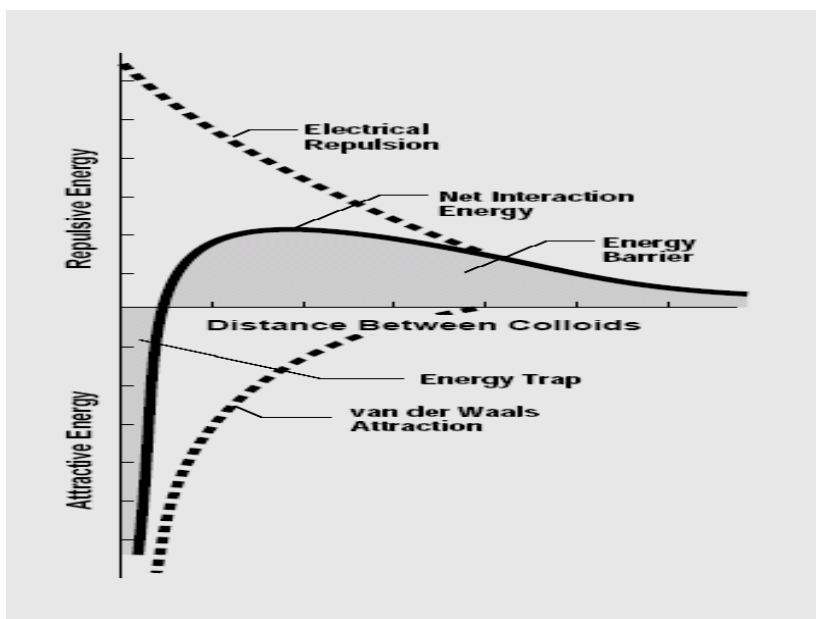


Figure 2.3 The net interaction energy curve (after Ravina (42))

For really effective coagulation, the energy barrier can be lowered or completely removed by either increasing the ionic strength, which compresses the double layer of particles, or reducing the surface charge of the particles hence reducing the repulsive energy. The destabilization and stabilization of negative particles by cationic polymers occur when the electrophoretic mobility of particles at the optimum flocculant concentration is close to zero (43). Therefore, the energy barrier is lowered to the point where the particle velocity from mixing allows the colloids to overwhelm it.

2.3.2 Coagulation Mechanisms of Cationic Polymer

The removal of colloidal and dissolved impurities during water treatment involves interacting with impurities and forming a stabilized dispersion. Bolto (1) stated that for the adsorption of polymers on the particle surface there must be some favourable interactions between the polymer segments and the particle surface. If the particles and the polymer have opposite charge, i.e., negative colloidal particles and a cationic polymer, then strong interaction and complete adsorption of the polymer will occur as a result of an electrostatic interaction. However, if the particles and polymer are of the same charge or if the polymer is non-ionic then there needs to be some specific interactions responsible for binding of polymer segments to the particle surfaces. These interactions can include hydrophobic bonding, hydrogen bonding or as a result of dipole crystal field effects.

Cationic polymers have been widely reported as significantly influencing the aggregation of anionic suspensions. Three principal mechanisms of cationic polymer-induced colloidal aggregation have been proposed: charge neutralization, polymer bridging and depletion flocculation. In comparison with polymer bridging and charge neutralization, which depend on the adsorption of polymer on particle surfaces, depletion flocculation occurs in systems where the polymer

has a very low adsorption affinity and a fairly high concentration. Due to the high operating and capital costs, depletion flocculation is not recommended in water treatment practice (12) and will not be considered here. However, in very many practical cases, it is generally difficult to distinguish between charge neutralization and polymer bridging, particularly, in a system containing colloids and cationic polyelectrolytes with high MW, where both mechanisms may lead to destabilization (19).

2.3.2.1 Charge Neutralization

Charge neutralization by the adsorption of the destabilizing chemical to the colloid is a key mechanism for optimizing removal of suspension particles from water. Inorganic coagulants (such as alum) and cationic polymers often work through charge neutralization due to the negative charge of impurity particles in natural water. Gregory (45) found that cationic polymers always interact strongly with surfaces of negative charge and are quantitatively adsorbed. From the results of coagulation for aqueous silica suspension, he has indicated that the destabilization and restabilization of negative particles by cationic polymers of moderate molecular weight occurred primarily by charge neutralisation and charge reversal (43). There is the possibility that flocculation could occur as a result of the reduced surface charge of the particles and hence a decreased electrical repulsion between them. Thus, it is practical to lower the DLVO energy barrier and form flocs (46). Gregory's findings have been supported by the results of Zhang *et al* (47). They reported that rapid aggregation of hematite particles induced by polyacrylic acid (PAA) occurred only in the particle region with low surface charge. In other studies (43), polyelectrolytes with high CD have been found to be more effective for charge neutralisation due to more charge delivered to the particle surfaces. It is believed that a stoichiometry exists between the dose of the coagulant and the surface area of the colloidal phase where charge neutralisation is the dominant aggregation

mechanism (48). Nevertheless, restabilization of particles can occur by overdosing the cationic polymer. In this case, the charge of colloid changes from negative to positive. The stoichiometric relationship between an optimal polymer dose and a solid concentration has been studied by determining the amount of opposite charge needed to neutralize the negative charge of particles. For design purposes, in order to estimate the optimum polymer dosage, different techniques have been undertaken to measure the surface potential and charge of particles, which include the measurement of zeta potential (or electrophoretic mobility) (46), colloid titration (18) and streaming current (49) techniques. Recently, an on-line photometric dispersion analysis technique has been developed and used successfully for sensitive monitoring of the state of aggregation (50). A brief description, application and comparison of each method are discussed later in Section 2.4.4.

The concept of “electrostatic patch” was first introduced by Gregory (51) for the coagulation of low charge density latex particles by polyelectrolytes with high charge density. In his later study on the flocculation of clay with cationic polymers, Gregory (52) stated that the positively charged adsorbed species might form small positively charged patches on the negatively charged surfaces of the particle. As a result, attractive forces could develop between positive patches and oppositely charged surface areas as particles collide during coagulation. In the electrostatic patch model, it is assumed that the cationic polymer has a high charge density and the particles have a relatively low surface charge density. Even though the polymer adsorbs where there are domains of opposite charge, there are still areas of negative charge on the surface of the particles as well as excess positive charge on the polymer. The simple reason for this is that the average distance between charged polymer segments is smaller than that between surface sites of particles. The “patchwise” model is shown schematically in Fig. 2.4.

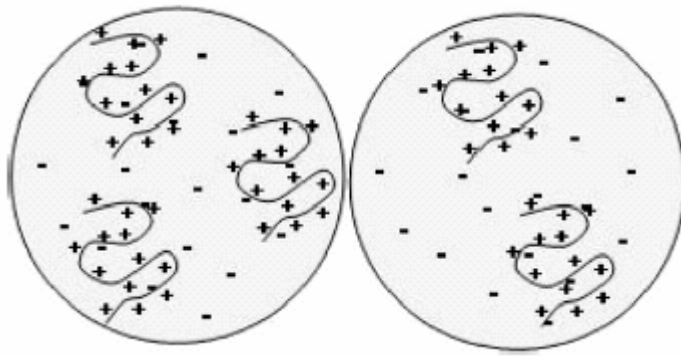


Figure 2.4 “Electrostatic patch” model for flocculation of negative particles by cationic polyelectrolytes (after Bolto and Gregory, (19))

For application in practice, the effectiveness of “electrostatic patch” mechanism probably depends on the ability of the polymer to form an uneven charge distribution on the surface of the particle. Ghosh (16) believed that for a given mass dosage of a polymer, the number of macromolecules adsorbed per colloid was lower for a high MW polymer than for a low MW polymer, therefore, the high MW polymer would form a more uneven charge distribution, encouraging better flocculation. Kozlova and Santore (53) using cationic polyDMAEMA of low MW (around 31,000), with silica particles, proved that only a few patches might be involved in the attachment of individual particles from adsorption experiments.

2.3.2.2 Polymer Bridging

“Polymer bridging” in flocculation by polyelectrolytes describes the destabilization mechanism by which the molecules of the added polymer attach onto two or more particles, causing aggregation. This concept was first proposed by Ruehrwein and Ward (54) from an experiment on the formation of clay aggregate. Graham (21) speculated the process of polymer bridging as follows: as a long-chain polymer comes into contact with a colloidal particle, some of its active groups adsorb onto the particle surface, while the rest of the segment of the

macromolecule stretches out from the surface into the solution phase as “loops” and “tails”. The widely accepted model of an adsorbed polymer chain is shown in Figure 2.5. If a second particle with vacant adsorption sites comes into contact with these extended segments a particle-polymer-particle arrangement may occur with the polymer acting as a bridge. In order for the bridging to work, the distance between the particles must be small enough for the loops and tails to connect two particles together (20).

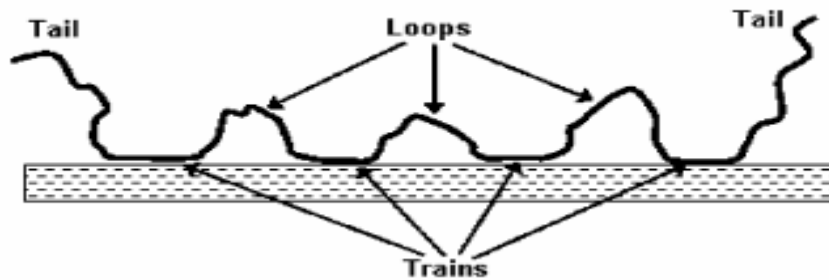


Figure 2.5 Model of an adsorbed polymer chain (after Bolto and Gregory (19))

It is generally found (55) that polymer bridging is favoured when linear chain polymers of high MW (up to several million), which do not have a high level of charge, are used in the flocculation process. Bolto and Gregory (19) reported that some degree of charge is beneficial since repulsion between charged segments gives expansion of the chain, thus enhancing the bridging effect. In contrast, the situation becomes more complex in the systems containing colloids and polyelectrolytes of highly opposite charge. In some studies (56), electron paramagnetic resonance has been applied to high cationic polymer-clay particle systems to determine the polyelectrolyte configuration on colloidal surfaces. It was found that segments of polymer adsorbed primarily in trains, rather than in the loop configuration. However, it is impossible for particle attachment to occur without a sufficient number of loops extending into the solution phase so that encounters with other particles can take place, based on polymer bridging. In this case, the positive polymer is assumed to be a flat configuration on the colloidal

surface, rather than a configuration with many segments extending into the solution. It can be well explained by the charge neutralization mechanism that when the polyelectrolyte has a high concentration of positive charge, it will adsorb onto the negatively charged particles in a rather flat configuration because of the strong ionic interaction, leading to high-intensity patches, then the direct electrostatic attraction between the particles results in agglomeration. The work of Yu *et al.* (57) appears to support this view by their study of the aggregation kinetics of kaolin particles using one high cationic polyDADMAC with low molecular weight, and one low cationic polyacrylamide with high molecular weight, although some of their assumptions are questionable. However, Ferretti *et al.* (58) noticed that the simple charge neutralization mechanism can not readily explain the following phenomena: (a) the breadth of flocculation zone with greater polymer molecular weight; (b) the higher flocculation rate than that with metal salts; (c) the zeta potential differing from zero at the optimal dosage; (d) the optimum dosage occurring at a lower concentration for larger polymers. The implication of these results is that charge neutralisation by cationic polymers may not be of great practical significance only. Gregory (51) studied the flocculation of latex particles by cationic polymers and recognized that both bridging and charge neutralization play important roles simultaneously for a high molecular weight polymer but a polymer of lower molecular weight appears effective entirely by virtue of its positive charge.

There are very few research publications concerned with the coagulation mechanisms of natural polymers. Some evidence has been found by Chen *et al.* (59) to support a bridging mechanism for coagulation of particles by chitosan. They observed an increasing removal of bentonite with increasing MW of chitosan. In contrast, Roussy *et al.* (60) have found that when a chitosan with MW exceeded $100,000 \text{ g mol}^{-1}$ was used as a primary coagulant for bentonite suspensions at pH5, the effective concentration of chitosan (0.17 meq l^{-1}) was much lower than that required for complete neutralization of the negative charge

on the bentonite particles ($1-2 \text{ meq l}^{-1}$), indicating that both charge neutralization and bridging mechanisms have been involved with the destabilization of bentonite.

For the case in which the amount of polymer and adsorption sites of the particle are in equilibrium, there should be an optimum dosage of the polymer for bridging flocculation, since bridging can no longer take place if the particle surface is highly covered by an overdosed polymer; so that there are insufficient adsorption sites available, and the suspension is re-stabilized by steric repulsion between adsorbed polymer chains. La Mer and Healy (61) found for bridging flocculation, the optimum dosage occurs at the “half surface coverage”. For practical design purposes, it is unfeasible to quantitatively define “surface coverage”. It is postulated by Bolto and Gregory (19) that the optimum dosage is directly proportional to the total particle surface area and hence to the particle concentration. However, Runkana *et al.* (62) found that theories of bridging flocculation assuming equilibrium conditions were of limited use in practice. Therefore, bridging interactions gave the possibility of non-equilibrium flocculation. Typical optimum results found by Bolto and Gregory (19) in practical systems, are of the order of $1 \text{ mg polymer g}^{-1}$ of suspended solids or less.

Generally, it is well known that high MW cationic polymers have diverse effects on the stability of a colloidal suspension. At certain concentrations, the adsorbed polymer reduces the inter-particle repulsion and provides attractive forces through bridging, “charge patch” or charge neutralization mechanisms. Although high molecular weight is often mentioned as a requirement for bridging flocculation, controversies still exist between the bridging and neutralization mechanisms, which concern their relative importance in the systems containing colloids and polymers of opposite charge. Very little is currently known about the quantitative comparison of these effects in flocculation processes.

2.4 Flocculation Behaviour of Cationic Polymer

2.4.1 Polymer Selection

As so many different types of cationic polymers are now used for water treatment, it is indicated that, apart from charge density and molecular weight, the monomer type used and other aspects of polymer product should be taken into account for the flocculation performance. There is a complex interrelationship involving monomer type, polymer structure, functional group, CD, MW and dose of polymer, and the amount and type of impurity in water (52, 63). The varieties available offer great flexibility in solving specific coagulation problems, but make selecting the right polymer more complicated. It has been reviewed previously that the mechanisms of coagulation are strongly correlated with the CD and MW of polymers. Thus, the coagulation performance is undoubtedly influenced by these properties. It is well known that when a charge neutralisation mechanism is dominant, the optimum dose of a polyelectrolyte depends on the CD. The study by Graham (64), who investigated the orthokinetic flocculation rates for amorphous silica microspheres with cationic polyelectrolytes, found that the rate of polymer flocculation and the optimal dosage depend on the polymer charge density and molecular weight. In general, 'screening' the optimal polymer type and determining the optimum dose of the polymer are commonly undertaken by jar tests, as is done for alum or ferric salts (15).

As discussed in section. 2.2.1.1, the chemical properties, e.g. the chemical structure of the polymer and the polymer chain, varies according to the polymer preparation. Basic acrylamide monomer yields varying polyacrylamides with different amines through co-polymerisation or Mannich reaction. For the polyacrylamides containing quaternary ammonium groups, the charge density is irrespective of pH, and hence more popularly used in water treatment, in comparison with the polyacrylamides with un-quaternary amine groups. Incidentally, linear polyamines or branched polyamines can be synthesized with

or without additives. It has been indicated previously that the polymer configuration is important in the flocculation process, particularly for cationic polymers. Ideally, this information should be supplied by the polymer manufacturer. Considering the complexity of natural polymers, the identification of these unknown polymers is necessary. A broad scheme for the examination of polymers involves qualitative and possibly quantitative elemental analysis and functional group analysis. Very useful information is often provided by running an infra-red or NMR spectrum on the sample and comparing the output with outputs obtained from a library of standard polymers under the same or similar experimental conditions. Other polymer physical properties and polymer microstructure can be an additional means of identifying the polymer (65).

2.4.2 Coagulation Performance

One of the present studies of particle aggregation in the flocculation process is based on the flocculation rate. Fler (66) has used a stopped-flow technique to measure the flocculation rate of a silver iodide sol by a polyvinyl alcohol with MW of 15,000, and found that the flocculation rate of the polymer appeared to be about twice that with a metal salt. However, Gregory (51) reported that in practice the method of mixing and the influence of different metal ions on the flocculation rate made the interpretation of this view difficult. At the moment of addition of the polymer into a suspension of particles, several rate processes are initiated: (a) mixing of polymer molecules among the particles; (b) attachment of polymer chains to particles (adsorption); (c) rearrangement of adsorbed chain to give an equilibrium configuration; (d) collisions between coated particles to flocculation (19). Rapid mixing is an important process in which the polymer becomes evenly distributed throughout the suspension, and hence giving uniform adsorption. Gregory (67) observed that the polymer adsorption rate under certain conditions can be considerably slower than the particle collision rate in this process. In the process of adsorption, according to Smoluchowski kinetics (68),

Gregory (69) found that the adsorption rate of polymer chains attaching to particles depended on their concentrations. An increasing particle concentration, generally corresponding with a higher optimum polymer dosage, would increase the adsorption rate remarkably due to a second-order adsorption rate process. Bolto and Gregory (19) have suggested that with a low particle concentration, as in low turbidity water, the time required for adsorption of polymer may be of the order of minutes, whereas for a high solid concentration the adsorption time can be less than a second. Although the time required for rearrangement (or reformation) of adsorbed chains is not well understood, Pelssers *et al.* (70) have studied the degree of flocculation in polystyrene dispersions by high molecular weight polyethylene oxide (PEO) and reported that for these high MW polymers, several seconds may be needed. When the adsorbed polymer is in an equilibrium conformation, collision step (d) results in the formation of aggregates, either by bridging or for electrostatic reasons. The flocculation is thought of as a second order rate process, so that the rate depends on the square of the particle concentration (19). At high solid concentrations, flocculation rates become very high. Schwoyer (12) suggested that the greater the particle concentration, the shorter the inter-particle distance, which leads to increased collision frequency. Although there is very little information available about the influence of pH values on suspension flocculation by cationic polyelectrolytes of high MW, Gill and Herrington (71) concluded that the effect of pH on the chain length of cationic polyacrylamides correlated with the largest flocs occurring at pH 5 to 9, since the configuration of the polymer molecule may depend on pH, and the viscosity data in their study showed polyacrylamides were in the most uncoiled state between pH 5-7.

Apart from the particle concentration and pH, the kinetic aspects of polymer adsorption and flocculation are considered partly in the optimal design of the mixing processes. The type and intensity of agitation are very important parameters for collision efficiency. In practice, turbulent mixing, characterized by

high velocity gradients (G), is desirable in order to provide sufficient energy for inter-particle collisions. It is well established that when a cationic polyelectrolyte is used as a primary coagulant, a G -value range of 300 s^{-1} - 700 s^{-1} is more appropriate. Nevertheless, Graham (21) indicated that the conventional rapid mix design parameters, $G=300 \text{ s}^{-1}$, $T=10$ to 30 s , may not complete particle destabilisation. Morrow and Rausch (72) have suggested that satisfactory performances of polymers as primary coagulants were obtained using velocity gradients in excess of 400 s^{-1} . By increasing the mean velocity gradient, they observed that the polymer dose and time of agitation could be decreased. However, there is an upper limit for the mixing intensity because high shear conditions can break up microflocs and delay or prevent visible floc formation. They concluded that rapid mixing must be completed within 2 min at $G = 400 \text{ s}^{-1}$ to prevent aggregate shearing.

It is evident from many studies that with polyelectrolytes, larger flocs often grow to full size significantly more rapidly and are less fragile than flocs of inorganic coagulants. However, at the end of its growth phase, flocs do not continue growing and reach a uniform size for a given shear condition. A comparative investigation has been undertaken by Li *et al.* (73), of the size, strength and structure of flocs formed by alum and cationic polyacrylamide with kaolin suspension using light scattering. They found that the floc strength varied with coagulation mechanisms and followed the hierarchy: bridging particle flocs > charge neutralized particle flocs > complexation flocs (charge sweep). Therefore, aggregates formed by polymer flocculants appeared to be significantly more resistant to breakage (74). Theoretically, floc strength is dependent on the inter-particle bonds between the components of the aggregate. An individual floc will break if the stress applied at its surface is larger than the bonding strength within the floc (75). Parker *et al.* (76) treated the rate of aggregation as a balance between floc formation and floc breakage. Based on the relationship between the velocity gradient in the flocculating vessel and aggregates size, they suggested an

empirical expression (2.1) for the stable floc size as:

$$d = CG^{-\gamma} \quad \text{----- (2.1)}$$

Where d is the floc diameter, C is the floc strength coefficient that strongly depends on the method used for particle size measurement; G is the average velocity gradient and γ is the stable floc size exponent. Furthermore, the correlation between floc size with the average velocity gradient, in log-log form, is given as:

$$\log d = \log C - \gamma \log G \quad \text{----- (2.2)}$$

Therefore, from equation 2.2, the steeper the slope, γ , the greater the reduction in the floc size with increasing G .

There are no straightforward techniques to experimentally characterize floc strength without destroying the flocs. However, a very important consequence of the nature of aggregates is that their density increases appreciably as the size decreases. Gregory (77) stated that a greater floc compaction by a higher velocity gradient, G , may increase the number of bonds holding the aggregate together, thus, leading to greater floc strength. According to equation 2.2, a decreased floc size is associated with the increasing average velocity gradient G . In this case, flocs at higher G value were smaller but with higher strength (78). As can be seen, in order to compare different flocs, the floc strength may be observed by following changes in floc size over a range of shear rates.

In comparison to the small number of studies of the coagulation mechanism by chitosan, relatively comprehensive investigations of the coagulation performance of chitosan have been carried out in suspension waters. It is well known that the characteristics of chitosan are dependent on the preparative conditions such as concentrations of acetic acid and hydrochloric acid and the degree of alkali treatment. Therefore, Huang (28) evaluated the coagulation efficiency of modified chitosan prepared under different conditions, and recommended that the optimal pre-treatment condition is deacetylation by

45% alkali for 60min and dissolution by 0.1% hydrochloric acid. Chitosan that was initially dissolved in acid media can precipitate when diluted into alkaline solutions. Guibal and Roussy (29) found for a given initial pH value the optimum dosage of chitosan correlated well with the initial concentration of colloidal particles. Decreasing in initial pH values resulted in a decrease of the dosage required for efficient coagulation. It has been stated (60) that the molecular weight of chitosan presented an important effect on its coagulation performance. Ten chitosan preparations with different MW have been tested for the coagulation of bentonite suspensions at pH5 and pH7 in the study by Roussy *et al.* (60), and the results showed that the removal of turbidity was best for the highest MW chitosans at both pH values. Pan *et al.* (79) have demonstrated how the mixing speed can affect the coagulation performance of bentonite, kaolinite and clay by chitosan in the settling rate, floc diameter and residual turbidity. He concluded that the increased speed during rapid mixing can reduce the amount of optimum dosage.

In summary, both experimental and theoretical analysis show that the flocculation rate and the size and strength of flocs are dependent on the molecular weight and charge density of polyelectrolytes, particle concentrations, pH and mixing conditions (velocity gradient). There is much opportunity for improved polymer flocculation performances by selecting the right polymer and optimizing the design of the mixing process.

2.4.3 Interaction with Dissolved Organic Matter

All of the above reviews involving coagulation mechanism and performance of the polyelectrolytes are in terms of particle removal processes. Actually, in water treatment, coagulation with cationic polymers is also important in removing natural organic matter (NOM).

In natural water, humic substances are by far the largest constituent of natural organic matter, which can cause odour, taste, colour, and bacterial re-growth problems, and furthermore, lead to the formation of disinfection by-products (DBPs) as well as increasing the chlorine demand in the disinfection process. Thurman and Morgan (80) have reported that dissolved humic substances generally comprise of approximately 30-50% of the dissolved organic carbon (DOC) in surface water. Studies to provide comprehensive insights into humic substance characterisation have been carried out by some researchers. Newcombe (81) has defined humic substances (humic and fulvic acid) as organic molecules with an approximate size of 500-250,000 Daltons, with heterogeneous structures composed of aromatic and aliphatic units and various functional groups. It is commonly recognized that humic substances are anionic in character at natural water pH values, which is partly responsible for their solubility in water. Thus, humic substances can be precipitated from water, if the charge is reduced by lowering the pH value (82).

The removal of NOM from drinking water is necessary to meet the quality regulations of drinking water. When using cationic polyelectrolytes as coagulants in water treatment, charge neutralisation of aquatic humic substances is thought to be the predominant mechanism of coagulation (83). These conclusions have been confirmed by Kvinnesland and Odegaard (30), who used different cationic polymers, including polyDADMAC, polyacrylamide and polyamine as coagulants to remove humic matter. In this case they found that the optimum dose corresponded closely with charge neutralisation and there was a clear stoichiometry between anionic charge of the humic substances and cationic charge carried by the added polyelectrolytes. Their recommendation is in agreement with the results from Bolto *et al* (63). In Bolto and co-worker's study, they compared the efficiencies of cationic polyacrylamide copolymer (CPAAM), polyDADMAC, polyethyleneimine (PEI) and chitosan in experiments on reconstituted humic water at pH6, and found that the effectiveness of

polyelectrolytes as coagulants for NOM increased with increasing charge densities. Incidentally, the coagulation behaviour using the natural polymer, chitosan, to treat natural organic materials seemed to be consistent with a charge neutralization mechanism, since a stoichiometry was observed between the concentration of humic materials and the required dose of chitosan (84).

Unless the raw water has a low total organic carbon (TOC) concentration, the coagulant dosages of polymers are determined by the content of NOM in raw water rather than by turbidity (85). Generally, the NOM removal performance by polymers was less pH dependent and there was a lower level of dissolved ions in the product water, in comparison to metal coagulants (86). The effect of polymer molecular weight on the removal of humic substances by cationic polyelectrolytes has also been investigated by Kam and Gregory (18), who compared a range of cationic polyacrylamide copolymers with MW from 0.05 to 15 million, and found that MW had no effect on coagulation kinetics or colour removal, indicating that 'polymer bridging' was not a pronounced mechanism. However, observations by Bolto *et al.* (63) recently concluded that higher MW polymers were more effective for NOM removing from water, and the effect of increasing MW was more important for colour removal than increasing charge density.

2.4.4 Monitoring System

There are a number of different methods to determine the optimum dosage and flocculation performance of polyelectrolytes. The most familiar and widely used coagulation test employed by those acquainted with water and wastewater treatment is the 'jar test'. Essentially, a jar test is a series of equal volume, identical samples that are exposed to a controlled variety of treatment conditions. Observation of the degree of clarification can be obtained by a complete laboratory analysis of resulting sample quality. The protocol of jar tests

has been commonly accepted to confirm the optimum type and dose of inorganic coagulants such as alum or iron salts (87). Recently, Bolto *et al.* (6) found a good result from jar test in NOM removal using comparative primary coagulants of synthetic cationic polyelectrolytes and alum. In bench-scale tests, the jar test was also employed to evaluate the effectiveness of natural chitosan as a coagulant by Kawamura (3). Although jar tests are particularly useful and remain popular for controlling coagulation-sedimentation and precipitation-sedimentation processes, these methods are limited in terms of their sensitivity and practical convenience since they are less suited to the control of direct filtration or in-line coagulation processes. Yeh (88) has demonstrated that alum and polymer doses required for direct filtration were lower than found from jar test results.

Zeta potential (ZP) is a measure of the electrostatic charge on the surface of particles suspended in water and is commonly related to the stability of the colloidal materials under any given set of water characteristics. The technique of measuring zeta potential has been successfully used to optimize the coagulant dose for metal salts (89). In natural water, colloidal suspensions are commonly found to possess ZPs of 20-30mV and are negatively charged (12). In order to achieve coagulation in suspension systems, the ZP must be reduced in value to less than 10mV (preferably to less than 5mV) (90). It has been reported that in a bentonite particle system, the optimum doses of natural chitosan resulted in a very negative zeta potential (~-15mV) (28). Previous attempts (91) to link the coagulation of NOM to ZP have found that optimum doses of alum occurred at a range of zeta potentials between -8 and +8 mV depending on the water source and pH values of coagulation. Theoretically, an optimum dose of the polyelectrolyte can be found to occur at or near the point of zero ZP. Graham (21) observed that the applicability of ZP measurement was largely dependent on whether the coagulation and flocculation mechanisms are predominantly due to Coulombic interactions. Therefore ZP dose not necessarily provide a proportional indication of the amount of coagulants required for destabilization. Many

researchers (92, 47) have used ZP measurement technique to evaluate the coagulation mechanism and flocculation rate of high MW cationic polyelectrolytes. However, the results from these studies cannot provide data for estimating the optimal dose in the flocculation process due to a complexity of interaction mechanisms of polymers. Although this method has several advantages such as its speed, relative ease of operation and on-line control, there is still a concern that in practice, the measurement of ZP is normally based on a small number of particles, and may not always be representative of the suspension at actual conditions (93).

The streaming current measurement has been recognized as an on-line, reliable way to monitor the coagulation state by charge neutralization. The streaming current is caused by the movement of counter ions beyond the shear plane of surfaces within a detector (94). Unlike the zeta potential measurement, this method does not directly measure the surface potential on individual particles. Rather, it measures a flow of electrical current that is statistically proportional to the average surface charge on the particles. Hence, it is possible to select the optimum dose of a coagulant, according to the reduction of the negative surface charge on the particles in the water. The mechanism of charge neutralization of clay particles has been examined by Barron *et al.* (95), who used a streaming current director to automatically control the coagulation performance of electrolytes for a drinking water product. Furthermore, Kam and Gregory (18) compared the streaming current detection with other monitoring methods in the interaction of humic substances with cationic polyelectrolytes (over a range from 0.05 to 15 million), and found that the non-stoichiometric interaction between the anionic sites of humic substances and the cationic charge of polyelectrolytes was indicated by the streaming current technique. In general, the literature suggests that most of the investigations related to the use of these methods are carried out to study the electrokinetic properties of polymers using model water (49). Very little attention has been given to both zeta potential and streaming current

techniques in selecting a particular polymer type or determining the polymer dose in practical water treatment. Of particular concern for streaming current detection is either sample pre-treatment such as large dilution of the sample in order to avoid coincidence effects of particles, or metal ions in water such as calcium ions, which affect the current and the coagulation process (96).

The laser light diffraction method has been advocated to measure the floc size distribution, thus optimising flocculation (97). However, Gregory and Nelson (50) found that light scattering is difficult to interpret unambiguously in terms of the aggregate size distribution, except under special conditions. In addition, detailed particle size distributions are not really necessary for monitoring of industrial suspensions and the control of process conditions.

The photometric dispersion analysis (PDA) instrument provides a valuable and convenient technique of assessing coagulation by means of a sensitive and rapid response to fluctuations in the intensity of light transmitted through a flowing suspension. Gregory and Nelson (50) proposed that a simple index by this technique, which is in correspondence with the state of aggregation of the particles, would be sufficient to give an insight to fit many experimental and industrial observations, since this could be conveniently derived from on-line measurements. By a photometric dispersion analysis monitor, the aggregation or disaggregation in the suspension can be quantified with respect to the ratio of V_{rms} to d_c by measuring the root mean square (rms) values of the fluctuation signal (V_{rms}) and the average transmitted light intensity (d_c). In this case, the ratio of V_{rms} to d_c is called the Flocculation Index (FI). This ratio can give immediate information on the state of aggregation of particle suspension over the entire period of coagulation. Huang and Liu (98) demonstrated that the PDA monitor with a designed control system could be successfully applied to the on-line control of coagulation dosing, by studying the coagulation of bentonite powder with alum. More definitely, Kam and Gregory (18) have shown that the optimum

dose for humic substance removal was easily achievable by the observation of the Flocculation Index when polymers are used as primary coagulants. In the flocculation process, FI is regarded as a representation of floc size, which is closely associated with floc strength, the other important parameter of the flocculation performance. Some researchers (99, 100) proposed that the FI values might be considered as a way of quantifying floc strength by changing the velocity gradient after the floc has formed. The effect of shear on the formation and break-up of flocs generated using alum and two cationic polyelectrolytes has been thoroughly investigated using a PDA by Yukselen and Gregory (101).

In summary, the ideal monitoring technique should be suited to on-line application and require no sample pre-treatment (such as dilution). Few available techniques satisfy these requirements in specific applications. The difficulties encountered in using either visual (semi-quantitative) or electrical technologies in practice to predict coagulant dose are that the actual treatment situation can vary outside the set of parameters for which dose relationships were established in routine experimentation. Thus, the use of the photometric dispersion analysis method in monitoring polymer feed during operation of a water treatment process has been found in many respects to be advantageous. This novel method has been successfully applied to study the dynamics and mechanisms of coagulation in dilute and concentrated suspensions with polymeric coagulants.

2.5 Application of Cationic Polymer in Water Treatment

All of the above discussions about the mechanisms and action of polymeric coagulants have been in terms of model water processes, involving either particles or dissolved organic matter. Actually, cationic polyelectrolytes have been widely used as the sole primary coagulants instead of conventional inorganic salts (alum, iron salts or lime), or flocculation aids in the drinking water industry.

2.5.1 Primary Coagulant Used in Drinking Water Treatment

In surface water, the principal contaminants include particulate matter, color, hardness, toxic organic, metal element (iron and manganese) and water borne pathogens. The typical purifying process consisting of coagulation/flocculation followed by settling or flotation, filtration and disinfection is used to produce water that is biologically and chemically safe for human consumption and also aesthetically pleasing in terms of odour, appearance and taste. Recently, increasing attention has been paid by the water industry to removal of natural organic matter in light of the potential for carcinogenic disinfection-by-product (DBP) to form during the disinfection process if organic carbon is insufficiently removed in the coagulation process.

Aluminium and iron salts are the most frequently used coagulants in drinking water treatment and their proven efficacy in the removal of turbidity, color, NOM and algae is achieved through their pH-dependent mechanisms, which are either the adsorption of soluble hydrolysis products or/and the reduction in particle charge. Under certain conditions, the hydroxide precipitate is formed and hence “sweep coagulation” could be regarded as “bridging” and enmeshing particles together. Amirtharajah (2) stated that the coagulation performance of humic substances, which are correlated to NOM and color, was best at pH values of about 5 to 6 with alum, and at pH values of 4.5 to 5.5 with iron. Previous studies have pointed out several serious drawbacks of using metal salts, for example, the coagulation performance is pH dependent; a higher dose of coagulant is applied, in proportion to the turbidity; and extra solids in the form of metal hydroxide arise adding to the burden of the separation process.

In the production of drinking water, cationic polyelectrolytes with high MW can be added as either primary coagulants or coagulant aids to partially replace inorganic coagulants (e.g., alum). In the last twenty years a world-wide major emphasis has been given to enhance the coagulation technique by

polyelectrolytes in removing turbidity and organic matter from surface water. A low dosage requirement of polyelectrolytes used as primary coagulants for raw water from river “Ganga”, India, has been proved in the study of Rout *et al* (102). In their study, with the maximum turbidity level of 1200NTU, the alum dose requirement was 75 mg l⁻¹ against the polyDADMAC dose of 1.5 mg l⁻¹. As compared to alum, the sludge generated during the polyelectrolyte treatment was 40-60% less in volume than that formed by alum. The coagulation properties of different synthetic polyelectrolytes combined with metal salts or polyelectrolytes alone used in surface water treatment to remove DOC have been investigated by Lindqvist (103). For comparison, cationic polyDADMAC, aluminium and ferric salts were included as coagulants in his study. Lindqvist observed from laboratory scale jar tests that as a primary coagulant, polyDADMAC achieved an inferior DOM removal (33%) from Lake Roine, Finland, in comparison to that of aluminium salt (55%) and ferric salt (65%). Moreover, when polyDADMAC was applied as a coagulant aid, which is added to raw water with a metal coagulant simultaneously, an increasing removal of DOC was found of about 70%, indicating cationic polyelectrolytes with high CD may be used to reduce the amount of metal salts in the coagulation process. In contrast, Bolto and co-workers (6) studied the removal of NOM with cationic polyDADMAC and polyacrylamide, by means of jar tests on reconstituted waters containing aquatic NOM obtained by reverse osmosis treatment of water from Moorabool River, Australia. It was found that organic polymers were as effective as alum for colour removal, and took out up to 85% of the UV absorbance removed by alum. However, an alum/polymer combination was the most attractive treatment option for natural organic matter. When they used a series of polyDADMAC polymers with different molecular weight and charge density as coagulants in jar tests, Bolto and co-workers observed that the performance of cationic polymers used as sole coagulants improved significantly with increasing charge density and molecular weight. Their results were confirmed by other studies. Chang *et al.* (104) found an effective removal of UV absorbance when they used

polyDADMAC as a coagulant for drinking water treatment. They also observed that a polymer with higher CD was more effective in reducing UV absorbance than that with low CD.

It is evident that the application of a polymer in conjunction with a metal salt as a primary coagulant has become increasingly of interest for the treatment of natural organic matter in surface water. Apart from the evidence from Lindqvist (103) and Bolto (6), experimental results obtained from bench-scale, pilot-scale and real scale tests by Filho *et al.* (105) have also shown that algae removal and turbidity removal were much better when a cationic polymer was added with ferric sulphate (compared to ferric sulphate alone) to treat raw water from Guarapiranga Reservoir, Brazil. Lee *et al.* (106) has also demonstrated that both cationic polyamine and polyDADMAC combined with metal salts were effective as coagulants to treat Nak-dong river water, Korea, and the addition of 1 mg l⁻¹ of organic polymers enabled a reduction of 50% of the consumption of inorganic coagulants.

As a natural polymer, chitosan has been applied as a primary coagulant to replace or partially replace alum in water treatment. In 1981, the United States Environmental Protection Agency (USEPA) approved chitosan's use in a drinking water treatment application up to a 10mg l⁻¹ dose. The effectiveness of turbidity removal by chitosan appeared to involve the alkalinity of different surface waters in Kawamura's study (3). When chitosan was used as filtration aid in the direct filtration process at pH 8.4 and temperature 14 °C, for raw waters with high alkalinity (200 mg l⁻¹ as CaCO₃), it was demonstrated that about 0.2 mg l⁻¹ chitosan improved the flocculation and sedimentation performance. In contrast, as sole coagulants, for low alkalinity water (~30-40 mg l⁻¹ as CaCO₃), chitosan presented a greater effectiveness in producing a settled-water turbidity of about 1 NTU with approximately 5 mg l⁻¹ of dosage compared to approximately 30 mg l⁻¹ of alum at pH 7.1 and temperature 10 °C. Even though the coagulation

mechanism of chitosan is still not fully understood, Kawamura indicated that the effectiveness of chitosan was especially significant for the high-turbidity water. This observation has also been shown in another study (107). Divakaran and Sivasankara (108) reported that chitosan as a primary coagulant at a dosage of 0.5 mg l⁻¹ achieved over 80% turbidity removal from an initial raw water of 10NTU. The combination of chitosan and alum as a primary coagulant has been considered for water treatment. A pilot filter investigation by Kawamura (3) has shown that the combination of chitosan and alum is more effective than the synthetic polymer-alum combination tested for turbidity removal from Colorado water, USA. The effectiveness of chitosan as a primary coagulant and a coagulant aid for different turbidity raw waters has been summarised in Table 2.4. However, the typical formula of alum in this study was not mentioned.

TABLE 2.4 Coagulation performance using chitosan and alum (after Kawamura (3))

Raw Water Turbidity (NTU)	Alum (mg l ⁻¹)	Residual Turbidity (NTU)	Chitosan as Primary Coagulant (mg l ⁻¹)	Residual Turbidity (NTU)	Chitosan as Coagulant Aid (mg l ⁻¹)	Residual Turbidity (NTU)
3200	300	90	1.00	10	0.15 + 20 mg l ⁻¹ alum	4
1400	100	10	1.00	10	0.1 + 20 mg l ⁻¹ alum	3
500	30	5	0.25	25	0.1 + 5 mg l ⁻¹ alum	5
70	10	14	0.25	18	0.05 + 8 mg l ⁻¹ alum	10

Moreover, chitosan has been shown to be an effective coagulant for the removal of humic substances from drinking water. From comparative

experiments using chitosan as a sole coagulant or combined with ferric salts to treat the river water from Glomma, Norway, Vogelsang *et al.* (109) found that 2 mg l⁻¹ chitosan and 2 mg l⁻¹ as Fe³⁺ at pH 5 led to 96% colour removal and 60% TOC removal, with an improvement from respectively 93% and 47% for chitosan alone. In contrast, iron salt used as a primary coagulant alone gave no significant removal of organic matter. A fractionation based on the molecular size of humic substances was measured by high-performance size exclusion chromatography (HPSEC) in this study, and the results indicated that by adding small amounts of iron salt together with chitosan, a substantially improved removal of the medium molecular weight fraction of the humic substances was obtained with a significantly reduced addition of chitosan.

Cationic polyelectrolytes have a distinct advantage over metal salts used in the direct filtration process due to an absence of the formation of additional solids in the form of a metal hydroxide precipitate. The uses of direct filtration preceded by polymeric coagulants to remove humic substances have been investigated by some researchers. An effective performance of colour removal from synthetic (humic acid solution) and natural colored waters using a bench-scale pilot filter with a 14-cm filter bed has been reported by Scheuch and Edzwald, (110) who used a chlorine-resistant cationic polymer (polyquaternary amine) with molecular weight about 50,000 as a coagulant. Furthermore, Edzwald *et al.* (111) employed a large-scale pilot dual-media filter and two natural colored waters to study the coagulation performance of three cationic polyelectrolytes (polyquaternary amine), and found an effective improvement in treatment and water quality were obtained in all cases. To minimize some of the drawbacks arising from the accumulation of polymers in the equipment of filtration and limited permissible-dosage range, Graham (112) used a low-to-moderate MW polymer based on polyamine to investigate the possibility of improved treatment by partially replacing alum with the polymer and noticed that there was less color removal using the combination of a polymer with alum

than alum alone by direct filtration; this study employed a pilot filter with 50-cm filter bed and humic extract from colored, upland water in the United Kingdom.

2.5.2 Polymer Toxicity and Residual Polymer

Although any relationship between aluminum and Alzheimer's disease is too tentative to justify changes in the use of aluminum compounds in water treatment, there is still a strict regulatory limit on the residual aluminum concentration of 0.2 mg l^{-1} in drinking water in the UK (113). The application of synthetic organic polymeric coagulants such as polyacrylamide or polyamine is also potentially problematic since there may be toxicity concerns under certain circumstances. These concerns have led to a ban on the use of polyelectrolytes in drinking water treatment in Switzerland and Japan (114), while other countries such as the United Kingdom, Germany and France have established stringent limits on the doses of polymeric coagulants.

For drinking water production, the maximum allowable dosage of commercial polymers in the source water at the treatment plant is recommended in the USA by the National Sanitation Foundation (115), the limits are generally $<50 \text{ mg l}^{-1}$ for polyDADMAC, $<20 \text{ mg l}^{-1}$ for ECH/DMA polymers and $<1 \text{ mg l}^{-1}$ for PAAs. The maximum authorised dose of polyacrylamide used as the coagulant in drinking water treatment is 1 mg l^{-1} . National Sanitation Foundation further restricts the application of polyDADMAC to not exceed 25 mg l^{-1} , which is based on a maximum carryover of the polymer into the product water of 50 ug l^{-1} (116).

In fact, even though cationic polymers are of high toxicity generally, it is well known that a monomer is likely to be more toxic than a polymer in drinking water (117). Some frequently used polymer coagulants such as polyDADMAC, polyacrylamide and epichlorohydrin-based polymers may release the unreacted

monomers acrylamide and epichlorohydrin in drinking water. Accordingly, limits on the level of monomer are strictly controlled. Especially, in the UK, for polyDADMAC the maximum allowed monomer content is 0.5% , and maximum residue in reservoirs is $500 \mu\text{g l}^{-1}$ (118); for polyacrylamide, as a general rule, the monomer content limit of free acrylamide is 0.025%, and the residual in drinking water is $0.1 \mu\text{g l}^{-1}$ (113); polyethyleneimines are generally not used in potable water treatment (119).

It is essential to determine the ultimate fate of polymers used in the coagulation process to see what quantities are present in the final water. A number of promising approaches have been explored for measuring polymer residuals in the last thirty years. Parazak *et al.* (120) were able to analyse residual polymers by colloid titration against a polyelectrolyte of opposite charge, using dyes as indicators. The method is not especially sensitive since the results ($0.5 - 1 \text{ mg l}^{-1}$) were found to be near the limits of detection. Other researchers have used fluorescence spectroscopy (121), size exclusion chromatography (122), ^{14}C -mark polymer (123), NMR spectroscopy (124) and fluorescent tagged polymer (125). Detection limits below 1 mg l^{-1} have been claimed for methods based on colloid titration ($500-1000 \mu\text{g l}^{-1}$); fluorescence spectroscopy ($<50 \mu\text{g l}^{-1}$); size exclusion chromatography ($10-20 \mu\text{g l}^{-1}$); fluorescent tagged polymer ($10-40 \mu\text{g l}^{-1}$) and NMR spectroscopy ($<500 \mu\text{g l}^{-1}$). However, the more extreme of these claims has been disputed or simply not reproduced by other researchers (126).

In summary, published methods for determining residual polymers generally have low sensitivities and may require a pre-concentration process. To date, there is still no accepted method to effectively measure the accurate amount of residual polymers in treated water. Consequently, the regulation of these published methods is arbitrary and inconsistent. It is felt that there should be more effort by polymer manufacturers to develop suitable methods.

2.5.3 Costs

Apart from the significant treatment effectiveness, economics should be considered as another merit of the complete or partial replacement of metal salts by polyelectrolytes as primary coagulants. The estimated costs of \$2-4 per kg (£1-2 per kg) for the polymer is consistent with the current market value in USA for organic flocculants in water treatment of approximately \$130 million per year (124). The market price of aluminium coagulant (8% w/w Al_2O_3) is approximately £80 per tonne, which is equal to £ 1.89 per kg Al. Accordingly, an approximate alum (9.1% w/w) cost can be estimated as £171 per tonne (£0.171 per kg). Mangravite (25) has found that the typical dose of primary coagulants for most polymers is 0.5 to 10 mg l⁻¹. From the previous reviews, the dose of alum for the surface water treatment is in the range of 30 mg l⁻¹ to 75 mg l⁻¹. Therefore, the cost of polymers varied from £0.00075/m³ to £0.015/m³, and the cost of alum is speculated as £0.00513/m³ to £0.0128/m³. It was found that ferric chloride, ferric sulphate and aluminum sulphate are very similar in cost. In addition, there is a major upward pressure on metal coagulant prices due to heavy usage of phosphate. Considering the reduced filter loading and volume of backwash water, and further convenient sludge deposit due to a lower amount of solids production, organic polymers give a greater cost benefit than inorganic coagulants. One experience from a water plant in South Africa on changing the coagulant from alum to a polymer demonstrated a 30% decrease in the cost over a three-year period (127).

Chitosan works well over a large pH and dosage range. However, a major drawback is its price, which is about \$18-20 per kg (£9-10 per kg) dry weight (109). Hence, dosage optimisation is of high priority. In Kawamura's study of different surface waters (3), the optimum dose of chitosan varied from 0.2 mg l⁻¹ to 5 mg l⁻¹, therefore, the cost of chitosan in water treatment was estimated from £0.002/m³ to £ 0.05/m³. This unrealistically high cost of chitosan

presents an opportunity to find cheaper natural polyelectrolytes to produce cleaner and safer water.

2.6 Modified Tannin-based Polymer (TBP) as Coagulant

One of the modified natural products, the tannin-base polymer (TBP), has been proposed as a flocculant for use in wastewater treatment in certain parts of the world due to its reasonable cost and biodegradability. In the USA, the National Sanitation Foundation (116) has restricted the maximum dose of tannin-based products as 3 mg l^{-1} in raw water.

Tannin is a plant extract mainly from bark and wood which can be subdivided into two groups, hydrolysable and condensed, based on their structures (128). In this study, the natural tannin extract is obtained from a tree called Black Wattle, which grows in Brazil. The type of tannin present in wattle extract is condensed tannin which consists of a molecular gradation of poly-flavinoids. Before the application of a Mannich type reaction and polymerisation, the original aqueous extract is composed of approximately 67-77% polyphenolic tannins and 25% non-tannins, which are mostly simple sugars and polymeric carbohydrates (hydrocolloid gums); the latter constitute 2% of the extract and heavily contribute to the extract viscosity (information from the supplier). The average molecular weight of tannin can range typically from about 300 to about 3000, dependent on the number of flavinoids (129). The structure of the main flavinoid unit present in condensed tannin has been published by Hemingway (130) (see Figure 2.6).

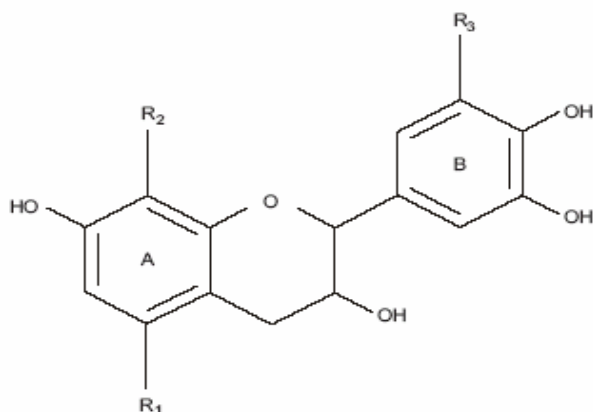


Figure 2.6 Chemical structure of condensed-tannin: flavan-3-ol unit of condensed-tannins (to A-ring: $R_1=OH$, $R_2=H$, phloroglucinolic; $R_1=R_2=H$, resorcinolic; $R_1=H$, $R_2=OH$, pyrogallolic; to B-ring: $R_3=H$, catecholic; $R_3=OH$, pyrogallolic) (after Hemingway (130))

The preparation process of the modified tannin-based polymer (TBP) is proprietary information, but is believed to involve two chemical steps: Mannich reaction and polymerization. In the Mannich reaction an aldehyde is condensed with an amino compound and an active hydrogen is supplied by the polyphenolic tannin. The common reaction procedure is: Aqueous formaldehyde and ammonium chloride solid are mixed and heated to give a mixture of (mainly) primary and secondary amines. Then the amine mixture reacts with the aromatic tannin chains (also under acid catalysis). The nitrogen in the resultant non-polymerized product protonates under acidic pH conditions to give an “ammonium tannate monomer” with positive charge. Consequently, the monomer polymerizes while the viscosity of the reacting mixture is monitored at low pH.

Some investigations related to the use of natural condensed anionic tannin as a coagulant aid for particle removal have been carried out by Özacar and co-workers (131). In their studies, jar tests were performed at pH 6 to 11, using kaolin clay to adjust the turbidity of the synthetic water. When tannin was used as a flocculant aid combined with alum, a very low tannin concentration of 1

mg l⁻¹ was found to effectively reduce the residual turbidity and the amount of required alum. However, the literature suggests that more attention has been given to the use of the modified cationic tannin polyelectrolyte instead of anionic natural tannin as a coagulant or flocculant aid in the waste water treatment field and its preparation method has been explored. In 1962, Fife (132) first disclosed the new application of the reaction product between tannin, formaldehyde and an amino compound for the flocculation of suspensions such as sewage and industrial waste. He found that clear supernatant water was obtained using 12 mg l⁻¹ Mannich reaction product as a coagulant, for an artificially turbid water of 100 mg l⁻¹ solid. The disclosed advantage of using this flocculant is believed that it does not affect the pH of the suspension solution and also the flocculant does not affect the dissolved inorganic contents of the final water. On the basis of this previous invention, Reed *et al.* (8) synthesized an alkylated Mannich polymer, which is prepared from a condensed tannin, amine, and formaldehyde, with an alkylating agent within a wide range of pH between 5 and 14. This polymer was proved to effectively remove color from waste water effluent streams.

A comprehensive study of the application of TBP in drinking water treatment and the relative merits of partial or complete replacement of alum by TBP as a primary coagulant in water treatment has not been undertaken so far; previous work with TBP has been related to wastewater treatment. The early work has been done on the assumed chemical structure of condensed-tannin. To date, there is little information available of the structure or functional groups of TBP, or how these vary with the preparation conditions (pH, viscosity). Thus it is not possible to predict the chemical properties of the final TBP product, and in particular the nature of the “ammonium tannate monomer”. There is virtually no prior literature about the fundamental mechanisms of coagulation using TBP as a primary coagulant for aqueous suspensions or/and dissolved organic matter, and therefore no clear understanding of the interrelationship between polymer chemical structure, polymer molecular weight and charge density with the

coagulation mechanism of TBP. Some information is available concerning the various manufacturing methods and basic flocculation performance of the tannin-based polymer in wastewater treatment, from published patents (8,129). Knowledge of the polymer's characterisation would be a significant step towards understanding the mechanisms, and hence flocculation ability when using TBP as a coagulant.

Since adequate attention has not yet been given to the use of TBP as a primary coagulant in surface water treatment, there is much opportunity to validate the coagulation effectiveness of TBP in this field of application and investigate ways of improving its performance by optimizing the mixing process and selecting the right combination with metal salts or micro-sands to either reduce the dose of inorganic coagulants or lower the residual TBP in final water. In addition, this investigation presents a broad challenge on the optimal monitoring of coagulation process and the accurate measurement of residual tannin in treated water.

2.7 Summary

The application of synthetic or natural cationic polymers in the production of drinking water has been reviewed, with emphasis on the type and characterisation of polymers commonly available, dominant mechanisms of coagulation, the coagulation behaviour of model waters, and the application in practical treatment with particular attention of residual polymers, and polymer cost assessment. A preliminary introduction of a novel and potential modified natural coagulant--- tannin-based polymer (TBP) has been included here.

The main concepts detailed in this chapter of the thesis can be summarized as follows:

a) The role of polymeric coagulants in water treatment is well established, with examples of benefits in conventional sedimentation and filtration, or in direct filtration, mostly due to the low solid volume production, and in particular the low cost of using a natural polymer.

b). Polymer bridging and charge neutralization have been recognized as the two most important mechanisms of coagulation by polymers. Theoretically, high MW, linear polymers are more preferable in bridging flocculation. In contrast, polymers with high CD are more effective in charge neutralisation. In fact, it is a matter of controversy and speculation between these two mechanisms, concerning their relative importance, when cationic polymers with high MW are used as primary coagulants.

c) It is often assumed that the polymer's type, molecular weight and charge density are the crucial parameters governing the mechanism and performance of coagulation in terms of the removal of particles or dissolved organic matter. The coagulation behaviour of polymers also depends on the particle concentrations in solution, the pH, and the mixing conditions. In practice, the presence of residual polymers and monomers in the product water are of particular health and environmental concern in drinking water treatment. To date, there is not yet a sufficiently sensitive and practical analytical technique available to determine the residual polymer concentration in treated water.

d). In comparison to synthetic cationic polymers, the number of investigations concerned with natural cationic polymers for drinking water treatment are relatively small and most of them were of the use of chitosan in water and wastewater treatment. Very little is currently known of the fundamental coagulation behaviour by natural polymers, and in particular, of the importance of the nature of these polymers.

e). A modified tannin-based polymer (TBP) is proposed as an alternative to synthetic organic polymers because of its availability from a renewable source material, giving rise to environmental benefits and potential cost advantages. Given its preparation via the Mannich reaction and polymerization, it is believed that TBP is a high molecular weight polymer possessing positive charge. While there has been some use of TBP in wastewater treatment, very little attention has been given to characterizing its fundamental properties and investigating in detail the use of TBP as a primary coagulant in surface water treatment.

3. OBJECTIVES OF STUDY

From the previous discussion it is clear that the chemical structure of TBP and the interrelationship between the chemical properties of TBP and coagulation mechanisms have not yet been investigated. Furthermore, the understanding of the coagulation performance using TBP as a primary coagulant to partially or completely replace metal salts in water treatment is still very poorly developed. To illustrate the potential in this regard, this study of its significance set out to achieve three broad aims:

(1) to provide a description of the polymer structure and physical properties, by qualitative functional group analysis in conjunction with quantitative methods, thereby characterizing the tannin-based polymer (TBP).

(2) to qualitatively assess the existence, significance and relative appropriateness of two well established coagulation mechanisms using TBP as a primary coagulant alone.

(3) to evaluate the coagulation performance of TBP alone and TBP combined with metal salts, and microsand, in both model water and raw water systems, in comparison with the effectiveness of inorganic and synthetic organic coagulants.

Considering the possibility of differences in the coagulation action of TBP using model systems containing either particle suspensions or dissolved organic matter, both of the systems were included in this study. Furthermore, the performance of TBP with raw surface water samples is investigated. It is emphasized that the objectives of this research fall into particular sections of the thesis. In the following discussion, section 5 is relative to objective (1), section 6 to objective (2), part of section 6 and sections 7, 8 and 9 to objective (3). The structure of the thesis is as follows:

Section 4: describes all experimental materials and the analysis methods used throughout this research. Although the research purposes of Sections 6, 7, 8 and 9 are different, the coagulants and equipment used in these sections are mostly the same. By concentrating the materials and methods in one section simplifies the structure of this thesis.

Section 5: outlines the experimental characterisation of the TBP using different techniques. A variety of quantitative analysis methods, including charge density, molecular weight and elemental identification, were undertaken, in conjunction with a number of qualitative analysis methods on functional groups and chemical bonds.

Section 6: evaluates the fundamental coagulation mechanisms of TBP in particle suspension and dissolved organic matter systems through an on-line measurement of Flocculation Index. The variation of optimum dosage of TBP and final floc size and strength were studied as indicators to determine the preference between polymer bridging and charge neutralisation. The preliminary coagulation stoichiometry and the influences of coagulation conditions on coagulation performance of TBP were considered.

Section 7: describes an experimental investigation of the coagulation performance and mechanisms using alum and cationic TBP as combined primary coagulants (partial alum replacement). Under a given set of conditions, coagulation matrix tests were studied for a full range of alum-TBP combinations to determine whether or not there is a unique optimal dosage combination of alum and TBP.

Section 8: The tentative application of TBP bonded to microsand was investigated in order to reduce the residual tannin in final water. Preliminary adsorption tests were carried out to determine the ratio of surface attachment between TBP and sand.

Section 9: to confirm the coagulation behaviour of TBP observed in tests with model waters, raw water from an organic-rich river source located in the UK was tested using TBP alone and TBP-alum as primary coagulants. Subsequently, the coagulation efficiency was compared experimentally with other coagulants under equivalent operational conditions.

4. MATERIALS AND METHODS

4.1 Introduction

All the materials and methods of analysis described here were used in either the characterisation or coagulation experiments through the whole investigation. Consequently, all the details are described in this section only.

In order to evaluate and compare the coagulant behaviour, four different coagulant chemicals were employed in this study. These can be classified as: modified natural polymer -- TBP, synthetic organic polymer -- polyDADMAC, inorganic metal coagulant – alum, and commercial product – TSL. The adsorption of polyelectrolyte on solid/liquid interface (clays, oxides and silica) has been largely investigated because significant modifications of surface properties within the adsorbed layer were observed (133), however, it is believed that the coagulation action by polymer in the dissolved organic matter system may be relatively complex since hydrophobic and hydrophilic fractions of NOM play different roles, which affect the coagulation mechanism (63). Therefore, two kinds of model water including kaolin particles and humic substances, respectively, were applied in assessing the coagulation performance in this research.

The methods used for TBP in this research fall into two categories: characterization experiments and coagulation experiments. In the TBP characterization experiments, some standard methods, such as Argentometric titration for element determination, and a number of new or modified techniques, such as size exclusion chromatography for MW measurement, were used. Accordingly, the details of the methods and apparatus/equipments are included in this section. In the coagulation experiments, a specially built reactor to control the velocity gradient, G , and on-line monitoring system were employed. In order to determine the quality of final water, a variety of measurements in terms of TOC,

turbidity, colour, UV, floc strength, residual Al and residual tannin were undertaken.

4.2 Cogulants

4.2.1 Tannin-based Polymer

Tannin based polymer (TBP) in this study was obtained from TANAC Ltd, Brazil. The TBP was supplied as a brown solid and was prepared in high purity water (de-ionised, 18.2mΩ) as a 0.3% w/v (3g l⁻¹), which was used as the stock solution for subsequent tests. The preparation involved agitating the solution (by magnetic stirrer) for one hour and then filtering through Whatman No.42 filter paper (pore size ~2.5µm). Considering the aging effect, all TBP solutions were used within 3 hours, except the samples used for ageing tests. After further filtering by a Gelman 0.45µM membrane filter, the Non-purgeable dissolved organic content (NPDOC) of working TBP solutions at different concentrations was measured by a TOC analyzer (discussed in Section 4.4.2.3). Colour and UV absorbance values were measured in terms of absorbance at 400 nm and 254 nm respectively, using a scanning UV-visible spectrophotometer (discussed in Section 4.4.2.6). The analysis results are shown in Table 4.1.

The results in Table 4.1 indicate that there a linear relationship between NPDOC /absorbance values at 254nm with TBP concentrations in accordance with Beer's Law theory. Although there is a linear relationship between absorbance values at 400nm (indication of colour) and TBP concentrations, the relationship does not go through origin, which was not expected. Although the reason for this is unclear, it may be caused by the complex nature of the raw tannin material.

TABLE 4.1 Variation of NPDOC and UV/Vis-absorbance (254nm and 400nm) with TBP solution concentration

TBP concentration (mg l ⁻¹)	NPDOC (mg l ⁻¹)	Abs (254nm) (cm ⁻¹)	Abs (400nm) (cm ⁻¹)
25	11.73	0.25	0.030
30	16.41	0.299	0.033
35	18.04	0.343	0.035
40	22.41	0.386	0.037
45	24.65	0.429	0.039
50	27.14	0.472	0.041
55	29.79	0.508	0.043
58	30.99	0.532	0.044
60	32.50	0.547	0.045
65	35.53	0.592	0.046
70	38.36	0.634	0.048

4.2.2 PolyDADMAC

Quantities of a commercial cationic polyDADMAC, Flobeads DB 45 SH, with 90% active content in weight, were kindly provided by SNF Ltd (UK). This synthetic polyDADMAC (poly diallyldimethylammonium chloride) has a molecular weight of approximately $1 \times 10^6 \text{ g mol}^{-1}$, which is quoted by the manufacturer. Information concerning charge density of this product was not available by the manufacturer but a previous study (19) strongly supported the assumption that polyDADMAC has a high CD of about 6.2 meq g^{-1} , which was believed to be insensitive to pH due to the quaternary ammonium, $R_1R_2R_3R_4N^+$ cationic group. The product was supplied in solid form and diluted in high purity water (de-ionised, 18.2mΩ) to give a stock solution of 2 g l^{-1} . Continuous gentle stirring was required to achieve complete solution of the granular polymers in the preparation of stock solutions.

4.2.3 Alum

Aluminium and iron salts are still widely used as coagulants in the water and wastewater industry. For comparative purposes, aluminum sulphate hydrate ($\text{Al}_2(\text{SO}_4)_3 \cdot 14\text{H}_2\text{O}$; Aldrich, UK), 'alum', was applied as a primary coagulant in this study. Several mechanisms such as charge neutralisation or sweep flocculation have been postulated for the coagulation of humic substances and turbidity particles by aluminium ions. The relative importance of these mechanisms depends on factors such as pH and coagulant dosage (134). It is well established that the optimal pH level is about 5.5 ~6 for aluminium sulphate and slightly lower for ferric salts, in the coagulation process (2). Stock alum solutions were prepared at a concentration of 0.1 mol l^{-1} . These were prepared weekly and kept at 4°C in the refrigerator.

4.2.4 Tanfloc SL

Tanfloc SL (TANAC Ltd, Brazil) is a solid mixture of TBP and Alum. Tanfloc SL solution does not jellify within the stated 3 month shelf-life. The composition of Tanfloc SL was given by the manufacturer, as solids (w/w): 8.4% aluminium sulphate and the rest as TBP. However, 1 g l^{-1} TSL solution was measured by an ICP Analyser (FISONS ARL 3580B), and gave a result of $8.8 \times 10^{-3} \text{ g l}^{-1}$ as Al^{3+} , which is equal to 5.6% $\text{Al}_2(\text{SO}_4)_3$ without water of hydration in TSL mixtures. This lower figure of Al content was used in comparative coagulation tests, because the higher weight value of aluminium sulphate salt (8.4%) given by the manufacturer is likely to be based on inclusion of some water of hydration.

4.3 Reagents and Chemicals

The other reagents or chemicals in preparation of the working buffer or

titration solution, except noted otherwise, were supplied by BDH (BDH, Dagenham, Essex, UK) and were all analytical reagent grade. They were used without further purification. High purity water (de-ionised, 18.2m Ω) was used in all experiments. To investigate the effect of pH values, two distinct buffer systems in the measurement of charge density and coagulation performance were adopted respectively. These categories can be described under the following headings:

(i) Characterisation tests: 1 mmol l⁻¹ buffer solutions were used to control the pH value of solution directly. The buffers that were used were: CH₃COOH/CH₃COONa for pH 3-5, NaH₂PO₄/Na₂HPO₄ for pH 6-7 and NH₄OH/NH₄Cl for pH 8-10.

(ii) Coagulation tests: 0.1 mol l⁻¹ NaHCO₃ solution was used as a buffer and the pH of model waters was maintained by adding 0.1mol l⁻¹ NaOH or HCl solution.

There were two types of standard titration analysis used in this study. These were colloid titration to measure the CD values and Argentometric titration (135) to determine the chloride content. The preparation of titration solutions are discussed below:

(i) Colloid titration: PPVS was obtained from Aldrich Chemicals, UK. The solution was prepared by dissolving 180 mg PPVS chemical in 1L of water. The charge density of PPVS solution used as anionic titrant was standardized with the cationic surfactant, cetyltrimethylammonium bromide (CTAB) which was prepared as a 1 meq l⁻¹ solution. *Ortho*-toluidine blue (*o*-Tb) was prepared as a 0.01% (v/v) aqueous solution, which was used as colour indicator in the colloid titration process.

(ii) Argentometric titration: Potassium chromate K₂CrO₄ (Aldrich Chemicals,

UK) was prepared as 50 g l^{-1} to indicate the end point of the silver nitrate titration of chloride in a neutral or slightly alkaline solution. Standard silver nitrate, AgNO_3 was obtained from Aldrich Chemicals, UK, and prepared as $0.0141 \text{ mol l}^{-1}$ titrant as the standard method defined. Silver chloride is precipitated quantitatively before silver chromate is formed. Sample pH was adjusted by $0.1 \text{ mol l}^{-1} \text{ H}_2\text{SO}_4$ or NaOH to the range from 7 to 10.

4.4 Model Water and Surface Water Sample

4.4.1 Model Water with Kaolin Suspension

Kaolin clay (Fisher Chemical, UK) was prepared as a model suspension. The particle size was analysed by Laser Diffraction Particle Size Analyser (Coulter LS Series, Beckman coulter Ltd., UK) and the geometric mean size of the particles in the suspension was $4.85 \mu\text{m}$. A working solution, normally 50 mg l^{-1} of concentration, was prepared by dispersing 100 mg of kaolin clay in 2 L of de-ionised water. To obtain full dispersion it was necessary to raise the pH of the suspension to about 7.5 (136), and blend at high rotational speed, which was achieved by adding 5 ml of $0.1 \text{ mol l}^{-1} \text{ NaOH}$ and vigorously stirring at 2000 rpm for 2 hours to obtain a solution with a turbidity value of $40 \text{ NTU} \pm 1\%$, determined by HACH turbidimeter (discussed in Section 4.4.2.4). It was observed that the light kaolin clay showed good dispersion and stability in the solution. Surface potentials were not determined but previous study indicated that kaolin has a net negative charge in natural water. Duan and Gregory (136) determined that the Electrophoretic Mobility values of kaolin particles range from about -0.8 at pH 3 to -2.5 at pH10 ($\mu\text{m s}^{-1} \text{ v}^{-1} \text{ cm}$). In this case several pH values were investigated, using $0.1 \text{ mol l}^{-1} \text{ NaHCO}_3$ as an appropriate buffer solution.

4.4.2 Model Water with Humic Acid

Humic acid (Aldrich Chemical Company, UK. Sodium salts, 42.2% Carbon content) was obtained as a commercial reagent grade solid. Stock solutions were prepared from 5g of dry humic acid product dissolved into 1L de-ionised water to give a HA concentration of approximately 5 g l^{-1} , after filtering by Whatman No.42 filter paper (pore size $\sim 2.5\mu\text{m}$). Working solutions of 10 mg l^{-1} and 30 mg l^{-1} concentration were prepared by diluting the HA stock solution with de-ionized water and adjusting the pH using 0.1 mol l^{-1} NaOH or HCl solution. 0.1 mol l^{-1} NaHCO_3 was used as the buffer solution to allow convenient adjustment of pH. The solution was then further filtered under vacuum through a $0.45\mu\text{M}$ membrane filter (Gelman Sciences). The Non-purgeable dissolved organic carbon (NPDOC) and UV/Vis-absorbance values of HA in pure de-ionised water at 10 mg l^{-1} and 30 mg l^{-1} concentrations were measured by TOC analyser and the UV Probe Ultraviolet Spectrophotometer. These are shown in Table 4.2.

TABLE 4.2 Variation of NPDOC and UV/Vis-absorbance (at 254nm and 400nm) with HA solution concentration

Concentration (mg l^{-1})	pH	NPDOC (mg l^{-1})	Abs (254nm) (cm^{-1})	Abs (400nm) (cm^{-1})	SUVA* $\text{m}^{-1}/\text{mg l}^{-1}$
10	8.45	2.672	0.285	0.090	10.7
30	8.60	9.957	0.748	0.227	7.5

*SUVA= $\text{UV}_{254}/\text{NPDOC}$; indicative of aromaticity

It has been shown that the UV/Vis-absorbance values of humic solution increased with increasing pH (89). This was confirmed by measuring the UV/Vis-absorbance values of 30 mg l^{-1} HA solution at different pH values (after filtration) and the results are shown in Table 4.3. The UV/Vis- absorbance values

of 10mg l⁻¹ HA solution at pH 9 are 0.293 and 0.096.

TABLE 4.3 Variation of UV/Vis-absorbance (at 254nm and 400nm) of HA solutions with pH (HA concentration 30mg l⁻¹)

pH	Abs (254nm) (cm ⁻¹)	Abs (400nm) (cm ⁻¹)
3	0.653	0.160
4	0.685	0.172
5	0.709	0.188
6	0.719	0.197
7	0.737	0.210
8	0.743	0.212
9	0.752	0.232
10	0.770	0.250

Considering the complications caused by the very rapid interaction of humic acid with TBP, especially at a high pH value, it was infeasible to determine the initial UV-visible absorbance of the combined HA and TBP at the beginning of the coagulation process. Hence, it is assumed that the initial absorbance value (at 254nm and 400nm) was the sum of the individual absorbance values of TBP and HA (values shown in Tables 4.1 and 4.3).

4.4.3 Simulated Water with Kaolin Suspension and Humic Acid

The tests involving model waters containing both suspended material and humic substances were undertaken to compare the TBP performance with that investigated previously by WRc using real water (River Thames water, Egham (137)). The model water was 2L de-ionised water (18.2mΩ) with 70mg of

kaolin clay and 2ml of humic acid solution (2g l^{-1}); to achieve the same pH (7.9) 10ml of 0.1mol l^{-1} HCl was added. The relevant quality parameters of the model water and real river water are shown in Table 4.4.

TABLE 4.4 Analysis of simulated water and real water used by WRc (137)

	Colour (Hazen)	NPDOC (mg l^{-1})	Turbidity (NTU)	pH
Model water	32.0	(8.51)*	27	7.9
River water (WRc study)	32.8	5.73	27	7.9

* This value is unexpectedly high (see Table 4.2) and therefore believed to be incorrect

4.4.4 Raw Surface Water

Raw water samples were received from an organic-rich river source at Bamford, UK (located in the north of England). A preliminary analysis of the water quality was undertaken before commencing the coagulation experiments. The results of the tests are given in Table 4.5. All parameters were measured after filtration by $0.45\ \mu\text{m}$ paper, apart from the Turbidity. To achieve the pH value at 6 in the samples, $0.1\ \text{mol l}^{-1}$ HCl solution was pre-determined and added to 2L raw water in these coagulation tests. The high colour and SUVA values indicate a highly aromatic, humic type organic content.

TABLE 4.5 Analysis of an organic-rich river water at Bamford, UK

	pH	NPDOC (mg l^{-1})	Colour (H°)	UV _{254nm} * (cm^{-1})	UV _{400nm} * (cm^{-1})	Turbidity** (NTU)
Raw water	7.9	3.66	70	0.248	0.039	1.5

* 1cm cell **No filtration

4.5 Analysis Methods

4.5.1 Polymer Characterisation

4.5.1.1 Dissociation, Precipitation and UV Absorbance Analysis

Simple chemistry analysis falls into three categories:

(1) pH Titration Analysis

A pH titration was performed by adding standard base (0.001 mol l^{-1} NaOH solution) to 100ml TBP solution (0.03 g l^{-1}). For comparison, the titration of the distilled water was also carried out with the standard base (0.001 mol l^{-1} NaOH solution). To avoid the influence of air effects, the solutions were contained within a desiccator and soda lime was used in the desiccator to absorb carbon dioxide and water during the titration. The beaker with TBP solution was placed in the desiccator, then 1ml of 0.001 mol l^{-1} NaOH was added carefully, until the pH value was stable. The pH was measured by pH electrode (Hydrus 300, Fisher, UK). Based on the TBP—base titration curve, the dissociation constant pKa of TBP was estimated.

(2) Solubility Analysis

Using 1 m mol l^{-1} pH buffers to dilute the 1 g l^{-1} stock (initially filtered) TBP solution, a series of solutions with concentrations from 0.02 g l^{-1} to 0.1 g l^{-1} over the pH range of 3-9 were prepared. All of these solutions after standing for 6 hours in the bench were subsequently filtered through Whatman No.42 filter paper (pore size $\sim 2.5 \mu\text{m}$) to determine the TBP solubility. In each case, clean filter paper was transferred to a crucible and dried at $50\text{-}55^\circ\text{C}$ for 12 hours, then placed in a desiccator to cool and equilibrate to ambient temperature before weighing the paper. This cycle of drying, cooling, desiccating and weighing was repeated until a constant weight was obtained or until the weight change was less than 4%. After filtration, the filter paper was dried and weighed using the same

procedure, and the final weight of filter paper was taken to calculate the m/v concentration of the polymer. It should be noted that the (un-buffered) solutions had a $\text{pH} < 6$.

(3) UV/visible Light Absorbance Analysis

The *UV-visible* light absorbance of the TBP was determined spectrophotometrically. TBP water solution with different concentrations in the range of 0.02 g l^{-1} --- 0.1 g l^{-1} were firstly scanned using the *UV Probe* Ultraviolet Spectrophotometer (Shimadzo, Japan; wavelength range from 190nm to 800nm, 10 mm quartz cell path) to determine the maximum absorbance wavelength. At this maximum wavelength, TBP solutions with different concentrations (from 0.02 g l^{-1} to 0.1 g l^{-1}) were analyzed over a range of pH from 4 to 9 by employing a 10mm quartz cell path. All tannin solutions were allowed to stand for 6 hours and then filtered to test. Blank buffer solutions were used as the reference solution in the instrument to exclude absorbance due to the buffer alone.

4.5.1.2 Charge Density Analysis

The charge density of the TBP was evaluated by colloid titration using PPVS (poly-potassium vinyl sulphate) as anionic titrant (18). The method is based on the stoichiometric reaction in the sense of 1:1 charge compensation between oppositely charged polyelectrolytes. The end point is determined by the interaction of the cationic indicator, o-toluidine blue (o-Tb, 3-amino-7-dimethylamino-2-methyl-phenothiazin-5-ium chloride) with anionic PPVS, which leads to a hypsochromic shift in the absorption spectrum of o-Tb and thus to a visible colour change. The charge density of PPVS solution was preliminary standardised with the cationic surfactant, cetyltrimethylammonium bromide (CTAB). Both visual titration and spectrophotometry were used to

determine the titration end point in order to compare the methods. The charge densities of the TBP and the polyDADMAC were evaluated for a range of solution pH values from 3 to 9 in this study. Results are expressed as the mean value of three replicate samples. To determine the TBP charge density at $\text{pH} \geq 6$, the titrant (PPVS) concentration was diluted to $1 \times 10^{-5} \text{ mol l}^{-1}$.

(1) Visual titration (procedure 1)

To determine the charge density of the cationic polymer by titration with the anionic polyelectrolyte PPVS, the charge density of PPVS should be determined. The PPVS solution was firstly standardised with CTAB; this involved 3 ml of CTAB (1 meq l^{-1}) solution with three drops of o-Tb solution titrated with PPVS until the colour of the solution changed from blue to red-violet. Then, the titration procedure was repeated for the filtered solutions of TBP (10 ml of 0.08 g l^{-1}) and polyDADMAC (10 ml of 0.05 g l^{-1}) at various pH values, using PPVS of a pre-determined charge density according to the above procedure.

(2) Spectrophotometry (procedure 2)

The titration procedure was the same as indicated for procedure 1. However, at the end point, the solution was tested by spectrophotometry, where the binding of o-Tb blue to PPVS produces a distinct colour shift from blue (absorption maximum at 635 nm) to red-violet (530 nm).

4.5.1.3 Functional Group and Chemical Bond Analysis

(1) FT-IR Analysis

One common method for investigating the chemical structure of organic molecules is by the use of FT-IR (Fourier Transform Infrared) Spectroscopy. In this case, a preliminary assessment of the chemical structure of the TBP was

determined by the use of a Magna-IR 560 Spectrometer (Nicolet Instrument Corporation, USA). The spectrometer was equipped with a Globar IR source CsI beam splitter, and a DTGS CsI detector. For comparative purposes, study was made of tannin extract (gel, non-Mannich reaction and non-polymerization) after freeze drying. Approximately 35g tannin extract (gel) was weighed and then placed in a conical flask in a low temperature refrigerator at -18°C. Freeze drying was carried out overnight in a laboratory freeze dryer (Birchover Instruments Ltd, UK) with a vacuum of 100 mT or less. With great care, the solid powder of TBP or solid tannin extract was further dehydrated at 60°C in an oven, was blended with dried KBr (1/40 w/w) and then studied by FTIR spectroscopy. For each spectrum 200 scans were taken in the range from 400 to 4000 cm^{-1} with the resolution of 8 cm^{-1} . The resulting FTIR spectral patterns were analyzed and the results were compared with known signatures of identified materials in the FTIR library.

(2) ^1H NMR Analysis

The arrangement of functional groups in TBP was measured by ^1H NMR (Nuclear Magnetic Resonance) Spectroscopy. A TBP sample was placed in a strong magnetic field of 5,000 to 23,000 gauss and irradiated by the radio frequency (RF), the value of which is dependent on the nuclei of interest. Absorption of the radio frequency occurs, corresponding to the energy required to bring the nuclear magnets (^1H) into specific orientations with respect to the magnetic field. The ^1H NMR analysis of the TBP samples was undertaken using a 600MHz instrument (Bruker Spectrospin AV600, USA). The TBP solid was dissolved in the solvent comprising 95% water: 5% D_2O , and water suppression was used to remove the water effects to the spectra generated. It had been the intention to use ^{13}C NMR, but due to the low solubility of the tannin and the low sensitivity of carbon to NMR, no signals were observed, hence the use of ^1H as the atomic species to study.

4.5.1.4 Element Content Analysis

(1) ICP Analysis

A polymer will contain several elements in addition to carbon, which need to be identified during a characterization process. A metal elemental analysis test was carried out by use of an ICP Analyser (FISONS ARL 3580B, UK). 100 mg l⁻¹ TBP solution and certified standard solutions (Merck, UK) were acidified with 1% (w/w) HNO₃ solution to the same pH. Results are expressed as the mean value of three replicate samples. Using ICP, the percentage content of prominent trace (mainly metal) elements of TBP (with dissolution in strong acid solution) was analysed.

(2) CHN Analysis

An elemental analysis test for carbon, hydrogen and nitrogen was carried out by a CHN elemental analyzer (Perkin-Elmer, USA) involving the catalysed combustion of a 10 mg accurately weighted TBP solid sample at high temperature (above 1800°C) in a stream of oxygen. After combustion, the generated CO₂, NO_x and H₂O flowed through a series of thermal conductivity cells (the detector) and then were measured to determine the C, N and H percentages, respectively.

(3) TOC Analysis

The organic carbon content analysis was carried out by a total organic carbon analyser, TOC-Vws (Shimadzo, Japan). Organic carbon in highly pure water (de-ionised, 18.2mΩ), and in 100 mg l⁻¹ TBP solution were measured to determine the organic carbon content of the TBP sample. For the TBP solution, samples were initially filtered by 0.45 μM membrane filter (Whatman,UK). The filtered solution was acidified with ortho-phosphoric acid and sparged with high purity (zero-grade) oxygen in a TOC analyzer prior to analysis. The solution was

then analyzed three times with mean results being quoted.

(4) Kjeldahl Nitrogen Analysis

The Kjeldahl method can be undertaken to determine ammonia nitrogen and organic nitrogen (138). In this study, a Skalar's SAN^{plus} analyzer (Skalar Analytical Ltd., Netherlands) was used for the nitrogen analysis in 1g l⁻¹ liquid TBP samples after digesting the sample with concentrated sulphuric acid, H₂SO₄, 5% (w/w) and a Kjeldahl catalyst. This result was adopted to validate the data from the CHN analysis.

(5) Argentometric Titration Analysis

An Argentometric titration method (135) was used to measure the chloride content of the TBP (counterion to the cationic charge). In a neutral or slightly alkaline solution, potassium chromate can indicate the end point of the silver nitrate titration of chloride. Silver chloride is precipitated quantitatively before red silver chromate is formed. To get the concentration of chloride in a sample, the following formula was used:

$$\text{Chloride Concentration} \frac{\text{mgCl}}{\text{L}} = \frac{(A - B)\text{mL} * M \frac{\text{mmol}}{\text{mL}} * 35.5 \frac{\text{mgCl}}{\text{mmol}}}{25\text{mL} * \frac{1\text{L}}{1000\text{mL}}}$$

----- (4.1)

Where:

A = mL titrant used for sample

B = mL titrant used for blank

M =molarity of silver nitrate

4.5.1.5 Molecular Weight Analysis

(1) Size Exclusion Chromatography (SEC) Analysis

SEC has been used to determine the molecular mass distribution of both natural and synthetic polymers (139). In SEC, elution time data of samples can be conveniently translated into molecular mass through a calibration curve. In this study, information concerning the molecular mass distribution of TBP was obtained by size exclusion chromatography with 1-methyl-2-pyrrolidinone (NMP) as the polymer solvent and chromatographic eluent (139). This work was carried out by colleagues in the Department of Chemical Engineering. Two appropriate SEC columns (300mm; 7.5mm i.d. packed with polystyrene/polydivinylbenzene beads) were selected in this study to fractionate the TBP sample at a temperature of 85°C and flow rate of 2ml min⁻¹. The SEC columns of different porosity ranges (Mixed-D and Mixed-A; Polymer Labs,UK) were used with detection by an evaporative light scattering detector (ELS) as well as Perkin-Elmer LC 290 UV-absorbance detector set at 280, 300 and 350nm. The method involves the use of a calibration curve obtained by plotting the logarithms of known molecular masses of standard polystyrenes or polysaccharides against their elution time. TBP concentrations at 1g l⁻¹ were used in this study. Although the solubility of polymer samples in NMP solvent was assumed, this needs to be confirmed in any future studies.

(2) Light Scattering Analysis

The amount of light scattered is directly proportional to the product of the weight-average molar mass and the macromolecule (solute) concentration (140). Light scattering method is widely used but it is valid only when the refractive index (specifically the refractive index—concentration gradient, dn/dc) of solution is known. In this study, the average molecular weight, $\langle M \rangle_w$, of the TBP was determined by a Wyatt DAWN EOS Light Scattering Photometer

(Wyatt Technology Ltd. UK) at 633 nm and 25°C. A known molar mass polystyrene (200,000 g mol⁻¹) dissolved in toluene was used as a standard sample. The stock solution with TBP concentration of 1 g l⁻¹ was prepared in 0.05 M NaCl solution and filtered through a 0.2 µm syringe filter to remove fine dust particles. To construct a Zimm plot, five dilutions at relative concentrations of approximately 80%, 60%, 40%, 20% and 10% of the stock concentration were introduced to the DAWN photometer in a batch mode by a syringe pump and the scattered light was measured as a function of angle for each concentration. From a single Zimm plot the molar mass M , rms radius r_g and the second virial coefficient A_2 can be determined (140). The refractive index of TBP solution was determined by Wyatt Technology UK Ltd.

4.5.2 Coagulation Experiments

4.5.2.1 Photometric Dispersion Analyser

Conventional jar test methods are limited in terms of their sensitivity and practical convenience, although they sometimes do provide a useful visual and semi-quantitative simulation of full-scale performance. In this study a photometric dispersion analyser (PDA 2000, Rank Brothers, Cambridge, UK) was used in a modified jar test procedure. This is a relatively new approach to evaluating coagulation performance which has been found to provide a sensitive and rapid response to the state of aggregation of colloidal suspensions. In the tests a constant flow from the stirred reactor to the PDA optical sensor was maintained by the use of tubing and a peristaltic pump (Matson 505S, UK) operating at about 25ml min⁻¹; the flow passes through the optical sensor where it is illuminated by a narrow light beam (850nm wavelength). In regard to the output of the PDA, the ratio of the root mean square (rms) value of the fluctuating component to the average transmitted light intensity (dc value) is called as the Flocculation Index (FI). The optical data was recorded every second and the results were logged by computer for subsequent spreadsheet analysis. Although inherently qualitative, it

is believed that the FI value is correlated with floc size and always increases as flocs grow larger (141). Therefore, this ratio can give immediate information on the state of aggregation of particle suspension over the entire period of coagulation.

The principle of this optical technique has been described by Gregory (142). A briefly description of this technique is illustrated as follows: a flowing suspension through the transparent tube is illuminated by a narrow light beam from a luminous light source. The transmitted light intensity passing through the suspension fluctuates randomly about some mean value, which can be converted to an electrical signal by a photometric detector. The output from detector consists of a steady (*dc*) signal and a fluctuating (*ac*) component. The *dc* value is a measure of the average transmitted light intensity and depends on the turbidity of the suspension. The fluctuating (*ac*) component is a result of random variation in the number of particles in the illuminated volume. Gregory concluded that the root mean square (RMS) value of the fluctuating (*ac*) signal is related to the average number concentration and the size of the suspended particles. In practice, it is convenient to divide the RMS value by the steady *dc* value to give a dimensionless term $R = \text{RMS} / dc$. Although the ratio *R* is qualitative information on aggregate size in nature, the relative change in the *R* value is a useful indicator of the degree of coagulation.

4.5.2.2 Gator Jar

A 2L square, acrylic reactor vessel of 21cm height and 11.5cm width was used in the coagulation tests as an alternative to standard glass beakers. This was partly because the glass beakers created a large amount of vortexing, which limited the attainable power input to the water, and partly to carry out tests where it is useful to quantify the prevailing mean velocity gradient (commonly referred

to as G). By assessing the coagulation performance at a known value of velocity gradient allows for direct comparison with other published studies and to full-scale practice. A ‘Gator jar’ reactor and a 7.6 cm flat paddle were fabricated from clear acrylic sheets in a form based directly on a standard design recommended by the AWWA (143). The flat paddle was driven by a standard top-mounting, variable speed stirrer (Heidolph, RZR2020, Germany). The AWWA design provides a linear log (paddle speed) versus log (velocity gradient) calibration curve that can be applied directly. The mean velocity gradient for the tests were pre-calculated as , 950 s^{-1} , 800 s^{-1} , 600 s^{-1} , 480 s^{-1} , 350 s^{-1} and 48 s^{-1} , corresponding to the following paddle speeds: 400rpm, 350rpm, 300rpm, 250rpm, 200rpm and 50rpm (Appendix I: Laboratory G Curve for Flat Paddle in 2L Gator Jar). All the coagulation experiments have involved pumping a sample flow from the stirred reactor to the PDA sensor and returning it to the reactor (see Figure 4.1 – clockwise direction).

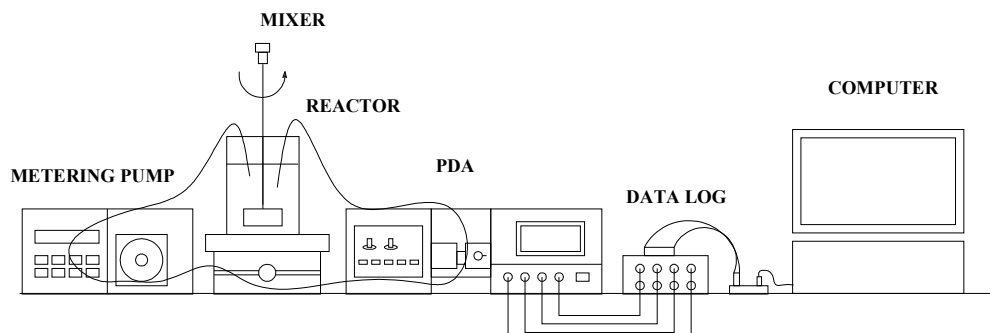


Figure 4.1 Schematic of coagulation apparatus

4.5.2.3 Coagulation Process

(1) Standard Coagulation Procedure

The optimum dosages of coagulants for the model waters and the raw surface water under different coagulation conditions were determined by the PDA at a temperature of approximately 23°C (laboratory room temperature). The

dynamic coagulation tests followed a standard approach: solution samples were pumped from a 2L gator jar at about 25 ml min^{-1} through the tubing and the average (dc) and fluctuating (rms) components of the transmitted light intensity were monitored by the PDA instrument. After allowing 1 minute for steady state readings to be established, coagulants at the required dosage were pipetted into the suspension and the suspension was stirred at a high mixing speed, generally with a G-value range of 300 s^{-1} - 700 s^{-1} , for 30 seconds. It was observed that alum and TBP were acidic and lowered the pH of model water. Therefore, to reach the desired pH, a pre-determined amount of 0.1 mol l^{-1} NaOH or HCl solution was added. The basic function of rapid mixing was to achieve complete mixing of the polymer in the water in as short a time as possible, thereby causing efficient destabilization. The stirring speed was subsequently reduced to a lower speed of 50 rpm (48 s^{-1}) and held at this value for a chosen time period (10-60 mins), which was determined as that required to obtain a steady FI, indicating flocs do not continue growing and have reached a steady-state size. The fundamental purpose of slow mixing was to promote collisions between destabilized particles so that flocs were formed. The speed of 50 rpm is believed to be the optimal stirring speed, which maintained the aggregates in suspension but without excessive breakage in solution. However, in some cases there was still fluctuation of the FI index at this speed in the stable phase of flocs, since large flocs were observed to accumulate on the bottom of the jar and were intermittently re-suspended.

(2) Procedure for the Study of Floc Strength

The formation, breakage and re-formation of flocs using TBP as coagulant were investigated by studying the FI response to different values in mean velocity gradient. Using a 2L gator jar, an indication of relative floc strength can be obtained by applying a sudden increase in shear rate to the formed aggregates and relating velocity gradient applied to the maximum 'floc size' (FI)

resulting. The procedure used is described as follows: after the coagulant at the required dosage was pipetted into the suspension, the suspension was stirred at 200 rpm (350 s^{-1}) for 30s, followed by slow stirring at 50 rpm for 10-30min (to achieve steady state with no significant change in the FI value and so no further floc growth). In order to study the floc strength, a series of tests were carried out in which the stirring speed was increased suddenly to either 200 rpm (350 s^{-1}), 250 rpm (480 s^{-1}), 300 rpm (600 s^{-1}), 350 rpm (800 s^{-1}), and 400 rpm (950 s^{-1}) for 60 seconds and then reducing the stirring speed back to 50rpm. A second series of tests of floc breakage and re-formation was carried out in which a sudden increase in stirring speed to 300 rpm was maintained for different time periods, ranging from 5 to 300 seconds, and then the speed was reduced back to 50 rpm. For each coagulant the flocculation indexes before floc breakage, and before and after the floc re-formation due to increasing mixing speeds, were measured.

(3) Procedure for the Study of Coagulation Performance of Dual Coagulant

A coagulation performance matrix was produced for a full range of alum-polymer combinations at different pH values. Initially, a series of coagulation tests using alum as the sole coagulant were carried out to determine the optimal alum dosage. From this specific value the alum dosage was systematically reduced, and at each dosage coagulation tests were carried out with a range of polymer dosages. The dynamic coagulation tests for this study were conducted in a 2 L gator jar and measured by the PDA, using a standard approach as described previously; in summary this was: after allowing 1 minute for steady state readings to be established, the required dosages of alum and TBP were pipetted into the solution simultaneously and the solution was stirred at 200 rpm (350 s^{-1}) for 30 seconds. The stirring speed was then reduced to a speed of 50 rpm (48 s^{-1}) and held at this value for the required time (30min).

(4) Procedure for the Study of Coagulation Performance of Solid Bound TBP

The sand used in this study was supplied by Universal Mineral Supplies Ltd, UK. Considering the organic contaminant on the surface of microsand, the received sand was first washed by either 20% (v/v) H₂O₂ or 5 % (v/v) Decon solution (Decon Laboratories Ltd, UK), then rinsed by de-ionised water for three times and finally dried in an oven at an appropriate temperature (105°C). After this pre-washing of the sand, the adsorption tests at pH4 were undertaken. Initial adsorption tests were carried out at pH 4 using 30 mg l⁻¹ TBP with different amounts of sand. A 2L gator jar with a high mixing speed of 300 rpm (600 s⁻¹) for 2 minutes was used in this test, and the final solution was filtered by 0.45µM filter paper. It was found that the maximum UV absorbance wavelength for TBP solution is 210nm, therefore the UV₂₁₀ absorbance of filtered solutions was measured to indicate the residual TBP in solution. Further, the absorption ratio of TBP and sand can be determined.

The modified method of applying TBP/sand mixture as a coagulant for HA solution treatment was investigated. In this case, the pH of solution was kept at a value of 4 and the coagulation test procedure of solid bound TBP was as follows: the solid bound TBP was prepared as described previously during 2 minutes rapid mixing of washed sand and soluble TBP in the correct concentrations; the suspension was settled for 15 minutes; as much supernatant solution was carefully decanted away without disturbing or losing the settled sand from the bottom of the gator jar; approximately 2 L humic acid solution at 30mg l⁻¹ was poured to the jar, with an amount of pre-determined HCl/NaOH solution to keep pH at 4; the contents of the gator jar were then rapidly mixed at 260 rpm (500 s⁻¹) to resuspend the sand and maintain uniform conditions for flocculation.

In general, all the bench-scale coagulation experiments have involved

pumping a sample flow from the stirred reactor to the PDA sensor and returning it to the reactor. Figure 4.1 shows the PDA and Gator jar equipped with a peristaltic pump and motorized stirrer for the coagulation tests.



Figure 4.2 Apparatus of coagulation tests

4.5.2.4 Analysis of Water Quality

Following a 30 min settling period after stirring, supernatant liquid was withdrawn by pipette in order to measure the quality parameters in terms of NPDOC, turbidity, colour, UV absorbance, floc volume and residual Al

concentration. All the analyses were carried out in accordance with standard methods (135).

The concentrations of non-purgeable dissolved organic carbon (NPDOC) in water were determined by a total organic carbon analyser, TOC-Vws (Shimadzo, Japan). The treated water was initially filtered by 0.45 μ M membrane filter (Whatman,UK) and then the filtered solution was acidified with ortho-phosphoric acid and sparged with high purity (zero-grade) oxygen in a TOC analyzer prior to analysis. The solution was analyzed three times with mean results being quoted.

Turbidity was measured by a turbidity meter (Model 2100A, Hach, UK), which was calibrated with standard solutions of 1 NTU, 10NTU or 100NTU. 50ml supernatant of final water was measured without filtration.

The Hazen colour values of the final water were measured by a Lovibond Nessleriser (BDH Chemicals Ltd, UK) after filtering through a Whatman 0.45 μ M membrane filter. The color was determined by visually matching a column of sample in a Nessler cylinder with pre-calibrated colored glass standards, which are stable-colored and not affected by UV light or extreme environmental conditions.

The absorption of light at ultra-violet wavelengths, such as 254nm, is believed to be caused by aromatic compounds and other organic substances with conjugated double bonds. Specific visible light absorbance at 400nm was used to represent true colour in the solution. In this case, UV-Vis measurements were recorded for filtered water by 0.45 μ M membrane filter (Whatman,UK) at 254nm (UV) and 400nm (colour), using the *UV Probe* Ultraviolet Spectrophotometer (Shimadzo, Japan; 10 mm quartz cell path).

Floc volume was measured by Imhoff cones after 1 hour settling. 2 L treated water is added to a pair of one-liter cone-shaped plastic containers. After settling for 45 min, the sample solution was gently agitated near the sides of the cone with a rod. Following a further 15 min settling period, the floc volume was recorded in milliliters, from graduations marked near the bottom of the cone.

The solution was further centrifuged at 2000 rpm for 30 min by centrifuge (Gallenkamp, UK), and then 20 ml of the solution was filtered through a 0.45 μM membrane filter (Whatman, UK). In order to determine the residual aluminum concentration, the filtrate was acidified with 2 ml of concentrated HNO_3 solution (0.2% w/w), and measured by a graphite furnace atomic absorption spectrometer (Perkin-elmer AAnalyst 800, USA).

4.5.3 Residual Tannin Measurement

(1) Determination Limit of Standard Method for Tannin Measurement

A standard method (144) was undertaken to determine the concentration of free tannin in final water. This colorimetric method measures the light absorbance at 700nm using the *UV Probe* Ultraviolet Spectrophotometer (Shimadzo, Japan; 10 mm quartz cell path) following progressive additions of a standard solution of Folin phenol reagent (tungstophosphoric and molybdophosphoric acids) and carbonate-tartrate reagent that participate in an association reaction with tannin in solution to form a blue color. According to the procedure describe in Section 5550B of Standard Methods (144), the minimum detectable concentration is approximately 0.025 mg l^{-1} for phenol and tannin acid with as 1-cm-path-length spectrophotometer. However, the detection limit of this method was determined in a preliminary study. For this purpose, seven replicates of 0.025 mg l^{-1} standard tannin acid solution were analyzed with a

1-cm-path length spectrophotometer. The Detection Limit (DL) for tannin acid and phenol was evaluated by use of the equation: $DL = S t_{(n-1, 1-\alpha=0.99)}$, where S = standard deviation of the replicate analyses, and $t_{(n-1, 1-\alpha=0.99)} = 3.143$, where 3.14 is the Student's t value for 7 degrees of freedom at 99% confidence level. Using a set of seven tannin samples in aqueous solution, and quantifying the light absorbance at 700nm, the DL in this method was found to be 0.018 mg l^{-1} for tannin acid. The method illustrated that in a single laboratory analyzing seven replicates for phenol at 0.1 mg l^{-1} the precision was $\pm 7\%$ and recovery was 107%.

(2) Standard Calibration Curve for Colorimetric Method

A calibration curve has been established by measuring the absorbance of Folin phenol reagent with different concentrations of standard tannin at 700nm. The calibration curves for low concentrations (0.025 mg l^{-1} to 0.5 mg l^{-1}) and relatively high concentrations (0.4 mg l^{-1} to 10 mg l^{-1}) of tannin acid are given in Figure 4.2 and Figure 4.3. It can be seen that although the linear relationship between absorbance and reagent concentration is less consistent at low concentration, compared with high concentration of reagent, the trend is still sufficiently linear for both concentration ranges. Figure 4.4 shows the calibration curve with the combined reagent concentration (i.e. from 0.025 mg l^{-1} to 10 mg l^{-1} ; the combination of the Figures 4.2 and 4.3), and the resulting overall equation: $Y = 0.0943X - 0.0043$ ----- (4.2), was used subsequently for the final calculation of residual TBP concentration. Having derived the calibration curve for tannin acid, it was used to estimate the concentration of residual TBP in various coagulation tests.

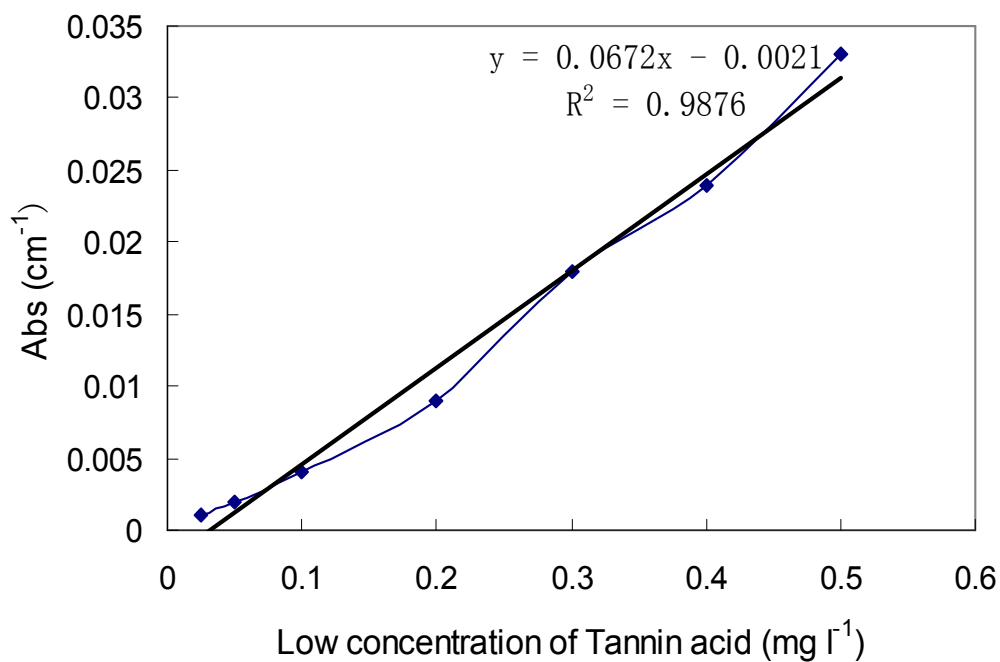


Figure 4.3 Absorbance at 700nm with low tannin acid concentration

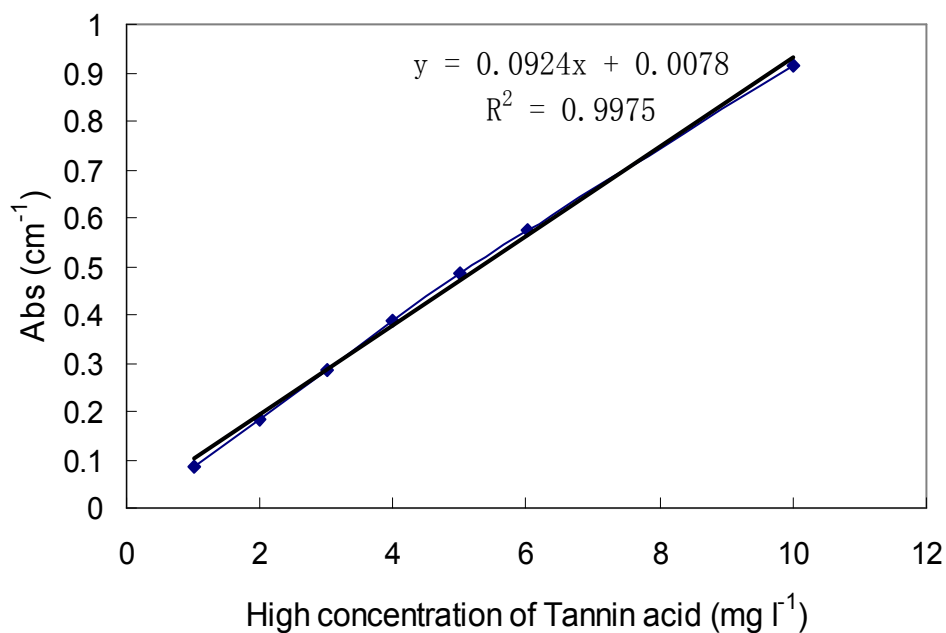


Figure 4.4 Absorbance at 700nm with high tannin acid concentration

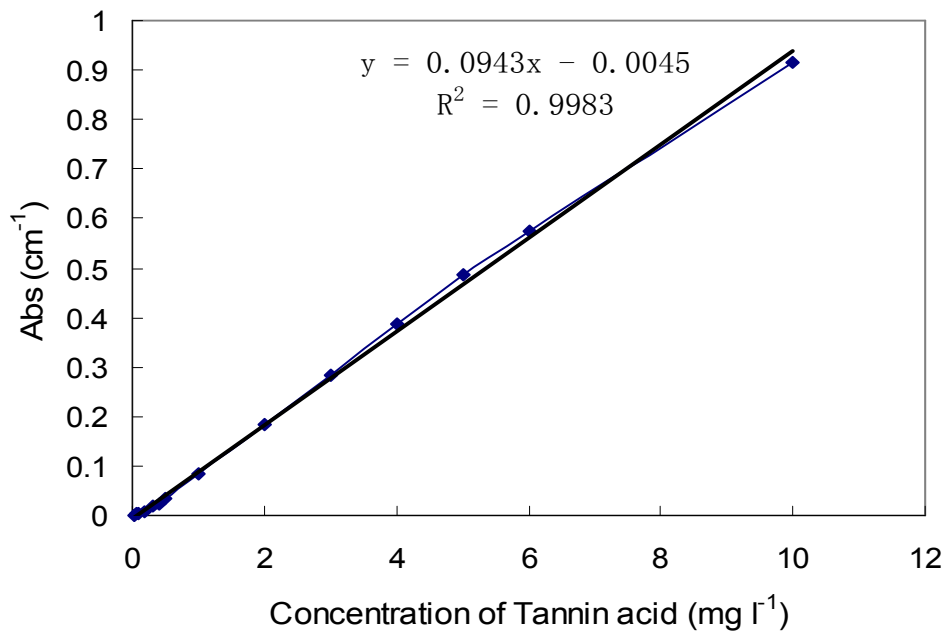


Figure 4.5 Absorbance at 700nm (10mm cell path) with whole range of tannin acid concentration

5. RESULTS: CHARACTERISATION OF TBP

5.1 Introduction

It is generally accepted that the molecular weight and charge density of polymers play important roles in coagulation mechanisms and should be taken into account for the coagulation performance. Dentel *et al.* (22) proposed that the monomer types and actual chemical structures of polymers were evidently related to their coagulation behaviors in water and wastewater treatment processes. However, sufficient attention has not been given to the improvement of the coagulation performance by optimizing the polymer structure for particular applications. To date, the theories on the coagulation mechanism of natural polymers are still at the broad and exploring stage, with, unfortunately, much of the early work having been done on poorly characterized natural polymers. Studies (27, 146) on the characterisation of modified chitosan by different techniques have been undertaken in some areas, for example, biomedicine, food packaging, and the cosmetics industry, but no attempt has been made to link the structure of these natural polymers with the coagulation mechanism and their application in water treatment.

The principal aim of this study was to determine the important parameters such as charge density and molecular weight, which is believed to affect the coagulation mechanism of TBP. Furthermore, working on an assumed tannin structure, shown in Figure 2.6, the other objective of this phase of the experimental work was to identify more clearly the chemical structure and functional group of TBP through the application of different techniques. Identification of TBP was carried out by a series of standard and modified analysis methods. The experimental steps are described briefly below:

- (a) Some preliminary tests were carried out, for example, on the polymer solubility, UV absorbance and pH titration. These simple tests do not provide conclusive information about the polymer structure, but provide useful

supporting information.

- (b) The charge density of TBP was determined under varying conditions. The results provide an assumption of the amine type in the TBP monomer and information concerning the structure of condensed-tannin and the modification process.
- (c) Identification of TBP functional groups was attempted by involving FTIR and NMR methods. The useful output is compared with outputs obtained for a library of standard polymers obtained under similar experimental conditions.
- (d) Qualitative and quantitative elemental analysis was employed to provide confirmatory evidence regarding the assumption by previous steps, and further information about the structure of the monomer of TBP.
- (e) Examination of the molecular weight of TBP was obtained in the final set of tests.

Overall, the intention was to assess the monomer type and functional groups of TBP, and to estimate two important parameters, charge density and molecular weight. It was considered therefore that by employing standard or modified test methods would advance the possibility to describe the chemical properties and structure of TBP.

5.2 Characterisations of TBP

5.2.1 Dissociation, Precipitation and UV Absorbance of TBP

In order to fully identify the polymer, it is first necessary to be familiar with the basic chemical properties of TBP in solution, such as its dissociation behaviour, solubility and UV/Vis absorbance.

5.2.1.1 Dissociation of TBP in Solution

Modified tannin-based polymer was observed to be water soluble and present a low initial pH value in de-ionised water. Since the relative strength of weak acids can be found by comparing their acid dissociation constant pK_a , a pH titration was initially carried out by adding standard base (NaOH solution) to TBP solution. A titration curve contains a relatively vertical section which represents a change of pH with a small volume of standard solution. The midpoint of the titration curve corresponds to the equivalence point for the reaction. Based on the TBP—base titration curve (Figure 5.1), the value of an approximate dissociation constant (pK_a) was determined.

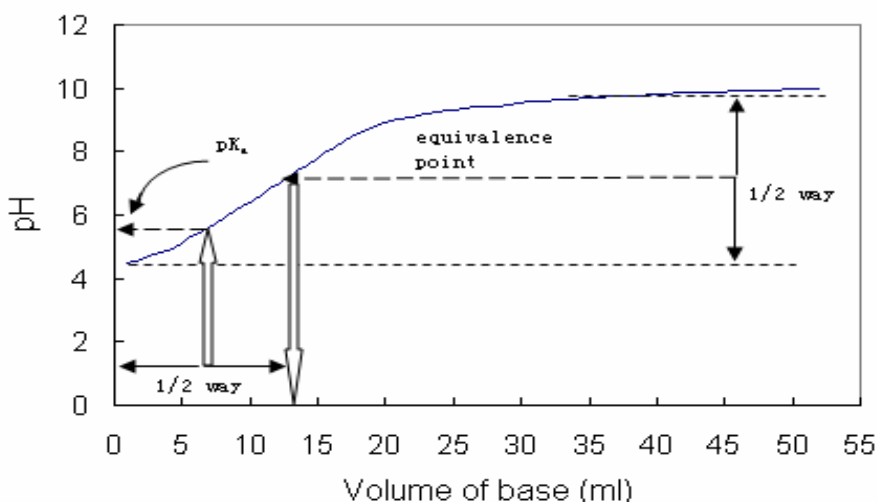


Figure 5.1 TBP solution titration curve: 100ml Tannin (0.03g l^{-1}) titrated with 0.001mol l^{-1} NaOH

From the pH titration curve, it can be seen that the titration curve of TBP solution is different from a strong acid- strong base titration curve. For a strong acid-strong base titration curve, the change in pH near the equilibrium point is sharper, so it is easier to locate the equivalence point with good precision. However, as can be seen from Figure 5.1, the pH titration curve is not indicative of the end point, which occurs when the acid and base in solution are stoichiometrically equivalent. Therefore, assuming the equivalence point is

around 12-14 ml NaOH, the pKa value is equal to the pH halfway to neutralization (equivalence point), around 5.6-6. This standard method only gave a rough pKa value of TBP, due to the different dissociation constants of multi function groups of TBP. Some researchers have reported the pKa value of the amine group on the polymer in the range of 5.5 to 6.5, depending on the source of the polymer (147).

5.2.1.2 Solubility of TBP in Solution

The influence of pH was observed on the solubility of TBP in solution by diluting the filtered 1 g l⁻¹ stock solution with pH buffers to produce a series of solutions with concentration from 0.02 g l⁻¹ to 0.1 g l⁻¹ over the pH range from 3 to 9. No precipitation was evident for pH<6 at any TBP concentration solution after 6 hours. The results shown in Table 5.1 to 5.4 indicate that the precipitation of TBP is pH-dependent. At pH≥6 some insoluble products were produced in solution during 6 hours deposition. It was found that the insolubility of TBP is about 25-35% at pH 6; these evidences from precipitation tests supported the belief that the relatively low value of the intrinsic pKa of TBP, which was determined in previous section, is associated with tannin insolubility in water above pH 6. However, the insolubility of TBP at the pH range of 7-9 is very high (~45-55%), but does not change much with TBP concentration increasing. This unexpected pattern of insolubility indicated that TBP may be a mixture of hydrophilic and hydrophobic fractions.

TABLE 5.1 Insoluble materials for a range of TBP solutions with pH 6

Concentration of TBP (g l ⁻¹) at pH=6	Pre-weight paper (g)	Final Weight1 after dry(g)	Final Weight2 after dry(g)	Final Weight3 after dry(g)	Precipitate (g)	Percentage %
0.04	0.5764	0.5899	0.5872	0.5875	0.0111	27.75
0.06	0.5744	0.5992	0.5897	0.5901	0.0157	26.16
0.08	0.5754	0.6024	0.6018	0.6016	0.0262	32.75
0.1	0.583	0.6153	0.6196	0.6195	0.0365	36.5

TABLE 5.2 Insoluble materials for a range of TBP solutions with pH 7

Concentration of TBP (g l ⁻¹) at pH=7	Pre-weight paper (g)	Weight1 after dry(g)	Weight2 after dry(g)	Weight3 after dry(g)	Precipitate (g)	Percentage %
0.04	0.5762	0.5962	0.5944	0.5944	0.0182	45.50
0.06	0.5761	0.6094	0.6055	0.6052	0.0291	48.50
0.08	0.5767	0.6162	0.6133	0.613	0.0363	45.37
0.1	0.5704	0.6162	0.614	0.6138	0.0434	43.40

TABLE 5.3 Insoluble materials for a range of TBP solutions with pH 8

Concentration of TBP (g l ⁻¹) at pH=8	Pre-weight paper (g)	Weight1 after dry(g)	Weight2 after dry(g)	Weight3 after dry(g)	Precipitate (g)	Percentage %
0.02	0.5647	0.5754	0.5742	0.5738	0.0091	45.50
0.04	0.5678	0.5856	0.5838	0.5839	0.0161	40.25
0.06	0.5644	0.5983	0.5957	0.5954	0.031	51.60
0.08	0.5768	0.6199	0.619	0.6189	0.0421	52.60
0.1	0.5619	0.6091	0.6083	0.6078	0.0459	45.90

TABLE 5.4 Insoluble materials for a range of TBP solutions with pH 9

Concentration of TBP (g l ⁻¹) at pH=9	Pre-weight paper (g)	Weight1 after dry(g)	Weight2 after dry(g)	Weight3 after dry(g)	Precipitate (g)	Percentage %
0.02	0.5667	0.5791	0.5766	0.5765	0.0098	49
0.04	0.5843	0.6064	0.604	0.6036	0.0193	48.25
0.06	0.5696	0.6049	0.603	0.6028	0.0332	55.34
0.08	0.5864	0.6478	0.6299	0.6295	0.0431	53.85
0.1	0.5722	0.6294	0.6218	0.6215	0.0493	49.30

5.2.1.3 UV/visible Light Absorbance

UV/visible light absorbance tests were carried out using an Ultraviolet Spectrophotometer (10mm quartz cell path; wavelength range from 190nm to 800nm) for 0.02g l⁻¹, 0.05g l⁻¹ and 0.1g l⁻¹ TBP solutions (no buffer). Figure 5.2 shows two absorbance peaks at wavelengths of 210±2nm and 280±5nm were found for TBP solutions with a range of concentrations, and the maximum absorption occurred at 210nm. These two distinct absorbance peaks at two wavelengths indicated the complex nature of TBP.

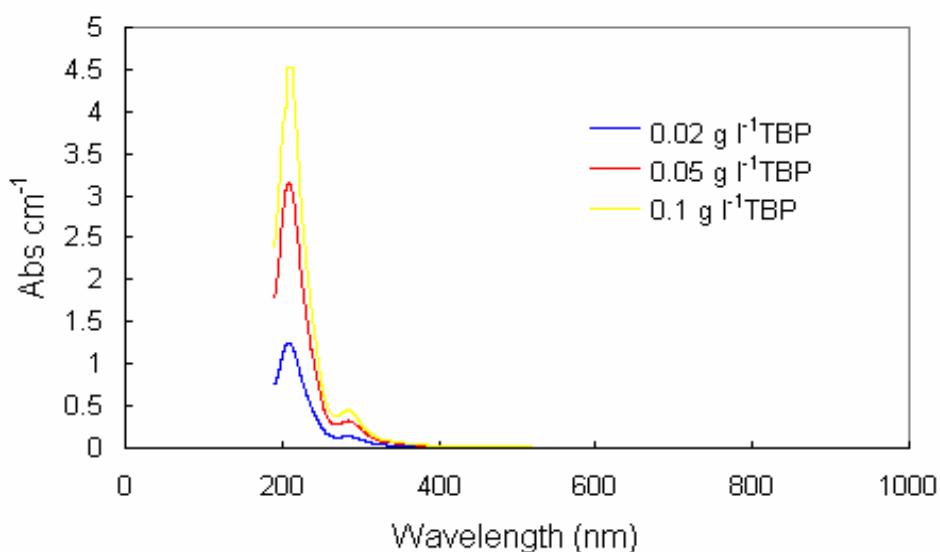


Figure 5.2 UV-Vis scan of TBP solution with a series of TBP concentrations

The results in Figure 5.3 clearly demonstrate the influence of pH upon the UV absorbance of TBP solution. For the TBP solutions at pH 4, 6 and 8, after 6 hours and filtration, there is an approximate linear relationship between UV absorbance (at 210nm) and TBP concentration in accordance with Beer's Law; that is, UV absorbance of solution increased directly with TBP concentration (148). However, the values of absorbance at 210nm decreased with the pH increasing, indicating the loss of precipitated polymer at $\text{pH} \geq 6$. It was observed that at pH 9, there was a non-linear relationship between UV absorption and TBP concentration, indicating a significant change in the chemical properties of the TBP. Therefore, UV absorbance measurement is infeasible to give a quantitative analysis for the content of TBP solution at different pH values.

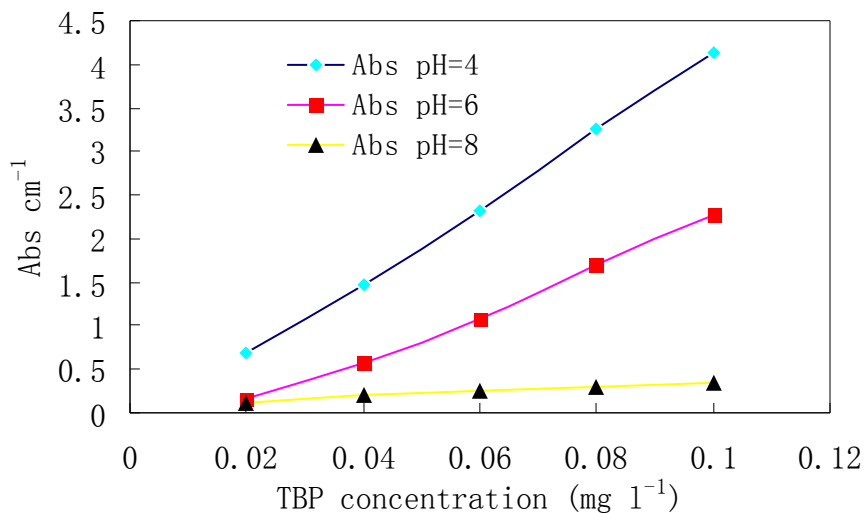


Figure 5.3 Variation of absorbance at 210nm (10mm cell path) with TBP concentrations (pH = 4, 6 and 8)

5.2.2 Variation of Charge Density with pH and Time

Colloid titrations with TBP solutions at a constant concentration of 0.05 g l⁻¹ were carried out to determine the variation of charge density with pH using PPVS of pre-determined charge density (0.512×10^{-3} meq l⁻¹). The titration end-point was measured by visual and spectrophotometric methods. For comparative purposes, a study was made of a quaternary ammonium polymer, polyDADMAC (DB 45 SH). In this case, the charge density is expressed as the milliequivalents of positive charge per gram of polymer. Through confirming the charge density of polyDADMAC, it was found that the spectrophotometric method (procedure 2) was more accurate than the visual method because the repeatability error was much smaller. Figure 5.4 shows the charge densities of TBP and polyDADMAC prepared in buffer solutions for 3 hours in the pH range from 4 to 9 and measured by spectrophotometry. It is clearly seen that the charge density values of polyDADMAC are in the range of 6.1 to 6.2 meq g⁻¹, and the value is not pH sensitive over a wide range of solution pH. This result agrees with the observations of Bolto and Gregory (19), that the charge density of

polyDADMAC is generally about 6.2 meq g^{-1} and unaffected by changes in pH. In contrast, the charge density of TBP was found to be pH-dependent as indicated in Figure 5.4. The results show that the charge density decreased from 3.07 meq g^{-1} to 0.2 meq g^{-1} with increasing pH values from 4 to 9.

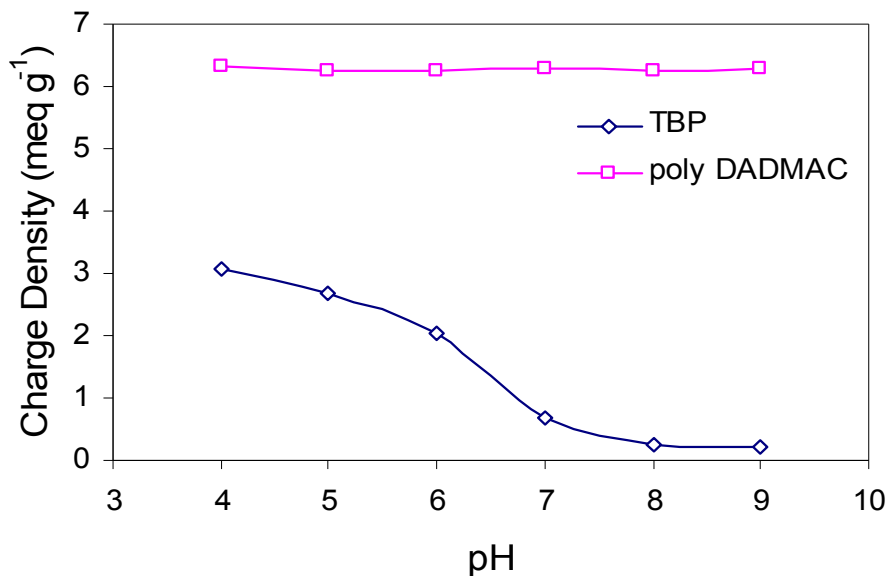


Figure 5.4 Charge density of TBP as a function of pH

In addition to the influence of pH, the charge density of TBP is also observed to be subject to an ‘ageing’ effect. Figure 5.5 represents the temporal variation of charge density of TBP at different pH. In this case, the initial charge density of 0.05 g l^{-1} TBP solution was colloid titrated within 2 standing hours, which give a higher value, compared with the results in Figure 5.4. Inspection of the varied curves of charge density revealed that with TBP storage time increasing, the charge density significantly decreased at all pH values. However, it is evident that even after 48 hours, the charge density was still significant at $\text{pH} < 7$. These phenomena are clearly related to the previous observations concerning the TBP solubility, and dissociation chemistry.

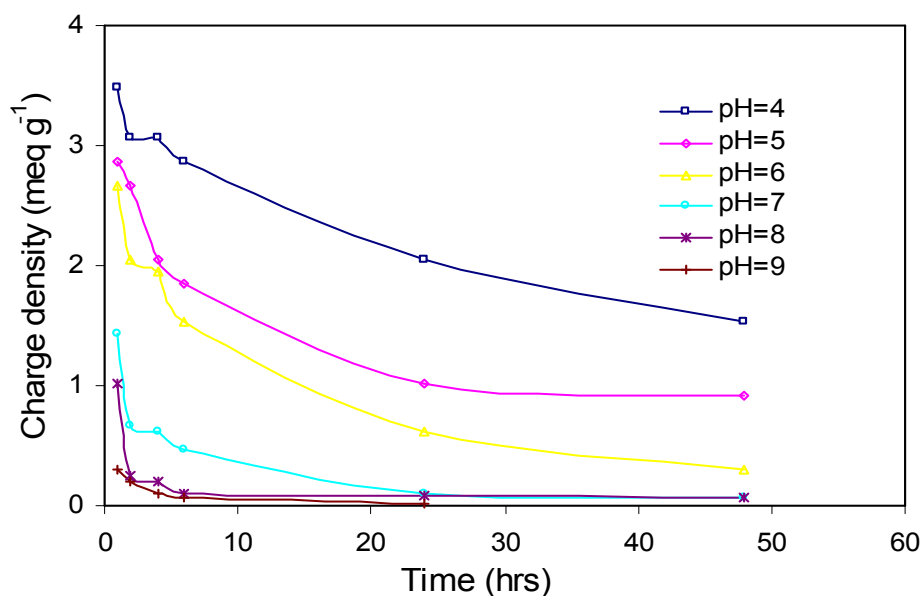


Figure 5.5 Temporal variation of charge density of TBP at different pH

5.2.3 Elemental Content Analysis

The elemental content of TBP was measured by several methods, namely: ICP for the metal elements; CHN for carbon, hydrogen and oxygen; and Argentometric titration for chlorine. The carbon content was validated by TOC analysis, and the nitrogen was validated by the Kjeldahl method. The results are shown in Table 5.5. These provide useful information in interpreting the repeating structure of TBP by considering the ratio of the elements. It is reasonable to assume that remaining content (~ 29%) of the polymer is oxygen.

TABLE 5.5 Results of elemental analysis of TBP product (mass %)

TBP Element	C	H	N	Metal (Sum)	Cl	Total
Mass %	42.77	5.88	7.16	1.6	13.4	70.81

5.2.4 Chemical Functional Group/Bond Analysis

Two major spectroscopic methods, Fourier Transform Infrared (FTIR)

and Nuclear magnetic resonance (NMR), were used to qualitatively study the chemical groups and bond types of TBP in this study.

5.2.4.1 Analysis of FT-IR Spectra

The absorbance of infrared rays plotted separately against wave number for TBP and tannin extract is displayed in Figure 5.6 and Figure 5.7. Based on the region of the absorption peaks and the notional structure of the TBP it is possible to speculate on the nature of some of the functional groups. Comparing the spectra in Figure 5.6 and 5.7, it can be seen that most of the functional groups in TBP are present in the spectra of tannin extract. In both spectra, the 1040-1150 cm^{-1} absorption band is attributed to C-O stretching; the 1370-1470 cm^{-1} absorption band belongs to the $-\text{CH}_3$ group; and the 700-900 cm^{-1} absorption band is characterised by adjacent or isolated H and aromatic H. The 2360 cm^{-1} absorption band is from the small CO_2 doublets, which appears in many spectra due to inequalities in path length. The 3600-3850 cm^{-1} absorption band is caused by sharp O-H stretching. It is also clear that the similar appearances of absorption peaks in Figure 5.6 and Figure 5.7 indicated that the absorbance bond between 1550 and 1600 cm^{-1} belonged to a benzene group rather than an amine group (148).

The distinct absorbance peak between 3300 and 3600 cm^{-1} in the FTIR spectrum of TBP is thought to be attributable to amine groups, for example, $>\text{N-H}$, $-\text{NH}_2$ and $-\text{NH}_3^+$. This absorbance peak is not shown in Figure 5.7 by the FTIR analysis of tannin extract, which was assumed not to have any significant nitrogen in the structure. This conclusion is consistent with the results of the Kjeldahl method which showed that for TBP, the organic-N content was found to be approximately 6.5% and inorganic ammonia-N content was approximately 1%, compared with a neglectable N content in tannin extract by the Kjeldahl method.

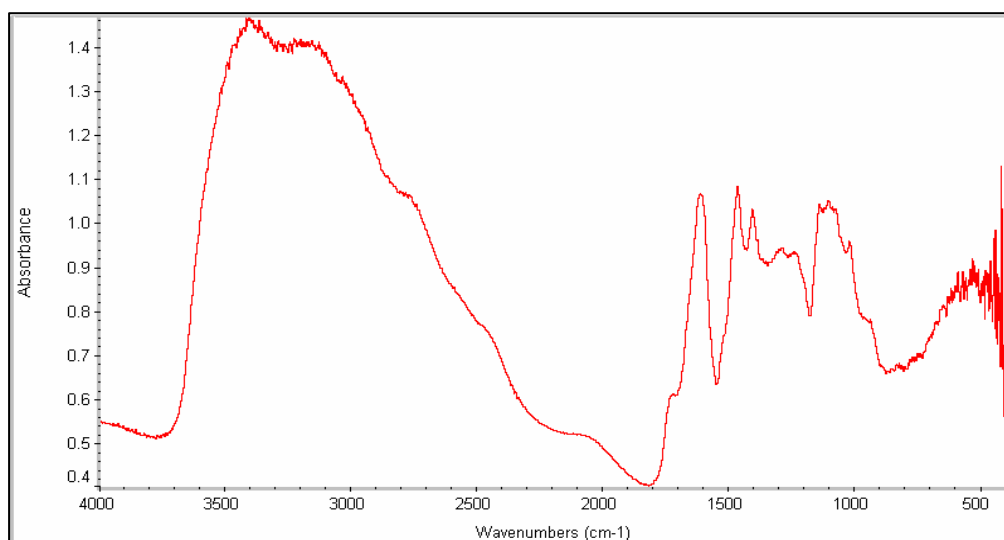


Figure 5.6 FT-IR spectra of TBP

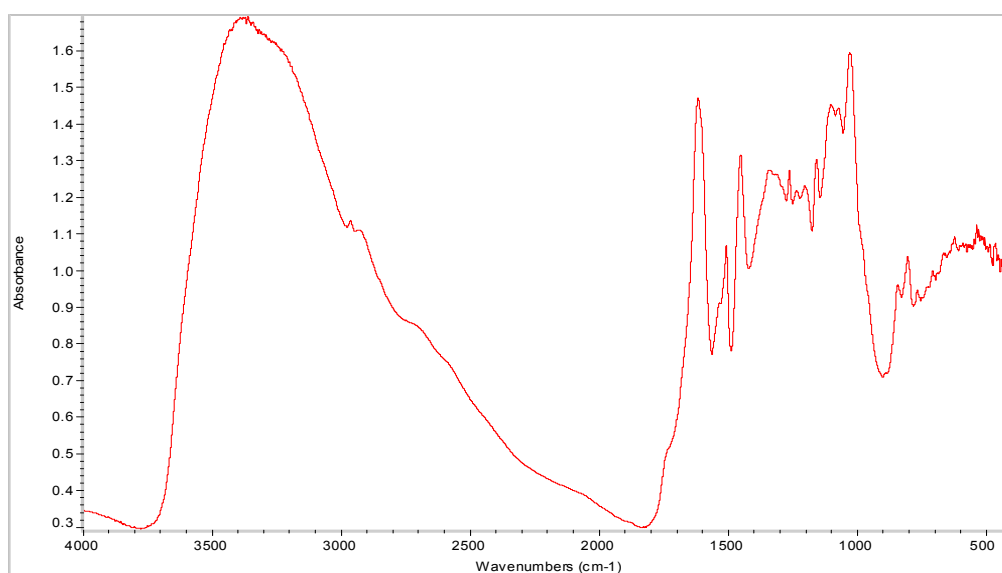


Figure 5.7 FT-IR spectra of tannin extract

5.2.4.2 Analysis of ^1H NMR Spectra

The resulting spectrum from the ^1H NMR analysis of the TBP solution is presented in Figure 5.8. Although ^1H NMR is a very versatile structural elucidation technique for hydrogen-containing compounds, the interaction between neighbouring hydrogens makes the resulting spectrum very complex, as can be observed from inspection of Figure 5.8 in the 2.5-4.4 ppm region. An

initial analysis of the spectrum has resulted in the breakdown of the data into three distinct regions: signals due to alkane protons (2.5-4.4 ppm); alkene protons (4.5-5.5 ppm) and aromatic protons (6.5-8.5 ppm). Several of the signals in the 1-4 ppm region could also be attributed to the numerous magnetically different O-H groups around the basic TBP structure. In addition, one of the signals in the 6.5-8.5 ppm region may also be tentatively attributable to the presence of an amine salt.

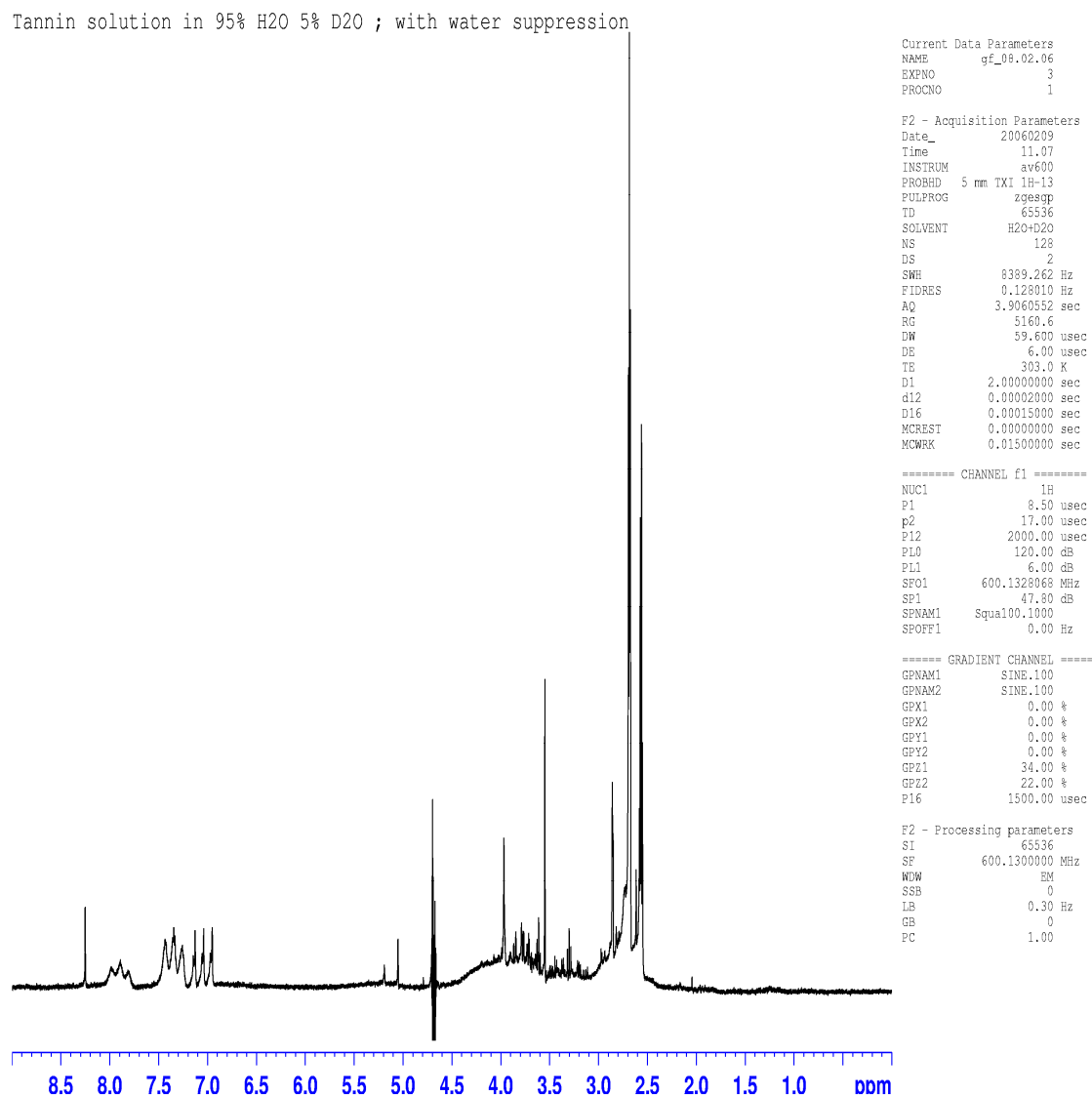


Figure 5.8 ^1H NMR spectra of TBP

5.2.5 Analysis of Molecular Weight

5.2.5.1 Molecular Weight Determined by SEC

The molecular weight of TBP can be defined experimentally by size exclusion chromatography (SEC). However, the precision is dependent upon the adequacy of reference polymers for calibration. The results from the SEC in Figure 5.9 show a narrow range of MW distribution for the TBP, with a mean MW differing widely from a possible 15 million (from calibration with polystyrenes) to 800,000 (from calibration with polysaccharides). Since the oxygen content deduced by the element analysis is approximately 30% by weight, the standard polysaccharides (highly oxygenated polysaccharides) were considered more appropriate to create the calibration curve to measure MWs in this case (139). The elution time for TBP was lower than 14 min, which is beyond the standard calibration curve (elution time range: 14min to 20min for standard polysaccharides). This indicated that the molecular weight was greater than 800,000 in comparisons with polysaccharide. Some additional information was provided by SEC, which is that another peak occurred at the elution time of 24 min, with a mean MW of 2-300. Even though the elution time is out of the standard calibration range, the result from the SEC showed that the TBP sample is a mixture of high molecular weight polymers (>800,000) and some low molecular weight components (<200-300), probably non-polymerized monomer.

Through the SEC study, the full dissolubility of TBP in NMP solvent was concerned. Therefore, further MW measurement by light scattering was taken.

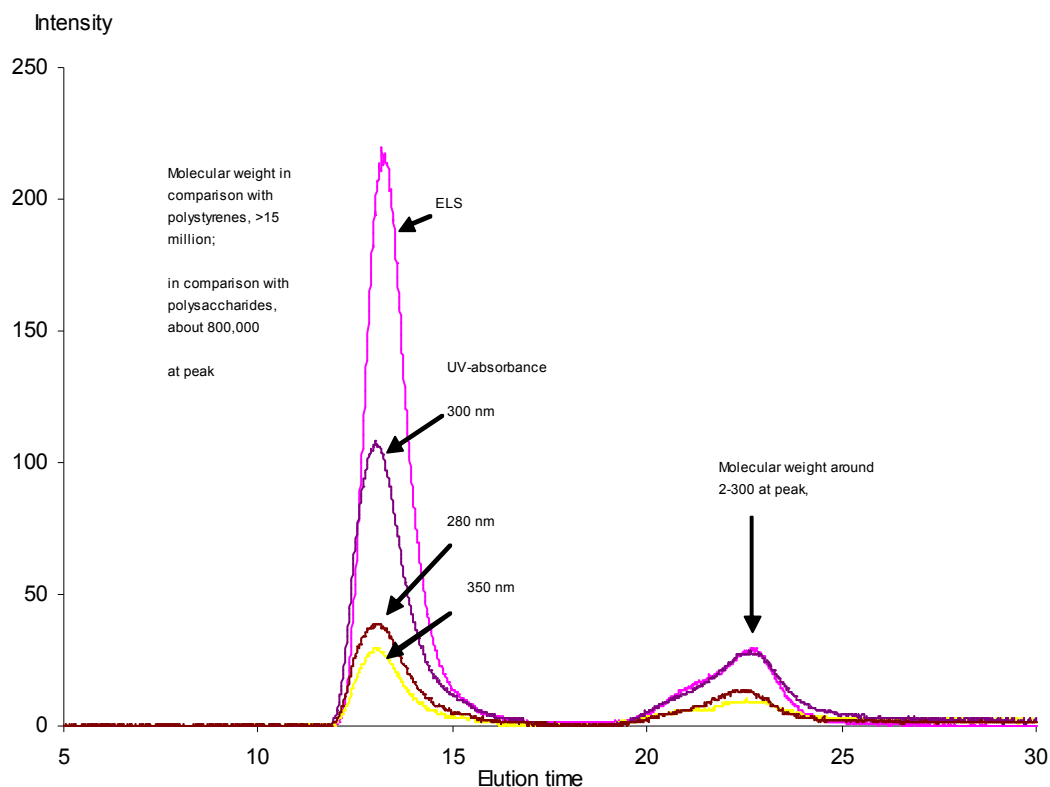


Figure 5.9 Elution curve of TBP by size exclusion chromatography

Note: ELS is the absorbance by evaporative light scattering detection.

5.2.5.2 Molecular Weight Determined by Light Scattering

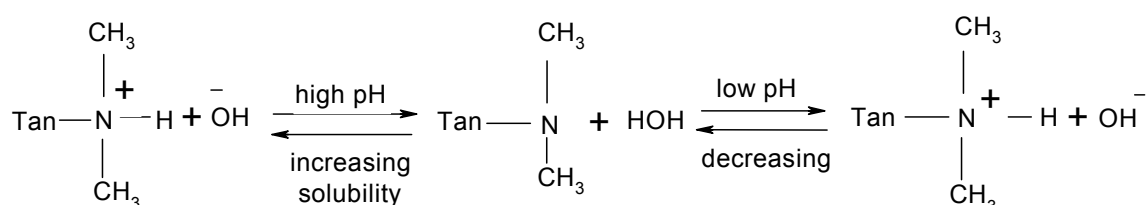
Light scattering is alternatively used to determine the molecular weight of polymers in solution. In order to calculate the molecular weight by the Zimm plot technique, it is necessary to know the refractive index/polymer concentration ratio (dn/dc) (149). The dn/dc value of TBP at 633nm and 25°C was determined to be 0.1846 ml g^{-1} (Determined by Wyatt Technology UK Ltd, see Appendix II). The construction of the Zimm plot of TBP was carried out by a Wyatt DAWN EOS Light Scattering Photometer and the plot is shown in Appendix III. In the Zimm plot, each combination of TBP concentration and scattering angle is represented by a solid circle, therefore, the molecular mass for tannin based polymer was determined as $5.7 \times (\pm 2.8) 10^5 \text{ g mol}^{-1}$, and the root mean square (rms) radius, or “radius of gyration” was $78.4 (\pm 19.3) \text{ nm}$.

5.3 Discussion

A series of analytical methods have been undertaken to fully understand the character and properties of TBP. A preliminary investigation by some standard methods showed that TBP solution exhibits a buffer behaviour and gives a dissociation constant pKa of 5.6-6. This assertion is further supported by the range of general pKa values for an amine group on the polymer, which is from 5.5 to 6.5 (150). The relatively low value of the intrinsic pKa of its amino functions may be linked to TBP's relative insolubility in water above pH 6. It was found that at $\text{pH} \geq 6$ the degree of insolubility increased dramatically with pH value (insolubility: ~25-35% at pH 6; ~40-55% at pH 7, 8 and 9). This strongly favours the conclusion that the solubility of amines increases with decreasing pH, as long as the solubility product of the protonated amine and the particular counter ion are not yet reached (151). These results point out the competition between protonation and complexation of the amino groups in relation with their pKa, around 6.0. The weak interactions observed at $\text{pH} > 6$ reflected the small percentage of free amino groups available under these conditions. The comparable UV spectroscopic results of TBP solution at acid and alkali conditions showed the maximum absorbance value at high pH is inferior and unstable, probably due to a change in the chemical properties of the TBP. Incidentally, the existence of two prominent UV/vis absorbance peaks indicated the complex form of components, probably, related to the polymeric TBP and non-polymerization monomer, when TBP solid dissolved in water.

Although TBP is classed as a cationic polymer, the charge density appeared to be strongly pH-dependent and subject to "ageing" effects. Increasing the pH value from 4 to 9 decreased the charge density from 3.07 meq g^{-1} to 0.2 meq g^{-1} for a 3 hours TBP solution sample. The sharp change of charge density occurred at pH7, where the net charge on TBP was less than 1 meq g^{-1} . The reason for this is that as a Mannich-reaction polymer, the cationic monomer of

TBP is non-quaternized. Thus, the cationic TBP is likely to be associated with a tertiary amine group, R_3NH^+ , which deprotonates at high pH, so variations in solution pH will affect the charge density. The mechanism of solubility and charge density can be described as:



More specifically, phenolic hydroxyl groups present on TBP have weak tendencies to lose the H^+ ion, thereby increasing the anionicity. This slow process of deprotonation at the hydroxide sites of TBP could be used to explain the diminished trend of charge density with time (at pH4, the charge density decreased from 3.07 meq g^{-1} to 2.04 meq g^{-1} after 24h).

The amine group on the TBP was further characterized by 1H NMR and FT-IR measurement in comparison with the results of tannin extract in this study. Both the NMR and FTIR analyses qualitatively and consistently identified the presence of the main functional groups, for example, aromatic rings; NH stretch; C-O stretching; O-H stretching; $-CH_3$ and amine salts, therefore aiding the evaluation of the structure of TBP.

The proposed monomer structure of TBP outlined in Figure 5.11 was derived from the experimental results and the information from the Mannich reaction of condensed tannin.

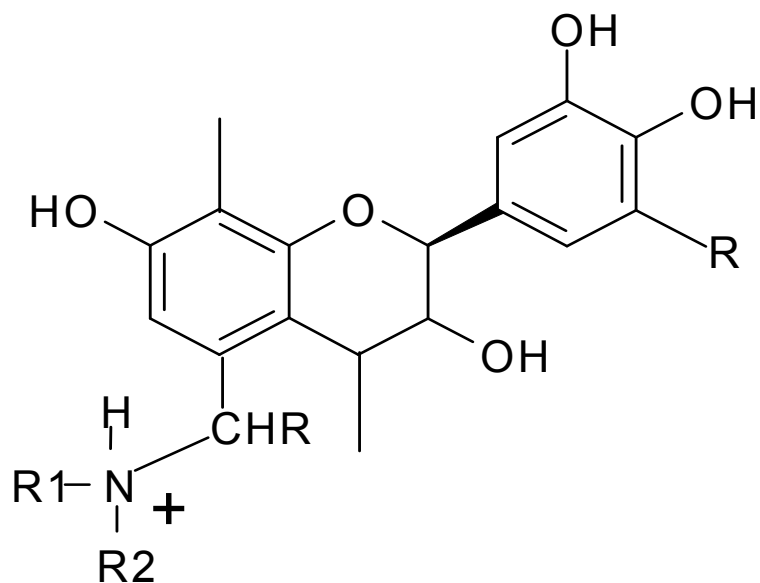


Figure 5.10 The proposed basic repeating unit of TBP

In Figure 5.11 it is believed that the CHR is the remainder of the aldehyde compound after the carbonyl oxygen has left. R₁ and R₂ are hydrogen or other organic moieties that were part of the original amino compound.

From the mass proportions, an approximate elemental ratio for the polymer can be deduced as: N: O: C: H = 1: 3.6: 7: 11.5. Clearly, there are some inconsistencies between the experimental results and the structure hypothesised. With the assumption that there are 16 carbon atoms per monomer group, there appear to be more nitrogen atoms present to account for the observed atomic ratio of 1:7 (N:C). From theory, in the Mannich reaction the molar ratio of the primary amine to the tannin monomer (assumed to contain 16 carbon atoms) is about 2.3:1. However, some studies (129) indicated that the preferred molar ratio of the primary amine, which was generated from the first reaction of an aldehyde and an amino compound, to the tannin repeating unit is in the range of about 1.5:1 to 3.0:1, which is consistent with the above theory. The less active secondary and tertiary amines were formed following the first reaction. In view of this, it can be

speculated that the solid TBP product contains additional nitrogen/amine mass which is not bound within the TBP monomer. Therefore a high amount of nitrogen was over estimated in the element content of TBP.

The molecular weight of TBP ($5.7 (\pm 2.8) \times 10^5 \text{ g mol}^{-1}$) determined by light scattering indicated that TBP is a medium-to- high MW polymer in the range of 10^5 - 10^6 g mol^{-1} and with a radius of gyration of 78.4 (± 19.3) nm. In solution, polymers adopt a random coil configuration with much smaller dimensions (usually less than 1 μm (145)). It is evident that the molecular weight of TBP determined in this study is broadly consistent with the US Patent (152), which disclosed that the average molecular weight of the tannin derived product after polymerization is generally within the range of 5,000 to 500,000.

6. RESULTS: COAGULATION ACTION OF TBP IN MODEL WATER

6.1 Introduction

The coagulation mechanisms of cationic polymers are believed to be a combination of charge neutralisation and polymer bridging. Even though it is still not clear which of these two mechanisms is predominant in the flocculation process, some investigations (153,154) have found that, for a given polymer, there was an optimum concentration, beyond which poorer flocculation performance was found. When charge neutralisation played the main role in the coagulation process, the optimal polymer concentration corresponded to the concentration required for zero particle surface charge. In the same way, when polymer bridging was the principal mechanism of coagulation, the optimum dosages should be directly proportional to the total particle surface area and hence to the particle concentration (19). Charge neutralisation of dissolved humic substances is thought to be the dominant mechanism of coagulation, specifically with cationic polyelectrolytes. There is a lot of evidence that the optimum dosage corresponds closely with charge neutralisation and that a stoichiometric relationship exists between the anionic charge carried by the humics and the cationic charge of the added polyelectrolyte (30).

In considering the kinetic processes of polymer flocculation for suspension particles, various types of interaction condition can be envisaged. It was well established that the rate of flocculation process depended on the concentration of polymer molecules and suspended particles, the intensity of agitation and the pH value of solution (145). These parameters are believed to greatly influence the flocculation effectiveness. In addition, ageing of polymer solutions is considered to have an important effect on their flocculation performance (19, 21). This is supported by the results of Owen *et al.* (155) who showed that polyacrylamide stock solutions, aged between 1 and 6 days, gave optimal flocculation after 72 h. Several 'screening' researches using different

polymers (16) to account for the influence of molecular weight on the flocculation effectiveness have been carried out, and there are some experimental results which can be cited as giving qualitative or quantitative evidence of their relationship (6, 31).

The strength of flocs formed during coagulation depends on many factors, such as the type and amount of coagulants, the nature and quantity of interacting contaminants and the hydrodynamic conditions prevailing during floc formation. An individual floc will break if the stress applied at its surface is larger than the bonding strength within the floc. Thus, increased floc compaction is believed to increase floc strength due to an increase in the number of bonds holding the aggregate together (78). The aggregates (flocs) formed by polymer bridging are considered to be much stronger than those formed by metal salts (19). Gregory (156) has stated that when comparing different flocs formed by the same coagulant, the size of the floc (or indirectly, the flocculation index) for a given shear rate indicates floc strength. It is believed that the density of aggregates increases as their size decreases (157), and increased floc density leads to greater floc strength (77). Floc size in a sheared suspension is limited by floc strength.

In general, the literature suggests that the coagulation performance of TBP has as yet only been investigated superficially, and very little attention has been given to the coagulation mechanism, stoichiometry, influences on performance and floc strength. A much clearer understanding of the reaction mechanism is required to optimize the application of TBP. In this study, to fully evaluate the fundamental mechanism of coagulation with the TBP, the coagulation performance of TBP was conducted by laboratory tests using, separately, clay suspensions (kaolin powder) and humic acid (HA) solutions as model water. Through the use of a 2 L Gator jar test reactor and PDA measurements, the optimal dosages of TBP in the pH range of 4-9 were

determined; this was to assess the relative importance of different coagulation mechanisms of TBP. Furthermore, the stoichiometry and the effect of TBP ageing phenomena and initial mixing speed were investigated. The results collected from the measurement of the turbidity reduction in clay suspensions, and the removal of UV-Visible absorbance and non-purgeable dissolved organic carbon (NPDOC) in HA solutions, in conjunction with the observation of floc strength formed by TBP were compared with the data obtained from the study of polyDADMAC and alum as coagulants.

6.2 Coagulation Mechanisms Using TBP as Sole Coagulant

6.2.1 Coagulation of Kaolin Suspensions

Using the PDA test method, the coagulation of 50 mg l⁻¹ kaolin suspension for a given pH in the range of 4-9, was conducted to determine the optimum dosage of TBP. In addition, at the end of the PDA monitoring period, the residual turbidity after settling for 30 mins was measured to further confirm the performance of the TBP. The results of flocculation tests in terms of the FI response and residual turbidity with different TBP dosages at pH4, 7 and 9 are shown in Figures 6.1-6.6.

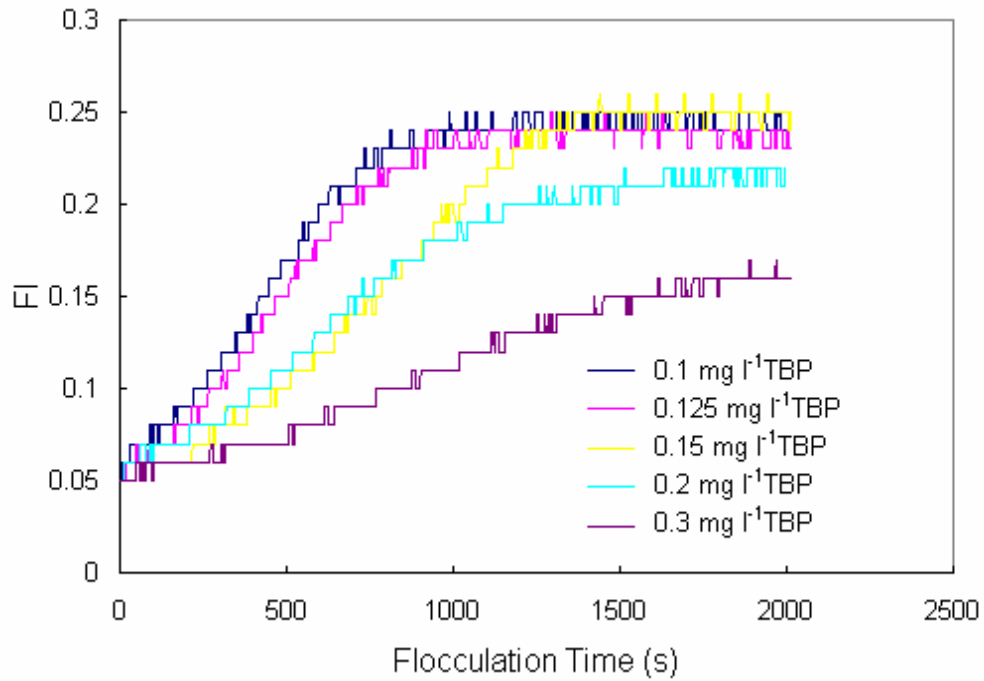


Figure 6.1 Flocculation index response with TBP dose at pH4 (50 mg l⁻¹ kaolin suspension)

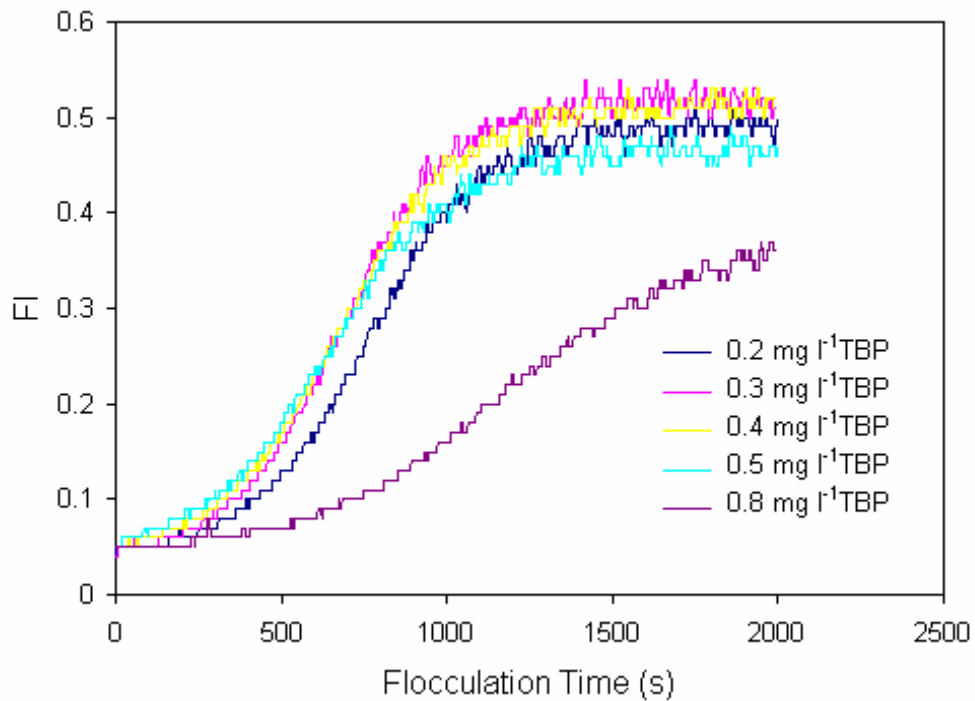


Figure 6.2 Flocculation index response with TBP dose at pH7 (50 mg l⁻¹ kaolin suspension)

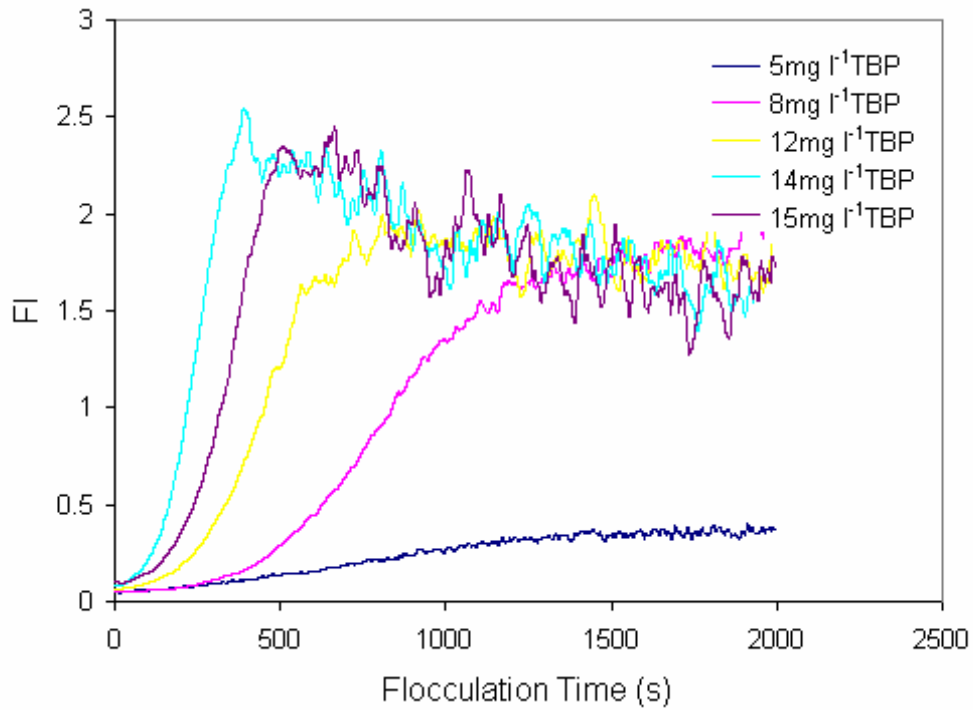


Figure 6.3 Flocculation index response with TBP dose at pH9 (50 mg l⁻¹ kaolin suspension)

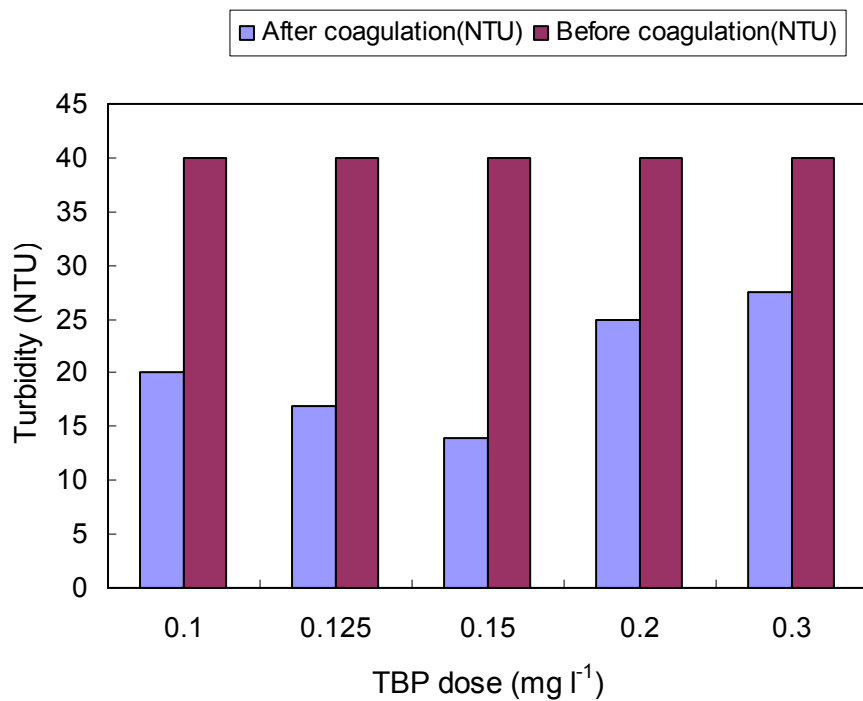


Figure 6.4 Residual turbidities before and after coagulation using TBP at pH 4 (50 mg l⁻¹ kaolin suspension)

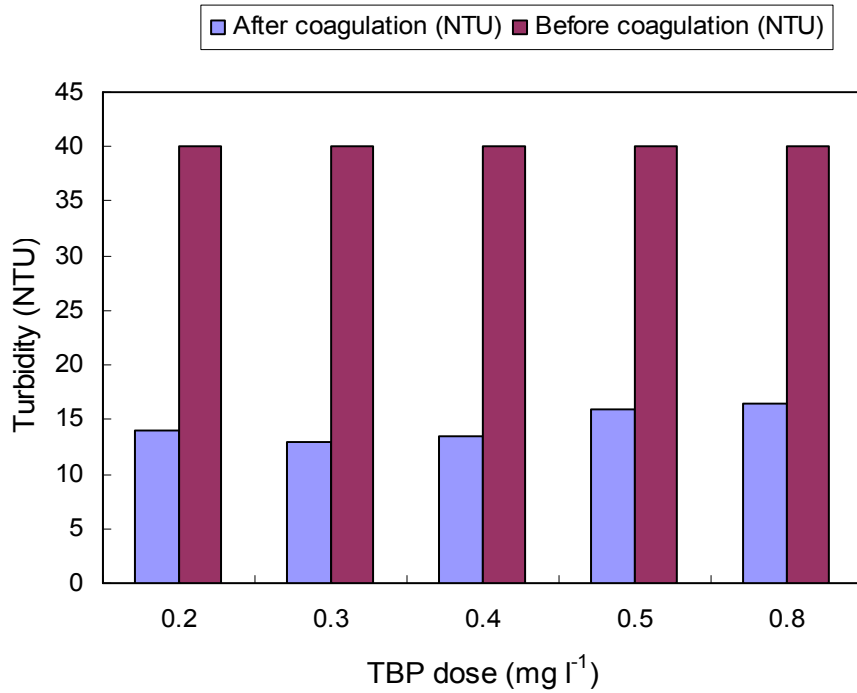


Figure 6.5 Residual turbidities before and after coagulation using TBP at pH 7
(50 mg l⁻¹ kaolin suspension)

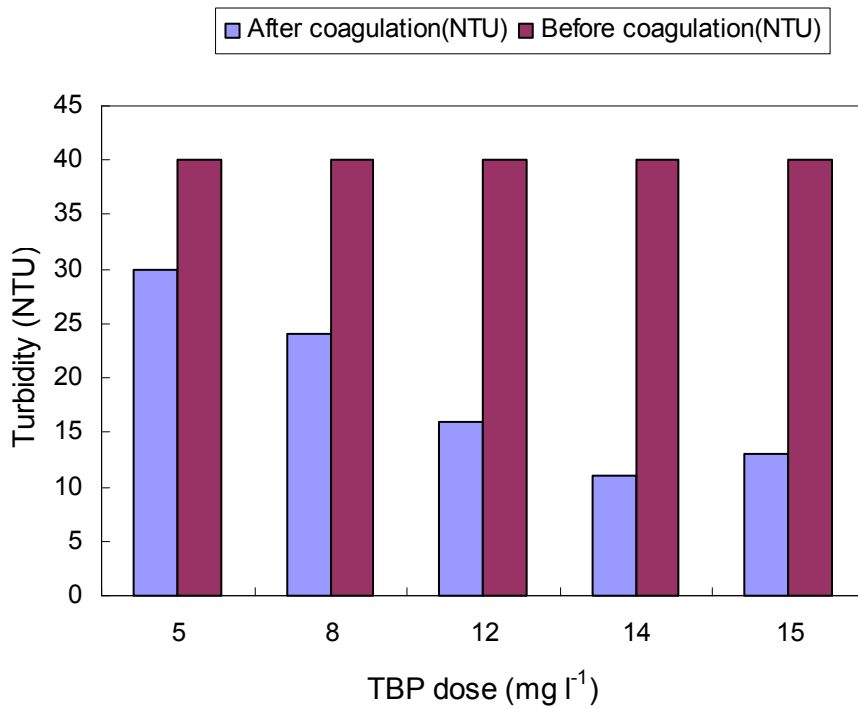


Figure 6.6 Residual turbidities before and after coagulation using TBP at pH 9
(50 mg l⁻¹ kaolin suspension)

The results given in Figures 6.1, 6.2, and 6.3 show that, near the optimum TBP dosage, the flocculation index rises rapidly with time and reaches a steady maximum value. At lower and higher dosages, less steep rises and lower maximum values are found, which indicate a poorer flocculation. At excess TBP concentrations, the negative particle (clay particle) surfaces become saturated with adsorbed polymer and the particles are re-stabilized. The optimum dosages are taken as those giving the steepest increase in FI value and agree well with those obtained by the measurement of residual turbidity, which can be seen in Figures 6.4, 6.5 and 6.6. The optimum dosage for TBP in the pH range from 4 to 9 was determined, and the results of the flocculation index and residual turbidity and residual tannin are summarised in Table 6.1. The reason for the declining FI values after the maximum value is reached, at pH 9 (Fig 6.3), is that the large sized flocs can not be kept uniformly dispersed in solution at the slow speed (50rpm; 48 s⁻¹), since large flocs were observed to accumulate on the bottom of the jar and are intermittently re-suspended.

TABLE 6.1 Comparison of coagulation performances of TBP (50 mg l⁻¹ kaolin suspension) with different charge density at different pH

pH	Charge Density (meq g ⁻¹)	Optimum Dosage (mg l ⁻¹)	FI	Residual Turbidity (NTU)	Residual Tannin (mg l ⁻¹)
4	3.07	0.15	0.25	14.5	0.088
5	2.66	0.25	0.32	18.5	0.090
6	2.05	0.25	0.35	17	0.097
7	0.67	0.3	0.52	13	0.099
8	0.26	12.5	1.6-1.8	12	0.421
9	0.21	14	2.3-2.5	11	0.449

From Table 6.1, it can be seen that with pH increasing from 4 to 9, the optimum dosage of TBP increased from 0.15 mg l⁻¹ to 14 mg l⁻¹, with an

increasing residual tannin matter in final water. The most significant increase of the optimum dose occurred at pH 8 and 9. In addition, the residual tannin matter in the final treated water was very low (less than 1 mg l^{-1}), due to the very small amount of initial TBP used as coagulant at low pH, and the good coagulation effectiveness at high pH. Also, at pH 8 and pH 9, the size of flocs (indicated by the FI) was distinctly larger than the size of flocs at pH 7 and below. These results seemed to be consistent with the observation that with increasing pH value, the charge density of TBP decreased, thus more TBP was needed to neutralize the negative particles in the model water. At high pH (8 and 9), the charge density of TBP was very low, close to zero, and precipitation occurred, therefore, the performance of flocculation suggested that polymer bridging and/or adsorption on to precipitating TBP (“sweep” coagulation) is considered as the dominant aggregation mechanism.

6.2.2 TBP Precipitation Measured by PDA

The previously observed TBP precipitation phenomenon in blank water at pH 7 and 9 was investigated using the PDA in order to get quantitative information of the precipitation kinetics. Using the optimum dose of TBP for each pH condition (0.3 mg l^{-1} at pH7; 14 mg l^{-1} at pH9), the precipitation response was determined and the results can be used as a reference for the coagulation tests. From the results shown in Figure 6.7 it is clear that at pH 9 the TBP precipitation was detectable by the PDA, giving a FI value about 0.25, but this response was small and unimportant compared to the FI value of kaolin coagulation with TBP at pH9. In contrast, the precipitation of TBP at pH 7 was not detectable by the PDA, probably because of the very small TBP dose (0.3 mg l^{-1}) that was added; clearly, under these conditions TBP precipitation is completely unimportant as a complicating factor in the coagulation measurements.

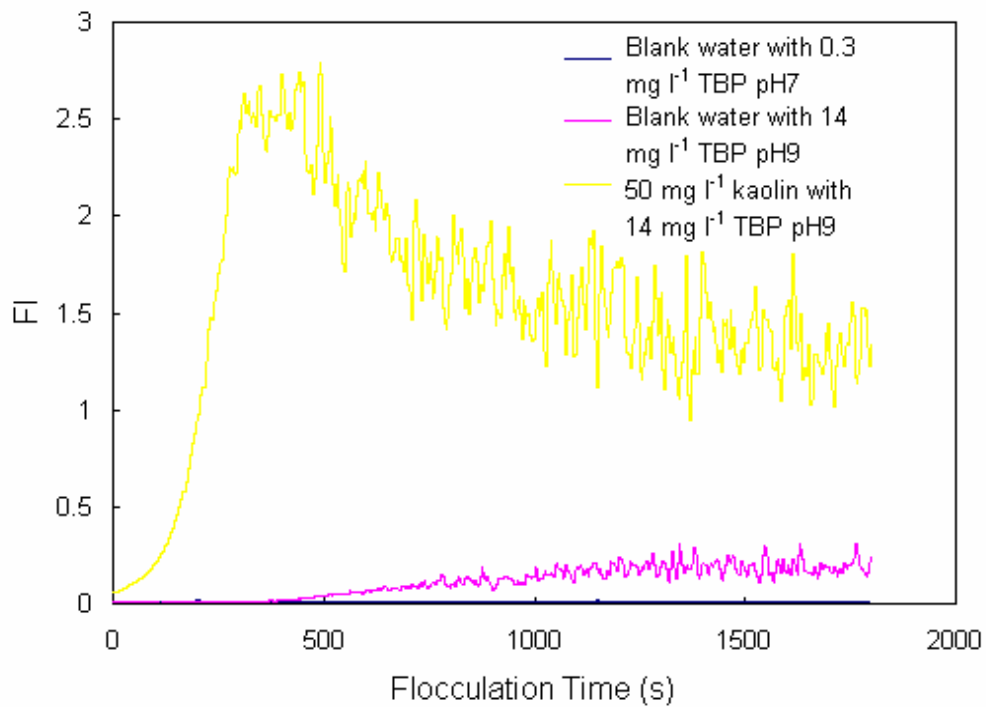


Figure 6.7 Comparison of the FI response between TBP precipitation in blank water and coagulation in kaolin suspension at pH 7 and pH 9

6.2.3 Coagulation of Humic Acid Solutions

At pH9, the model water had a lower humic acid concentration, 10 mg l^{-1} , compared to 30 mg l^{-1} at pH4 and 7; this was necessary for experimental convenience bearing in mind the much higher dosage of TBP needed at pH9. The optimum TBP dosages for the selected pH conditions were determined by the FI response of PDA and the changes in the solution NPDOC and UV-Vis absorbance.

It is commonly believed that the absorption of light at ultra-violet wavelengths is caused by aromatic compounds and other organic substances with conjugated double bonds. Although UV absorbance is a good measure of the required dose of metal coagulants, the complications caused by the very rapid

interaction of humic acid with TBP, especially at a high pH value, made it infeasible to determine the initial UV-visible absorbance (combined HA and TBP) at the beginning of the coagulation process. Hence, the initial absorbance value at 254nm and 400nm (Section 4.2.1 and 4.4.2) was assumed as the sum of the individual absorbance values of TBP and HA. By this means it was possible to evaluate approximately the coagulation performance of TBP by comparing the final absorbance value with the calculated initial value.

From the results shown in Figure 6.8, Table 6.2 and Table 6.3, the optimum dose of TBP at pH 4 appeared to be 30 mg l^{-1} (equivalent to a TBP:HA ratio of 1:1), which gave a maximum NPDOC reduction of 83.5%.

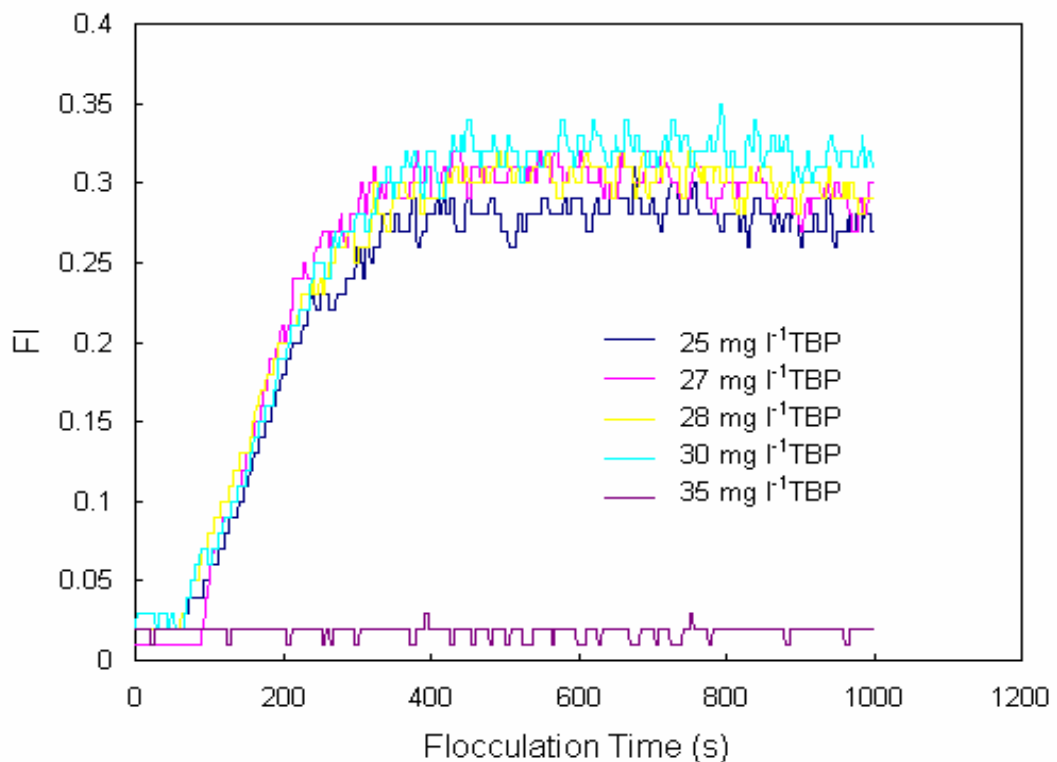


Figure 6.8 Flocculation index response with TBP dose at pH 4 (30 mg l^{-1} HA)

TABLE 6.2 NPDOC before and after coagulation with TBP dosage at pH 4
(30 mg l⁻¹ HA)

TBP dosage (mg l ⁻¹)	NPDOC 30mg l ⁻¹ HA (mg l ⁻¹)	NPDOC-TBP (mg l ⁻¹)	SUM NPDOC before coagulation (mg l ⁻¹)	NPDOC after coagulation (mg l ⁻¹)	NPDOC Reduction %
25	9.957	11.73	21.687	5.914	72.7
27	9.957	14.60	24.557	4.675	81.0
30	9.957	16.41	26.367	4.353	83.5
32	9.957	17.45	27.407	6.626	75.8

TABLE 6.3 Absorbance at 254nm and 400nm before and after coagulation with TBP dosage at pH 4 (30 mg l⁻¹ HA)

TBP dosage (mg l ⁻¹)	Abs 254nm Before coagulation	Abs 254nm After coagulation	Abs 254 nm Reduction %	Abs 400nm Before coagulation	Abs 400nm After coagulation	Abs 400 nm Reduction %
25	0.935	0.059	93.7	0.202	0.009	95.5
27	0.958	0.051	94.7	0.203	0.006	97.0
30	0.984	0.076	92.3	0.205	0.016	92.2
32	0.9997	0.097	90.3	0.206	0.016	92.2

From the results shown in Figure 6.9, Table 6.4 and Table 6.5, the optimum dose of TBP at pH 7 appeared to be 58 mg l⁻¹ (equivalent to a TBP:HA ratio of ~2:1), which gave a maximum NPDOC reduction of 83.3%.

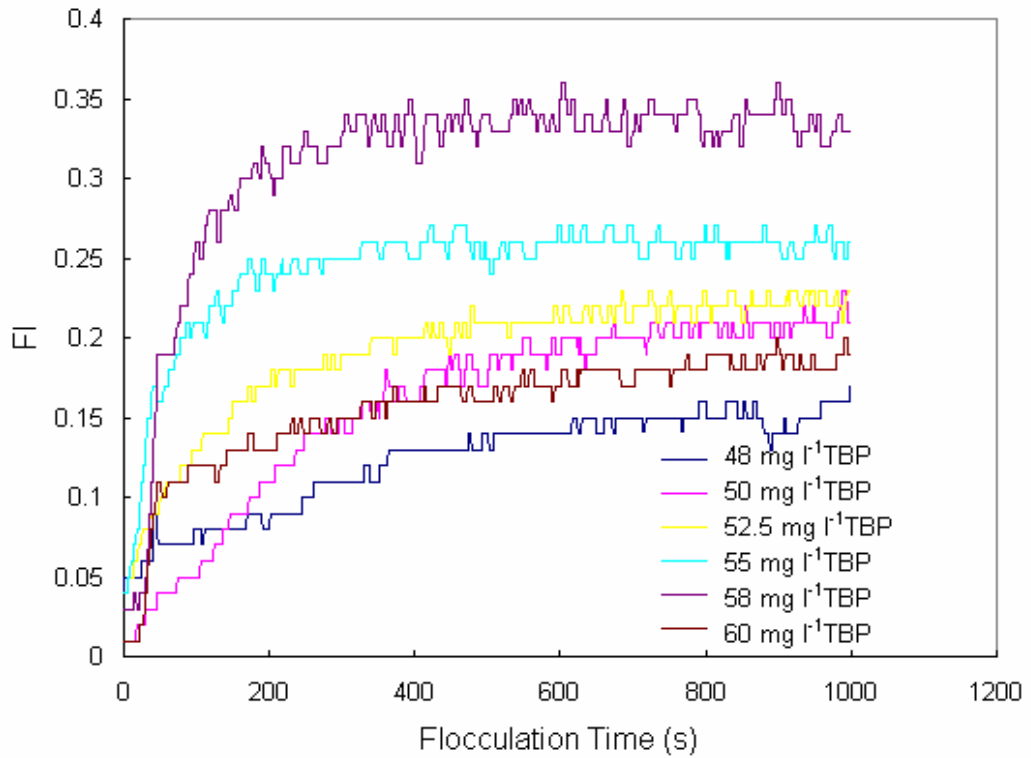


Figure 6.9 Flocculation index response with TBP dose at pH 7 (30 mg l⁻¹ HA)

TABLE 6.4 NPDOC before and after coagulation with TBP dosage at pH 7 (30 mg l⁻¹ HA)

TBP dosage (mg l ⁻¹)	NPDOC-30 mg l ⁻¹ HA (mg l ⁻¹)	NPDOC-TBP (mg l ⁻¹)	SUM NPDOC before coagulation (mg l ⁻¹)	NPDOC after coagulation (mg l ⁻¹)	NPDOC Reduction %
48	9.957	26.36	36.317	16.12	55.6
50	9.957	27.14	37.097	12.67	65.8
52.5	9.957	28.68	38.637	10.06	74.0
55	9.957	29.79	39.747	15.04	62.2
58	9.957	30.99	40.947	6.853	83.3
60	9.957	32.5	42.457	9.195	78.3

TABLE 6.5 Absorbance at 254nm and 400nm before and after coagulation with TBP dosage at pH7 (30 mg l⁻¹ HA)

TBP dosage (mg l ⁻¹)	Abs 254nm Before coagulation	Abs 254nm After coagulation	Abs 254 nm Reduction %	Abs 400nm Before coagulation	Abs 400nm After coagulation	Abs 400 nm Reduction %
48	1.186	0.097	91.8	0.250	0.012	95.2
50	1.209	0.092	92.4	0.251	0.012	95.2
52.5	1.224	0.083	93.2	0.251	0.011	95.6
55	1.245	0.077	93.8	0.253	0.010	96.0
58	1.270	0.073	94.3	0.254	0.008	96.9
60	1.284	0.062	95.2	0.255	0.008	96.9

From the results shown in Figure 6.10, Table 6.6 and Table 6.7 gave the optimum dose of TBP at pH 9 is approximately 60 mg l⁻¹ (equivalent to a TBP:HA ratio of ~6:1), which gave a maximum NPDOC reduction of 80.5%.

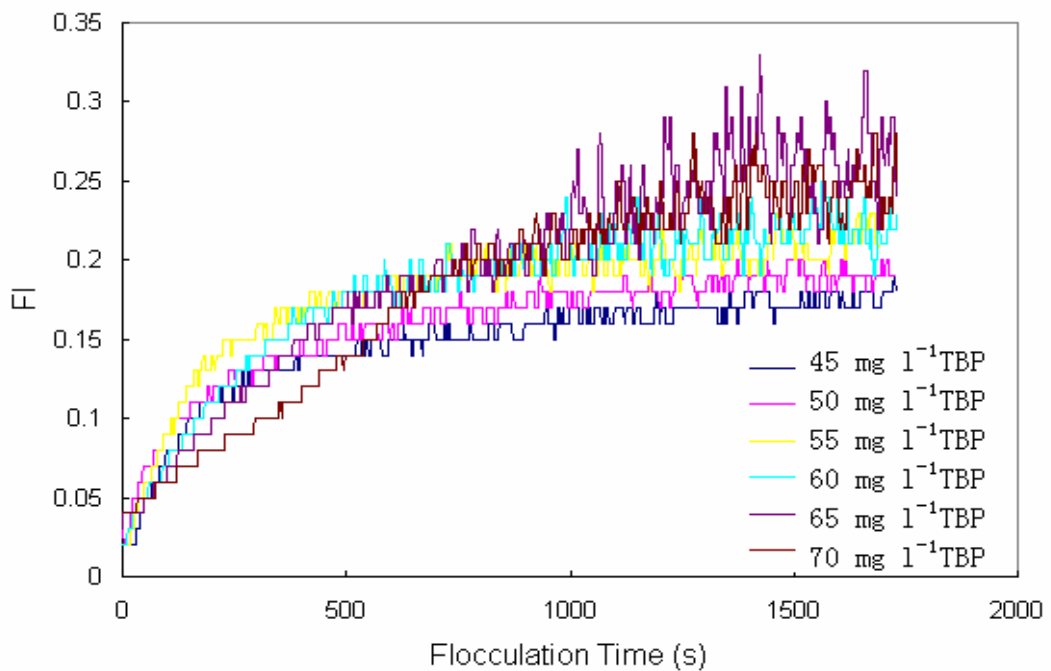


Figure 6.10 Flocculation index response with TBP dose at pH 9 (10 mg l⁻¹ HA)

TABLE 6.6 NPDOC before and after coagulation with TBP dosage at pH 9(10 mg l⁻¹ HA)

TBP dosage (mg l ⁻¹)	NPDOC- 10 mg l ⁻¹ HA (mg l ⁻¹)	NPDOC-TBP (mg l ⁻¹)	SUM NPDOC before coagulation (mg l ⁻¹)	NPDOC after coagulation (mg l ⁻¹)	NPDOC Reduction %
45	2.672	24.65	27.322	16.97	37.9
50	2.672	27.14	29.812	15.47	48.1
55	2.672	29.79	32.462	15.04	53.7
60	2.672	32.50	35.172	6.853	80.5
65	2.672	35.53	38.202	9.195	75.9
70	2.672	38.36	41.032	8.564	79.1

TABLE 6.7 Absorbance at 254nm and 400nm before and after coagulation with TBP dosage at pH 9 (10 mg l⁻¹ HA)

TBP dosage (mg l ⁻¹)	Abs 254nm Before coagulation	Abs 254nm After coagulation	Abs 254 nm Reduction %	Abs 400nm Before coagulation	Abs 400nm After coagulation	Abs 400 nm Reduction %
45	0.722	0.070	90.3	0.135	0.011	91.9
50	0.765	0.060	92.2	0.137	0.009	93.4
55	0.801	0.067	91.6	0.139	0.009	93.5
60	0.840	0.070	91.7	0.141	0.009	93.6
65	0.885	0.078	91.2	0.142	0.010	92.9
70	0.927	0.083	91.0	0.144	0.011	92.4

In these experiments with HA, the onset of flocculation occurred rapidly and a very short time (~6 min) was needed to attain the maximum FI value at pH 4 and 7. It was noted that at higher pH, say pH 9, the floc size was much smaller (as indicated by a small FI value) than the corresponding flocs (at optimum TBP dose) made by flocculation of the clay suspension. As with the clay suspension, there was a clear trend of increasing optimal TBP dose with increasing pH value for HA solution (Table 6.8). This may be explained by both the loss of TBP charge density, and increasing deprotonation of the humic acid (thus, increasing electronegativity), with pH increasing. From Table 6.8, it can be seen that for the model water with humic acid solution at low pH (≤ 7), the residual tannin matter was still lower than 1 mg l^{-1} , indicated by a high removal of NPDOC. It is also noted that at pH9 the residual tannin matter in final water was higher than that at lower pH. It is mostly caused by a higher amount of TBP used as a coagulant at pH9.

TABLE 6.8 Variation in optimum TBP dose and coagulation performance (HA solutions) with pH

pH	Charge Density (meq g^{-1})	Optimum Dosage		FI	NPDOC Reduction %	Residual Tannin (mg l^{-1})
		mg l^{-1}	(TBP:HA)			
4	3.07	30	1	0.33	83.50	0.396
7	0.67	58	2	0.34	83.26	0.618
9	0.20	60	6	0.32	80.51	1.318

The slight lack of agreement in the value of the optimal TBP indicated by the UV-Visible absorbance measurements, compared to that indicated by the FI and NPDOC, is probably the consequence of the complex interaction between

the various organic fractions of the TBP and HA. Clearly, the simple approach of summing the individual UV-Visible absorbance values for TBP and HA is not scientifically rigorous and inevitably leads to inaccuracies. It is also noted that in these tests the residual NPDOC after coagulation was still at a relatively high level, despite a high degree of overall NPDOC (>80%), mainly due to the large TBP dose added.

6.3 Coagulation Stoichiometry using TBP as Sole Coagulant

Model waters with kaolin suspension were obtained by dispersing 25mg, 50mg, 100mg and 200mg of kaolin clay in 2L of de-ionised water to give mass concentrations of 25 mg l⁻¹, 50 mg l⁻¹ and 100 mg l⁻¹, respectively. A series of working solutions with different clay concentrations were used for the TBP dose-stoichiometry tests. 50 mg l⁻¹ kaolin suspensions were chosen as standard kaolin mixtures (turbidity ~ 40 NTU) to investigate the floc strength (floc break-up and re-formation) under controlled conditions. For comparison purposes, model waters with different concentrations of humic acid were also used to investigate the existence of a TBP dose-stoichiometry. Working solutions with concentration of 15 mg l⁻¹, 30 mg l⁻¹ and 50 mg l⁻¹ were prepared by diluting HA stock solution with de-ionized water.

6.3.1 Coagulation Stoichiometry in Kaolin Suspension

The results of the flocculation tests using a series of concentrations of kaolin suspension in terms of the FI response with different TBP dosages at pH4 are shown in Figures 6.11 to 6.12.

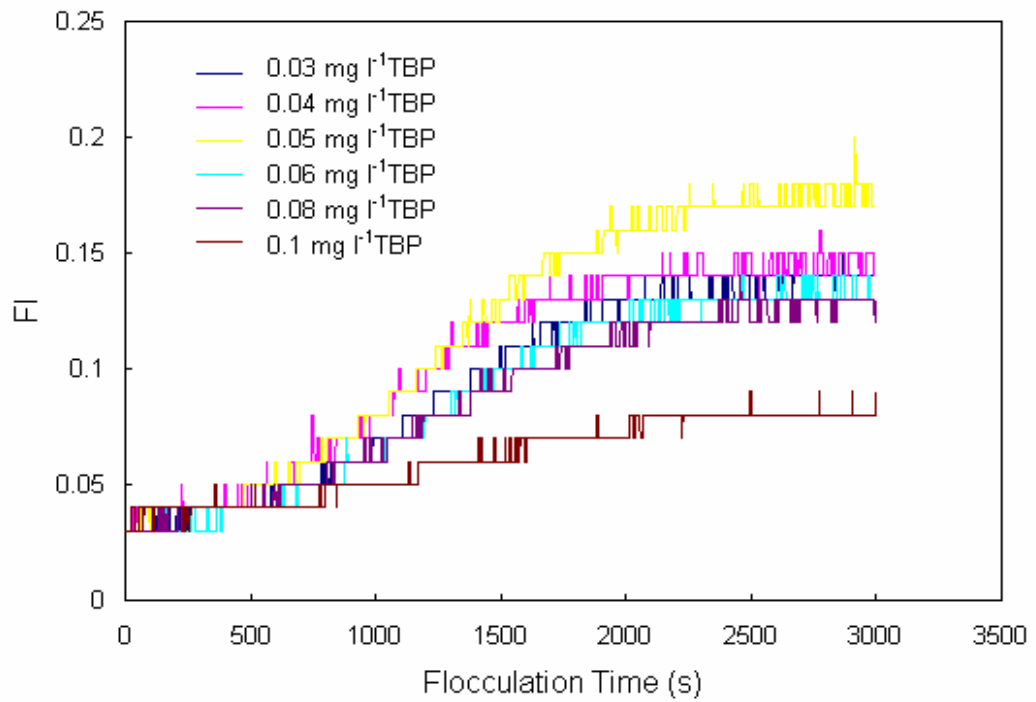


Figure 6.11 Flocculation index response with TBP dose at pH4 (25 mg l⁻¹ kaolin suspension)

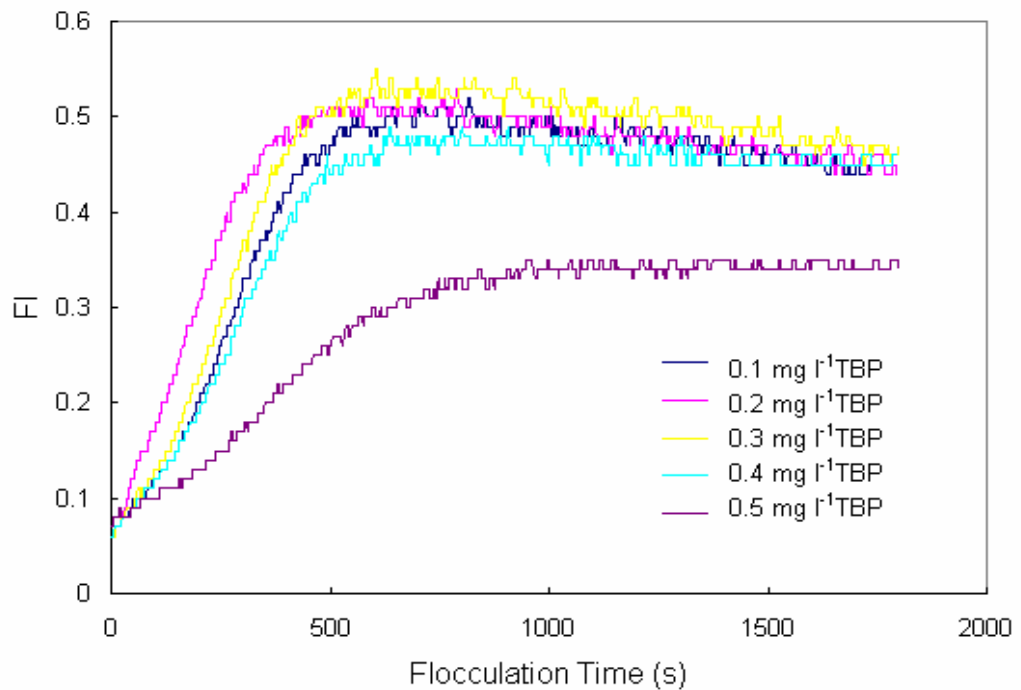


Figure 6.12 Flocculation index response with TBP dose at pH4 (100 mg l⁻¹ kaolin suspension)

Table 6.9 summarises the results of the tests by giving the TBP optimum dosage and turbidity reduction for the different kaolin concentrations at 25 mg l⁻¹, 50 mg l⁻¹ and 100 mg l⁻¹, at pH 4.

TABLE 6.9 Optimum dosage of TBP with different kaolin concentrations at pH 4, and the corresponding peak flocculation index and turbidity reduction

Kaolin Concentration (mg l ⁻¹)	TBP optimum Dosage (mg l ⁻¹)	Peak FI	Turbidity Reduction %
25	0.05	0.18	40
50	0.1	0.25	63.8
100	0.2	0.54	75

The corresponding results of the flocculation tests at pH 7 are shown in Figures 6.13 to 6.14.

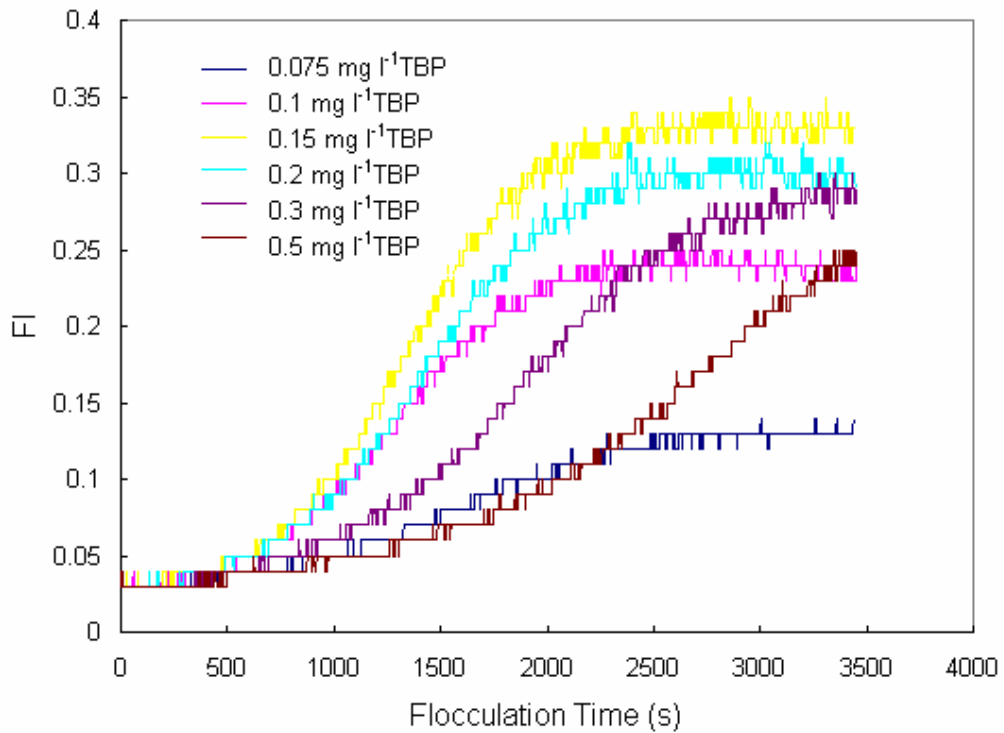


Figure 6.13 Flocculation index response with TBP dose at pH7 (25 mg l⁻¹ kaolin suspension)

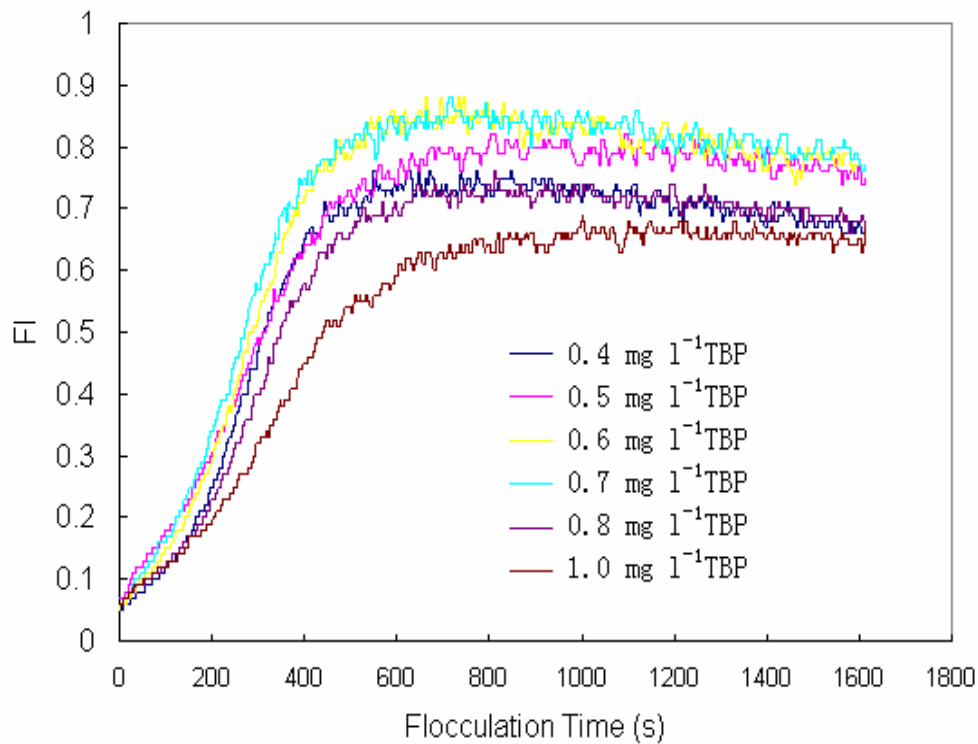


Figure 6.14 Flocculation index response with TBP dose at pH7 (100 mg l⁻¹ kaolin suspension)

Table 6.10 summarises the results of the tests by giving the TBP optimum dosage and turbidity reduction for different kaolin concentration at 25 mg l⁻¹, 50 mg l⁻¹ and 100 mg l⁻¹, at pH 7.

TABLE 6.10 Optimum dosage of TBP with different Kaolin concentrations at pH 7, and the corresponding peak flocculation index and turbidity reduction

Kaolin Concentration (mg l ⁻¹)	TBP optimum Dosage (mg l ⁻¹)	Peak FI	Turbidity Reduction %
25	0.15	0.34	50
50	0.3	0.52	67.5
100	0.6	0.83	84.8

It is clear from Tables 6.9 and 6.10 that the optimum TBP dosage increased linearly with increasing kaolin concentration, suggesting that a stoichiometric relationship exists between TBP and kaolin clay. This confirms that at pH 4 and 7, where the TBP has a significant cationic charge, the charge neutralisation is the dominant coagulation mechanism; since the counterions with a very high affinity are quantitative. Furthermore, it can be seen that the flocculation rate, peak flocculation index and turbidity reduction are also dependent on the concentration. From Figures 6.11 to 6.14, and Figure 6.1 and 6.2, a distinct trend was evident, which is that the onset of flocculation occurred more rapidly, and the time needed to attain the maximum FI reduced, with increasing concentration of kaolin clay, from 25 mg l⁻¹ to 100 mg l⁻¹, at both pH 4 and 7. It is reasonable to assume that the kinetics of TBP flocculation (indicated by the floc growth rate) at low pH are dependent on the concentration of particles and polymer molecules (as indicated by Smoluchowski flocculation theory (67)).

Using model waters with different concentrations of kaolin clay, the optimum dosages of TBP at pH 9 were determined. The results summarised in Figures 6.15, 6.16 and 6.17 show the flocculation performance of TBP at pH 9 for different concentrations of kaolin clay. It can be seen that at 50 mg l⁻¹ kaolin clay, the optimum dosage of TBP was in the range of 14-25 mg l⁻¹. At the lower kaolin concentration of 25 mg l⁻¹, the optimum dosage of TBP was in the range of 20-25 mg l⁻¹, and at the lowest clay concentration of 12.5 mg l⁻¹, the optimum dosage of TBP was 20 mg l⁻¹. A relatively constant dose of TBP (say around 20 mg l⁻¹) could be chosen as the optimum dose for all of the kaolin concentrations tested at pH 9. Thus, there appears to be no clear TBP dose stoichiometry at pH 9. This behaviour is consistent with previous findings that TBP polymer has little cationic charge at pH 9. Yukselen and Gregory (101) proposed that the mechanism of polymer bridging is considered to be more important for long-chain polymers that are not highly charged. Therefore, in this case, the principal coagulation mechanism is likely be polymer bridging rather than charge interaction. However,

the obviously large amount of dosage indicated that at higher pH, TBP precipitation occurs and this might play a part in the process, leading to the “sweep coagulation”.

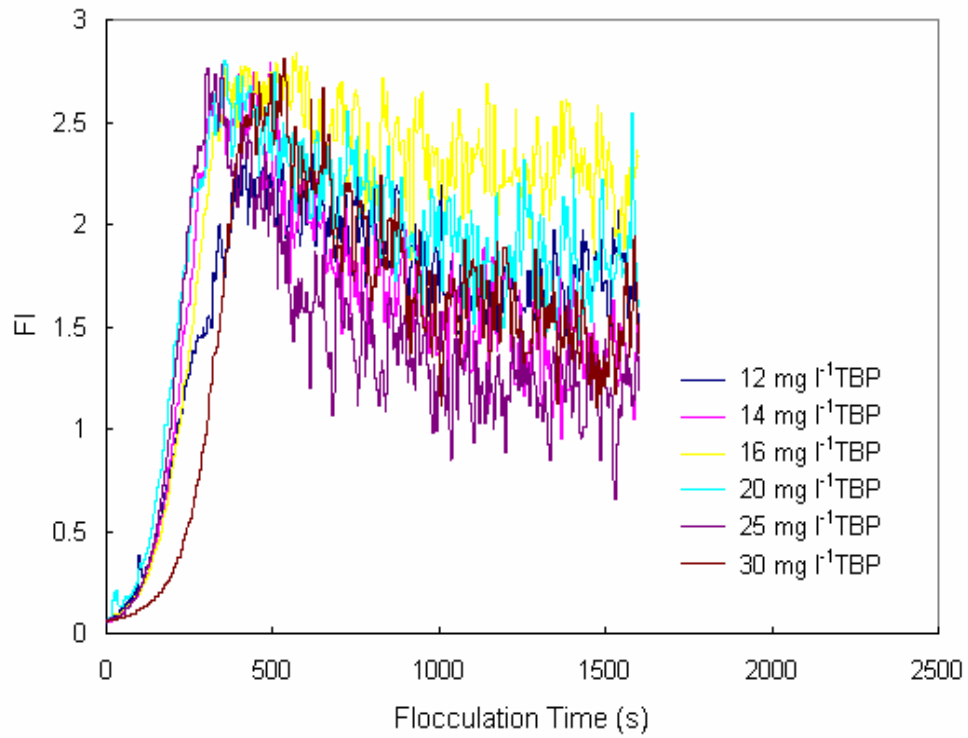


Figure 6.15 Flocculation index response with TBP dose at pH9 (50 mg l⁻¹ kaolin suspension)

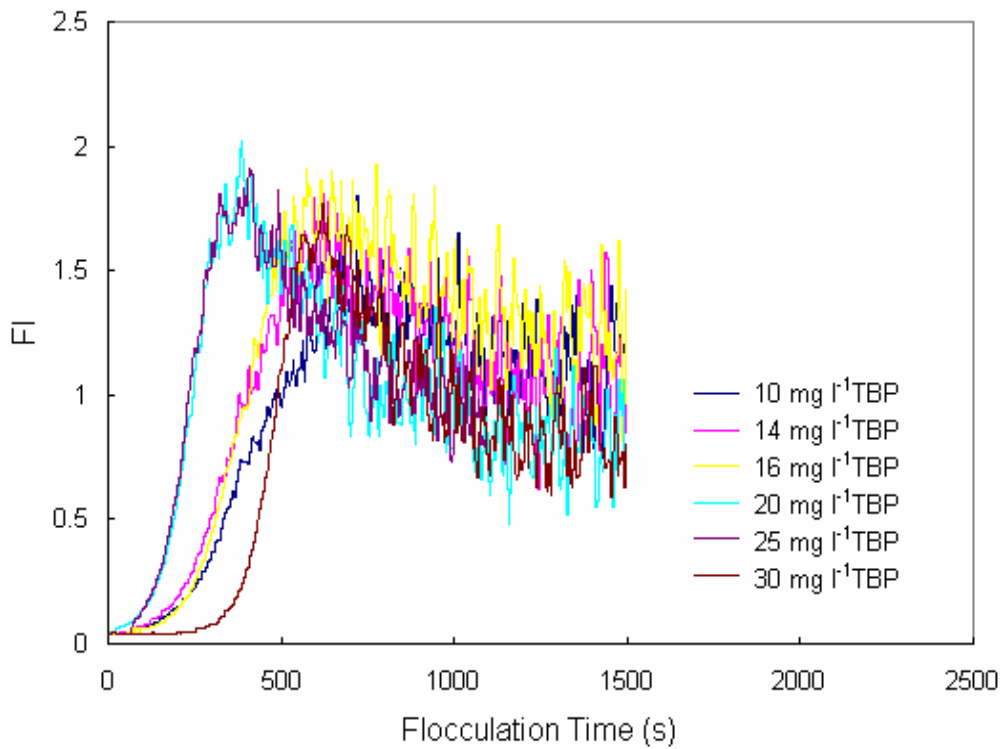


Figure 6.16 Flocculation index response with TBP dose at pH9 (25 mg l⁻¹ kaolin suspension)

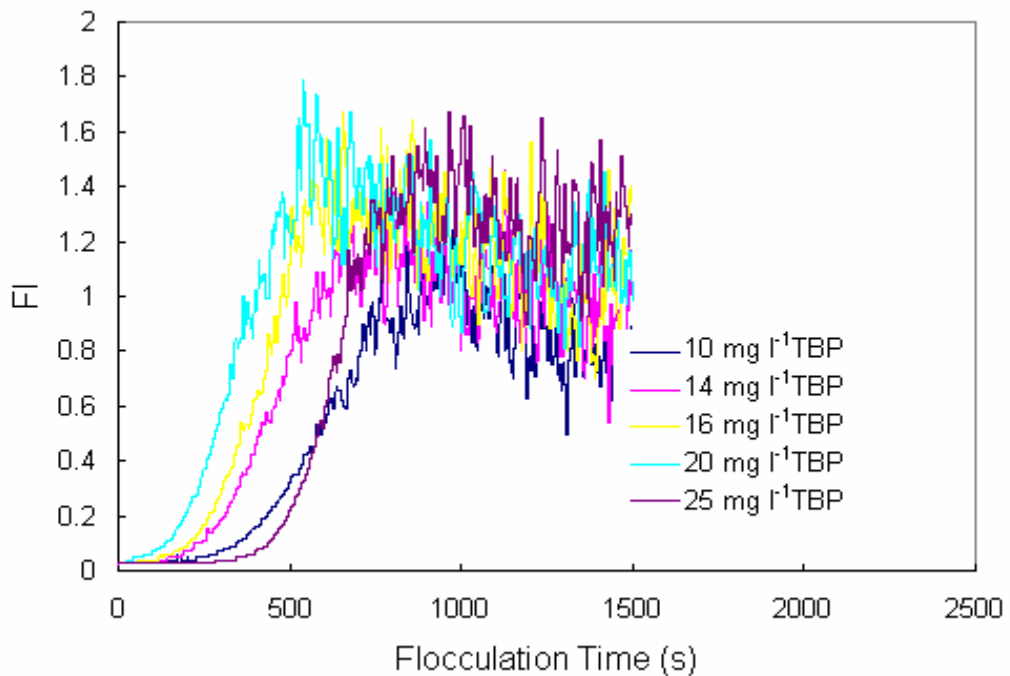


Figure 6.17 Flocculation index response with TBP dose at pH9 (12.5 mg l⁻¹ kaolin suspension)

6.3.2 Coagulation Stoichiometry with Humic Acid Solution

The results of flocculation tests using a series of concentrations of humic acid in terms of the FI response with different TBP dosages at pH 4 are shown in Figures 6.18 to 6.19.

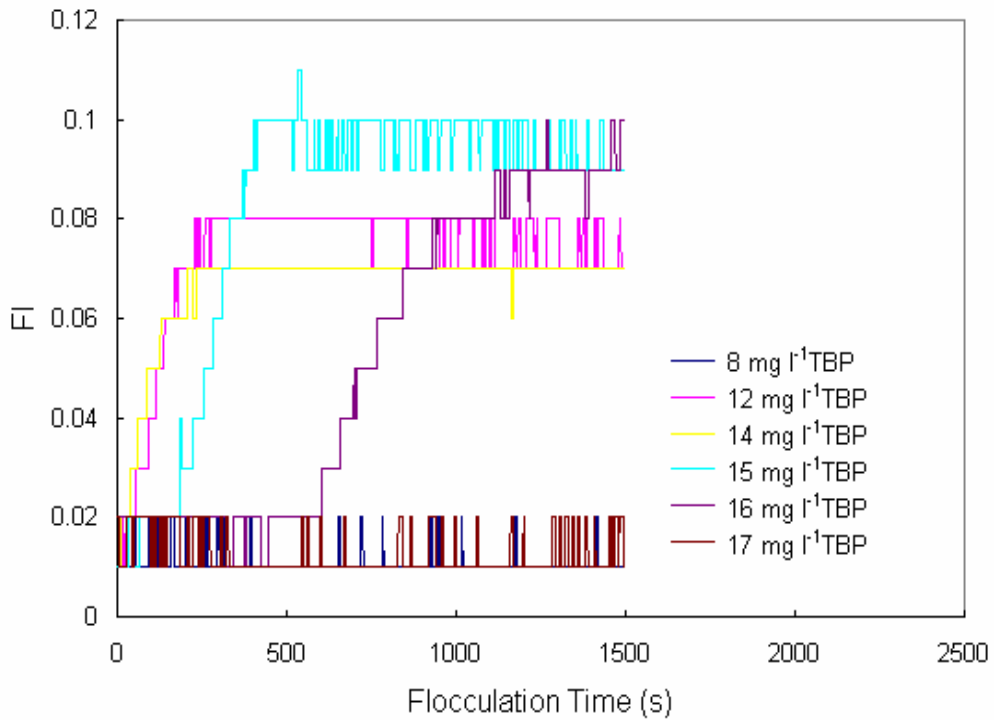


Figure 6.18 Flocculation index response with TBP dose at pH4 (15 mg l⁻¹ HA)

From Figure 6.18 and Figure 6.19, it is observed that at low FI values there is a spiky or discontinuous variation in the FI response curve. The precise reason for this is unclear but it seems that small size flocs at low concentration present a more sensitive and intermittent fluctuation in the intensity of light transmitted through a flowing suspension. Secondly, this may be the result of the resolution of the data acquisition.

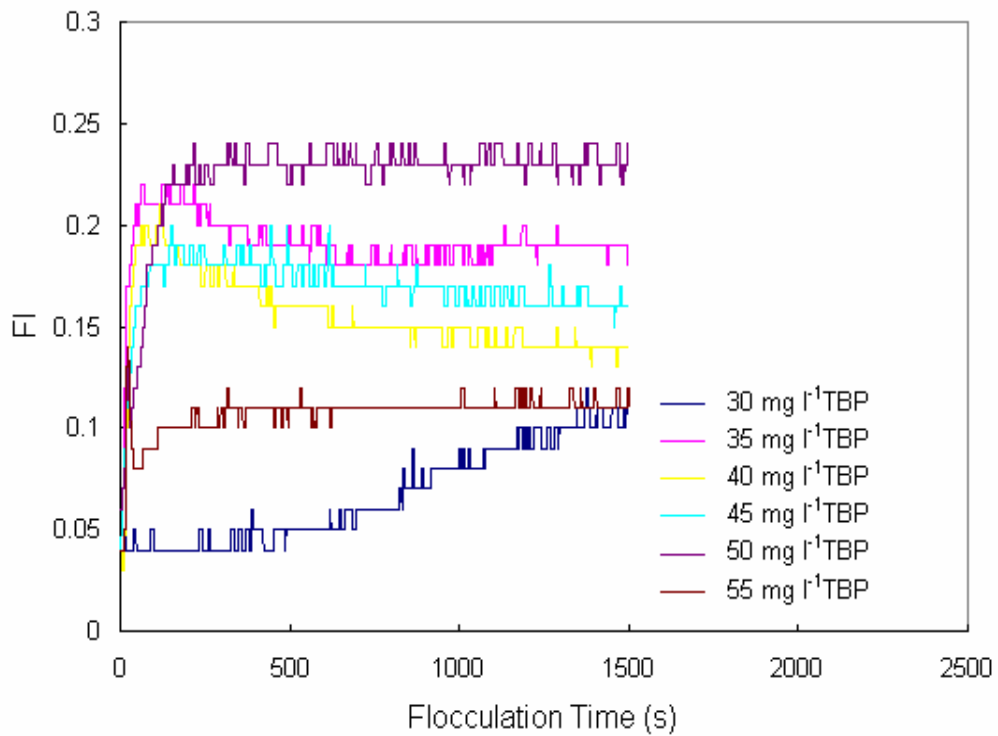


Figure 6.19 Flocculation index response with TBP dose at pH4 (50 mg l⁻¹ HA)

Table 6.11 summarises the results of the tests by giving the TBP optimum dosage for the different HA concentrations of 15 mg l⁻¹, 30 mg l⁻¹ and 50 mg l⁻¹, at pH 4.

TABLE 6.11 Optimum dosage of TBP with different HA concentration at pH 4, and the corresponding peak FI and reduction in NPDOC and colour

HA concentration (mg l ⁻¹)	Optimum Dosage		FI	NPDOC Reduction %	Colour Reduction %
	mg l ⁻¹	(TBP:HA)			
15	15	1	0.1	68.6	96.80
30	30	1	0.33	83.5	97.02
50	50	1	0.24	89.9	97.14

The corresponding results of the flocculation tests at pH 7 are shown in Figures 6.20 to 6.21.

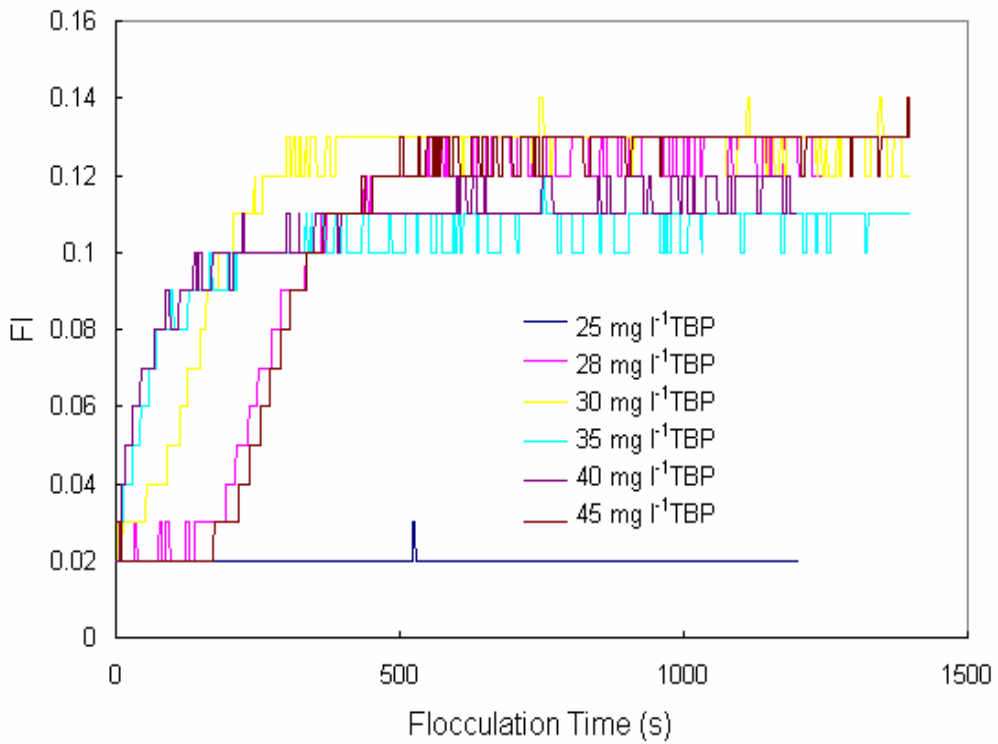


Figure 6.20 Flocculation index response with TBP dose at pH7 (15 mg l⁻¹ HA)

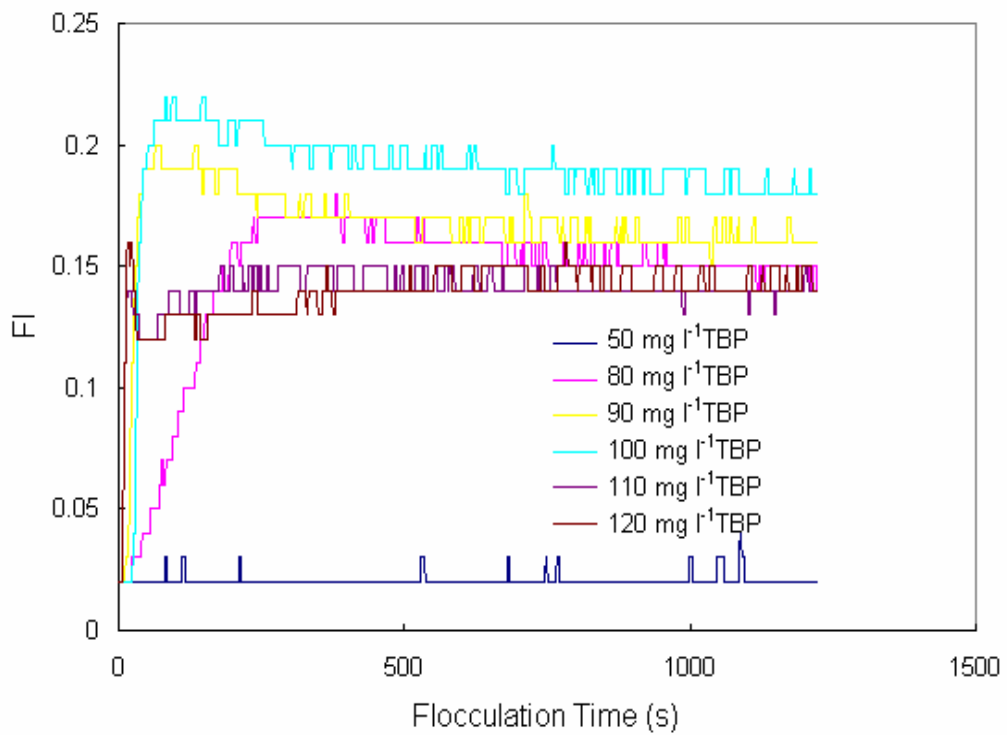


Figure 6.21 Flocculation index response with TBP dose at pH7 (50 mg l⁻¹ HA)

Table 6.12 summarises the results of the tests by giving the TBP optimum dosage for the different HA concentrations of 15 mg l⁻¹, 30 mg l⁻¹ and 50 mg l⁻¹, at pH 7.

TABLE 6.12 Optimum dosage of TBP with different HA concentration at pH 7, and the corresponding peak FI and reduction in NPDOC and colour

HA concentration (mg l ⁻¹)	Optimum Dosage		FI	NPDOC Reduction %	Colour Reduction %
	mg l ⁻¹	(TBP:HA)			
15	30	2	0.13	64.9	92
30	58	2	0.34	83.26	93.8
50	100	2	0.22	85.5	97.6

For HA flocculation, it is clear that there is a strong agreement in the concentration ratio of TBP: HA, confirming that the TBP optimum dosages were proportional with the HA concentration at low and neutral pH (≤ 7). This result is consistent with the tests using kaolin suspension.

The previous study (in Figure 5.4) showed that the charge density of TBP at pH 4 is 4-5 fold greater compared to the charge density at pH 7. Due to the deprotonation of HA with pH decreasing, if the charge neutralisation is the only coagulation mechanism, the optimum dosage of TBP at pH 7 should be much more than double the optimum dosage at pH4. The results from table 6.11 and 6.12 indicated that other mechanisms were involved, such as ‘polymer bridging’, which reduced the optimum dosage at pH 7, although stiochiometry exists at pH4 and 7 respectively.

6.4 Influence of Conditions on Coagulation Performance

6.4.1 Variation of Coagulation with Ageing Time of TBP

The results in Figures 6.22, 6.23 and 6.24 show the flocculation performance of TBP at pH4, 7 and 9 for different polymer aging times used for 50 mg l⁻¹ kaolin suspension. It can be seen that with increasing aging time the flocculation index decreased, possibly due to the reduction of charge density with time. At pH4, although the charge density of TBP decreased from 3.07 meq g⁻¹ to 2.04 meq g⁻¹ with the ageing time increasing from 3 hours to 24 hours, the charge density was still sufficient to achieve charge neutralisation (small flocs were observed) and the resulting FI response was only slightly inferior. At pH7, because the charge density has substantially decreased from 1.2 meq g⁻¹ to 0.1 meq g⁻¹ at 3 hours to 24 hours of ageing, there was a more marked reduction in the FI response. For pH9, the onset of flocculation was delayed as a consequence of the aging (72hrs compared to 3hrs) but the peak flocculation index was unchanged. Since at this pH value the polymer has very little cationic charge, it seems likely that the flocculation effect is the result of other phenomena, such as the extent of precipitation and polymer bridging effects.

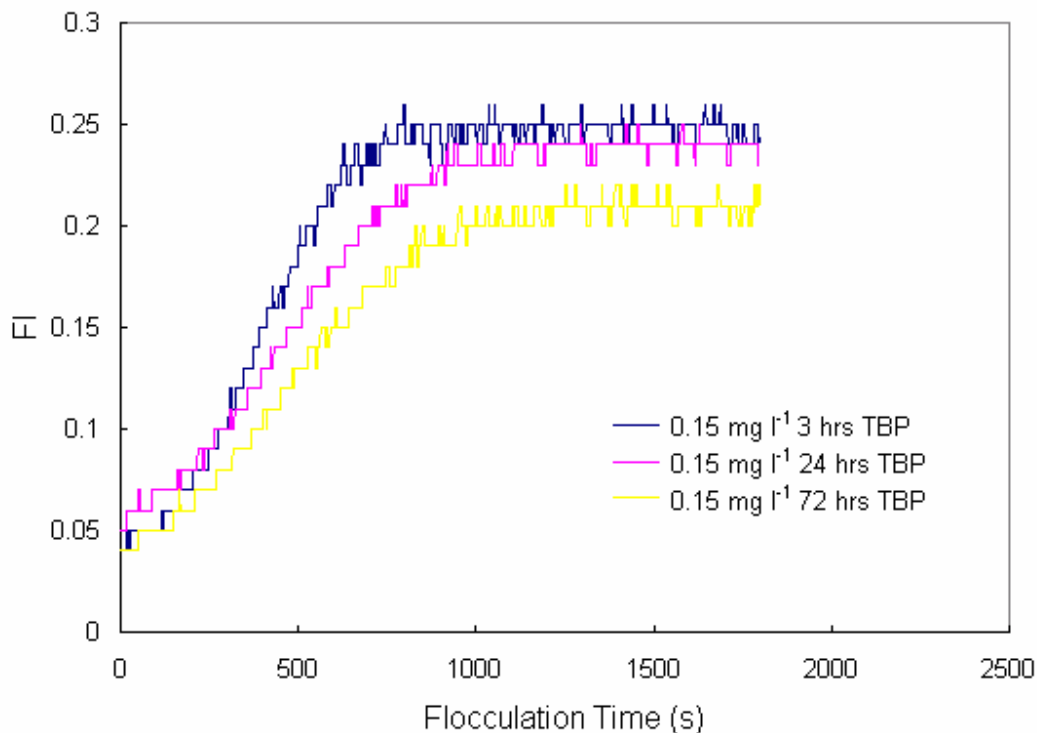


Figure 6.22 Flocculation index response for different aging periods at pH 4 (50mg l⁻¹ kaolin suspension)

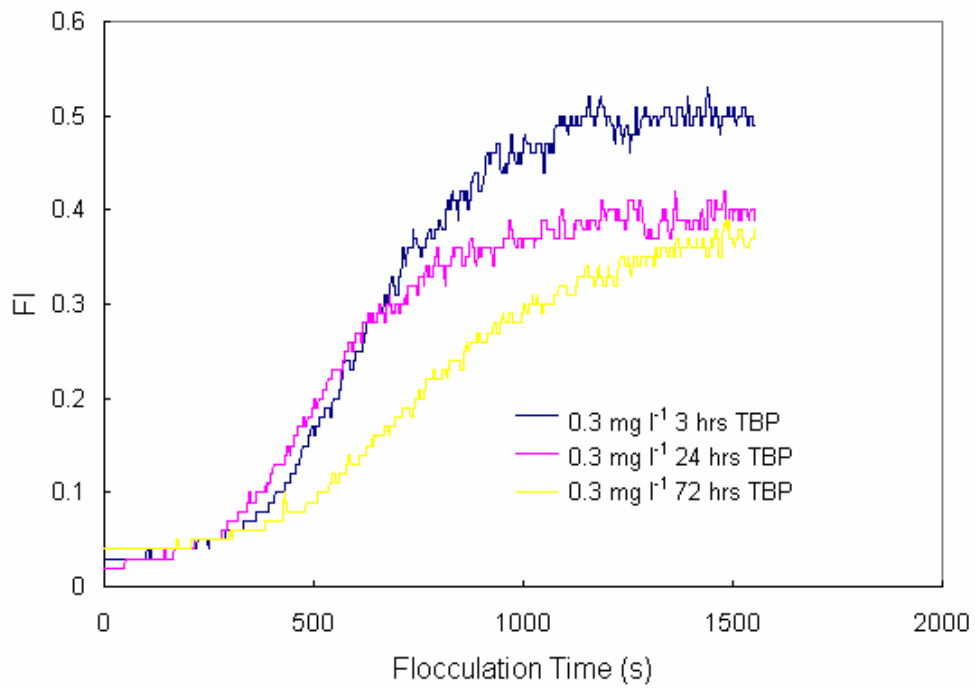


Figure 6.23 Flocculation index response for different aging periods at pH 7 (50mg l⁻¹ kaolin suspension)

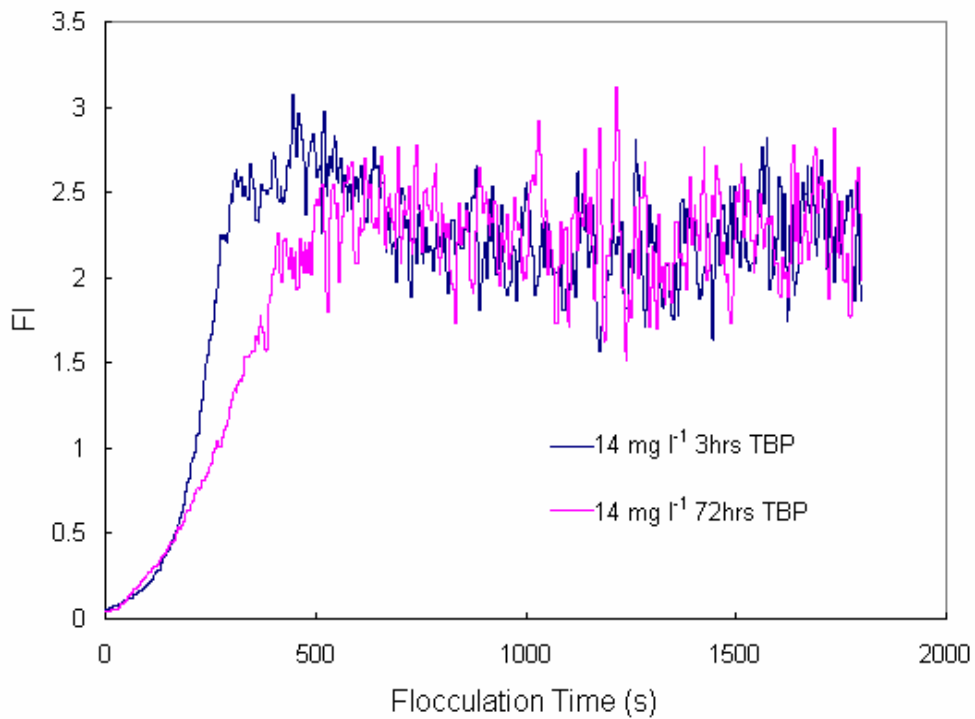


Figure 6.24 Flocculation index response for different aging periods at pH 9 (50mg l⁻¹ kaolin suspension)

The coagulation performance of the TBP at the previously determined optimum dose was studied for the following TBP aging times: 3 hrs, 24hrs and 48hrs, used in humic acid solution. Figures 6.25, 6.26 and 6.27 present the coagulation results of 30 mg l⁻¹ and 10 mg l⁻¹ humic acid solutions at pH 4, 7 and 9; these display a very similar behaviour to that observed with the clay suspensions. At pH 4 and 7, the charge density of TBP decreased with aging, and therefore the coagulation performance decreased. However, at pH 9, the charge density of TBP, even fresh, is very low (close to zero), and thus aging effects on charge are not important. In these conditions the coagulation is likely to be influenced by the relative extent of TBP precipitation and polymer bridging effects; thus, Figure 6.27 shows that TBP aging had little effect on performance.

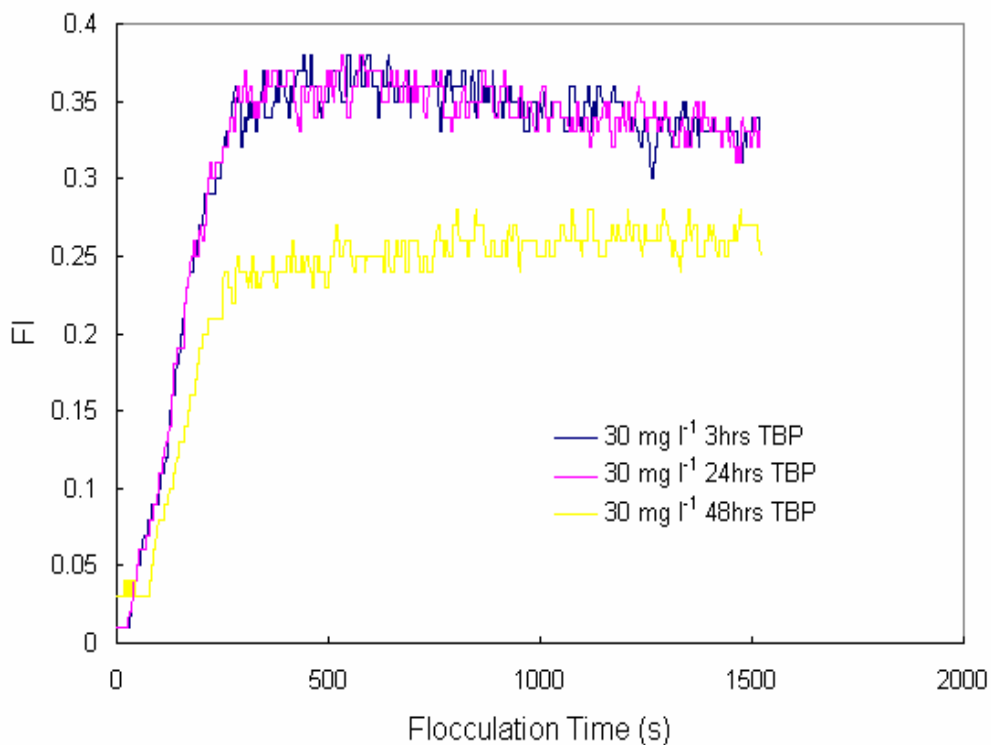


Figure 6.25 Flocculation index response for different aging periods at pH 4 (30 mg l⁻¹ HA)

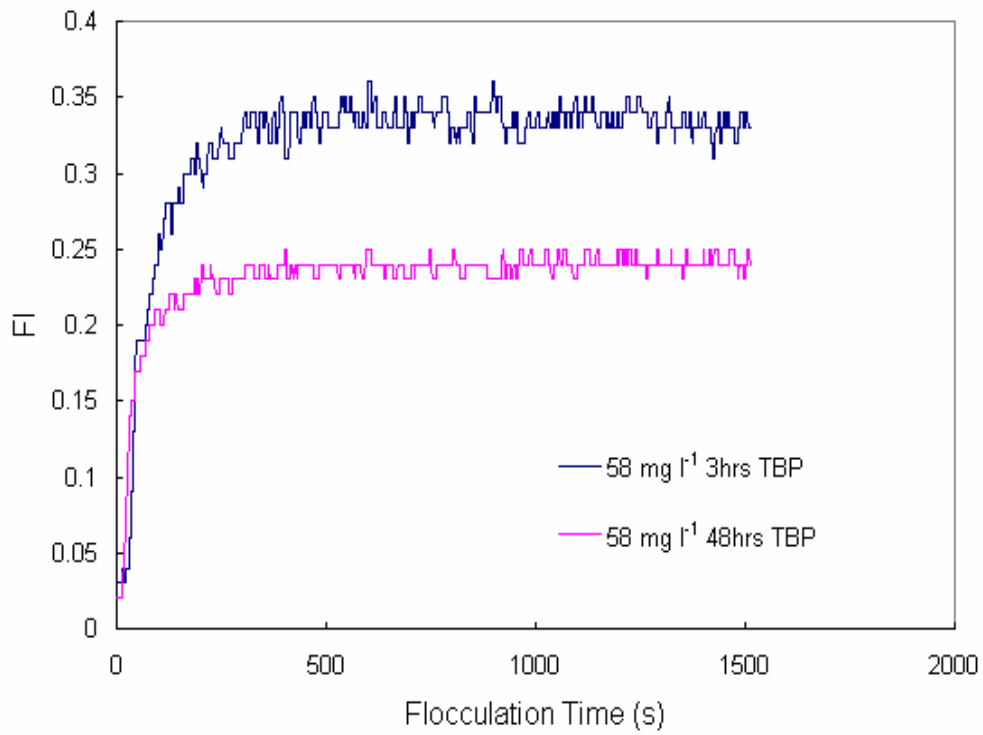


Figure 6.26 Flocculation index response for different aging periods at pH 7 (30 mg l⁻¹ HA)

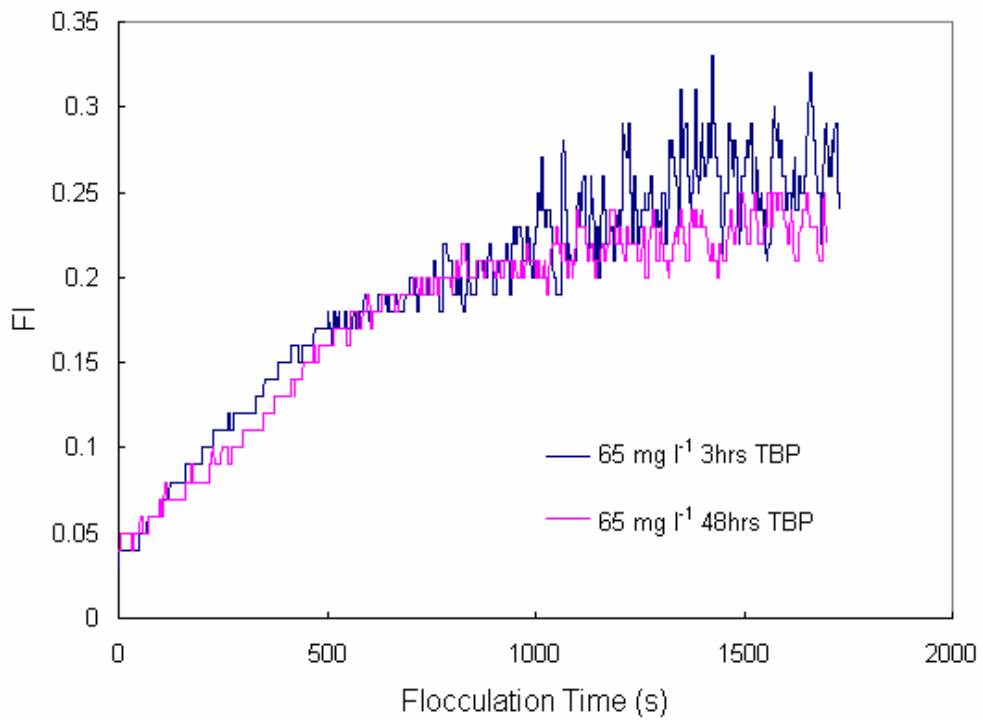


Figure 6.27 Flocculation index response for different aging periods at pH 9 (10 mg l⁻¹ HA)

6.4.2 Variation of Coagulation with Mixing Speed

According to the paddle speed-velocity gradient calibration line for the Gator reactor (Appendix I), a series of velocity gradients, 950 s^{-1} , 800 s^{-1} , 600 s^{-1} , 350 s^{-1} and 48 s^{-1} can be obtained with the following paddle speeds: 400 rpm, 350 rpm, 300 rpm, 200 rpm and 50 rpm. Using these conditions for the rapid mixing phase of the coagulation experiments, and a set mixing time of 30 s, followed by a constant slow coagulation phase at 50 rpm, the influence of the mixing rate was studied. The coagulation results of 50 mg l^{-1} kaolin suspension in Figure 6.28 show that at pH 4, with an optimal TBP dose of about 0.15 mg l^{-1} , the FI response was very similar for all mixing conditions and any differences probably within experimental error, suggesting that the conventional rapid mix design parameter, $G = 350 \text{ s}^{-1}$ may complete particle coagulation when TBP was used as primary coagulant. However, at the highest velocity gradient of 950 s^{-1} , the peak FI value was discernibly lower than for the other conditions, suggesting the possibility of floc break-up.

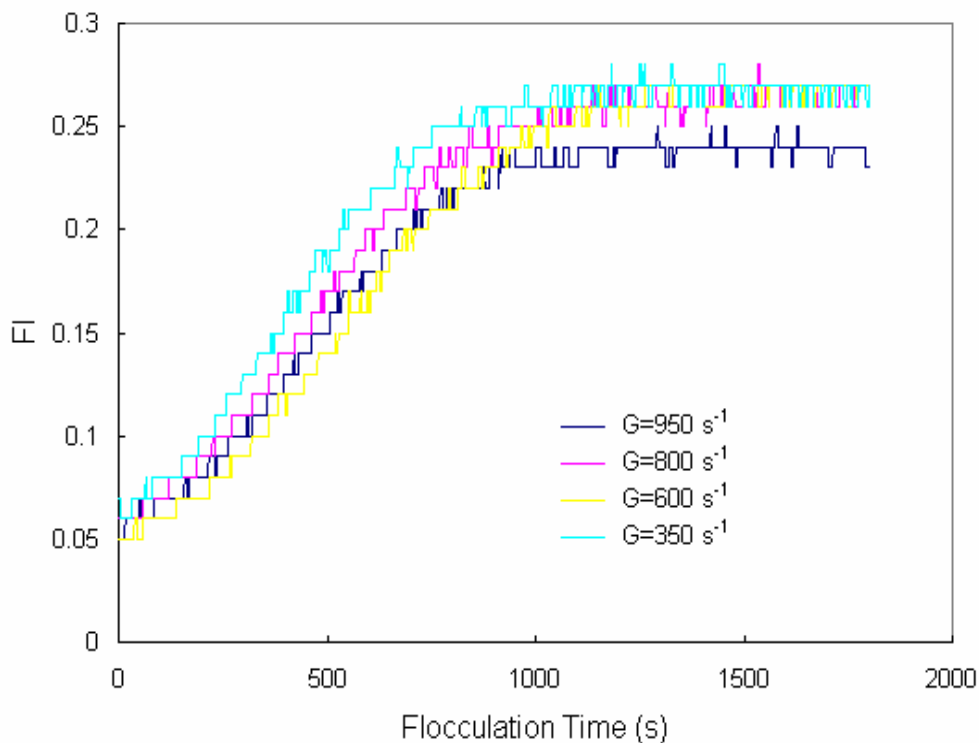


Figure 6.28 Flocculation index response for different mixing intensities at pH 4 (50 mg l^{-1} kaolin suspension)

6.4.3 Variation of Coagulation with Reactor

Coagulation tests for 50mg l^{-1} kaolin suspension were carried out under nominally similar mixing conditions (~ 50 rpm), but under optimal chemical conditions for pH9 and 7 (ie. 14 mg l^{-1} TBP at pH9, and 0.3 mg l^{-1} TBP at pH7) using two different jar test reactors (viz. glass beaker and Gator). The results indicated no significance difference at pH 9, but a better performance by the gator jar at pH 7 (see Figures 6.29 and 6.30). As noted previously the power transfer seemed less efficient for the glass beaker as indicated by a large amount of vortexing, and this effect may have been more influential for charge neutralisation process under the slower coagulation conditions at pH 7. It seems likely that in the case of “sweep coagulation”/polymer bridging, the initial mixing conditions are not so important.

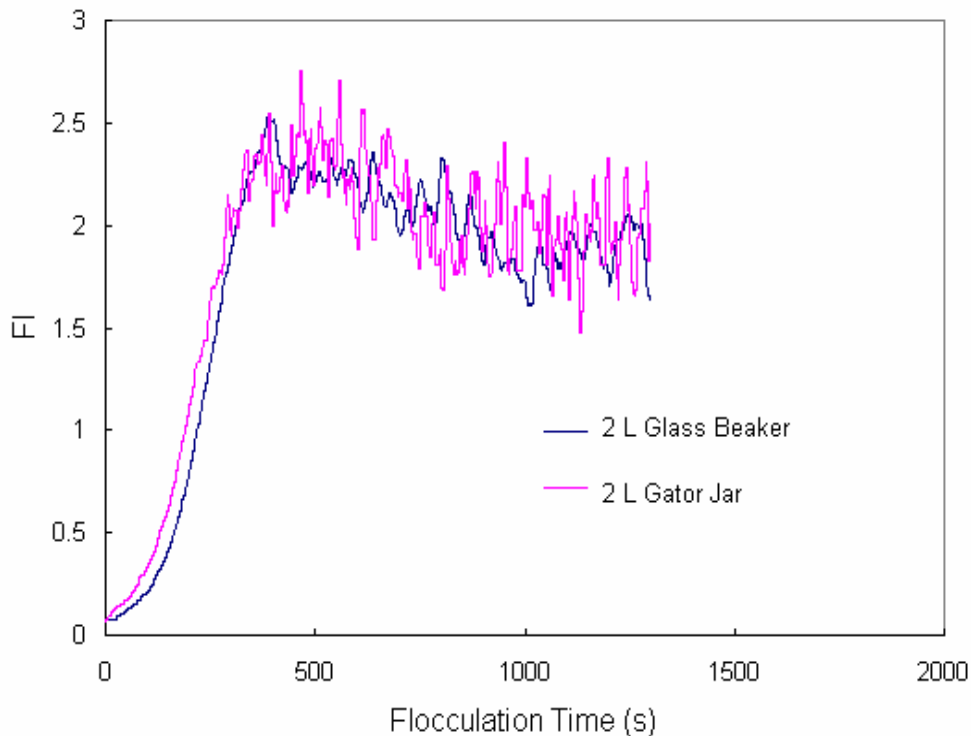


Figure 6.29 Flocculation index response for different reactors at pH 9 (50mg l^{-1} kaolin suspension)

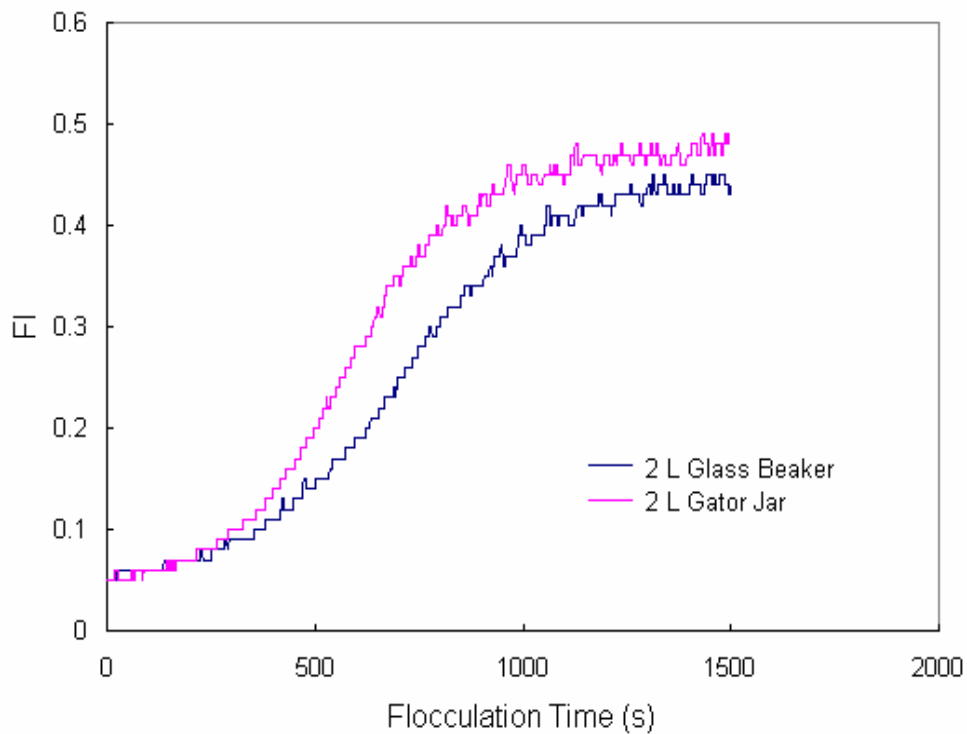


Figure 6.30 Flocculation index response for different reactors at pH 7 (50mg l⁻¹ kaolin suspension)

6.5 Coagulation Effectiveness in Comparison with Other Coagulant

Alum and polyDADMAC were chosen as reference chemicals for comparing the coagulation performance of TBP with 50 mg l⁻¹ kaolin clay suspension. The optimal dosage for alum was found to be 3.4 mg l⁻¹ (as Al³⁺) at pH 7, and for polyDADMAC (Flobeads DB 45 SH) the optimal dose was about 0.12 mg l⁻¹, and independent of pH. The comparable results are summarised in Figures 6.31 and 6.32.

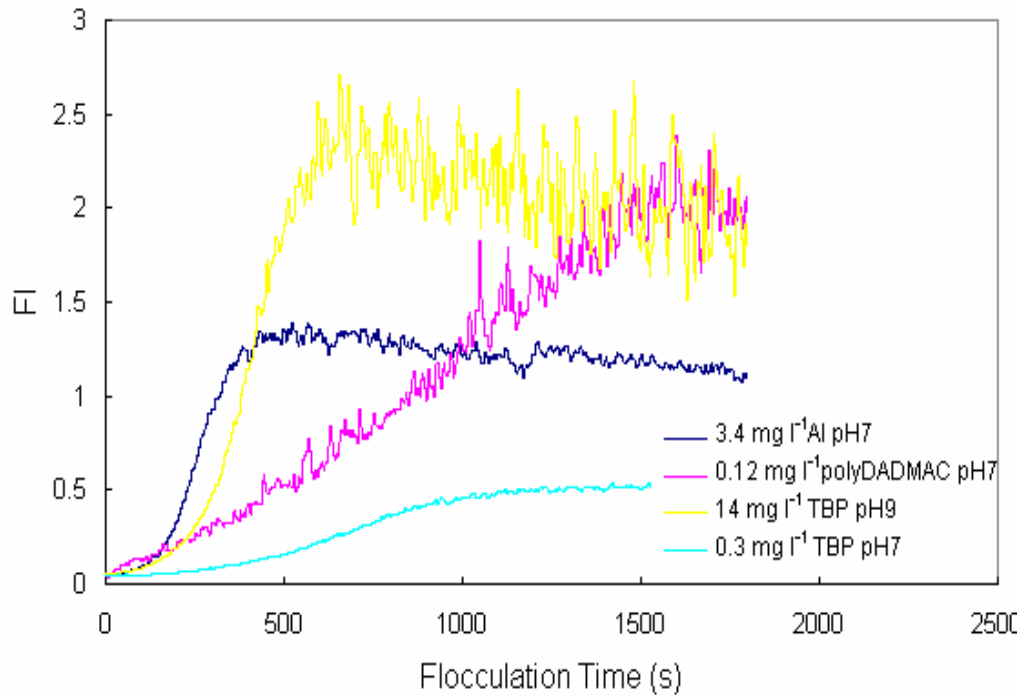


Figure 6.31 Flocculation index response with different coagulants at pH 7, and TBP at pH 9 (50 mg l⁻¹ kaolin suspension)

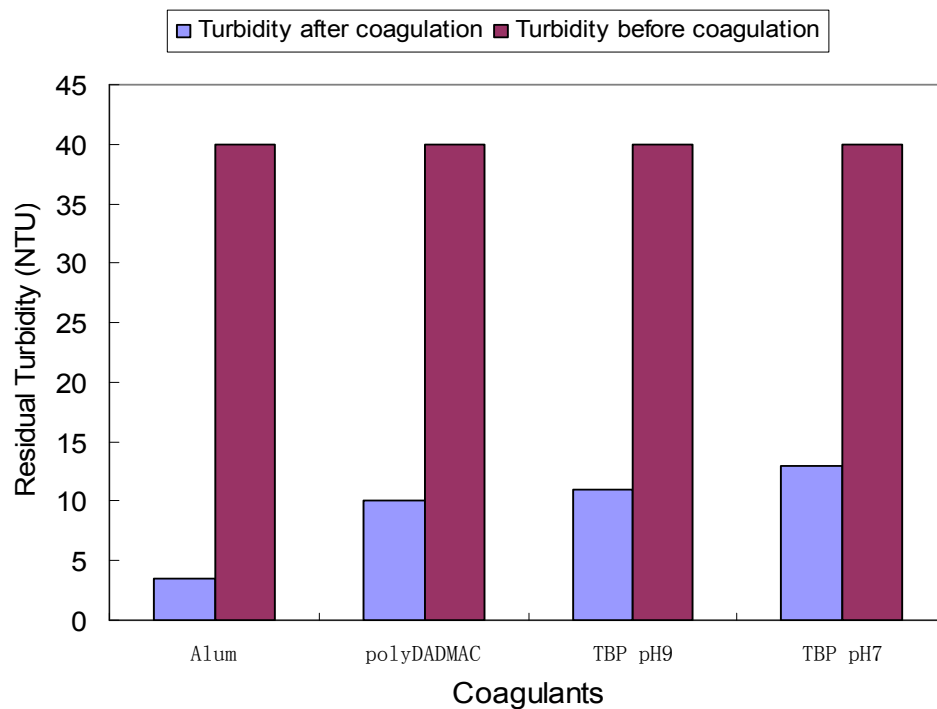


Figure 6.32 Residual turbidity before and after coagulation with different coagulants at pH 7 (50 mg l⁻¹ kaolin suspension)

From Figure 6.31, it can be seen that at pH 7, the onset of flocculation using TBP and polyDADMAC occurred rather later than for alum, and longer times were needed to attain the maximum flocculation index (FI) value. The use of polyDADMAC promoted the growth of very large flocs, with FI values about twice as high as those with alum and four times as those with TBP. At pH 9, using a higher optimal dosage of TBP, the time to attain the maximum value was reduced significantly, and large flocs were formed. The peak value of the FI is similar to that using the polyDADMAC as coagulant. Figure 6.32 shows that the residual turbidity in solution after coagulation using alum was lowest, 3.5 NTU, followed in performance by polyDADMAC where the residual turbidity was 10 NTU. At pH 9, the performance of TBP was virtually identical to the polyDADMAC, although the mechanism of coagulation is believed to be different.

The optimum dose for alum in the coagulation of 30 mg l⁻¹ HA at pH 7 was found to be 6.75 mg l⁻¹ (as Al³⁺), and for polyDADMAC (Flobeads DB 45 SH) the optimum dose was about 14 mg l⁻¹. It was also found that a higher alum dosage was required at higher pH because of increasing HA deprotonation (increasing electronegativity of HA) and the decreasing cationic nature of the Al coagulant species. For PolyDADMAC, being a quaternary ammonium cationic polymer, the cationic charge does not vary with pH. Thus, its performance in removing the HA only reflects the change in HA deprotonation with pH. At pH 4, the optimum polyDADMAC dose was 10 mg l⁻¹, compared with the optimum dose of 14 mg l⁻¹ at pH 7.

Figure 6.33 summarises the coagulation performance of 30 mg l⁻¹ HA solution for the different chemicals at their optimum doses and at pH 7. It can be seen that both cationic polymers promoted the growth of large flocs, with the FI values about 1.5 times higher than those with alum. Significant differences in the

reduction of NPDOC were observed (Table 6.13); viz. alum 88.1%, TBP, 83.3%, and polyDADMAC 63.3%. However, the residual NPDOC in filtered water using 58 mg l⁻¹ TBP was about 7 mg l⁻¹, which is higher than that with the other two coagulants.

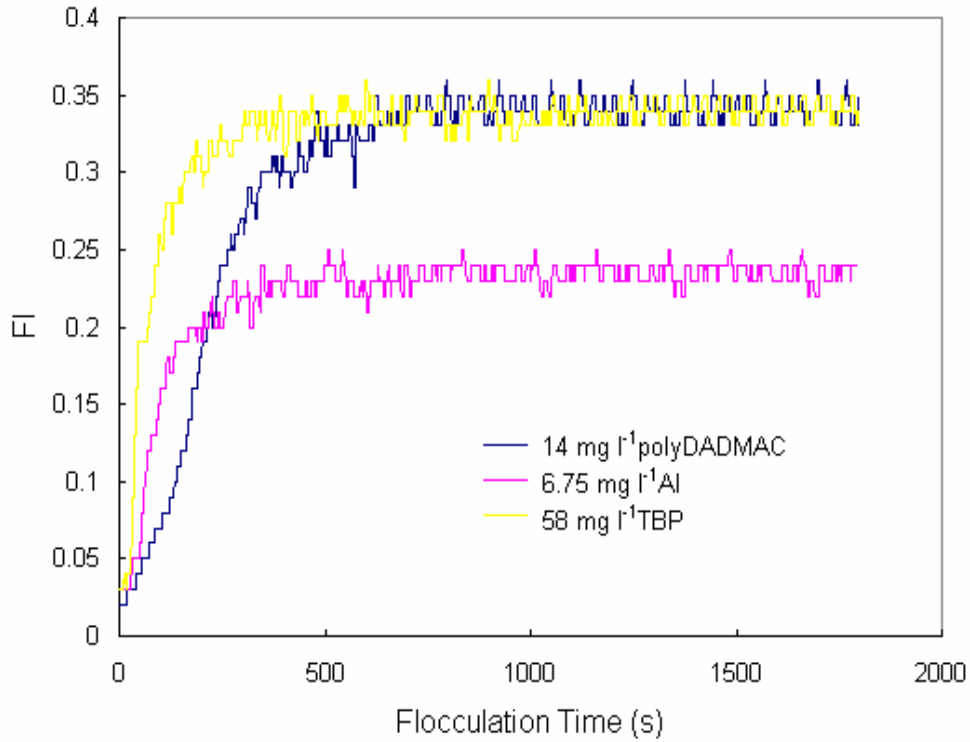


Figure 6.33 Flocculation index response with different coagulants at pH 7 (30 mg l⁻¹ HA)

TABLE 6.13 Optimum dose of coagulants at pH 7, and NPDOC reduction (30 mg l⁻¹ HA)

Coagulants	NPDOC-- 30mg l ⁻¹ HA (mg l ⁻¹)	NPDOC-- Coagulant (mg l ⁻¹)	SUM NPDOC before coagulation (mg l ⁻¹)	NPDOC after coagulation (mg l ⁻¹)	Reduction %
6.75 mg l ⁻¹ Al ³⁺	9.957	0.05	10.007	1.189	88.1
14 mg l ⁻¹ PolyDADMAC	9.957	3.926	13.883	5.097	63.3
58 mg l ⁻¹ TBP	9.957	30.99	40.947	6.853	83.3

6.6 Floc Strength of TBP

Using a 2L gator jar, an indication of the relative floc strength can be obtained by applying a sudden increase in shear rate to the formed aggregates and relating velocity gradient applied to the maximum floc size resulting. In this study, simple indices of floc strength have been applied based on the FI response, which allows the relative floc strength with different coagulants to be compared.

6.6.1 The Effect of Rapid Mixing on Floc Re-formation

The formation, breakage and re-formation of flocs using TBP as coagulant were investigated by studying the FI response to a sudden increase in mean velocity gradient within the Gator reactor. In this experiment, the optimum dose of 0.3 mg l^{-1} TBP was pipetted into 50 mg l^{-1} of kaolin suspension at pH 7, and an initial period of 25 minutes for the slow stirring at 50 rpm (48 s^{-1}) was chosen since no significant changes were observed in the FI after this. Floc breakage was brought about by suddenly increasing the stirring speed after the initial period, and maintaining this for 60 seconds. Thus, a series of tests were carried out whereby the stirring speed was varied from 200 rpm (350 s^{-1}) to 400 rpm (950 s^{-1}), and the floc formation conditions were otherwise the same in all cases. Figure 6.34 shows the results of dynamic monitoring for the optimum dosage of TBP at pH 7. The initial parts of the flocculation curves show the reproducibility of the process.

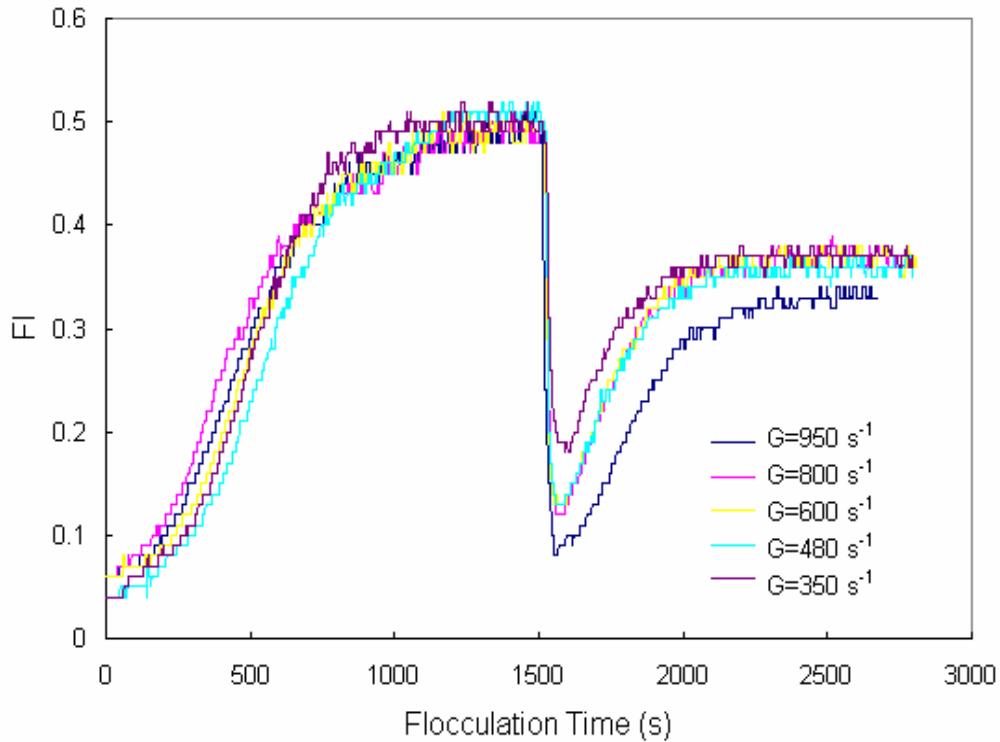


Figure 6.34 Monitoring of floc formation at 50 rpm (48 s^{-1}) with varying breakage speed (200 rpm (350 s^{-1}) to 400 rpm (950 s^{-1})) and re-formation at 50 rpm (48 s^{-1}) (50 mg l^{-1} kaolin suspension at pH7)

From Figure 6.34, it can be seen that by increasing the stirring rate from 50 rpm (48 s^{-1}) to a higher rate ($\geq 350 \text{ s}^{-1}$), there is an immediate and rapid decrease in FI, corresponding to a rapid breakage of flocs. The minimum FI value was found to decrease from 0.18 to 0.08 with increasing stirring rate from 200 rpm (350 s^{-1}) to 400 rpm (950 s^{-1}). After the stirring speed was reduced back to 50 rpm (48 s^{-1}) there was a clear but limited re-growth of flocs, to about the same FI value for all the previous stirring speeds, with the exception of 400 rpm which gave a lower FI. Clearly, when flocs formed by TBP are subjected to an increased velocity gradient ($\geq 350 \text{ s}^{-1}$), irreversible floc breakage can occur, since the FI value recovers to only a fraction of its value than that for the original flocs.

The differences in the dynamic monitoring results are reflected in the

residual turbidity values. The residual turbidity after settling for 30 minutes was measured to compare the potential removal after sedimentation. The values shown in Figure 6.35 are for samples taken before breakage and after re-formation. There is an apparent increasing of residual turbidity after re-formation of the flocs at 400 rpm (950 s^{-1}). This residual turbidity is discernibly higher than for the other conditions, suggesting the lower recovery of flocs after breakage.

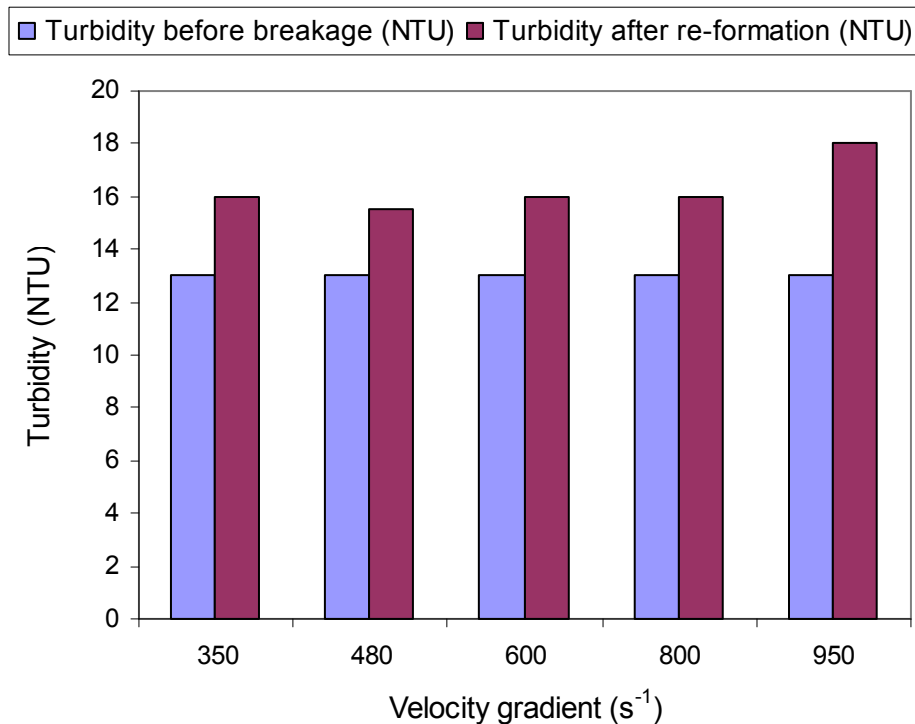


Figure 6.35 Variation of residual turbidity before breakage and after re-formation, with velocity gradient at pH7 (50 mg l^{-1} kaolin suspension)

The influence of the duration of the fast stirring rate was investigated at a constant rate of 300 rpm (600 s^{-1}); the results are shown in Figure 6.36. It can be seen that with increasing duration from 10 s to 300 s at 300rpm (600 s^{-1}), there is evidence of:

- a greater severity of floc breakup (lower minimum FI);
- a more delayed re-growth phase;

- a more limited final floc growth (steady state FI).

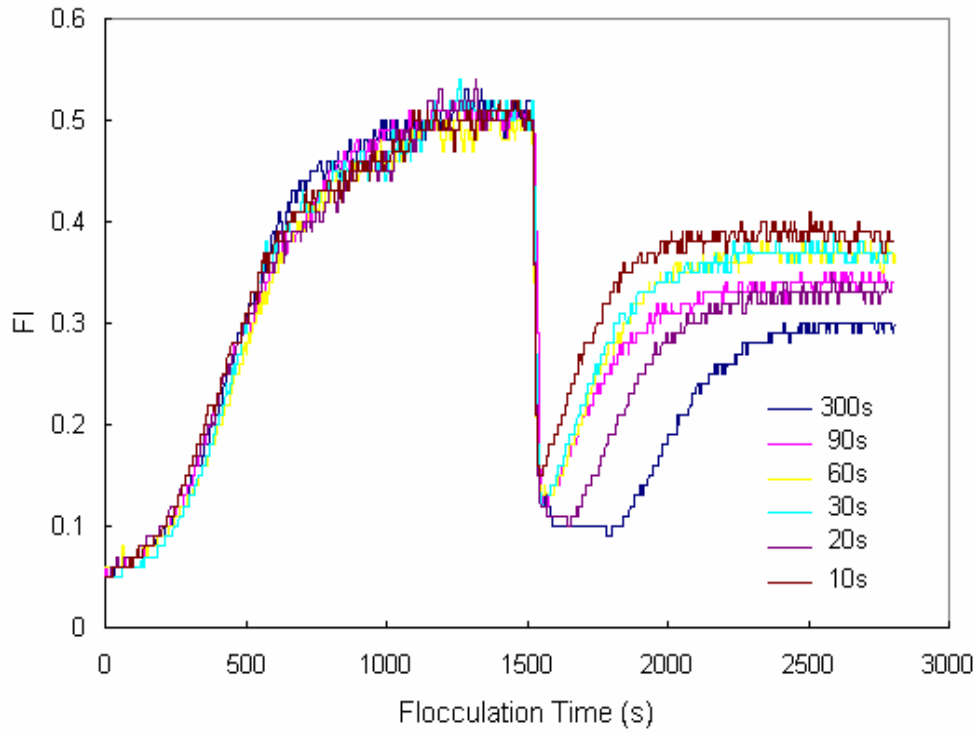


Figure 6.36 Monitoring of floc formation at 50 rpm (48 s^{-1}), breakage at 300 rpm (600 s^{-1}) for different periods and re-formation at 50 rpm (48 s^{-1}) at pH7 (50 mg l^{-1} kaolin suspension)

A general trend was found that the floc strength decreased with increasing floc size. In Figure 6.36, the original flocs formed at the slow stirring speed (at 50 rpm; with a high FI value of 0.5) were believed to have lower floc strength than re-formed final flocs with a lower FI value of 0.4. Furthermore, the results of residual turbidity before breakage and after re-formation with different breakage periods are shown in Figure 6.37. It is apparent that floc breakage for the longer period (300s) gives the highest residual turbidity.

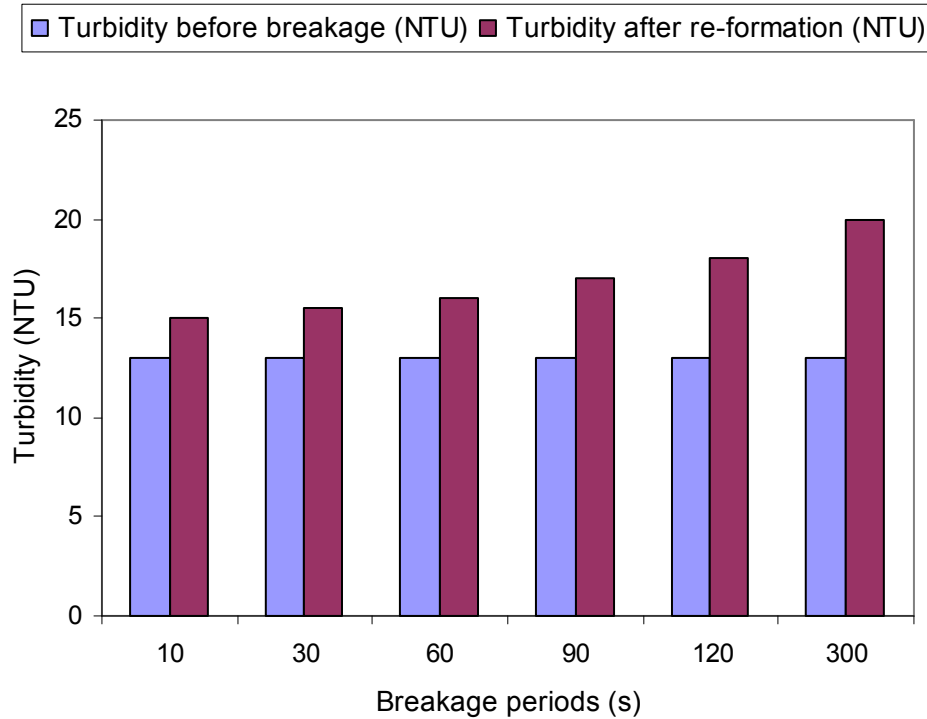


Figure 6.37 Variation of residual turbidity before breakage and after re-formation, with breakage period at pH 7 (50 mg l⁻¹ kaolin suspension)

6.6.2 Floc Strength of TBP in Comparison with Other Coagulants

A comparison of floc strength tests with alum and polyDADMAC, as coagulants, was investigated. For the test conditions used in this study (50 mg l⁻¹ kaolin suspension, pH 7), previous work had found that the optimum dosage for alum was about 3.4 mg l⁻¹ as Al³⁺, and 0.125 mg l⁻¹ for polyDADMAC. Some researchers (99, 100) have used ‘strength factor’ and ‘recovery factor’ to quantify floc strength. The Flocculation Index values for initial (FI₁), broken (FI₂) and reformed (FI₃) flocs are used as a surrogate for floc size in the strength equations, which are defined by Gregory (101,158) as:

$$\text{Strength factor} = (FI_2 / FI_1) \cdot 100 \quad \text{----- (6.1)}$$

$$\text{Recovery factor} = [(FI_3 - FI_2) / (FI_1 - FI_2)] \cdot 100 \quad \text{----- (6.2)}$$

However, the strength factor only represents the breakage factor, which may not be the best representative measure of the strength of flocs.

At pH 7, the formation, breakage and re-formation of flocs formed by alum, polyDADMAC and TBP under two different conditions of breakage (300 rpm for 60 s; and 300 rpm for 300 s) were measured by PDA using the 2L Gator jar. The results in terms of the FI response are shown in Figures 6.38 and 6.39. Strength and recovery factors obtained for flocs obtained using the different coagulants under the two different conditions of breakage (300 rpm for 60 s; and 300 rpm for 300 s) are given in Tables 6.14 and 6.15.

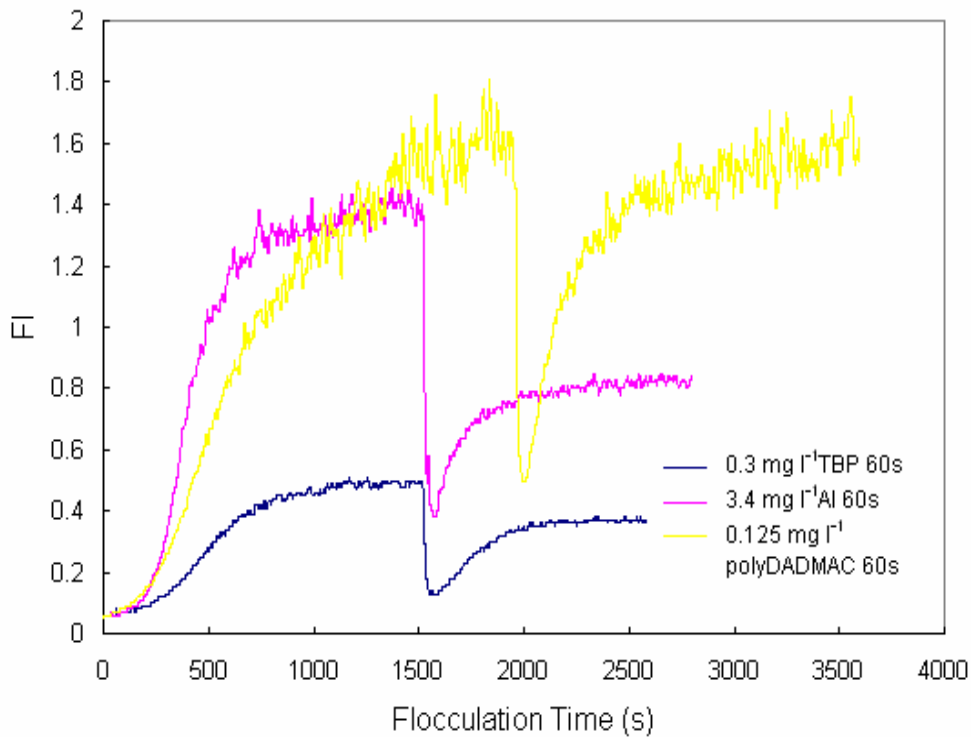


Figure 6.38 Monitoring of floc formation at 50 rpm, breakage at 300 rpm for 60 s and re-formation at 50 rpm using different coagulants at pH 7 (50 mg l⁻¹ kaolin suspension)

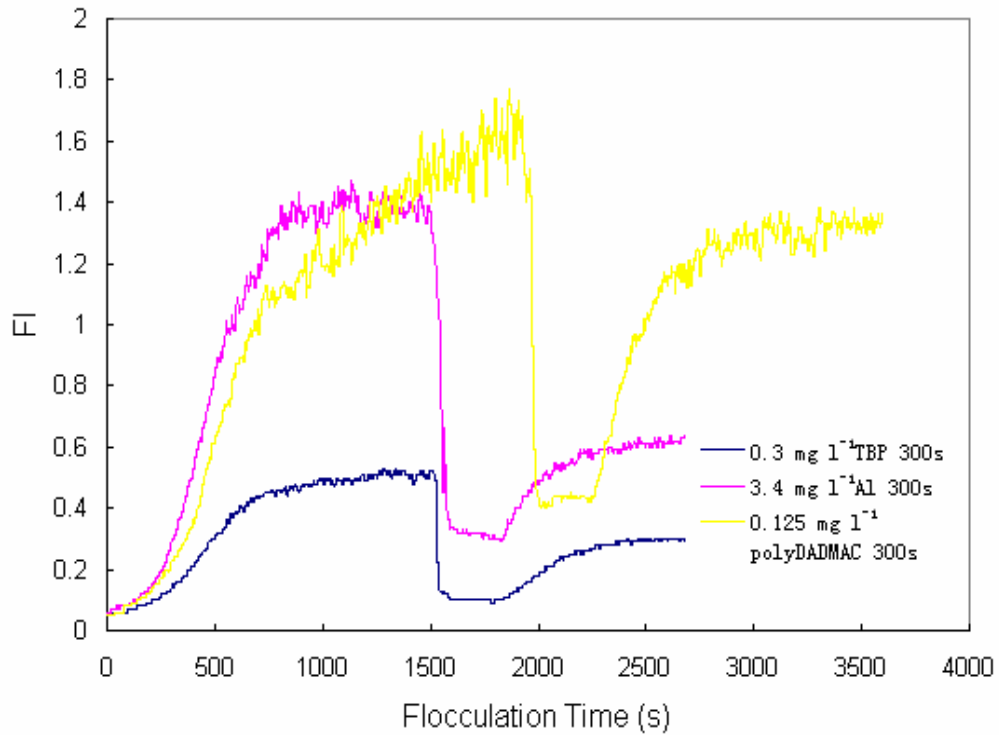


Figure 6.39 Monitoring of floc formation at 50 rpm, breakage at 300 rpm for 300 s and re-formation at 50 rpm using different coagulants at pH 7 (50 mg l⁻¹ kaolin suspension)

TABLE 6.14 Strength and recovery factors obtained for different coagulants (floc breakage at 300 rpm and 60 s) at pH 7 (50 mg l⁻¹ kaolin suspension)

	Alum	polyDADMAC	TBP
Strength factor	26.8	27.8	25.0
Recovery factor	42.3	96.2	61.5

TABLE 6.15 Strength and recovery factors obtained for different coagulants (floc breakage at 300 rpm and 300 s) at pH 7 (50 mg l⁻¹ kaolin suspension)

	Alum	polyDADMAC	TBP
Strength factor	20.3	22.3	19.2
Recovery factor	30.7	70.1	47.6

The results given in Table 6.14 and 6.15 show that for both breakage conditions, the strength factor for the three coagulants were very similar, with polyDADMAC producing marginally the greatest floc strength, and TBP marginally the lowest floc strength. However, the recovery factor for the two polymer coagulants was significantly greater than that with alum. This is consistent with other studies, for example, Yukselen and Gregory (101) found that alum gave lower floc strength and recovery values than cationic polyelectrolytes (including polyDADMAC). However, the recovery factor with TBP was substantially lower than that obtained with polyDADMAC. It is relevant to note that under the test conditions (ie. pH 7), polyDADMAC retains a high cationic charge ($\sim 6 \text{ meq g}^{-1}$), in sharp contrast to the TBP which has a greatly reduced cationic charge ($< 0.7 \text{ meq g}^{-1}$); this may be a key factor influencing the capability for floc re-formation.

The formation, breakage and re-formation of flocs formed by TBP at pH 9 were also investigated since previous studies have shown rapid coagulation at this elevated pH (at the optimal TBP dose), and the results are shown in Figure 6.40. At pH 9, for floc breakage times of 60 s and 300 s (at 300 rpm), the strength factors of TBP were 35.3 and 29.6, respectively, and the recovery factors were 71.5 and 54.6, respectively. Comparing with the TBP performance at pH 7, the strength and recovery factor of TBP at pH 9 were significantly increased. It is also interesting to note that the TBP floc strength at pH 9 was superior to alum at pH 7.

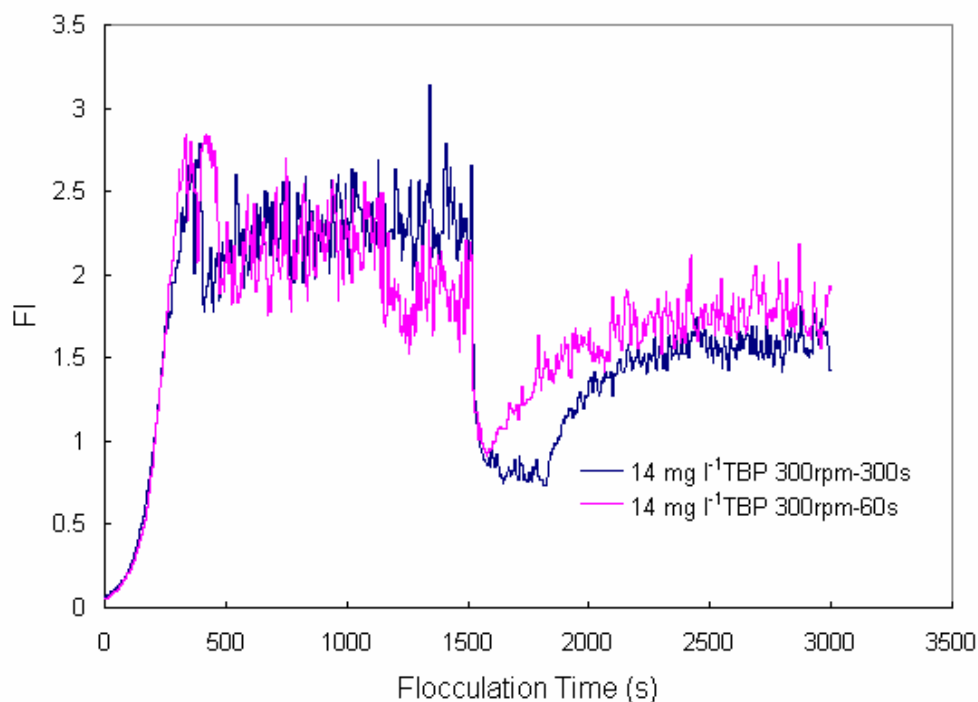


Figure 6.40 Monitoring of floc formation, and re-formation at pH9 using TBP
(50 mg l⁻¹ kaolin suspension)

6.7 Discussion

It was well established and demonstrated in this study that the optimum dose and coagulant mechanisms of TBP are pH dependent. Under acidic and neutral conditions, the charge density of TBP decreases with increasing pH value, thus, more TBP is needed to interact with the negative particles in the model water. This is quite consistent with the charge neutralization hypothesis, which requires that the optimal polymer concentrations correspond to the opposite charge on the surface of particles and are quantitatively adsorbed to the point of charge neutralization. This is supported by the previous evidence that the optimal polymer dose occurs at the point of zero particle mobility (159). In this case, the restabilization effect may be simply a result of charge reversal. With higher charge density, the ionisable group may lead to significant repulsion between segments of the polymer chain and hence an expansion from the typical random

coil configuration. Because of the strong electrostatic interaction, polyelectrolyte chains should adopt a rather flat configuration on oppositely charged surfaces, which would reduce the possibility of bridging (45). In contrast, at high pH, the remarkable distinction was observed from the change in flocculation kinetics, floc size and the amount of the flocculant. With regard to the low or non-charge of TBP at alkali conditions, 'polymer bridging' was able to provide an adequate explanation. Graham (21) indicated that for the optimal bridging effect, the number of bound polymer segments available for interparticle adsorption should equal the number of vacant sites of particles. Increasing the amount of the polymer with non-charge would increase the number of adsorbed segment loops thereby enhancing the possibility of interparticle bridging. At excess coagulant concentrations, surfaces of particles become saturated with the adsorbed polymer and the particles are re-stabilized.

During charge neutralisation, counterions are adsorbed on colloidal particles and the particle charge is reduced. The concentration of specifically-adsorbing counterions required to cause flocculation is called the critical flocculation concentration (cfc) (160). Stumm and O'Melia (161) employed the term 'stoichiometric' to describe the linear dependence of cfc on particle concentration. At acid and neutral pH values, the optimum dosage of TBP is directly proportional to the particle or humic substance concentrations, strongly suggesting the existence of charge neutralization. In theory, when polymer bridging is the principal mechanism of coagulation, the optimum dosages should be also directly proportional to the total particle surface area and hence to the particle concentration (19). However, Runkana *et al.* (62) found that theories of bridging flocculation assuming equilibrium conditions were of limited use in practice. In this case, evidence of non-stoichiometry between particle suspension and a higher dosage of TBP at pH 9 implied that complications may arise from the possible effects of 'polymer bridging' and the relative extent of TBP precipitation at higher pH values.

It was clearly found that the flocculation kinetics and the effectiveness of TBP are strongly dependent on pH and the concentrations of the particles and the polymer. Furthermore, the flocculation performance at the optimal TBP dosage was also found to be considerably influenced by some other factors, namely the polymer age, mixing speed and the type of reactor. The apparent diminution of the peak flocculation index at low pH for 'ageing' TBP is thought to be the consequence of changes in the deprotonation of the charge group with time.

Further evidence from the PDA results shows that, for all coagulants, there is a variation in coagulation effectiveness with model waters of suspensions and humic substances. In terms of Flocculation Index, a synthetic polymeric coagulant, polyDADMAC, presented a consistently high performance in both model waters at different pH values. In contrast, TBP only exhibited a superior performance in humic solution or particle suspension with higher pH, compared to the traditional metal coagulant, alum. Once more, aggregates formed by 'polymer bridging' using TBP at pH 9 or polyDADMAC (independent of pH) appeared to be significantly more resistant to breakage (hence higher strength factor) in comparison to the flocs produced by charge neutralization using alum as the primary coagulant. The effectiveness of polymeric coagulants was largely the result of the forming of strong flocs. This result is consistent with the observation of Yukselen and Gregory (101), who proposed that the flocs produced by cationic polymers can be much stronger than those formed when particles are destabilized by simple salts. But, from the other parameters of treated water, for the model water containing kaolin suspension, the treatment performance (turbidity reduction) of the alternative coagulants decreased in the following order (pH 7): alum, polyDADMAC, TBP; for the model water containing HA, the treatment performance (DOC reduction) of the alternative coagulants decreased in the following order (pH 7): alum, TBP and polyDADMAC.

7. RESULTS: IMPROVEMENT OF TBP COAGULATION PERFORMANCE USING DUAL COAGULANTS OF TBP WITH ALUM IN MODEL WATER

7.1 Introduction

The use of a high molecular weight, long-chain polymer in conjunction with a metal salt as a primary coagulant has become the most attractive treatment option for water treatment. It is logical to combine inorganic coagulants with some cationic organic polymers that should strengthen both the aggregating and charge neutralizing capabilities (5). This is supported by the results of Bolto *et al.* (6), who, using jar tests on reconstituted waters with alum and cationic polyDADMAC, indicated synergistic benefits from the combination of the two. The use of polymers in this way resulted in a substantial lowering of the alum dose required, a 40-60% reduction being possible (92). In addition, the work of Edzwald *et al.* (7) showed that for water containing 5 mg l⁻¹ humic acid, adding a polymer in conjunction with 10 mg l⁻¹ of alum gave a 95% reduction in DOC, in comparison with only 20% removal when 75 mg l⁻¹ of alum was used as the sole coagulant. Yu *et al.* (162) has observed that the most effective removal of humic substances prior to reverse osmosis treatment was achieved by the combination of an inorganic coagulant with a cationic polymer such as polyDADMAC.

As a novel natural modified polymer, the application of TBP in water treatment is still in the tentative and superficial stage. At the start of this work, the relative merits of partial or complete replacement of alum by TBP as primary coagulant in water treatment were still not determined. This chapter is concerned with the coagulation performance in model waters using alum and cationic TBP as combined primary coagulants (partial alum replacement). Other reported studies (112, 134) have concluded that particles / color coagulation and removal with alum are pH-dependent. Although the optimal pH for particles / color

removal is less than 6, some research evidence (163) has shown with natural water samples that the optimum pH for minimum residual aluminium is between 6 and 7. Thus, in order to investigate the coagulation mechanism and the effectiveness of alum-TBP combination in model water with particle suspension, two pH values of 5 and 7 were chosen in this study. Furthermore, using humic substances as model water, the study also summarized the results of extensive laboratory experiments designed to investigate whether a unique optimal dosage of combined alum and cationic TBP exists at a given pH value of 6, at which the coagulation performance was believed to be maximized.

7.2 Coagulation Action of Dual Coagulant in 50 mg l⁻¹ Kaolin Suspension

The primary aim of the laboratory tests in this stage is to assess the coagulation performance of TBP/alum with a model water (50 mg l⁻¹ kaolin suspension) using the PDA coagulation system. Initial tests were undertaken at pH 5.0 and 7.0 with a view to reduce the aluminium dose in the usual pH range where aluminium is used as the sole coagulant. To select the optimum conditions for the alum/TBP dose matrix and provide more insight into the nature of the coagulation mechanism of TBP combined with aluminium, floc volume and turbidity were measured. Efforts to employ Graphite furnace AAS have been undertaken in order to measure the residual aluminium concentration after filtration by 0.45µM filter paper.

7.2.1 Effect of Solution pH and Optimum Dosage of Alum

In order to investigate the effectiveness of partial replacement of alum by TBP in the coagulation processes, it was necessary to determine initially, as a reference, the optimum performance of the coagulation using alum as the sole coagulant at different pH values. Prior to this, a preliminary assessment was made of the influence of solution pH and alum dosage on particle coagulation using

PDA. The laboratory experiments have been undertaken over a wide range of aluminium concentrations (0.05 mg l^{-1} - 200 mg l^{-1} as Al^{3+}) to determine the optimum dose at pH4, 5, 7 and 9.

At pH4, very fine floc was observed using three broad aluminium concentration ranges—low (0.5 mg l^{-1} - 8 mg l^{-1} as Al^{3+}), medium (10 mg l^{-1} - 100 mg l^{-1} as Al^{3+}) and high (greater than 100 mg l^{-1} as Al^{3+}). The wide concentration ranges of Al^{3+} considered here were based on some previous research studies (89,164-169). The PDA results are summarised in Figure 7.1.

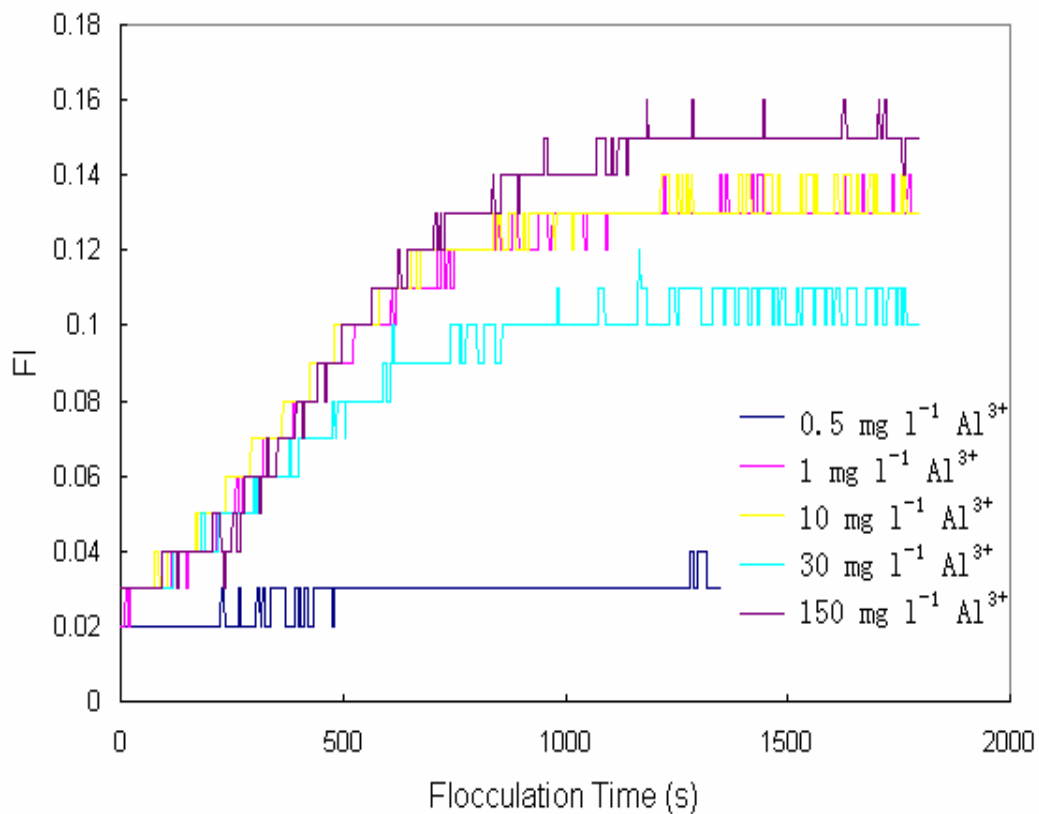


Figure 7.1 Dynamic monitoring of kaolin coagulation (50 mg l^{-1}) at pH4 using different dosages of alum

It can be seen that at pH 4, for the 50 mg l^{-1} kaolin clay suspensions, the maximum Flocculation Index, 0.15, was found when using 150 mg l^{-1} Al^{3+} as coagulant. However, most of other dosages also gave similar FI values around

0.13 to 0.15, and the values of final turbidity were all close to 37 to 39 NTU, compared with the initial turbidity of model water, 40 NTU. This indicates that there was a poor coagulation performance over a wide range of alum doses at pH4.

At pH5, there was a clear optimal Al^{3+} dose of 0.2 mg l^{-1} , which gave a maximum FI of around 0.3. The results are shown in Figure 7.2. Lower alum concentrations (0.02 mg l^{-1} as Al^{3+}) gave a poorer coagulation performance, suggesting insufficient coagulant for destabilisation. At the highest alum dosage (0.4 mg l^{-1} Al^{3+}), the FI was less than at lower dosages, most likely indicating that charge restabilisation was occurring.

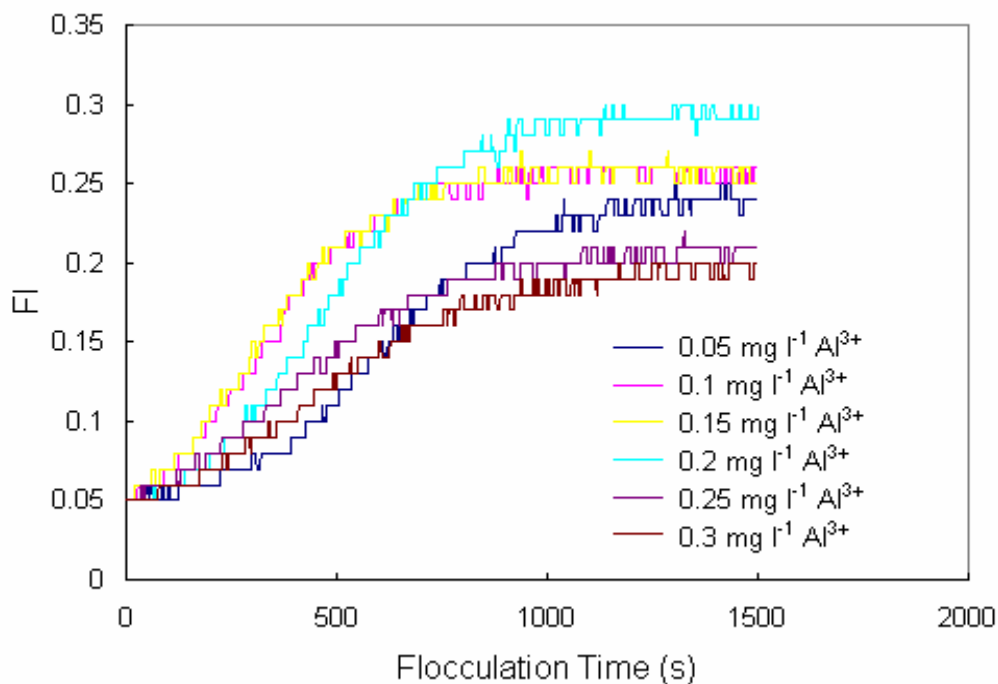


Figure 7.2 Dynamic monitoring of kaolin coagulation (50 mg l^{-1}) at pH5 using different dosage of alum

At pH 7, the optimal Al dose, 3.4 mg l^{-1} as Al^{3+} , has been determined as reported in section 6.5. Figure 7.3 shows the PDA results using different doses of alum as coagulant at pH 7.

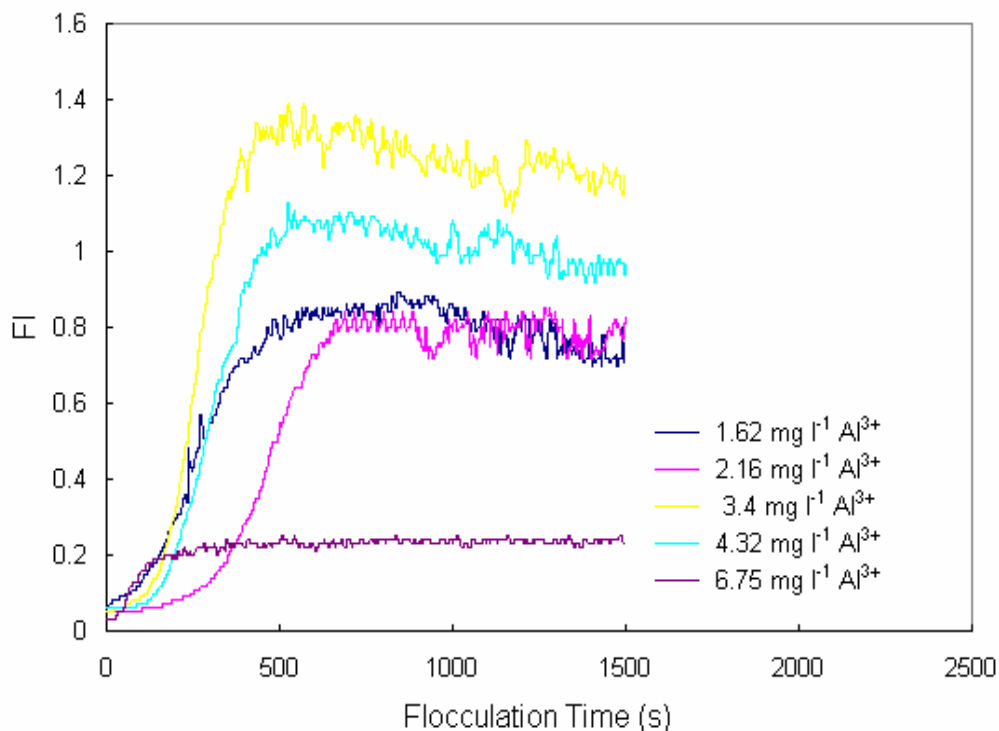


Figure 7.3 Dynamic monitoring of kaolin coagulation (50 mg l^{-1}) at pH7 using different dosage of alum

At pH 9, there was no FI response observed by the PDA using different doses of alum, indicating that the coagulation dose not occur at such high pH values; this is believed to be because the soluble anionic form Al(OH)_4^- becomes the dominant Al species at high pH (~ 9).

In general, it is well-known that the coagulation mechanism of alum is pH dependent. At pH 5.0 and below, the dominant Al soluble species are monomeric and dimeric cations (eg. Al^{3+} , Al(OH)^{2+} , Al(OH)_2^+) and the mechanism involves aggregation of particles by charge neutralisation. At pH 6 (minimum Al solubility) and above, the dominant mechanism is believed to be adsorption of particle species on precipitated Al(OH)_3 , known as ‘sweep flocculation’. At high pH 9, the soluble anionic form Al(OH)_4^- occurs, thus, no coagulation is observed (134). In view of these results, pH 5 and 7 were chosen as

the solution pH values for investigating the coagulation performance and mechanism of combined alum/TBP as coagulants.

7.2.2 Optimum Alum-TBP Combination at pH 7

The optimal dosage of TBP for 50 mg l⁻¹ kaolin suspension at pH7 is about 0.3 mg l⁻¹, giving a maximum FI around 0.52, and the lowest residual turbidity about 13 NTU, compared with other dosages of TBP. The optimal dose of alum is about 3.4 mg l⁻¹ as Al³⁺, with an FI value of 1.39 and residual turbidity of 3.5 NTU. These results were reported in section 6.5. Based on the optimum dose of Al³⁺ at pH7, a series of tests have been undertaken by reducing the dosage of aluminium from 3.4 mg l⁻¹ to 1.0 mg l⁻¹. At each dosage coagulation tests were carried out with a range of polymer dosage from 0.05 mg l⁻¹ to 0.4 mg l⁻¹. The dynamic monitoring results are shown in Figures 7.4 to 7.9.

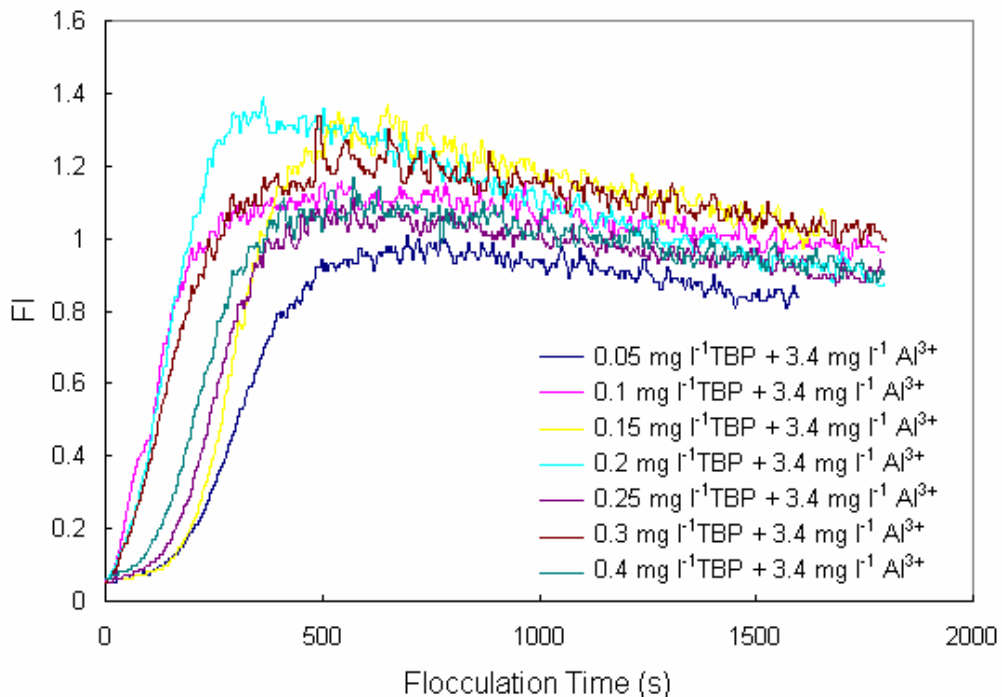


Figure 7.4 Flocculation index response with TBP dose and 3.4 mg l⁻¹ Al³⁺ at pH7 (50 mg l⁻¹ Kaolin suspension)

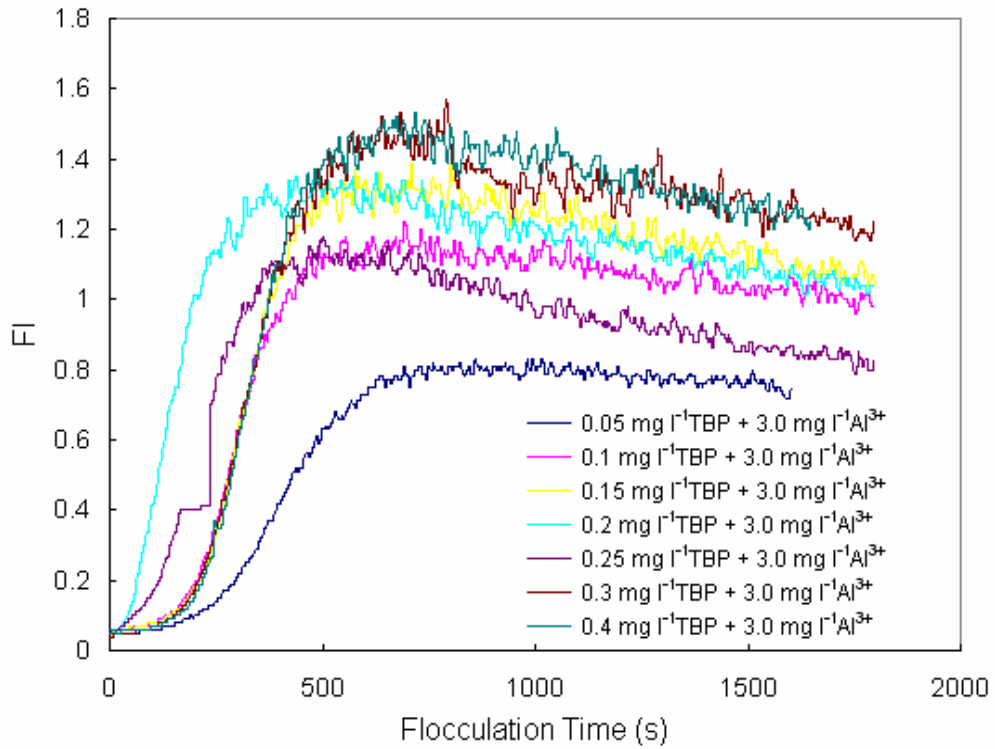


Figure 7.5 Flocculation index response with TBP dose and $3.0 \text{ mg l}^{-1} \text{ Al}^{3+}$ at pH7 (50 mg l^{-1} kaolin suspension)

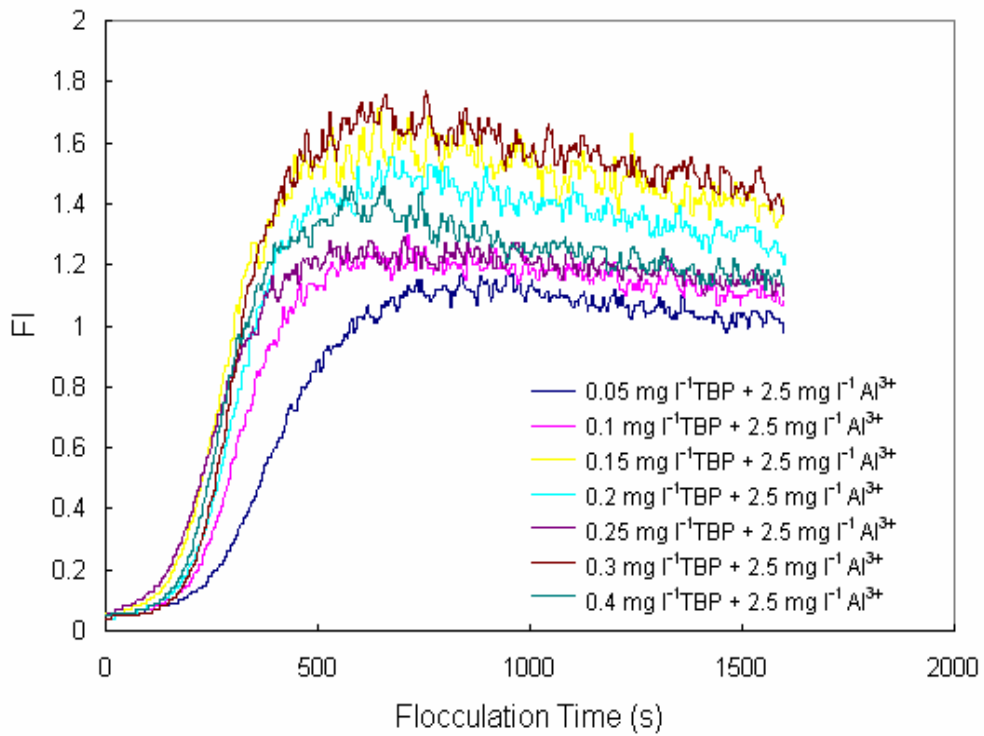


Figure 7.6 Flocculation index response with TBP dose and $2.5 \text{ mg l}^{-1} \text{ Al}^{3+}$ at pH7 (50 mg l^{-1} kaolin suspension)

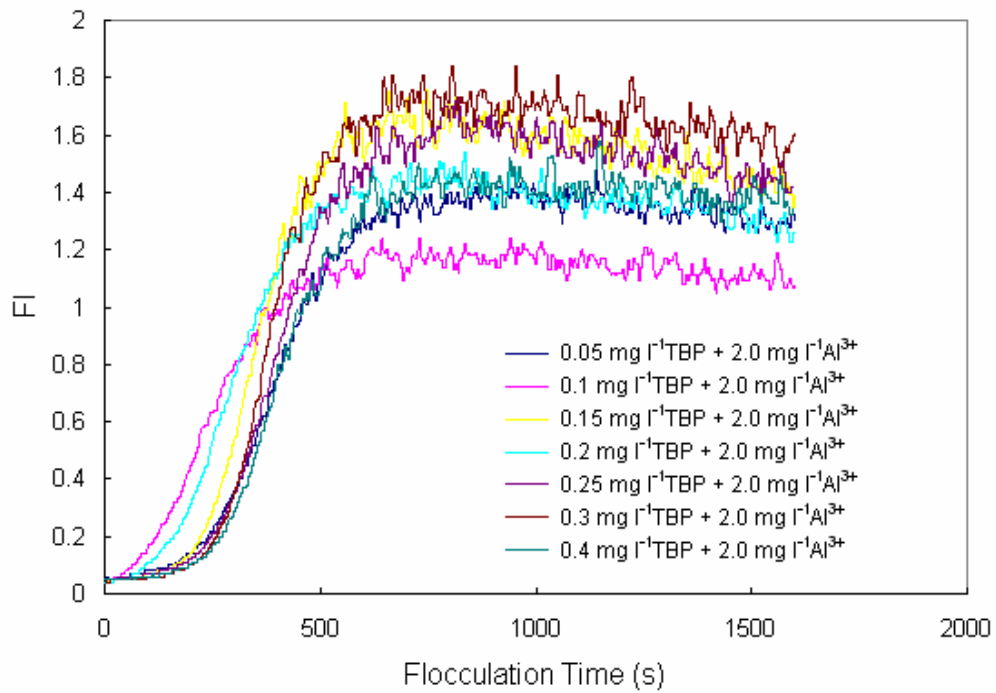


Figure 7.7 Flocculation index response with TBP dose and 2.0 mg l⁻¹ Al³⁺ at pH7 (50 mg l⁻¹ kaolin suspension)

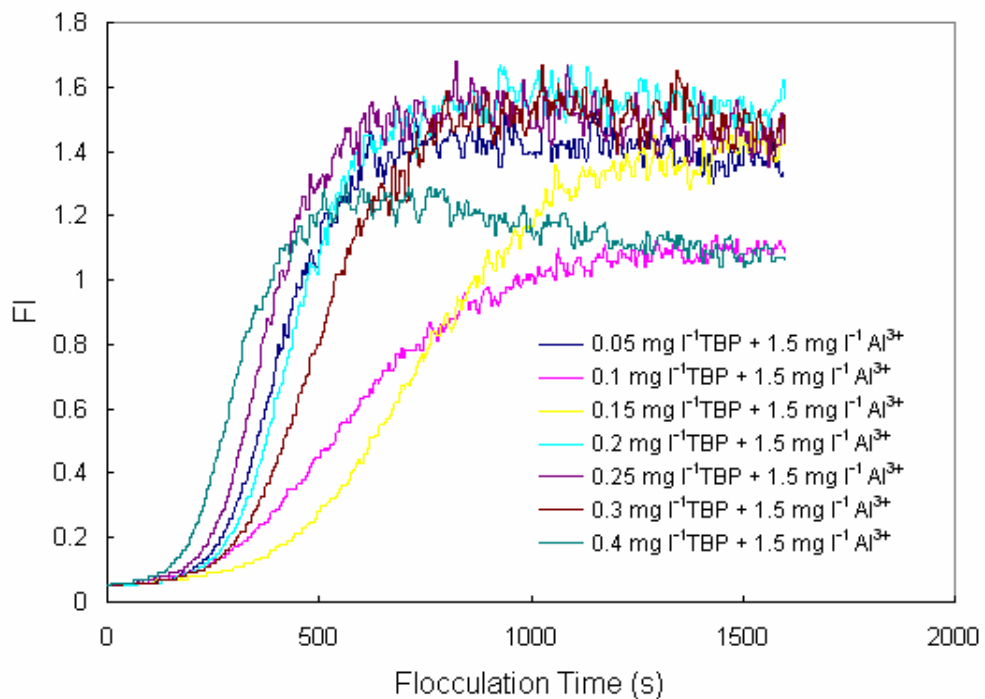


Figure 7.8 Flocculation index response with TBP dose and 1.5 mg l⁻¹ Al³⁺ at pH7 (50 mg l⁻¹ kaolin suspension)

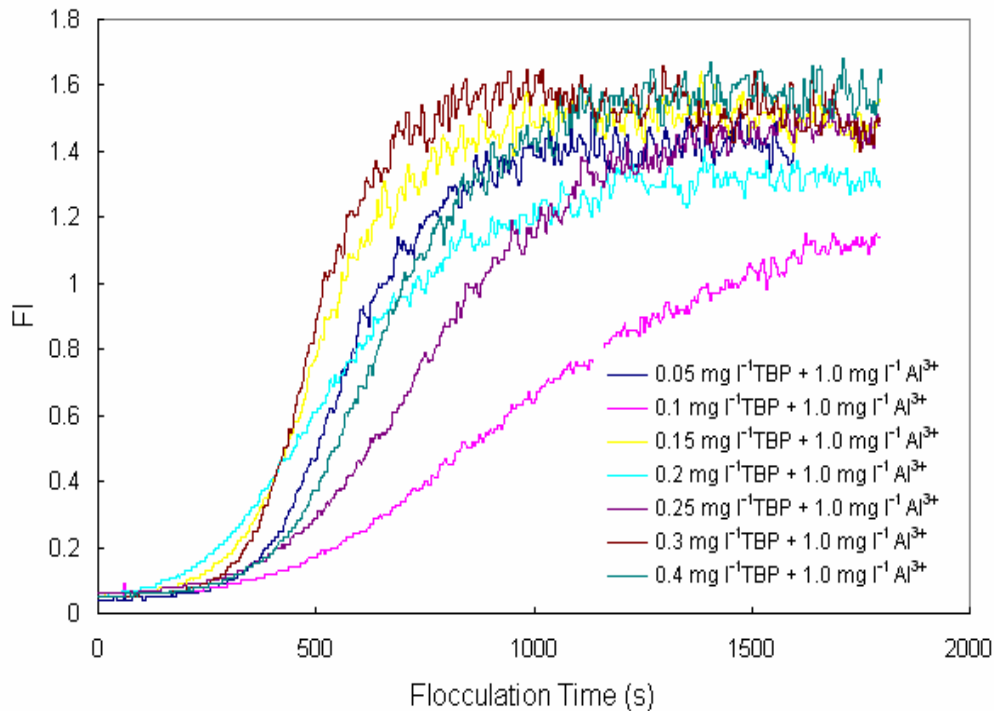


Figure 7.9 Flocculation index response with TBP dose and $1.0 \text{ mg l}^{-1} \text{ Al}^{3+}$ at pH7 (50 mg l^{-1} kaolin suspension)

The variation of Flocculation Index with the doses of alum and TBP is summarised in Figure 7.10, where it is noted that in most cases the maximum Flocculation Index values were found when 0.3 mg l^{-1} TBP was used in combination with different doses of alum. Previous work has provided evidence that for the flocculation of kaolin suspension at $\text{pH} \leq 7$, a stoichiometric relationship exists between TBP and kaolin clay, indicating that charge interaction and neutralisation was the dominant mechanism for the flocculation using TBP. However, in this series of tests there was no clear evidence of a need for increasing TBP dosage to achieve a large Flocculation Index as the alum dosage decreased. Consequently, it seems likely that the flocculation effect is influenced by other phenomena (than simply charge interaction), such as the extent of $\text{Al}(\text{OH})_3$ precipitation.

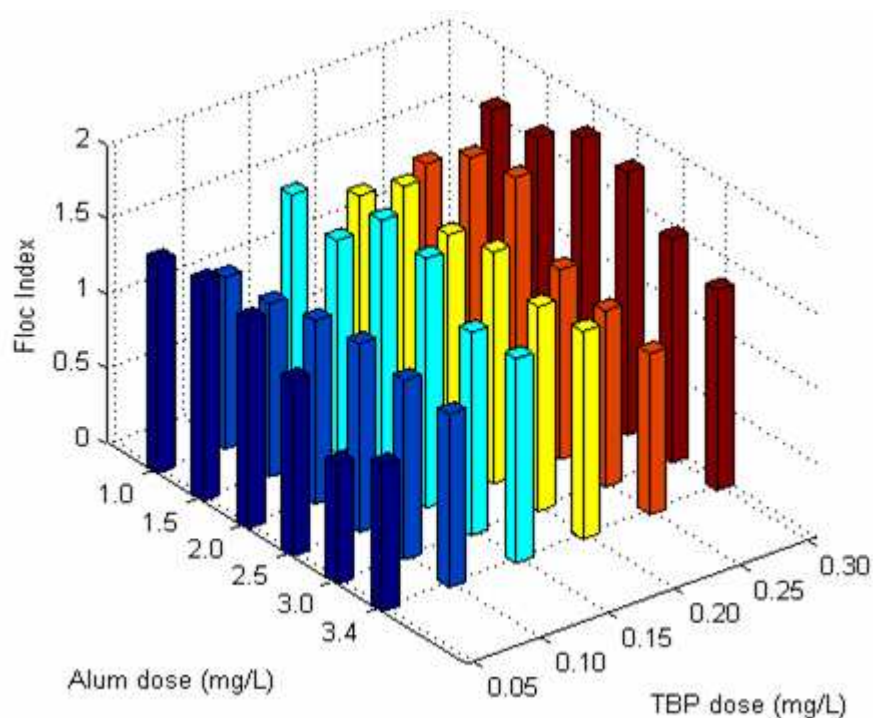


Figure 7.10 Variation of Flocculation index with alum (as Al) and TBP doses at pH7 (50 mg l⁻¹ kaolin suspension)

The optimum dosage for TBP at each alum dose (as Al, at pH 7) was determined, and the results for the flocculation index, residual turbidity and floc volume are summarised in Table 7.1. From Table 7.1, it can be seen that at pH 7, the optimal dose of TBP was insensitive to the alum dose and in most cases equal to the maximum TBP dose applied. Compared with the use of alum or TBP as sole coagulant, the use of dual coagulants with a TBP/Al mass ratio of 0.3/2.0 improved the coagulation performance in terms of the highest FI (1.80) and floc volume. It can be seen that compared to alum alone, the performance was not as good in terms of the residual turbidity. However, compared to the use of TBP alone, the TBP/Al combination was better in terms of a lower residual turbidity. Subsequent analysis of the residual aluminium concentration was carried out by Graphite furnace AAS after filtration. Even though there was no obvious relationship between residual aluminium with the dose combinations of

TBP/alum, very low concentrations of aluminium in the final water indicated a good coagulation performance using the dual coagulant.

TABLE 7.1 Coagulation performance for the optimum dosage of TBP at each alum dose (in terms of maximum flocculation index, residual turbidity and aluminium, and Floc volume) at pH7 (50 mg l⁻¹ kaolin suspension)

Al dosage (mg l ⁻¹)	TBP dosage (mg l ⁻¹)	FI	Residual Turbidity (NTU)	Floc Volume (ml)	Residual [Al ³⁺] (µg l ⁻¹)
3.4	0.0	1.39	3.5	5.0	10.1
3.4	0.2	1.39	16.0	4.5	11.9
3.0	0.3	1.50	14.0	6.5	3.4
2.5	0.3	1.76	12.5	6.5	8.6
2.0	0.3	1.80	9.0	6.5	8.1
1.5	0.25	1.65	10.0	3.5	7.2
1.0	0.3	1.62	15.0	3.5	6.7
0.0	0.3	0.52	13.0	4.0	--

Note: "--" indicated the value is out of the calibration range of Graphite furnace AAS.

7.2.3 Optimum Alum-TBP Combination at pH 5

The optimum dosage of TBP for 50 mg l⁻¹ kaolin suspension at pH 5 is about 0.25 mg l⁻¹, giving a maximum FI of about 0.32, and the lowest residual turbidity about 18.5 NTU; these results were reported previously in Section 6.2.1. As noted in Section 7.2.1, at pH 5, the optimal Al³⁺ dose for 50 mg l⁻¹ kaolin suspension is 0.2 mg l⁻¹, which gave a maximum FI of approximately 0.3. Based on the optimum dose of Al³⁺ at pH5, a series of tests have been undertaken by reducing the dosage of alum from 0.2 mg l⁻¹ to 0.05 mg l⁻¹ as Al³⁺. At each dosage coagulation tests were carried out with a range of polymer dosages from 0.01 mg l⁻¹ to 0.25 mg l⁻¹. The dynamic monitoring results are shown in Figures 7.11 to 7.14.

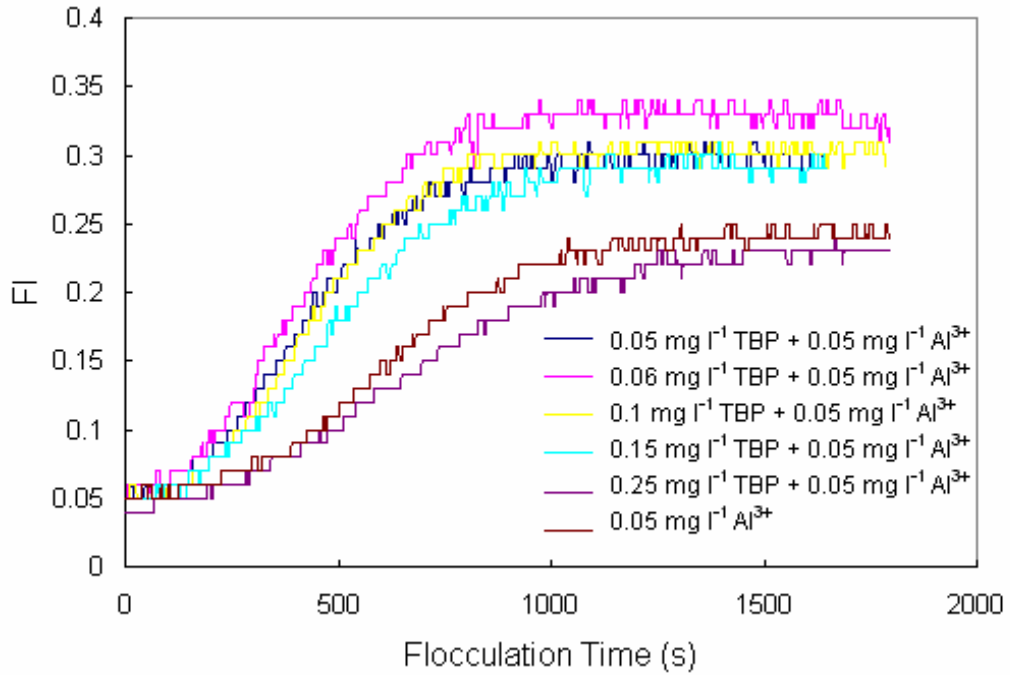


Figure 7.11 Flocculation index response with TBP dose and 0.05 mg l⁻¹ Al³⁺ at pH5 (50 mg l⁻¹ kaolin suspension)

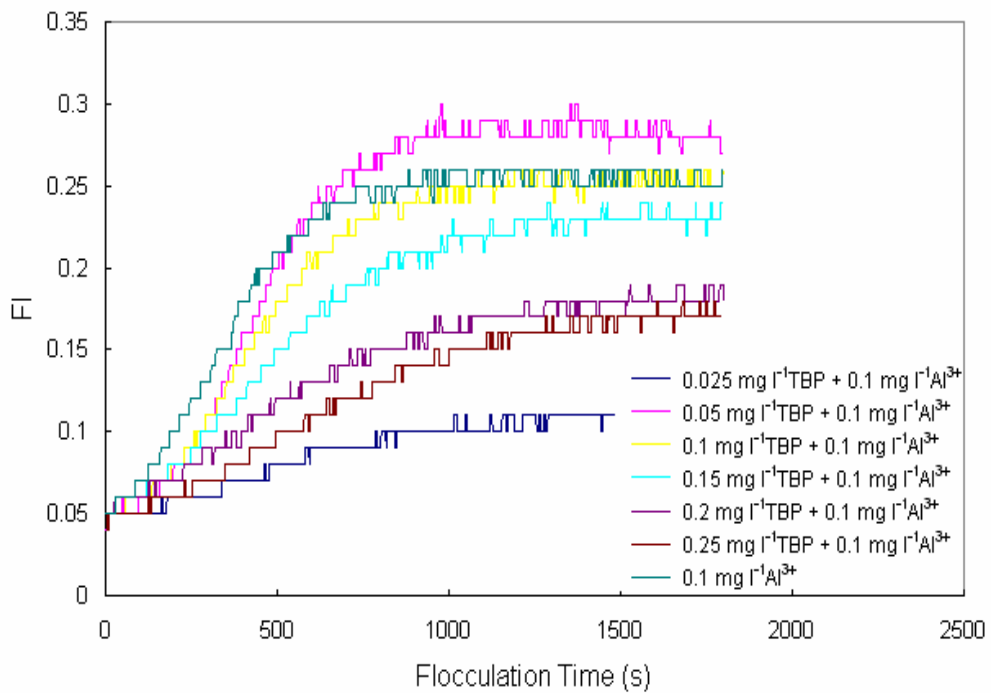


Figure 7.12 Flocculation index response with TBP dose and 0.1 mg l⁻¹ Al³⁺ at pH5 (50 mg l⁻¹ kaolin suspension)

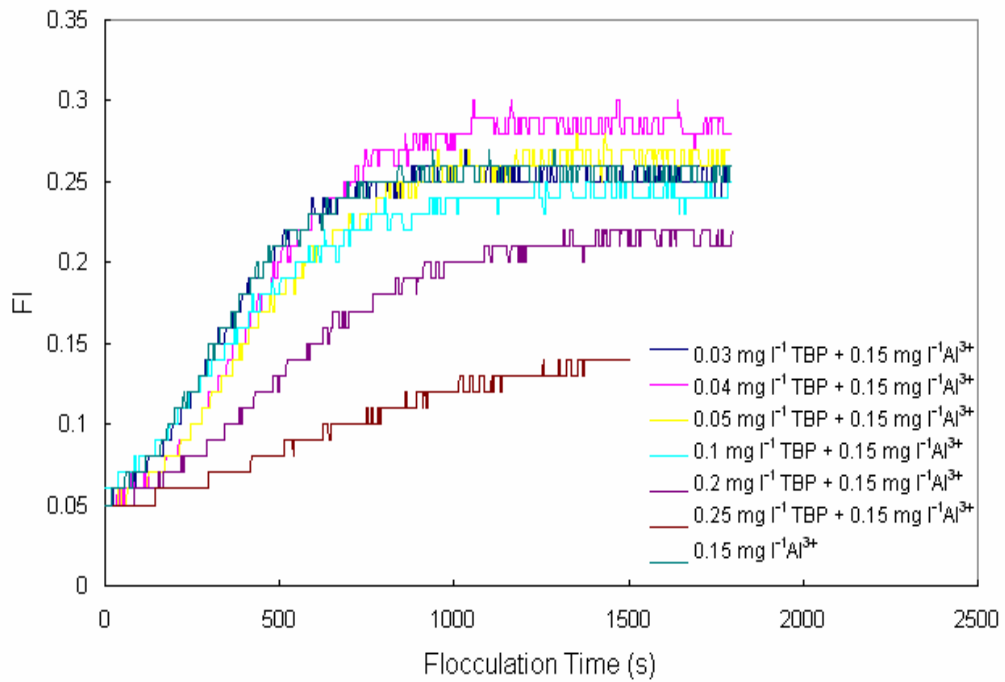


Figure 7.13 Flocculation index response with TBP dose and $0.15 \text{ mg l}^{-1} \text{ Al}^{3+}$ at pH5 (50 mg l^{-1} kaolin suspension)

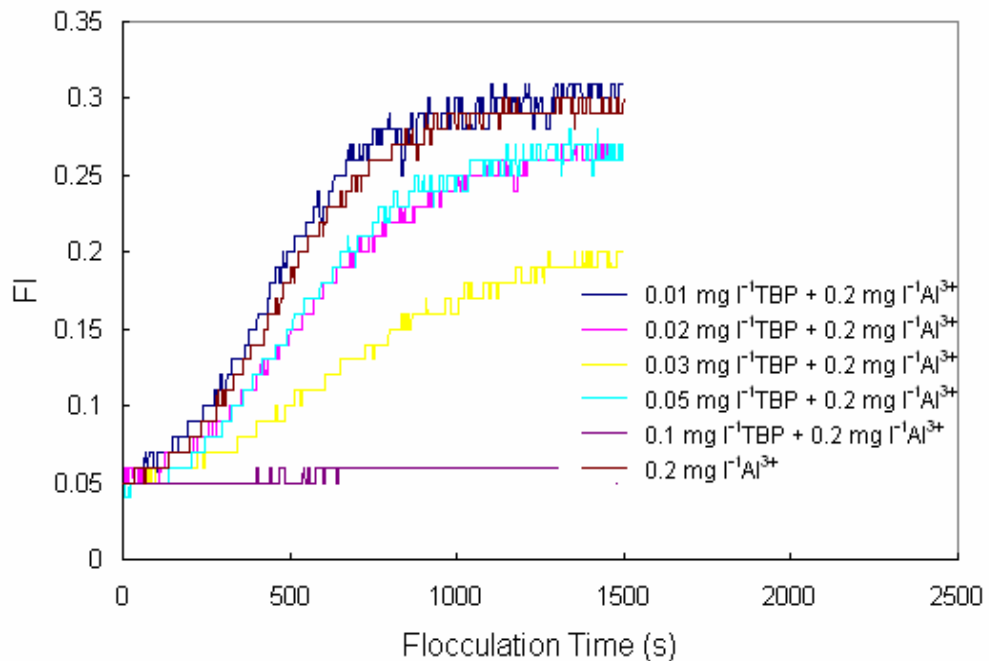


Figure 7.14 Flocculation index response with TBP dose and $0.2 \text{ mg l}^{-1} \text{ Al}^{3+}$ at pH5 (50 mg l^{-1} kaolin suspension)

The variation of Flocculation index with the doses of alum and TBP is summarised in Figure 7.15, where it is noted that at each alum dose, from 0.2 mg l⁻¹ to 0.05 mg l⁻¹ as Al³⁺, there is an optimal TBP dose corresponding to the maximum FI. This can be seen clearer in Table 7.2, which gives the coagulation performance at each alum-TBP dosage combination in terms of FI, residual turbidity and floc volume.

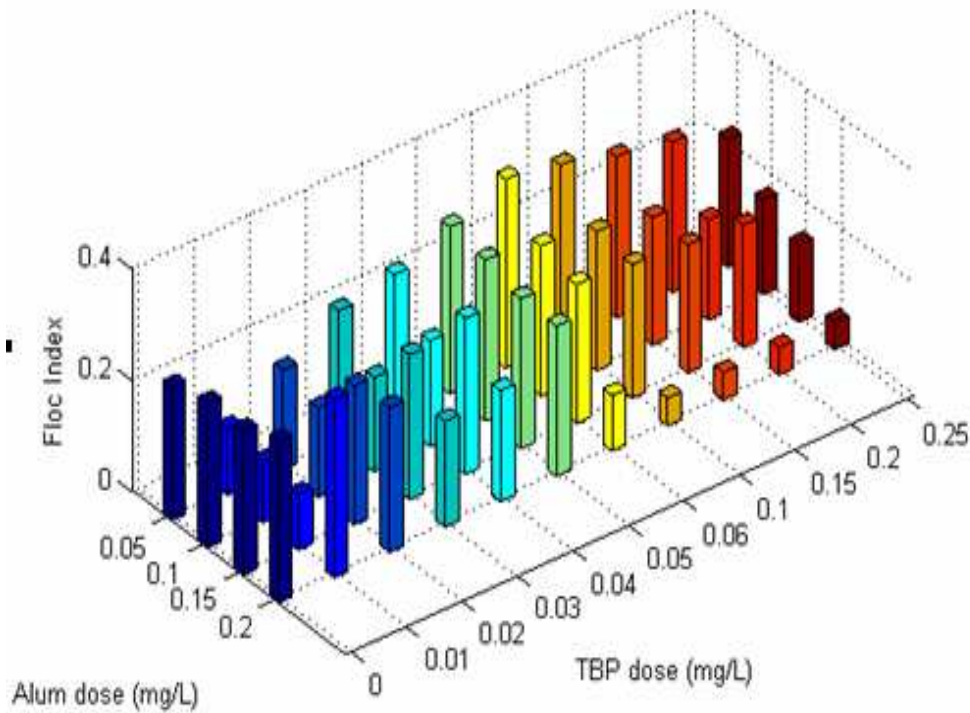


Figure 7.15 Flocculation index with alum (as Al) and TBP doses at pH 5 (50 mg l⁻¹ kaolin suspension)

From Table 7.2, it is clear that the optimum TBP dosage increased with decreasing Al concentration. Although nonlinear, the two coagulants are clearly complementary, and this is consistent with a coagulation mechanism based on charge neutralization between the TBP/Al cationic species and the kaolin suspension at pH 5. The locus of the optimal alum-polymer dosage combinations for the 50 mg l⁻¹ kaolin suspension at pH 5 is shown in Figure 7.16.

TABLE 7.2 Coagulation performances for the optimum dosage of TBP at each alum dose (in terms of maximum flocculation index, residual turbidity and aluminium, and Floc volume) at pH 5 (50 mg l⁻¹ kaolin suspension)

Al dose (mg l ⁻¹)	TBP dosage (mg l ⁻¹)	FI	Residual Turbidity (NTU)	Floc Volume (ml)	Residual [Al ³⁺] (µg l ⁻¹)
0.05	0.06	0.34	32.0	1.2	4.4
0.10	0.05	0.29	32.0	0.8	5.8
0.15	0.04	0.28	32.0	0.8	5.9
0.20	0.01	0.32	34.0	1.0	5.6
0.20	0.00	0.30	34.5	0.8	4.8
0.00	0.25	0.32	18.5	0.7	--

Note: "--" indicated that the value is out of the calibration range of Graphite furnace AAS.

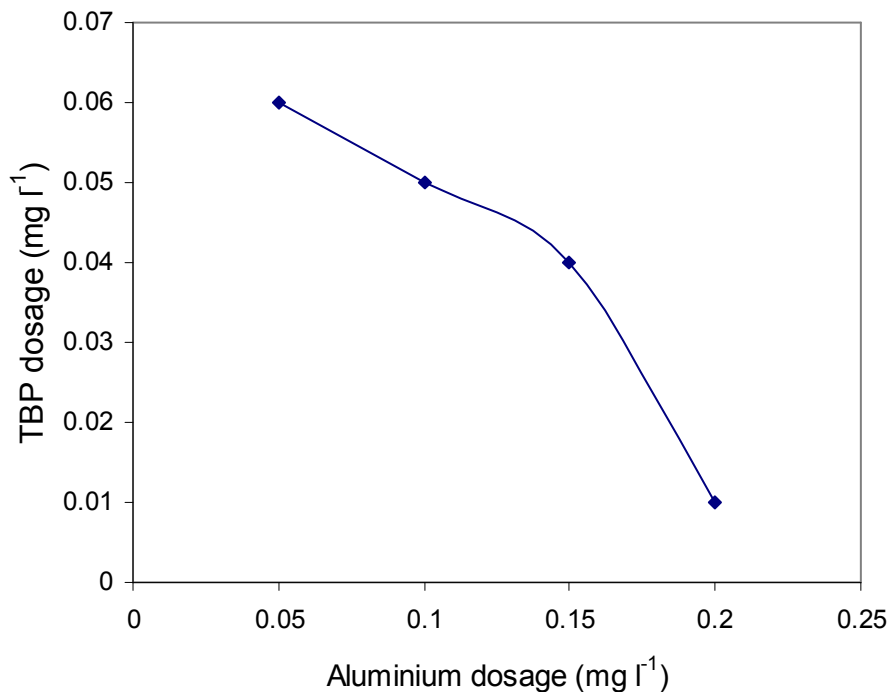


Figure 7.16 Locus of alum-polymer dosage combinations for 50 mg l⁻¹ kaolin at pH5

Compared to the use of the optimum dose of alum (0.2 mg l^{-1} as Al^{3+}) or TBP (0.25 mg l^{-1}) as sole coagulant, the use of the combined coagulants in the Al/TBP dose ratio of 0.05/0.06 gave the best coagulation performance in terms of the FI (0.34); however, it is noted that the FI values were very similar for all of the alum/TBP combinations and for the sole coagulants. This dual coagulant gave a minor improvement to the residual turbidity compared to Alum alone, but a much higher floc volume (1.2 ml). Nevertheless, the use of 0.25 mg l^{-1} TBP as the sole coagulant was substantially better than the use of dual coagulants or alum alone for the removal of turbidity, whilst giving a high FI and low floc volume.

7.3 Coagulation Action of Dual Coagulant in Humic Acid Solution at pH6

In order to investigate the dosage stoichiometry with respect to coagulation performance at pH 6, the locii of the optimal alum-TBP dosage combinations were established at two different HA concentrations of 15 mg l^{-1} (NPDOC approximately 4.01 mg l^{-1}) and 30 mg l^{-1} (NPDOC approximately 9.96 mg l^{-1}). Prior to studying the effect of partial replacement of alum by TBP, a series of laboratory experiments were undertaken to determine the optimum performances of the coagulation using alum and TBP, respectively, each as sole coagulant. Based on these optimum dosages, further coagulation tests were carried out by systematically reducing the alum dose with a range of TBP dosages. The coagulation performance by the optimal alum-TBP dose was subsequently compared with the result from a new commercial product TSL, which is a mixture of TBP and Alum.

7.3.1 Optimum Alum-TBP Combinations in 15 mg l^{-1} HA Solution

Using the PDA test method, the flocculation of 15 mg l^{-1} HA solution at pH6 was conducted to determine the optimum dose of different coagulants. In addition, at the end of the PDA (flocculation index) monitoring period, the floc

volume and the colour removal were measured to further describe the performance of the coagulation. Although the use of UV-visible absorbance for monitoring the performance of the coagulation is complicated because of the interaction between the organic fractions of the TBP and HA, and infeasible for determining the optimum dose of TBP (see Section 6.2.3), the measurement of light absorbance at 254nm and 400nm was carried out nevertheless, since it was considered that the parameters may provide some further insight into the effect of different alum-TBP combinations.

Figure 7.17 shows the variation of Flocculation Index with the flocculation time using a range of alum concentrations (1.35 mg l⁻¹ as Al³⁺ to 4.86 mg l⁻¹ as Al³⁺) for 15 mg l⁻¹ HA solution at pH6. The results indicate clearly the existence of an optimal dose of 2.03 mg l⁻¹ as Al³⁺, corresponding to a maximum FI of approximately 0.27.

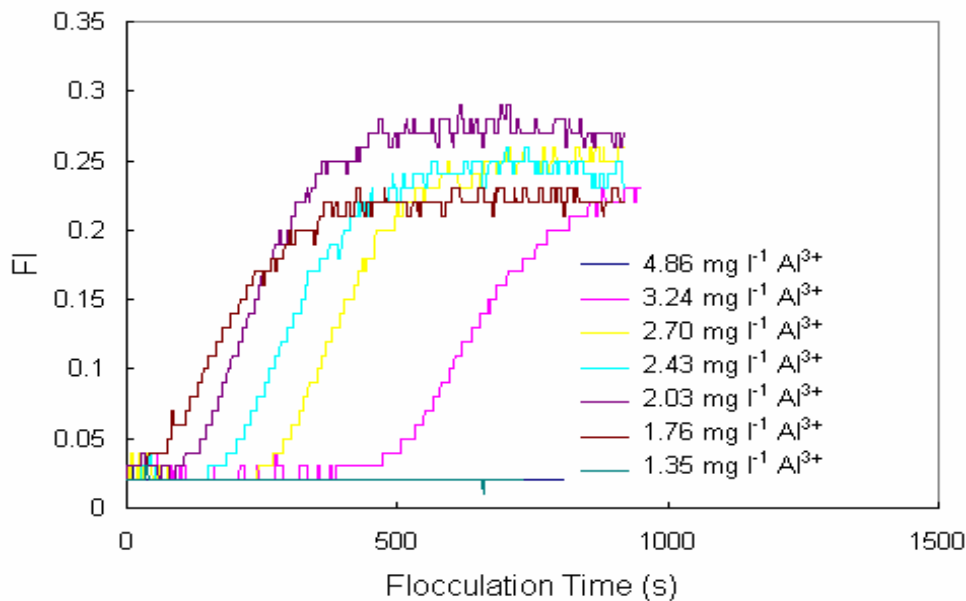


Figure 7.17 Dynamic monitoring of 15 mg l⁻¹ HA at pH 6 using different dosages of alum

In the range of 1.35 mg l⁻¹-2.7 mg l⁻¹ Al³⁺ using alum as coagulant, very

small floc volumes of about 0.25 ml to 0.5 ml were measured, while the decrease in colour and UV-absorbance was high; the results are shown in the Table 7.3.

TABLE 7.3 Coagulation performance for the different dosage of alum at pH6 (15 mg l⁻¹ HA)

Alum (mg l ⁻¹ as Al ³⁺)	Residual Colour (Hazen)	Colour Removal %	Abs(254nm) (cm ⁻¹)	Abs 254nm Reduction %	Abs(400nm) (cm ⁻¹)	Abs 400nm Reduction %
1.76	10	92	0.019	95.2	0.004	96.3
2.03	7.5	94	0.014	96.5	0.004	96.3
2.43	15	88	0.049	87.7	0.007	93.5
2.70	10	92	0.021	94.7	0.007	93.5
3.24	15	88	0.052	87	0.012	88.9

* **15 mg l⁻¹ HA solution pH 6.** Initial colour: 125 Hazen; Initial Abs (254nm): 0.4; Initial Abs (400nm): 0.108

The results obtained here, indicating an optimum alum dose of about 2.03 mg l⁻¹ as Al³⁺ at pH6 with model water containing 15 mg l⁻¹ HA (NPDOC approximately 4.011 mg l⁻¹), can be compared with previous studies (85) of the coagulation of natural organic matter (TOC approximately 10 mg l⁻¹) at pH 5-6.5, which have indicated a maximum reduction of UV-absorbance at an alum dose of about 2.7 mg l⁻¹ as Al³⁺ (100 µM as Al³⁺). The higher dose of alum is consistent with a dose stoichiometry, as originally reported by Hall and Packham (170) in which an increasing presence of humic substances at pH > 5 leads to an increase in the alum dosage required.

Figure 7.18 and Figure 7.19 give the coagulation monitoring results using TBP and Tanfloc SL as sole coagulants for 15 mg l⁻¹ HA, respectively.

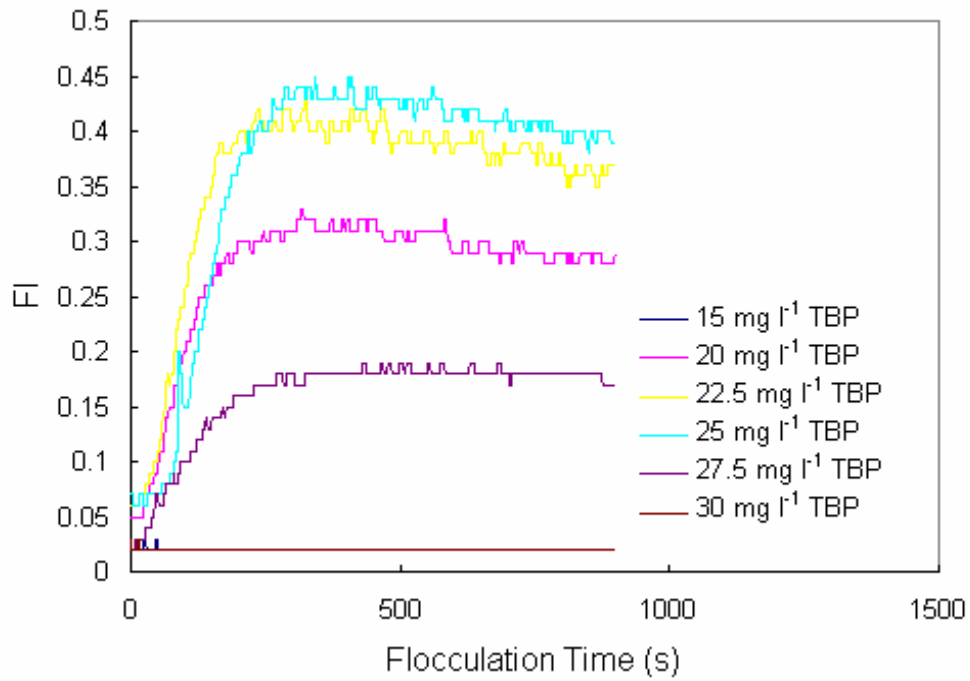


Figure 7.18 Flocculation index response with TBP dose at pH 6 (15 mg l⁻¹ HA)

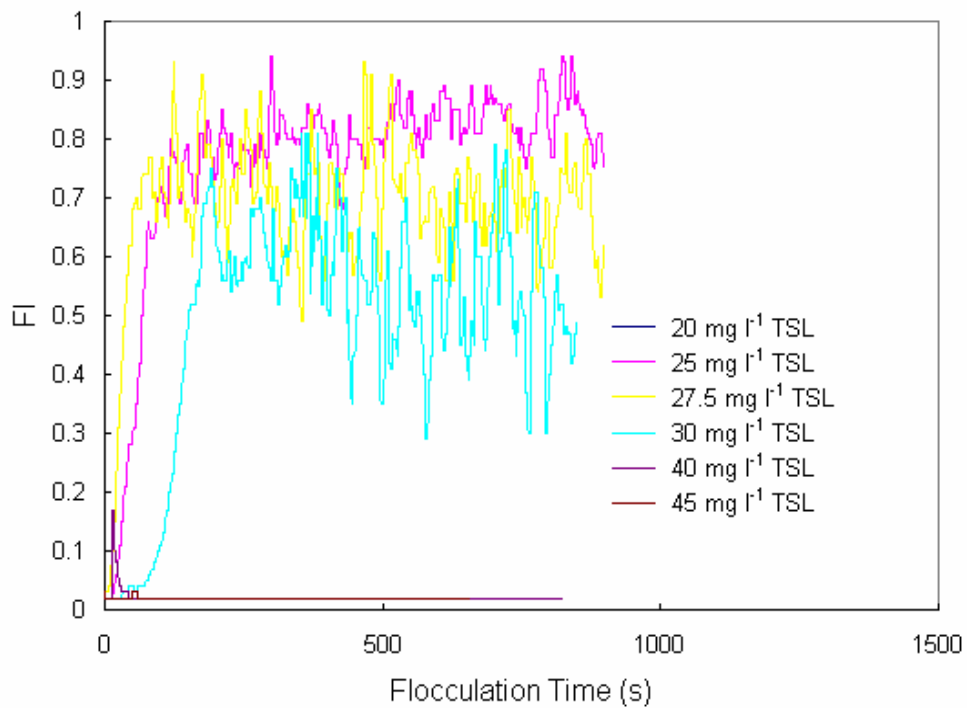


Figure 7.19 Flocculation index response with Tanfloc SL dose at pH 6 (15 mg l⁻¹ HA)

It was found that at pH6, the optimum TBP dosage was around 22.5 mg l⁻¹, which produced a maximum floc volume (10ml) and colour removal percentage (92%). In a previous report (Section 6.3.2), the optimum dosages of TBP for 15 mg l⁻¹ HA at pH4 and 7 were determined as 15 mg l⁻¹ and 30 mg l⁻¹. Clearly, there is a consistent trend of increasing optimal TBP dose with increasing pH. From Figure 7.19, the optimum dose of TSL at pH6 appeared to be 27.5 mg l⁻¹, which gave a maximum FI value of 0.92.

Based on the optimum dose of Al at pH6, a series of tests have been undertaken with a reducing dosage of aluminium from 2.03 mg l⁻¹ to 0.027 mg l⁻¹. At each dosage coagulation tests were carried out with a range of TBP dosage. A coagulation performance matrix was produced for a full range of alum-TBP combinations. Figures 7.20, 7.21 and 7.22 are examples of the dynamic monitoring results obtained for the coagulation tests.

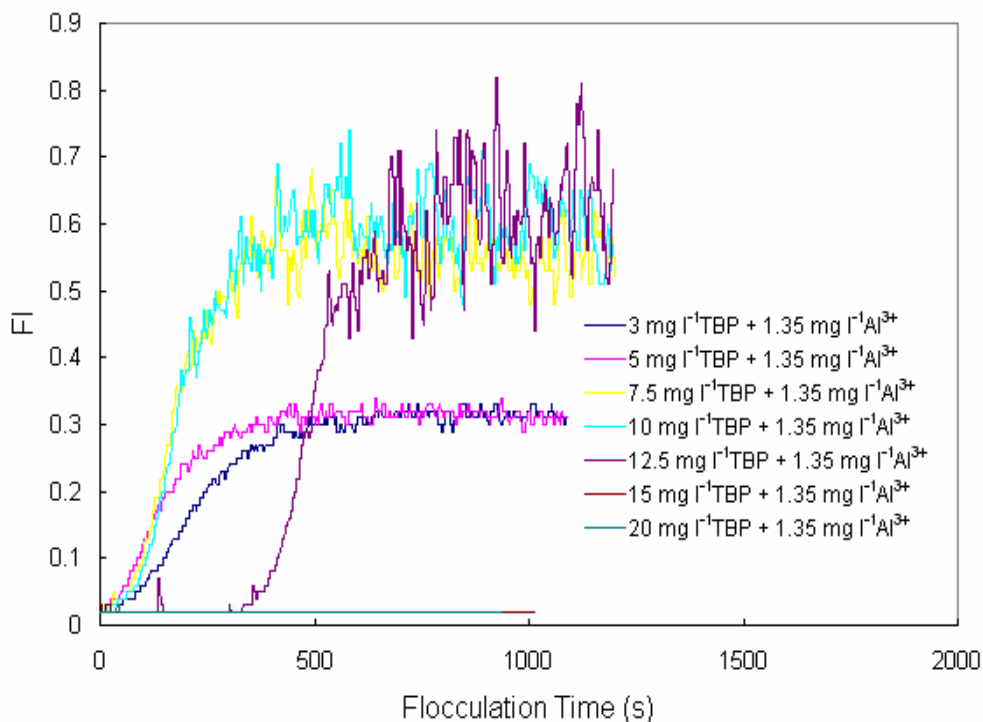


Figure 7.20 Flocculation index response with 1.35 mg l⁻¹ as Al³⁺ and different TBP dosages at pH 6 (15 mg l⁻¹ HA)

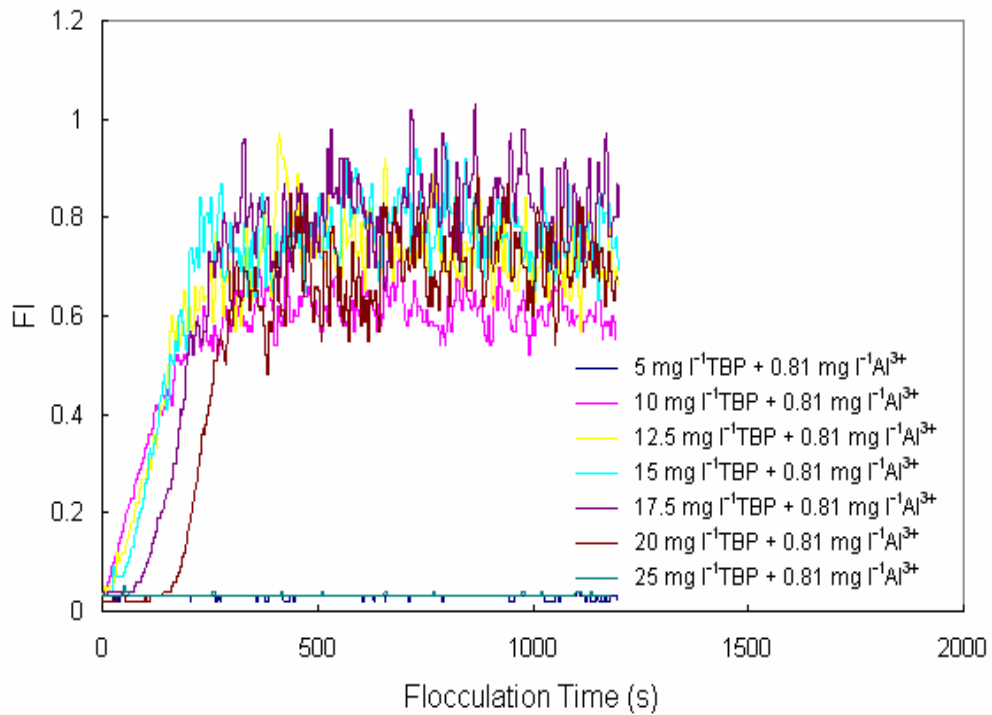


Figure 7.21 Flocculation index response with 0.81 mg l^{-1} as Al^{3+} and different TBP dosages at pH 6 (15 mg l^{-1} HA)

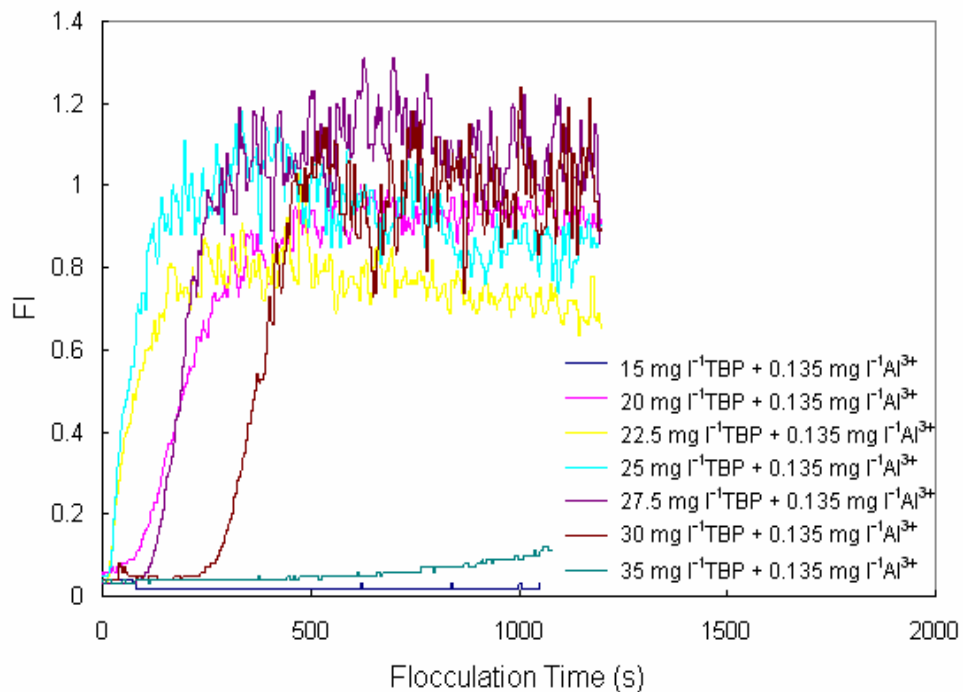
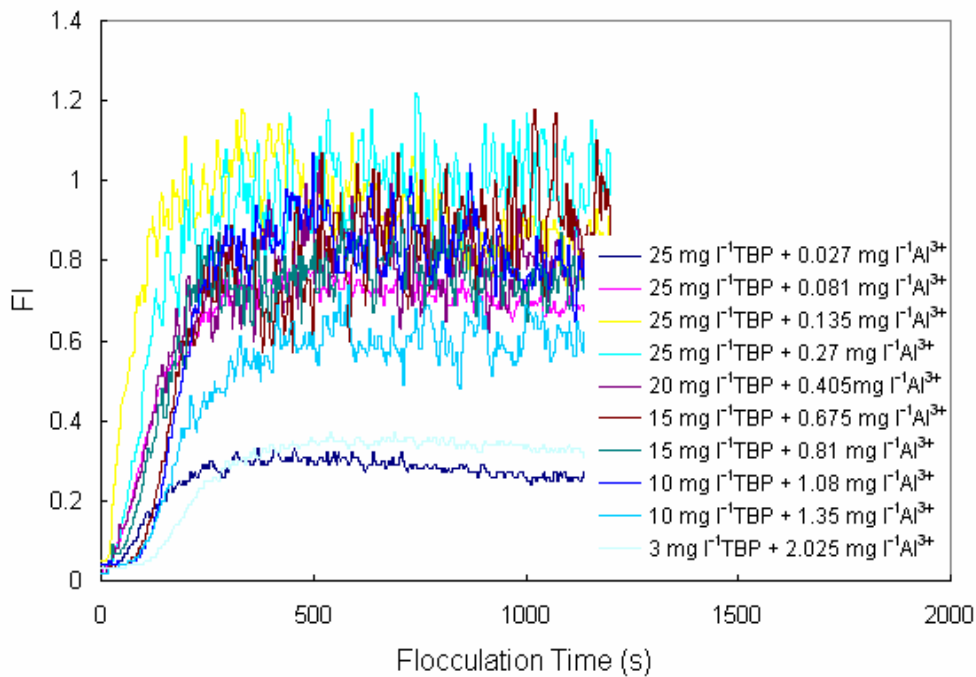


Figure 7.22 Flocculation index response with 0.135 mg l^{-1} as Al^{3+} and different TBP dosages at pH 6 (15 mg l^{-1} HA)

For each alum dose, the optimum dose of TBP was determined by measurement of the maximum value of FI, floc volume, and colour removal in each case. A summary of all the results for the range of alum doses and corresponding optimal TBP doses is given in Table 7.4; the performance of each coagulant combination is given in terms of FI, floc volume, colour removal and UV-visible absorbance. The variation of FI with flocculation time for each alum-optimal TBP dose is shown graphically in Figure 7.23.



Fi

Figure 7.23 Flocculation index response with TBP dose and different Al concentrations at pH 6 (15 mg l⁻¹ HA)

From Table 7.4, it can be seen that at low alum doses (0.027 mg l⁻¹ to 0.27 mg l⁻¹ as Al³⁺) the maximum Flocculation Index value corresponded to the combination of 25 mg l⁻¹ TBP with 0.135 mg l⁻¹ as Al³⁺. This TBP dose is very close to the optimum dose of TBP when used as the sole coagulant (22.5 mg l⁻¹). However, compared with the coagulation performances using alum and TBP as sole coagulants, the small addition of the alum (0.135 mg l⁻¹ as Al³⁺) significantly improved the coagulation efficiency in terms of the FI (1.15), floc volume

(12.5ml), and colour removal (98%). Although UV absorbance is not a good measurement of the required optimum dose of organic coagulants, in this case it appears that the optimal alum-TBP combination (0.135 mg l^{-1} as Al^{3+} with 25 mg l^{-1} TBP) gave a high UV absorbance reduction (94%) and visible absorbance reduction (98.1%). At higher alum dosages, it is evident from the results shown in Table 7.4 that the corresponding polymer dosage for optimal coagulation performance decreases.

Tanfloc SL, TBP and Alum were chosen as reference chemicals for comparing the coagulation performance with the overall optimal alum-TBP combination (0.135 mg l^{-1} as Al^{3+} with 25 mg l^{-1} TBP). This latter combination is of considerable interest in terms of achieving low residual Al in treated waters since the initial aluminium dose of 0.135 mg l^{-1} is well below the UK water quality standard for aluminium of 0.2 mg l^{-1} . From Table 7.4, it is noted that the alum-TBP combination of 1.08 mg l^{-1} as Al^{3+} with 10 mg l^{-1} TBP, also provided a good coagulation performance. In view of a possible dose limitation for tannin-based products, where the current DWI guideline (171) defines a maximum dose of 10 mg l^{-1} of active material, the alum-TBP combination of 1.08 mg l^{-1} as Al^{3+} with 10 mg l^{-1} TBP, is particularly of interest since it meets this regulatory guideline. The results of the coagulation by the different coagulants are summarised in Figure 7.24.

TABLE 7.4 Coagulation performance for the optimum TBP dosage with different alum doses at pH6 (15 mg l⁻¹ HA)

Al ³⁺ dosage (mg l ⁻¹)	TBP dosage (mg l ⁻¹)	Peak FI	Floc Volume (ml)	Colour (Hazen)	Colour Removal %	Abs 254nm Reductio %	Abs 400nm Reductio %	Residual [Al ³⁺] (µg l ⁻¹)
2.03	3	0.34	6.5	10	92	81.5	82.4	8.1
1.35	10	0.69	7	5	96	94	96.3	5.8
1.08	10	0.89	8.5	5	96	94	95.4	8.5
0.81	15	0.77	8	12.5	90	88.8	88.9	9.1
0.68	15	0.8	12	10	92	88.5	90.7	8.4
0.41	20	0.96	10	10	92	91.3	92.6	9.1
0.27	25	1.07	10	5	96	93.5	95.4	13.2
0.135	25	1.15	12.5	2.5	98	94	98.1	--
0.081	25	0.75	10	7.5	94	85.5	94.4	--
0.027	25	0.3	----	80	96	89.3	62.9	--
2.03		0.27	6.5	7.5	94	94.8	93.5	6.9
	22.5	0.41	10	10	92	91.5	92.6	--
	27.5	0.92	15	10	92	88.75	91.7	4.5
	mg l⁻¹							
	TSL							

* **15 mg l⁻¹ HA solution pH 6.** Initial colour: 125 Hazen; Initial Abs (254nm): 0.4; Initial Abs (400nm): 0.108

Note: All residual Al concentrations were < 14 µg l⁻¹; "--" indicated the value is out of the calibration range of Graphite furnace AAS.

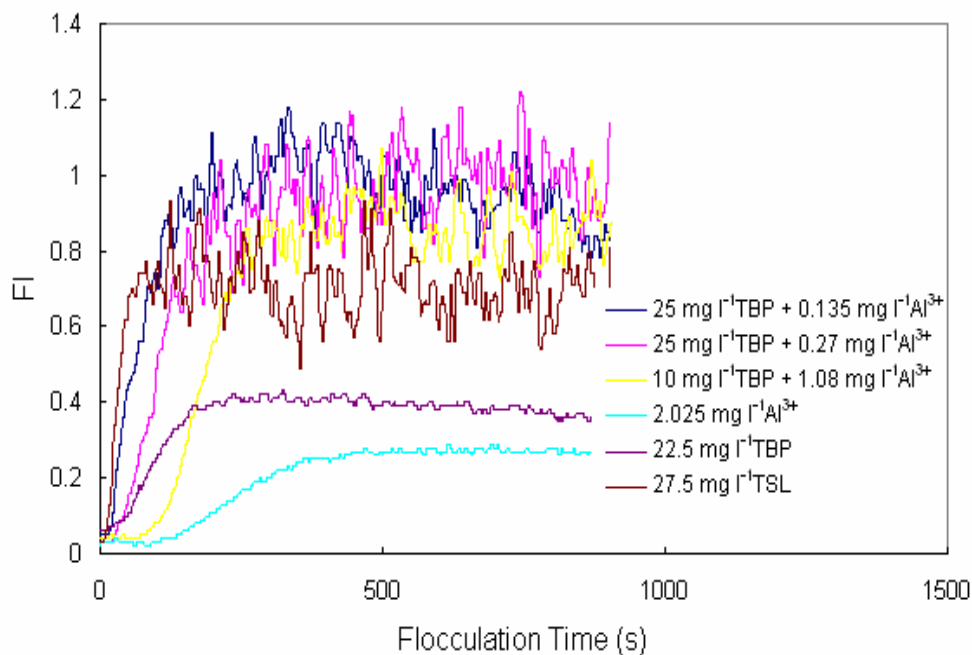


Figure 7.24 Flocculation index response with different optimum coagulants at pH6 (15 mg l⁻¹ HA)

From Figure 7.24 it can be seen that at pH 6 both the alum-TBP combinations of 0.135 mg l⁻¹ Al³⁺ with 25 mg l⁻¹ TBP, and 0.27 mg l⁻¹ Al³⁺ with 25 mg l⁻¹ TBP, presented good coagulation performances with a rapid response and high FI values, compared with the use of alum or TBP as sole coagulant. In terms of maximum FI achieved, these combinations outperformed the TSL, although TSL still performed well. It is interesting to note that for the alum-TBP combinations the 0.135 mg l⁻¹ Al³⁺ dose corresponds to a percentage of aluminium sulphate (assuming no water of hydration) of 3.3%, which is less than the corresponding figure for TSL (5.6% aluminium sulphate). However, the 0.27 mg l⁻¹ Al³⁺ dose corresponding to a percentage of aluminium sulphate (assuming no water of hydration) of 6.4%, is higher than the corresponding figure for TSL (5.6% aluminium sulphate). For the alum-TBP combination of 1.08 mg l⁻¹ Al³⁺ with 10 mg l⁻¹ TBP, the coagulation response was much slower than for the other combinations, but the maximum FI was only slightly inferior (see Figure 7.24)

and significantly superior to the TSL.

7.3.2 Optimum Alum-TBP Combinations in 30 mg l⁻¹ HA Solution

Figure 7.25 shows the variation of Flocculation Index with the flocculation time using a range of alum concentrations (1.35 mg l⁻¹ Al³⁺ to 4.86 mg l⁻¹ Al³⁺) for 30 mg l⁻¹ HA solution at pH6. It can be seen that the maximum FI of around 0.36 was obtained by using 4.05 mg l⁻¹ Al³⁺. This performance at this dose also corresponded to a maximum floc volume (15.5ml), colour removal (89.6%), and reduction in light absorbance at 254nm (74.1%) and at 400nm (84.8%). Since the optimal dosage of alum with 15 mg l⁻¹ HA was 2.03 mg l⁻¹ as Al³⁺ (Section 7.3.1), it is clear that the optimal dosage of alum is proportional to the HA concentration, indicating a charge stoichiometry. This suggests that the range of alum doses used, ≤ 4.05 mg l⁻¹ as Al³⁺, are not sufficient at pH 6 to cause rapid precipitation of aluminium hydroxide, and thus coagulation occurs principally by charge neutralization of the HA by cationic aluminium hydrolysis species.

Figure 7.26 and Figure 7.27 give the coagulation results using TBP and Tanfloc SL as sole coagulants for 30 mg l⁻¹ HA, respectively. The optimum dose of TBP and Tanfloc SL were determined as 45 mg l⁻¹ and 50 mg l⁻¹, respectively. The results were also confirmed by the measurement of floc volume, colour removal and UV-visible absorbance reduction, and these are summarised in Table 7.5.

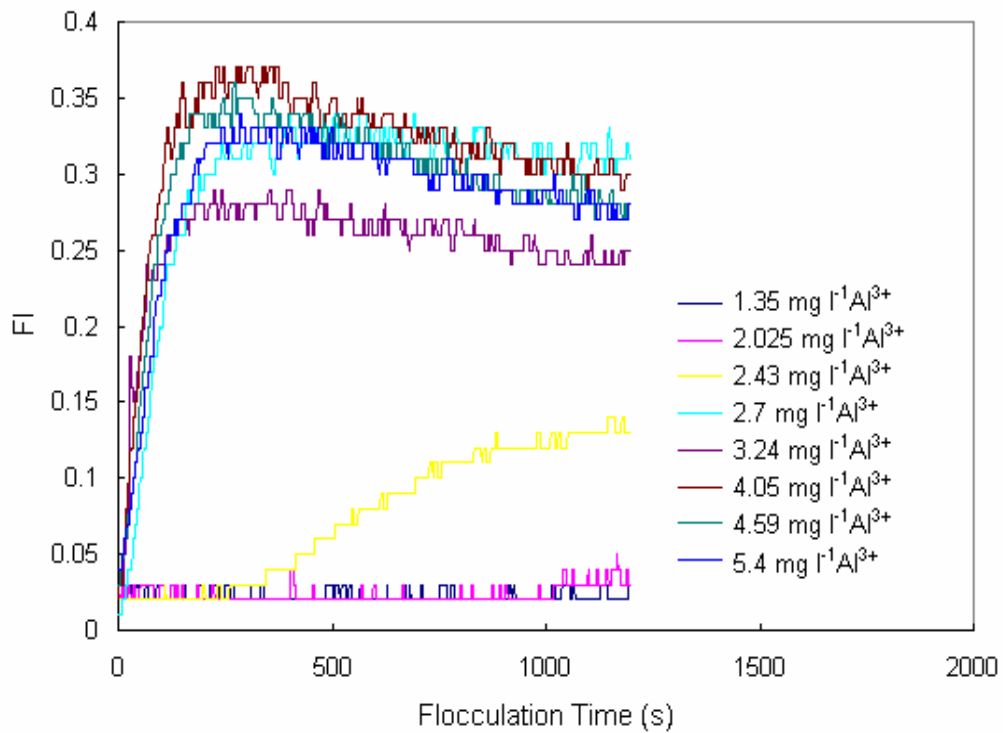


Figure 7.25 Dynamic monitoring of 30 mg l⁻¹ HA at pH 6 using different dosages of alum

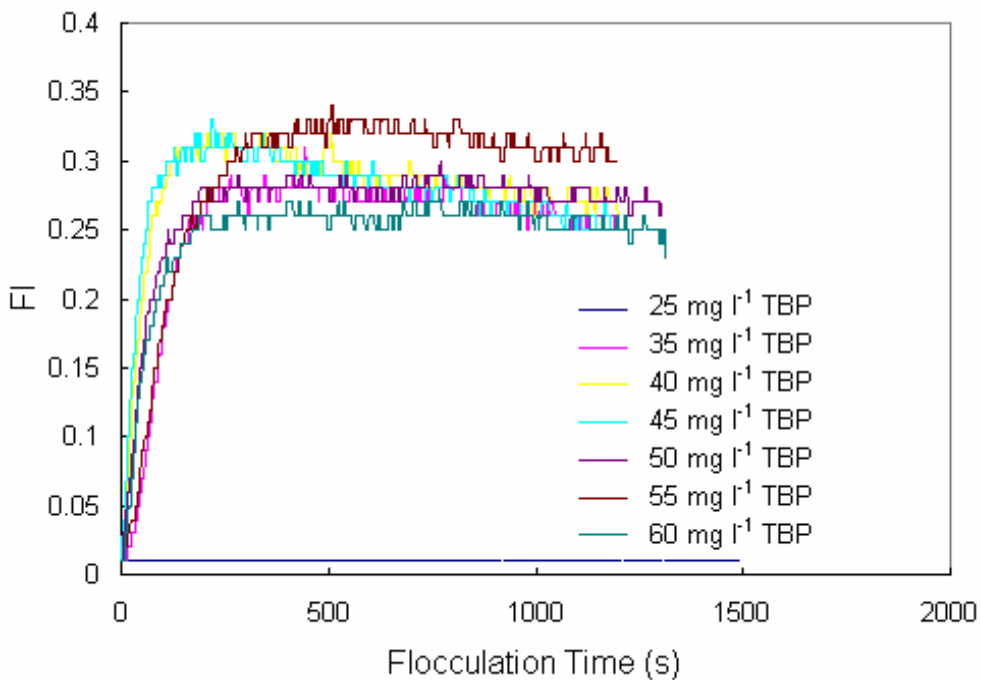


Figure 7.26 Flocculation index response with TBP dose at pH 6 (30 mg l⁻¹ HA)

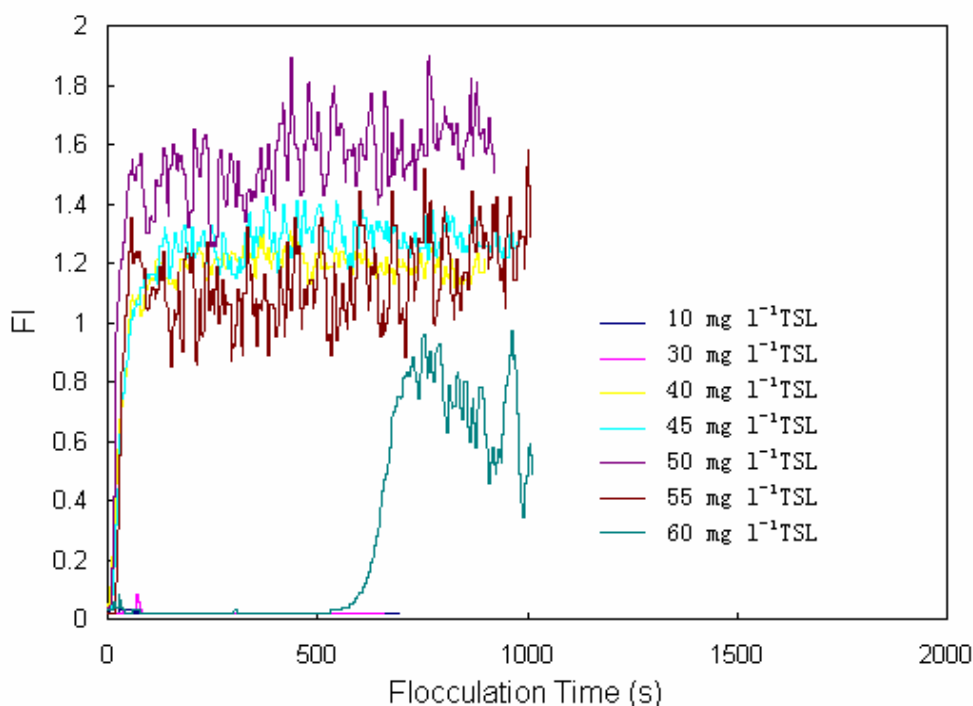


Figure 7.27 Flocculation index response with TSL dose at pH 6 (30 mg l⁻¹ HA)

It is clear that at pH6, the TBP optimum dosage is proportional to the HA concentration and therefore it is assumed that charge neutralisation is the dominant mechanism of coagulation. This assumption is consistent with previous tests using HA at pH4 and 7 (see Section 6.3.2). With TSL there is a slight departure in a strict dose stoichiometry at the two HA concentrations (viz: 15 mg l⁻¹ HA and 27.5 mg l⁻¹ TSL; 30 mg l⁻¹ HA and 50 mg l⁻¹ TSL), which may indicate a more complicated mechanism of coagulation than charge interaction.

Based on the optimum dose of alum (4.05 mg l⁻¹ as Al³⁺) at pH6, a series of tests have been undertaken by systematically reducing the dosage of aluminium from 4.59 mg l⁻¹ to 0.027 mg l⁻¹. At each dosage coagulation tests were carried out with a range of TBP dosages. Thus, a coagulation performance matrix was produced for a full range of alum-TBP combinations. Figure 7.28, 7.29, 7.30 and 7.31 are examples of the dynamic monitoring results obtained for the coagulation tests.

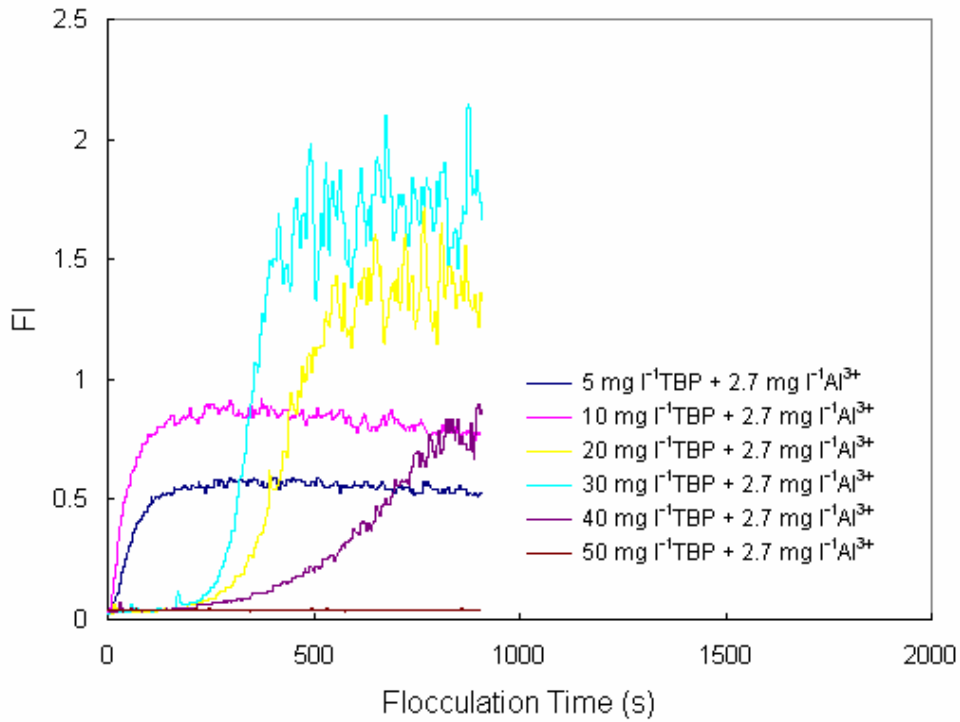


Figure 7.28 Flocculation index response with 2.7 mg l^{-1} as Al^{3+} and different TBP doses at pH 6 (30 mg l^{-1} HA)

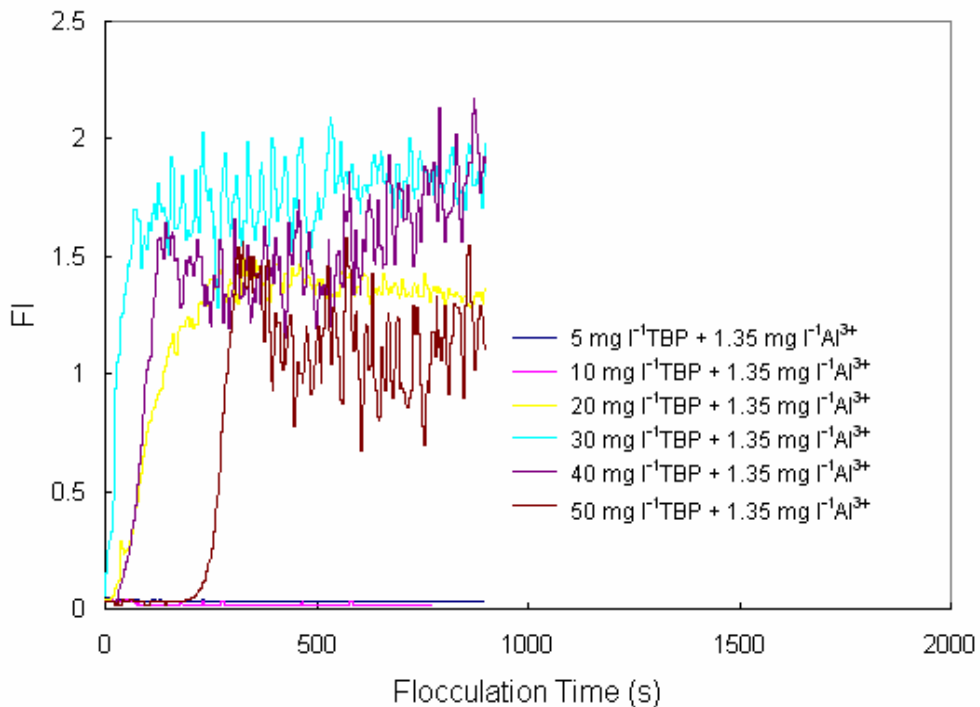


Figure 7.29 Flocculation index response with 1.35 mg l^{-1} as Al^{3+} and different TBP doses at pH6 (30 mg l^{-1} HA)

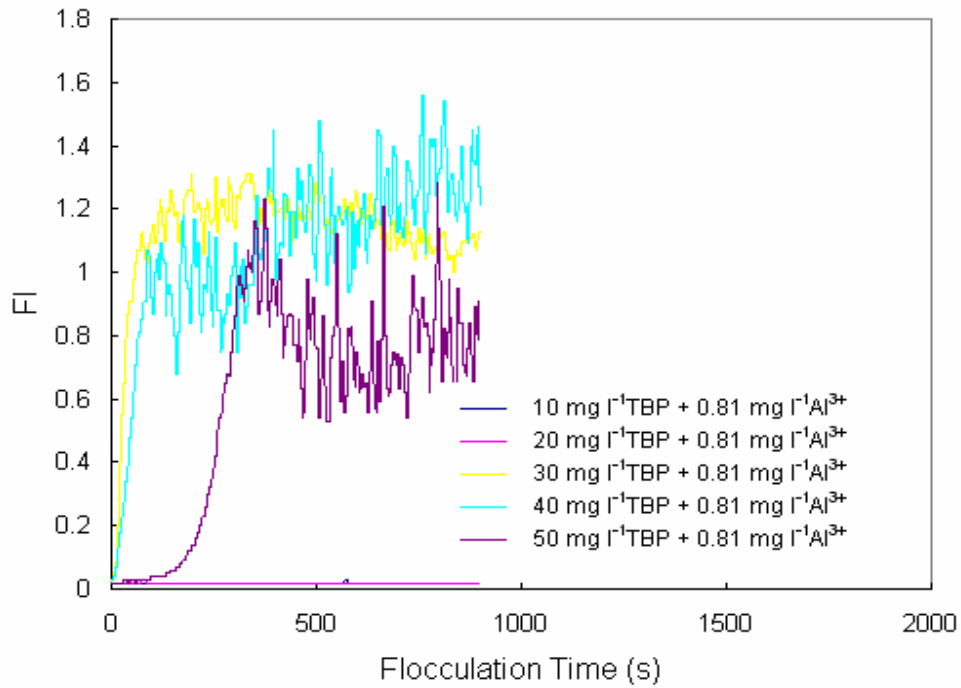


Figure 7.30 Flocculation index response with 0.81 mg l^{-1} as Al^{3+} and different TBP doses at pH6 (30 mg l^{-1} HA)

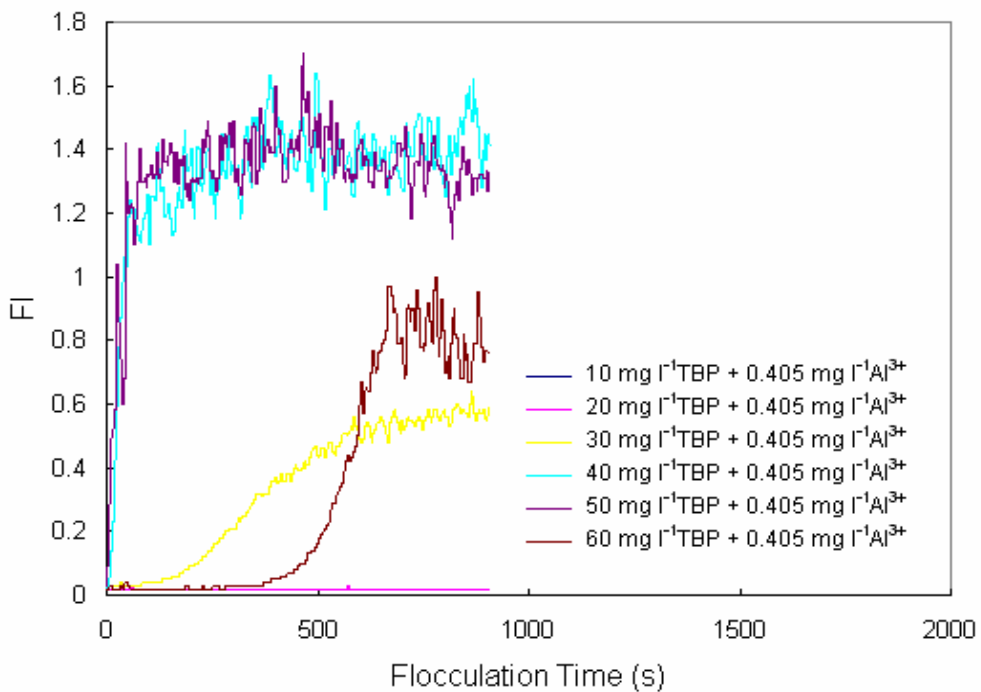


Figure 7.31 Flocculation index response with 0.405 mg l^{-1} as Al^{3+} and different TBP doses at pH6 (30 mg l^{-1} HA)

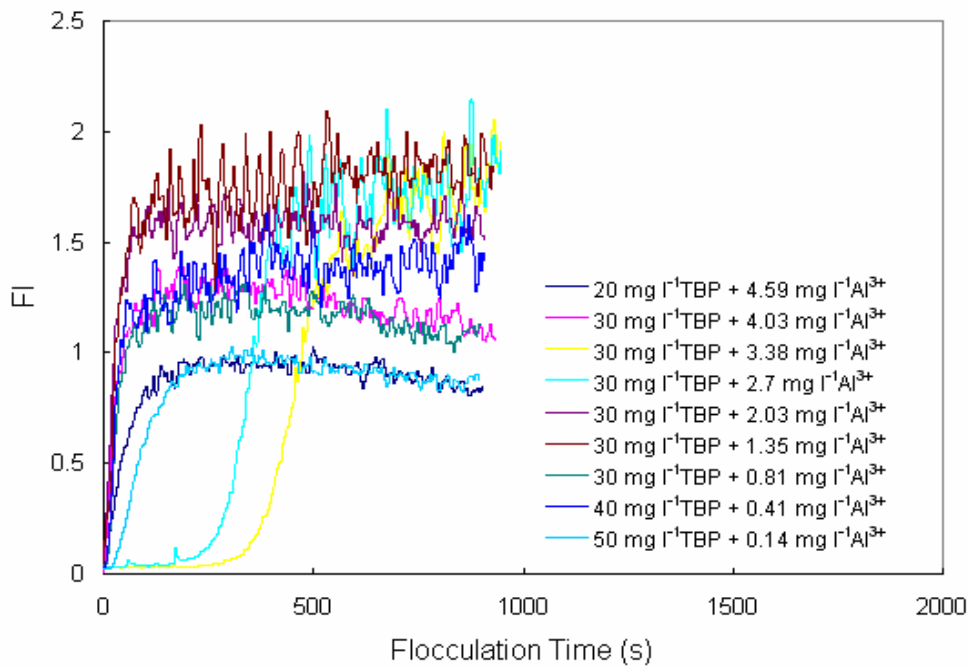


Figure 7.32 Flocculation index response with TBP dose and different Al concentrations at pH6 (30 mg l⁻¹ HA)

The maximum variation of Flocculation Index with flocculation time using different doses of alum with TBP is summarised in Figure 7.32, and the overall optimum coagulation results of flocculation index, floc volume, colour removal and UV-visible absorbance are summarised in Table 7.5. From Table 7.5, it is clearly seen that the alum-TBP combination of 1.35 mg l⁻¹ Al³⁺ with 30 mg l⁻¹ TBP gave the best coagulation performance in term of the maximum FI (1.98), floc volume (45ml), and colour removal (97.9%). In this case, the residual tannin matter in final water was still very low, 0.311 mg l⁻¹, and less than that for 45 mg l⁻¹ TBP as the sole coagulant, which gave a residual tannin of about 0.459 mg l⁻¹. Table 7.5 also shows that when the alum dose increased from 0.14 mg l⁻¹ as Al³⁺ to 0.81 mg l⁻¹ as Al³⁺, the optimal TBP dosage decreased from 50 mg l⁻¹ to 30 mg l⁻¹, confirming that the two coagulants are complementary.

TABLE 7.5 Coagulation performance for the optimum dosage of TBP with different alum dose at pH6 (30 mg l⁻¹ HA)

Al ³⁺ dosage (mg l ⁻¹)	TBP dosage (mg l ⁻¹)	Peak FI	Floc Volume (ml)	Colour (Hazen)	Colour Removal %	Abs 254nm Reduction %	Abs 400nm Reduction %	Residual [Al ³⁺] (µg l ⁻¹)
4.59	30	0.97	25	30	87.5	95.8	74.6	11.3
4.05	30	1.18	28	10	95.8	94.9	94.9	8.4
3.38	30	1.85	28	15	93.7	86.1	92.9	6.0
2.70	30	1.87	30	5	97.9	91.4	98.5	8.1
2.03	30	1.76	25	15	93.7	90.4	90.9	5.7
1.35	30	1.98	45	5	97.9	93.7	95.4	6.5
0.81	30	1.16	40	15	93.7	89.1	92.9	7.1
0.41	40	1.44	33	25	89.6	73.9	82.2	4.5
0.14	50	0.98	30	20	91.7	86.1	90.4	--
4.05	-	0.36	15.5	25	89.6	74.1	84.8	13.0
-	45	0.31	38	30	87.5	76.5	82.2	--
-	50mg l ⁻¹ TSL	1.81	40	10	95.8	90.9	94.9	6.2

* **30 mg l⁻¹ HA solution pH 6** Initial colour: 240 Hazen; Initial Abs (254nm): 0.742; Initial Abs (400nm): 0.197

Note: All residual Al concentrations were < 12µg l⁻¹; and "--" indicated the value is out of the calibration range of Graphite furnace AAS.

However, with increasing alum doses from 0.81 mg l⁻¹ as Al³⁺ to 4.59 mg l⁻¹ as Al³⁺, there was no substantial further reduction in the optimal dose of TBP. It is speculated that under these conditions of much higher humic and alum concentrations, the coagulation mechanism is probably caused both by charge neutralisation and adsorption on to solid phase aluminium hydrolysis species.

The comparative coagulation performances (in terms of FI) of alum, TBP, TSL and alum-TBP combination (1.35 mg l^{-1} as Al^{3+} with 30 mg l^{-1} as TBP) at their optimal doses are summarised in Figure 7.33. It is clear that compared with alum and TBP alone, the TSL (5.6% aluminium sulphate) and alum-TBP combination, which has a percentage of aluminium sulphate (assuming no water of hydration) of about 22%, produced a dramatically better coagulation performance; this was also the case in terms of colour and UV-absorbance removal. Comparing specifically the performance of the TSL with that of the alum-TBP combination showed a slight superiority of the alum-TBP combination.

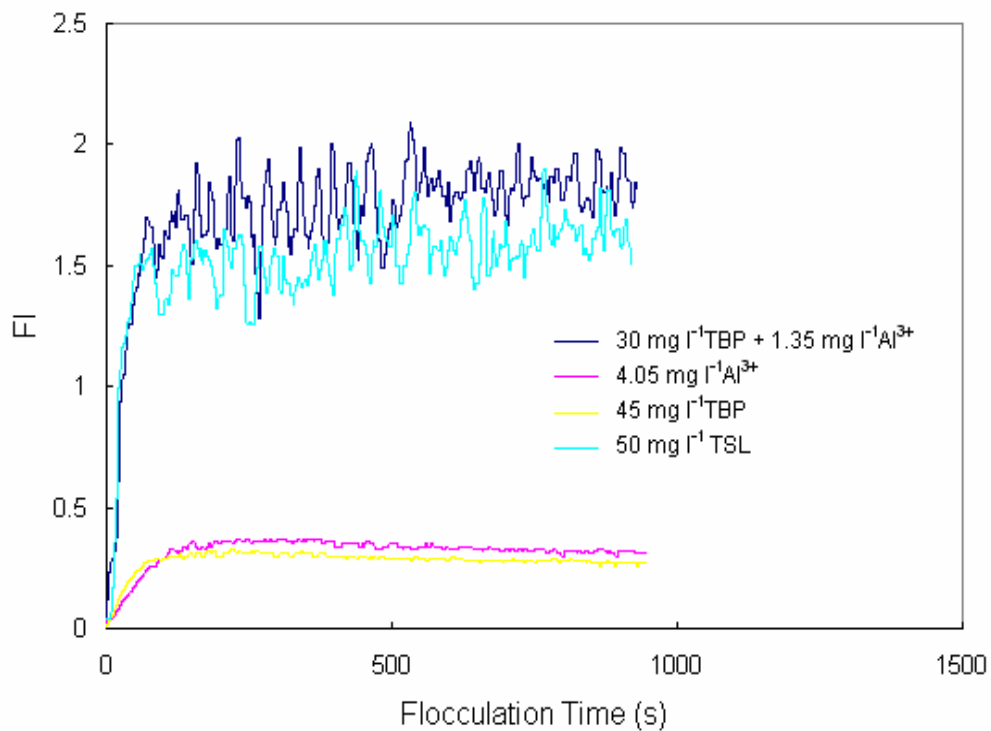


Figure 7.33 Flocculation index response with different optimum coagulants at pH6 (30 mg l^{-1} HA)

7.3.3 Loci of the Optimal Alum-TBP Dosage Combinations

From the optimal alum-TBP combinations summarised in Tables 7.4 and 7.5, the locus lines of the optimal alum-TBP dosage combination for 15 mg l⁻¹ and 30 mg l⁻¹ HA are shown in Figure 7.34.

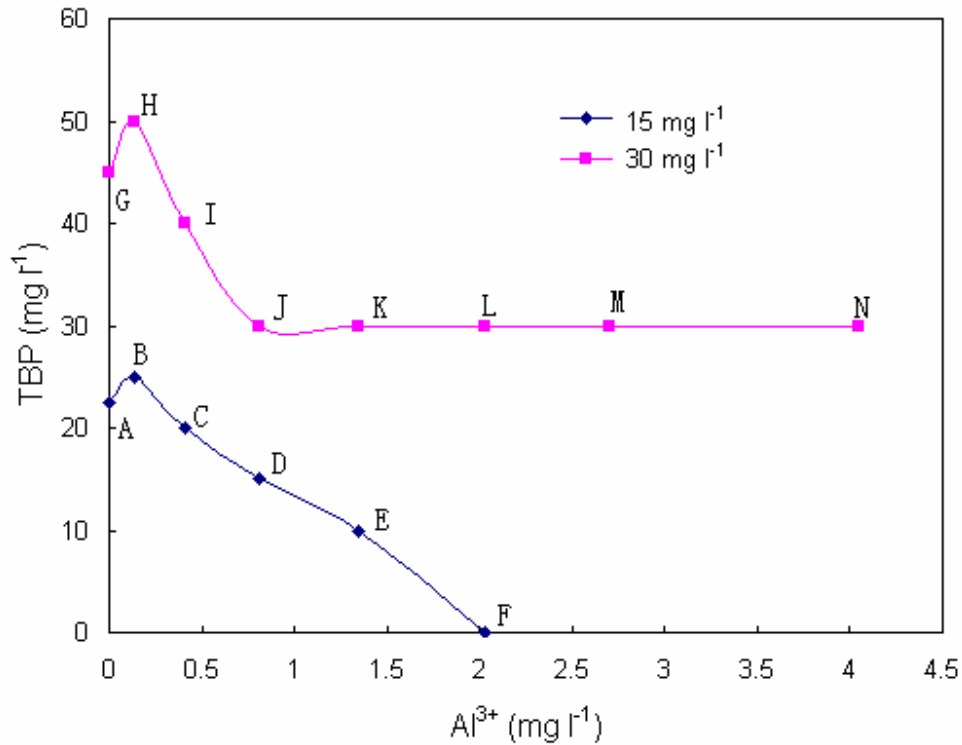


Figure 7.34 Loci of alum-TBP dosage combinations for optimal coagulation performance at pH6 at two HA concentrations

It can be seen that at relatively low Al³⁺ doses (≤ 0.81 mg l⁻¹), the alum and TBP are complementary, as discussed before, and the two locii show a close dose stoichiometry with respect to humic acid concentration. Thus, the coagulant dosages at point H, I and J are approximately twice those at point B, C, and D.

At higher Al³⁺ doses (>0.81 mg l⁻¹) and for the lower HA concentration

(15 mg l⁻¹), although the locus line is strictly nonlinear, it continues to follow an approximately linear inverse form (i.e., $y = -mx + c$, in very general terms) demonstrating the complementary relationship between the two coagulants. In contrast, for the higher HA concentration (30 mg l⁻¹), the locus line levels off, and the TBP dose has a constant value (30 mg l⁻¹) as the alum dose increases. The precise reason for the constant trend of the TBP dose with increasing alum is not obvious, but clearly this represents a departure from a mechanism of simple charge neutralisation. The corresponding values for FI and colour removal at each point along the locus lines are shown in Figures 7.35 and 7.36. The results show that while colour removal is fairly insensitive to the alum-TBP dose combination over the full range considered, the FI is strongly influenced by the dose combination. Thus, for case of 15 mg l⁻¹ HA, point B is clearly the optimal dose combination, while for 30 mg l⁻¹ HA, the optimal dose combination is approximately point K.

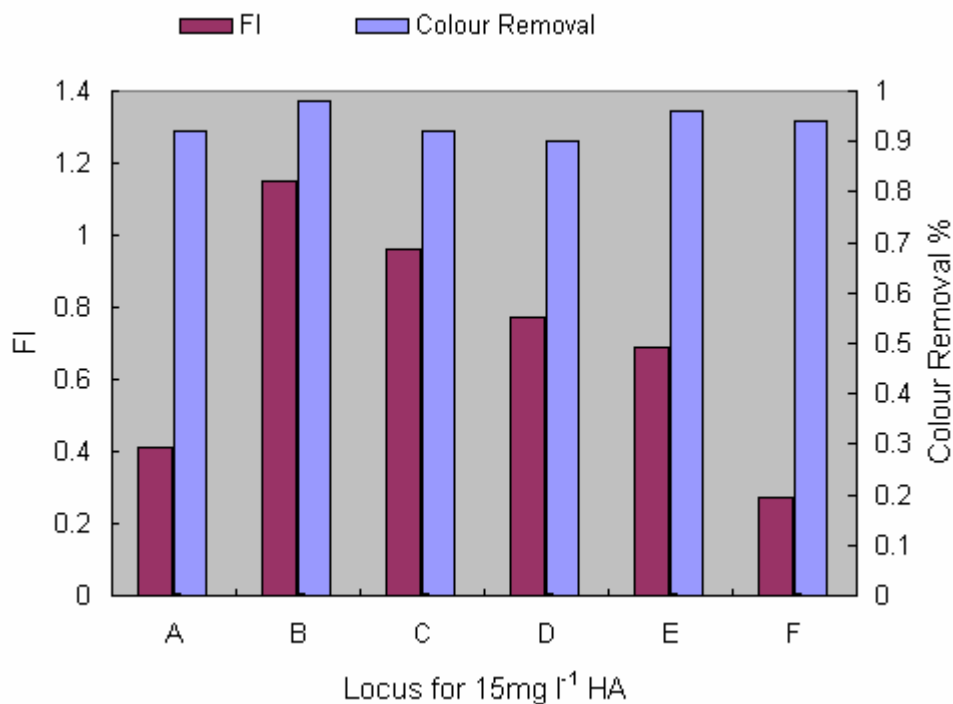


Figure 7.35 Variation of Flocculation Index and colour removal along coagulant dosage locus for 15 mg l⁻¹ HA at pH6

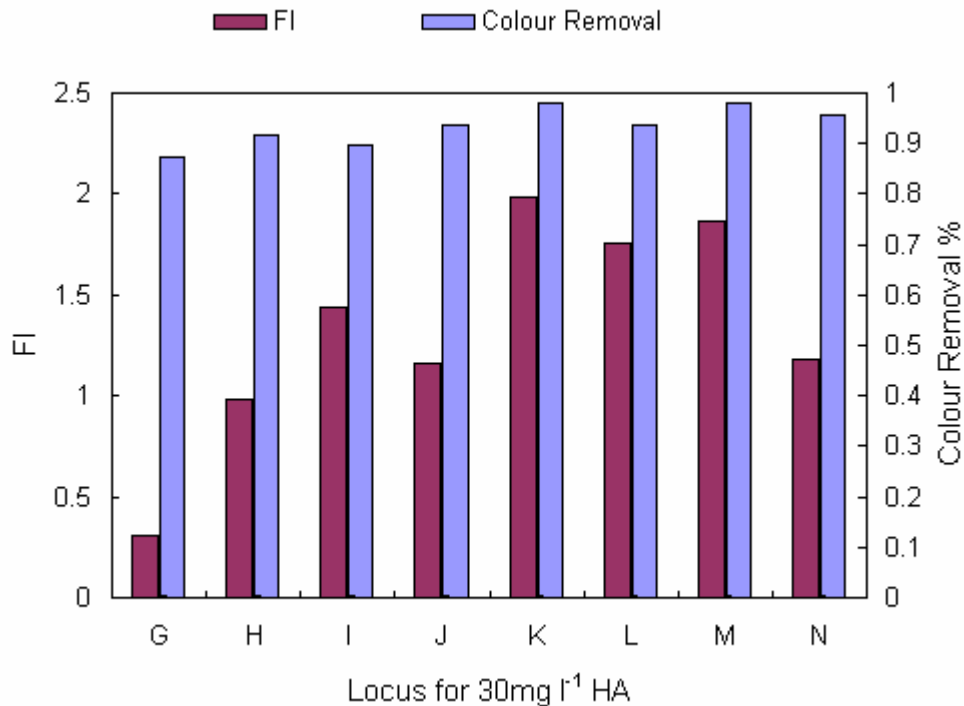


Figure 7.36 Variation of Flocculation Index and colour removal along coagulant dosage locus for 30 mg l⁻¹ HA at pH6

7.4 Discussion

When a cationic polymer has been used to partially replace alum as the primary coagulant in water treatment, coagulation/flocculation was observed to occur over a wide concentration range and reduced the dosages of the reagents (163). The results of the coagulation performance by the combination of TBP with alum in this investigation have confirmed this phenomenon.

From the results collected from the first set of flocculation tests using particle suspensions as model water at two different pH values, it can be concluded that at pH 5 (and below), the dominant coagulant species are cationic aluminium hydrolysis species and cationically charged TBP polymer, and this gives rise to coagulation of the kaolin particles by charge neutralisation. This mechanism was supported by the observed inverse relationship between the alum and TBP dosages required for optimal coagulation which suggested a

quasi-charge stoichiometry between the coagulant and the suspension. In contrast, at pH 7, the dominant mechanism of flocculation was believed to be adsorption of kaolin particles onto and within precipitated $\text{Al}(\text{OH})_3$, known generally as ‘sweep flocculation’(136). However, the influence of charge neutralisation from the TBP-cationic charge may still be significant under these conditions. Thus, the Al dose can be reduced from the optimum dose of 3.4 mg l^{-1} as sole coagulant, to 2.0 mg l^{-1} with the complementary presence of approximately 0.3 mg l^{-1} of TBP, which thereby contributes to the neutralisation of negative surface charge on the kaolin particles before and during sweep flocculation.

It is believed that at pH6, depending on the colour (humic) concentration and alum dosage, the dominant coagulation mechanisms are partly ‘humate’ precipitation by polymeric aluminium hydrolysis species (charge neutralisation) and partly adsorption of organic species onto aluminium hydroxide precipitate (‘sweep flocculation’), leading to a maximum removal of the humic substances (172). However, at the lower colour and humic substance concentration (15 mg l^{-1}), the small alum dose ($< 2.03 \text{ mg l}^{-1}$ as Al^{3+}) may not be sufficient for a rapid precipitation of aluminium hydroxide, and coagulation occurred principally by charge neutralization of the humic substances with the cationic TBP and aluminium hydrolysis species. In support of this, there is the observed increase in optimal polymer dose with decreasing alum dose, indicating an overall charge stoichiometry in order to achieve charge neutralization. In contrast, from the results obtained under the conditions of much higher humic concentrations (30 mg l^{-1}), it is speculated that the coagulation mechanism is probably caused both by charge neutralisation and adsorption on to solid phase aluminium hydrolysis species. The general shape of the alum-polymer dosage locus for optimal coagulation performance at the low concentration of HA is in accordance with the mechanism of cation charge stoichiometry. However, the nonlinear nature of the locus at high concentration of HA reflects the complex interaction between humic substances with coagulants.

For all model waters, it has been established that the reduction of the alum coagulant with a distinct improvement of coagulation efficiency are possible by a combination of TBP with alum used as a primary coagulant. The optimal dosages of combined alum and TBP that maximizes the coagulation performance and the reduction of alum at different conditions are summarized as:

For 50 mg l⁻¹ kaolin suspension at pH 5, the optimum Al/TBP dose ratio was identified as 0.05/0.06 mg/mg, suggesting that the addition of TBP at the same time as alum would allow a 75 % reduction of aluminium coagulant for a similar coagulation performance (in terms of FI and residual turbidity).

For 50mg l⁻¹ kaolin suspension at pH 7, the optimum Al/TBP dose ratio was 2.0/0.3 mg/mg, indicating that the addition of TBP at the same time as alum would allow a 41% reduction of aluminium coagulant with an improvement of coagulation efficiency (in terms of FI, but not with residual turbidity).

For the lower concentration of HA (15 mg l⁻¹) at pH6, the optimum Al/TBP dose ratio was identified as 0.135/25 mg/mg, suggesting that the addition of TBP at the same time as alum would allow a 93.4 % reduction of aluminium coagulant (as sole coagulant) with an improvement of coagulation efficiency (in terms of FI and colour removal).

For the higher concentration of HA (30 mg l⁻¹) at pH6, the optimum Al/TBP dose ratio was 1.35/30 mg/mg, indicating that the addition of TBP at the same time as alum would allow a 67 % reduction of aluminium coagulant with a distinct improvement of coagulation efficiency (in terms of FI and colour removal).

8. RESULTS: IMPROVEMENT OF TBP COAGULATION PERFORMANCE USING SOLID BOUND TBP WITH MICROSAND IN MODEL WATER

8.1 Introduction

In this part of the research, a novel approach of applying TBP as a TBP/microsand mixture (sand-TBP) for water treatment has been investigated. Preliminary work has been undertaken on the feasibility of attaching the TBP to an inert solid (fine sand), with the aim of being able to dose the polymer as a particle suspension ('solid bound TBP') coagulant. The potential benefits of this approach instead of simply dosing TBP as a solution are more rapid floc settling (due to the weight of the sand) and minimising residual soluble polymer in treated waters; the latter is important given the difficulties of measuring low concentrations of TBP (say, by the titration method) in the presence of other high molecular weight organic substances (e.g. humic substances). In practice, the use of one specific ballasted flocculation method, trade-name ACTIFLO[®], was introduced in the 1990s (173). Although the use of a microsand and a polymer together increases the weight of flocs and the settlement rate in this coagulation-flocculation-settling methodology, the polymer used in the applied ACTIFLO process is only to help the microsand attach to the flocs, which are chiefly formed by metal coagulants (e.g., alum).

The method of preparing the sand-TBP mixture was based on the adsorption of the cationic-charged TBP (at low pH) by the negatively charged sand grains; this was carried out in a simple mixed reactor with high speed mixing at 300 rpm (600 s^{-1}) for 2 min contact time with TBP solution and sand introduced simultaneously (this time is based on the ACTIFLO process design). The sand (Micro Sand Grade 90') used in this study was supplied by Universal Mineral Supplies Ltd, UK (via WRc, UK). The size of the sand was in the range

from 63 microns to 250 microns. It has a specific gravity of 2.65 and a bulk density of about 1450 kg m^{-3} , and is used by Yorkshire Water for the ACTIFLO process. After discarding the un-adsorbed TBP retaining in the solution, the resulting sand-TBP solid can be applied (dosed as a suspension) for coagulation.

To quantitatively determine the ‘active’ TBP attached on the surface of sand, which can be further used to aggregate the fine particles in model water, it was necessary to primarily measure the ratio of adsorption between TBP and sand. Based on previous studies (see Section 5.2.1.3), the absorbance of UV at 210 nm provides a satisfactory measure of the concentration of TBP in pure water. Therefore, in the preparation of the sand-TBP, the degree of TBP adsorption by a given mass of sand can be determined by the change in soluble TBP (measured by UV_{210} absorbance) over a given time period of exposure. In summary, the aim of this study was:

- To evaluate the maximum adsorption of TBP by sand at pH 4.
- To determine the optimum coagulation dose of the sand-TBP at pH 4 and 6 using a model water containing 30 mg l^{-1} humic acid. The coagulation performance was evaluated by PDA monitoring and changes in solution NPDOC, and UV-Visible absorbance at 254 nm and 400 nm.

8.2 Adsorption of TBP on Sand

8.2.1 Preparation of a Solid Bound TBP

Initial adsorption tests were carried out at pH 4 (maximum TBP charge density) using 30 mg l^{-1} TBP with different amounts of sand, with the sand used as received. A 2L gator jar with a high mixing speed of 300 rpm (600 s^{-1}) for 2 minutes was used in this test, and the final solution was filtered by $0.45\mu\text{m}$ filter paper. The results for the filtered water gave erratic UV_{210} absorbance values, with some absorbance higher than that corresponding to the initial 30 mg l^{-1} standard TBP solution, indicating some organic contamination on the surface of

microsand was present.

The method was modified to employ washing of the sand by either 20% (v/v) H₂O₂ or 5 % (v/v) decon solution (Decon Laboratories Ltd, UK), and drying of the washed sand in an oven at an appropriate temperature. After this pre-washing of the sand, the adsorption tests at pH4 were undertaken, and the UV₂₁₀ absorbance of filtered solutions is shown in Tables 8.1 and 8.2, for each washing method. From Tables 8.1 and 8.2, it can be seen that after the 2 min rapid mixing at 300 rpm (600 s⁻¹), a partial and systematic adsorption of TBP by the washed sand was observed. It was also observed that the optimum adsorption of TBP occurred at a sand concentration of 50 mg l⁻¹, and that the degree of adsorption was greater with the sand washed by Decon solution compared to that washed by hydrogen peroxide solution. Although the quantification of residual TBP by measurement of NPDOC is not believed to be as accurate as UV absorbance, the optimal ratio of TBP/sand (30mg l⁻¹/50mg l⁻¹) was confirmed, as shown in Table 8.3. At the optimal TBP/sand ratio, the residual TBP concentration in filtered water was 14.29 mg l⁻¹ (Table 8.2), which corresponded to nearly half of the original TBP dose (30 mg l⁻¹-14.29 mg l⁻¹=15.71 mg l⁻¹), indicating a polymer adsorption of 52%. The amount of TBP adsorbed in 1mg sand surface was shown in Table 8.1, the reason for the unstable change is unknown, and need to further studied.

TABLE 8.1 Residual TBP in solution after 2 min mixing with sand (20% H₂O₂ solution washed, 30 mg l⁻¹ TBP)

TBP (mg l ⁻¹)	Sand (mg l ⁻¹)	UV ₂₁₀	Residual TBP concentration (mg l ⁻¹)	The amount of TBP/sand (mg/mg)
30	15	1.815	29.50	0.03
	25	1.658	26.86	0.13
	50	1.273	20.39	0.19
	100	1.595	25.81	0.04
	150	1.766	28.69	0.008
	250	1.802	29.28	0.003

TABLE 8.2 Residual TBP in solution after 2 min mixing with sand (5% Decon solution washed, 30 mg l⁻¹ TBP)

TBP (mg l ⁻¹)	Sand (mg l ⁻¹)	UV ₂₁₀	Residual TBP concentration (mg l ⁻¹)	The amount of TBP/sand (mg/mg)
30	15	1.633	26.44	0.24
	25	1.589	25.70	0.29
	40	1.324	21.25	0.22
	45	1.204	19.23	0.24
	50	0.910	14.29	0.31
	55	1.421	22.88	0.13
	60	1.512	24.41	0.09
	100	1.602	25.92	0.04
	150	1.611	26.07	0.03
	250	1.672	27.10	0.01

TABLE 8.3 Residual NPDOC in solution after 2 min mixing with sand (5%Decon solution washed, 30mg l⁻¹ TBP)

	TBP 30 mg l ⁻¹	TBP 30 mg l ⁻¹ With Sand 15mg l ⁻¹	TBP 30 mg l ⁻¹ With Sand 25mg l ⁻¹	TBP30 mg l ⁻¹ With Sand 50mg l ⁻¹	TBP30mg l ⁻¹ With Sand100mg l ⁻¹	TBP30 mg l ⁻¹ With Sand150mg l ⁻¹
Residual NPDOC (mg l ⁻¹)	11.76	8.81	9.76	7.079	10.90	10.86

To check the uniqueness of the optimal TBP/sand ratio, a further test at pH 4 was carried out at double the previous TBP concentration used, 60mg l⁻¹, with different amounts of sand washed by Decon; the results are shown in Table 8.4.

TABLE 8.4 Residual TBP in solution after 2 min mixing with sand (5% Decon solution washed; 60mg l⁻¹ TBP)

TBP	Sand (mg l ⁻¹)	UV ₂₁₀	Residual TBP concentration (mg l ⁻¹)	The amount of TBP/ sand (mg/mg)
60mg l ⁻¹	80	3.194	52.68	0.09
	90	2.782	45.75	0.16
	100	2.321	38.01	0.219
	110	3.061	50.44	0.09
	120	3.202	52.81	0.06
	150	3.495	57.73	0.02

It is clear that the minimum residual TBP, 38.01 mg l⁻¹, was found at the optimum ratio of 60 mg l⁻¹ TBP/100 mg l⁻¹ Sand. This optimal ratio is virtually identical to that found for 30 mg l⁻¹ TBP solutions, but the degree of TBP adsorption was lower at 37%. The overall results are shown graphically in Figure 8.1. No further tests were carried out at higher concentrations of TBP (> 60mg l⁻¹) since the absorbance of UV₂₁₀ was out of the spectrophotometer's limit, indicating that the TBP-UV₂₁₀ calibration relationship was unreliable.

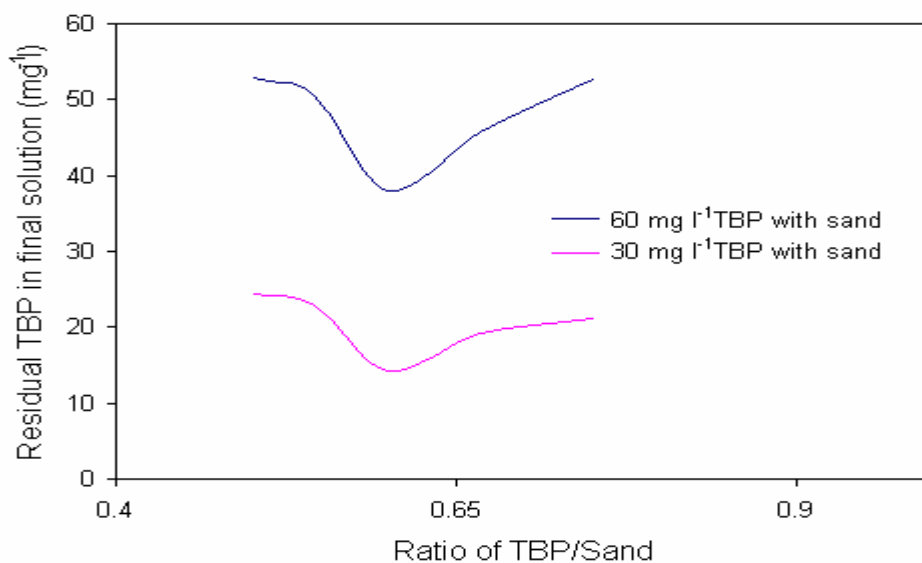


Figure 8.1 Variation of the residual TBP with TBP/Sand Ratio

8.2.2 The Effect of Mixing Time to Solid Bound TBP

The mixing time for the interaction of TBP and sand has been investigated by changing the time from 2 min to 45 min at high mixing speed (300rpm). Bearing in mind that the subsequent coagulation experiments would be carried out with 30 mg l⁻¹ HA at pH6, which previously required an optimal dose of 45 mg l⁻¹ TBP as coagulant alone, a series of tests using 60 mg l⁻¹ TBP with 100 mg l⁻¹ sand was undertaken to see whether an increased mixing time improves the adsorption effectiveness or causes desorption between TBP and sand. The results in Table 8.5 showed that with increasing mixing time, the solution absorbance at 210nm increased systematically, suggesting an increased quantity of TBP remaining in the solution. The results of UV absorbance with different mixing time were consistent with the NPDOC results, which showed the minimum NPDOC in the final solution was 15.42 mg l⁻¹ for the 2 min mixing, compared to the highest NPDOC, 22.96 mg l⁻¹ for 45 min mixing. It is clearly seen that the optimum adsorption of TBP with sand occurred with the shortest mixing time (2 min), and that further mixing leads to polymer desorption from the sand. Further test results showed that mixing times less than 2 min gave higher UV absorbance values compared to that with 2 min mixing.

TABLE 8.5 Residual TBP in solution with different mixing time (5% Decon solution washed; 60 mg l⁻¹ TBP)

TBP& Sand	Mixing time (min)	UV ₂₁₀ (cm ⁻¹)	Residual TBP concentration (mg l ⁻¹)	NPDOC (mg l ⁻¹)
60mg l ⁻¹ TBP and 100mg l ⁻¹ sand	2	2.321	38.01	15.41
	5	2.475	40.59	17.29
	10	2.962	48.78	18.85
	15	3.385	55.89	20.42
	30	3.475	57.40	22.22
	45	3.475	57.40	22.96

8.3 Coagulation Action of Solid Bound TBP in HA Solution

8.3.1 Coagulation Performance of Solid Bound TBP at pH 4

The coagulation performance of solid bound TBP was studied and compared with the optimum dose of solution phase TBP at pH 4 for 30 mg l^{-1} humic acid solution; the latter was determined as 30 mg l^{-1} , giving a maximum FI of 0.34 (see Section 6.2.3). Different doses of TBP have been used in the coagulation tests while maintaining the optimum TBP/Sand ratio, determined in Section 8.2.1. In this case, the TBP doses were chosen in the range of 50 mg l^{-1} to 1.5 g l^{-1} . The HA model water with the solid bound TBP were rapidly mixed in the 2L gator jar at 260 rpm (500 s^{-1}) and held at this value for the required time (20-25 min). This rather high speed was found to be the optimum speed to uniformly suspend the solid bound TBP in water. The results of the coagulation tests with the solid bound TBP, in terms of the PDA Flocculation index for the different amounts of TBP (optimum TBP/sand ratio), are shown in Figure 8.2.

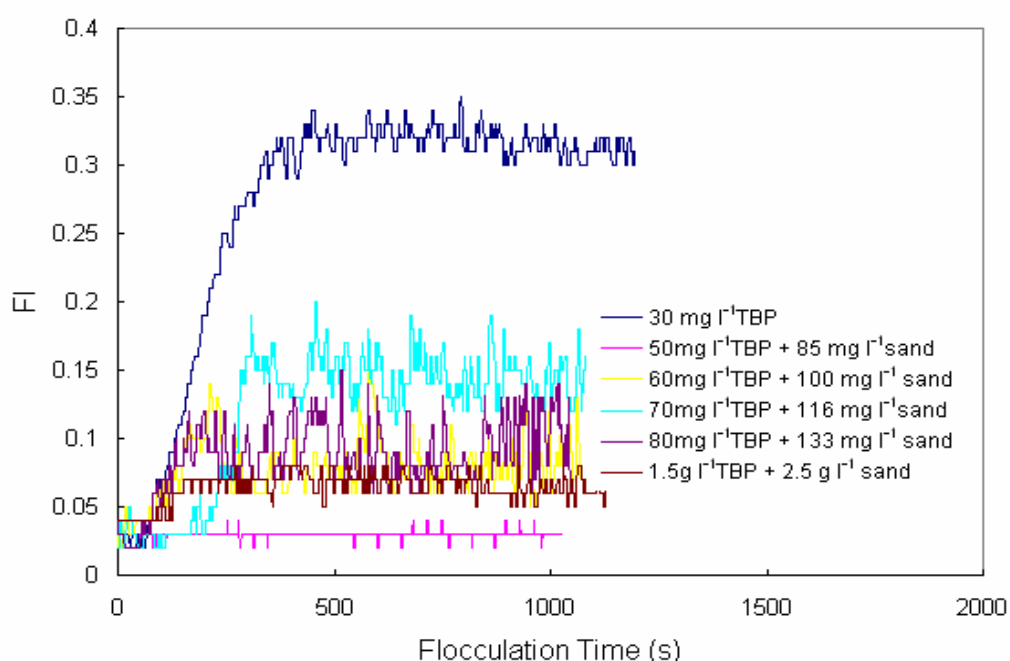


Figure 8.2 Flocculation index response with the solid bound TBP at pH4 (30 mg l^{-1} HA)

In Figure 8.2, it can be seen that the solid bound TBP was capable of achieving some degree of HA coagulation. However, the maximum FI (0.14-0.17) observed, corresponding to the solid bound TBP produced from 70 mg TBP with 116 mg sand, was substantially less than that produced by solution phase TBP (30 mg l⁻¹ TBP). With the increasing or decreasing TBP mixed with sand at the optimum ratio, the FI value clearly decreased. It is speculated that the charge density of TBP adsorbed on the surface of sand after mixing at the optimal ratio (70 mg l⁻¹ TBP/116 mg l⁻¹ sand) is similar to that of the optimum dose of solution phase TBP (30 mg l⁻¹), which interacts and neutralises the negative charge of the humic acid at pH 4. The relatively smaller FI value, in comparison with that using the 30 mg l⁻¹ solution phase TBP, is possibly explained by the high mixing speed required to maintain the sand in suspension, which may be sufficient to shear weak flocs and prevent significant floc formation. For example, in the previous studies with solution phase TBP, the maximum FI was reduced from 0.34 to 0.14, when the stirring rate was increased suddenly from 50 rpm to 300 rpm (Section 6.6). The much greater fluctuation in FI in this study was possibly caused by the variation of sand size and the presence of air bubbles in solution produced by the extended period of high speed mixing. The quality of the treated water after settling and filtering was measured in terms of NPDOC and UV-visible light absorbance at 254nm and 400nm. The results are shown in Table 8.6. From Table 8.6, it is clear that the sand/TBP combination of 116 mg l⁻¹ sand/70 mg l⁻¹ TBP, gave the best coagulation performance compared with the performances of the other sand/TBP combinations; this is consistent with the observed FI results. Assuming that no residual TBP remains in the filtered water, the removal of NPDOC and UV₂₅₄ absorbance by the solid bound TBP are 29.25% and 7.21%, which are much lower compared to the corresponding values for 30mg l⁻¹ solution phase TBP (30 mg l⁻¹ HA solution at pH4) of NPDOC 83.5% and 92.3%, respectively. Thus, the corresponding values for the residual NPDOC in the final water were 5.906 mg l⁻¹ for solid bound TBP and 4.353 mg l⁻¹ for the solution phase TBP.

TABLE 8.6 NPDOC and UV-visible light absorbance at 254nm and 400nm in filtered water at pH4 (30 mg l⁻¹ HA)

Sand (mg l ⁻¹)	TBP (mg l ⁻¹)	Abs at 254nm (cm ⁻¹)	Abs at 400nm (cm ⁻¹)	NPDOC (mg l ⁻¹)
0	0	0.707	0.176	8.348
85	50	0.705	0.175	7.247
100	60	0.702	0.173	6.997
116	70	0.656	0.153	5.906
133	80	0.684	0.161	6.644
150	90	0.700	0.174	6.892
2500	1500	0.678	0.146	7.171

8.3.2 Coagulation Performance of Solid Bound TBP at pH 6

A further series of tests were carried out to measure the coagulation performance of solid bound TBP with 30 mg l⁻¹ HA at pH 6, involving the prior preparation of sand with TBP for 2 min fast mixing at 300 rpm under pH 4. The results of the coagulation tests with the solid bound TBP, in terms of the PDA Flocculation index for the different amounts of TBP (optimum TBP/sand ratio), are shown in Figure 8.3. As found previously at pH4, it can be seen that the solid bound TBP was capable of achieving some degree of HA coagulation. However, the maximum FI of 0.15 observed, corresponding to the solid bound TBP produced from 160 mg TBP with 266 mg sand, was substantially less than that produced by solution phase TBP (45 mg l⁻¹ TBP). It also can be seen that the coagulation performance by 160 mgTBP/266 mg sand is close to the performance by 180 mgTBP/313 mg sand, suggesting that charge neutralization is not the dominant mechanism in this case at pH6. However, it is possible in these tests that the high speed mixing may have caused floc breakage.

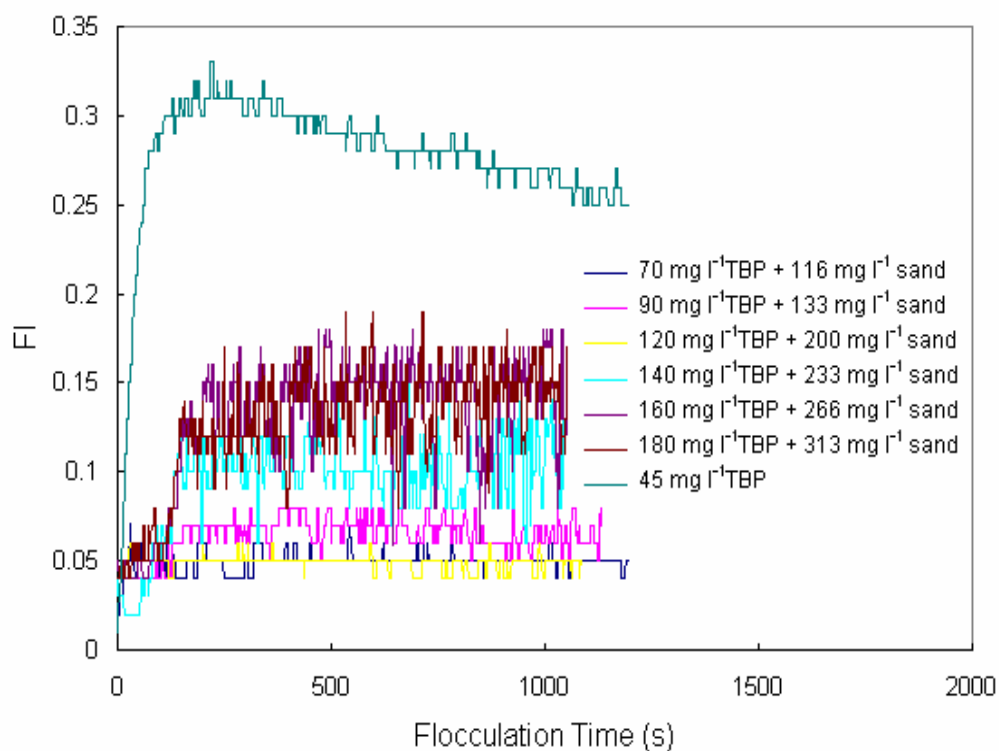


Figure 8.3 Flocculation index response with the solid bound TBP at pH6 (30mg l⁻¹ HA)

TABLE 8.7 NPDOC and UV-visible light absorbance at 254nm and 400nm in filtered water at pH6 (30mg l⁻¹ HA)

Sand (mg l ⁻¹)	TBP (mg l ⁻¹)	Abs at 254nm (cm ⁻¹)	Abs at 400nm (cm ⁻¹)	NPDOC (mg l ⁻¹)
0	0	0.707	0.176	8.348
116	70	0.704	0.129	8.375
133	90	0.702	0.129	8.420
200	120	0.707	0.129	7.05
233	140	0.701	0.128	6.501
266	160	0.700	0.127	6.427
313	180	0.707	0.127	6.331

8.4 Discussion

When polymeric coagulants are used in the treatment of potable waters, attention must be paid to their possible toxicity. Generally speaking, the presence of residual polymer or/and residual monomer can present a hazard. However, a practical problem with high molecular weight polymers is that they are difficult to measure in solution at low concentrations (eg. $< 1 \text{ mg l}^{-1}$)(44). To date, a standard colorimetric method is still considered a feasible means to measure the phenol and tannin acid in water treatment. However, although the Determination limit (DL) of this standard method has been determined by UV spectrophotometry as a very low value (0.018 mg l^{-1} as tannin acid, Section 4.5.3), there is still concern whether in real waters the TBP product or monomer could be determined accurately at sufficiently low concentrations. Unfortunately, no published work has considered the determination of residual TBP concentration, possibly due to the complex nature of this polymer.

Under the circumstances of a certain optimal adsorption ratio of TBP/sand, the combination of TBP and sand as 'solid bound TBP' was encouraging with respect to the use of the coagulant whilst minimizing residual TBP in the final water (following conventional filtration). This novel approach is based on the theory that if there is some affinity between polymer segments and particle surfaces, then adsorption of polymer chains may occur (19). In this case, for sands carrying a net negative surface charge and cationic TBP, the bound ratio of TBP/sand was found to be influenced by mixing time. It was observed that an equilibrium arrangement was achieved within 2 min of interaction between the TBP and the sand. The optimal bound ratio obtained in this mixing system was found to be consistently of the order of $0.6 \text{ mg TBP/mg micro sand}$. Beyond this optimal value, the adsorption effectiveness between sand with polymer was worse.

According to a widely accepted model of an adsorbed polymer chain (7), the tails and loops of TBP which is un-attached to the surface of sand and projecting into the solution are able to interact with the humic substances in the model water. Notwithstanding the evidence of coagulation between the solid bound TBP and the humic solution in this study, the effectiveness (the removal of NPDOC and UV_{254} absorbance) was inferior at pH 4 and 6, in comparison with the performance by solution phase TBP. It is speculated that in practice, the quantitative adsorption between TBP and sand is difficult to achieve at a very high mixing speed. The overdose of sand possibly depleted too much cationic charge of TBP, hence restricting the further interaction with humic acid to aggregate in solution. On the other hand, the vigorous agitation may cause the scission of polymer chains into small units and affect the coagulation effectiveness of TBP.

9. RESULTS: COAGULATION EXPERIMENTS OF RAW WATER

9.1 Introduction

In the treatment of surface water, a cationic polyelectrolyte with high CD and medium or high MW such as polyDADMAC or polyamine can be used to replace a metal salt as the primary coagulant. However, there are fewer examples of polymer-only coagulation in conventional coagulation/sedimentation/filtration plants, compared to the use of polymer in conjunction with a metal salt, due to the high polymer dose that would be required. A number of workers (102-105) have found that the most effective removal of either turbidity or humic substances from natural waters was achieved by the combination of an inorganic coagulant and a cationic polymer such as polyDADMAC. In addition, Bolto(1) has also indicated that for high turbidity waters, the alum dose required for effective coagulation and filtration could be the limiting factor, with 12-15 mg l⁻¹ as Al³⁺ suggested as the upper limit. In fact, the strategy of partial replacement of alum with a polymer has been applied in treatment practice for years (105, 106). In recent years, the combination of a natural polymer chitosan with alum as a primary coagulant has been considered for raw water treatment. Very good removal of turbidity and TOC from natural water by the combination of chitosan with metal salts has been reported by Kawamura (3) and Vogelsang *et al.* (109), respectively. Although these results indicated that chitosan was a potential alternative flocculant for synthetic polymers, its economic aspect must be considered in practice.

This chapter considers the coagulation effectiveness of TBP in 'synthetic' real waters using bench-scale tests with a photometric dispersion analyzer to investigate whether TBP would be a workable substitute for alum and polyDADMAC. Based on the previous results of model water tests, samples of a real water from an organic-rich river source at Bamford, UK, were also included for the bench-scale coagulation tests to raise the possibility of maximizing and

optimizing the performance using certain doses of TBP alone and dual coagulants (alum/TBP) as primary coagulants.

9.2 Coagulation Performance of TBP in Simulated Water

A simulation test using a mixture of kaolin clay and humic acid as model water was undertaken to simulate the performance of TBP with a real water and to compare the results with those reported previously for real waters by WRc (137). Details of the two waters and test methods were given in Section 4.4.3. The results of the coagulation performance with the artificial model water are shown in Figure 9.1.

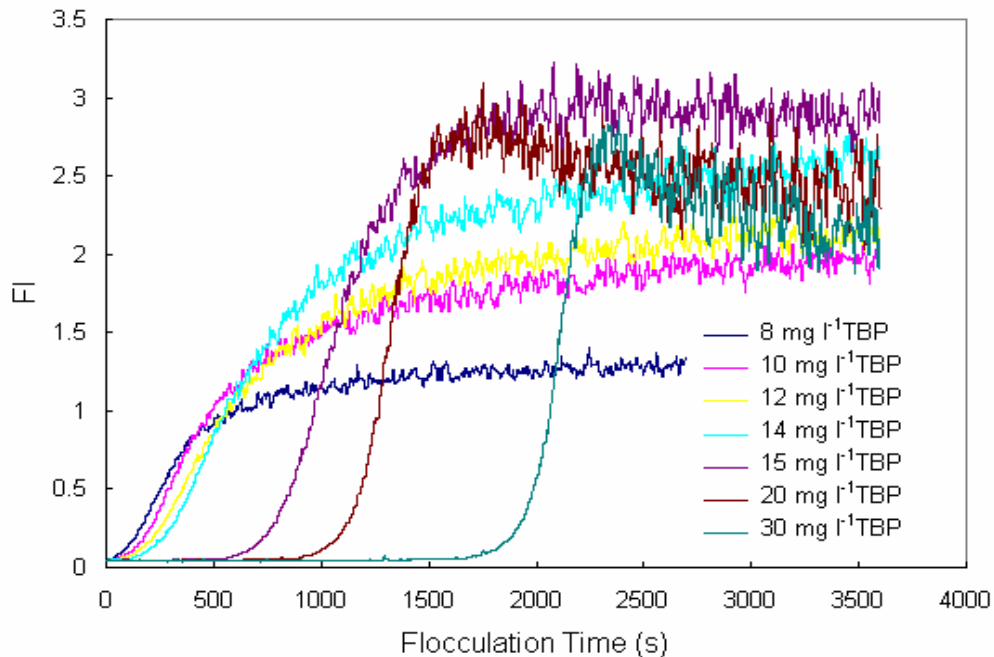


Figure 9.1 Flocculation index response with TBP dose for artificial water

The coagulation tests indicated that a relatively high dose (15-20 mg l⁻¹) of TBP gave a good performance of colour, turbidity and NPDOC removal, although at a lower dose, the onset of flocculation seemed to occur earlier. The delayed flocculation phenomena at high dosage are difficult to explain by Smoluchowski flocculation theory. It is likely affected by the precipitation of TBP at high pH, however, the details need to be further studied. Even though the

nature of the organic matter in the real water is different to the HA used in the model water, the optimum dose of around 15-20 mg l⁻¹ for the model water is consistent with the results of the WRc study, in which a similar dose of 15-20 mg l⁻¹ of TBP was required to produce the minimum residual turbidity. A comparison of the results of the two types of water at a common TBP dose of 15 mg l⁻¹ tests are given in Tables 9.1 and 9.2.

TABLE 9.1 Coagulation results for the artificial water using 15 mg l⁻¹ TBP

	pH	NPDOC* (mg l ⁻¹)	NPDOC Reduction	Colour (Hazen)	Colour Reduction	Turbidity (NTU)	Turbidity Reduction
Initial artificial water	7.9	(15.26)**	17.8%	32	75%	27	70.37%
Final filtered water	7.1	(12.55)**		8		8	

* Initial NPDOC value is the sum of NPDOC values of TBP and artificial water.

** As indicated in Table 4.4, these values are believed to be incorrect.

TABLE 9.2 Coagulation results for the real water using 15 mg l⁻¹ TBP (137)

	pH	NPDOC (mg l ⁻¹)	NPDOC Reduction	Colour (Hazen)	Colour Reduction	Turbidity (NTU)	Turbidity Reduction
Initial River water	7.9	5.73	18.32%	32.8	67.98%	27	99.48%
Final filtered water	6.9	4.68		10.5		0.14	

9.3 Coagulation Performance of Different Coagulants with Raw Water

9.3.1 Coagulation Tests of Raw Water without pH Adjustment

In this study, TBP was dosed to samples of raw water from Bamford, UK (see Section 4.4.4) without adjustment of pH and the coagulation performance was investigated. The PDA results are shown graphically in Figure 9.2. From

these and the values of the other water quality parameters, shown in Table 9.3, it is clear that a TBP dose of 30 mg l⁻¹ gave the maximum FI, around 0.2, and the optimal coagulation performance overall. The corresponding pH was 7.6.

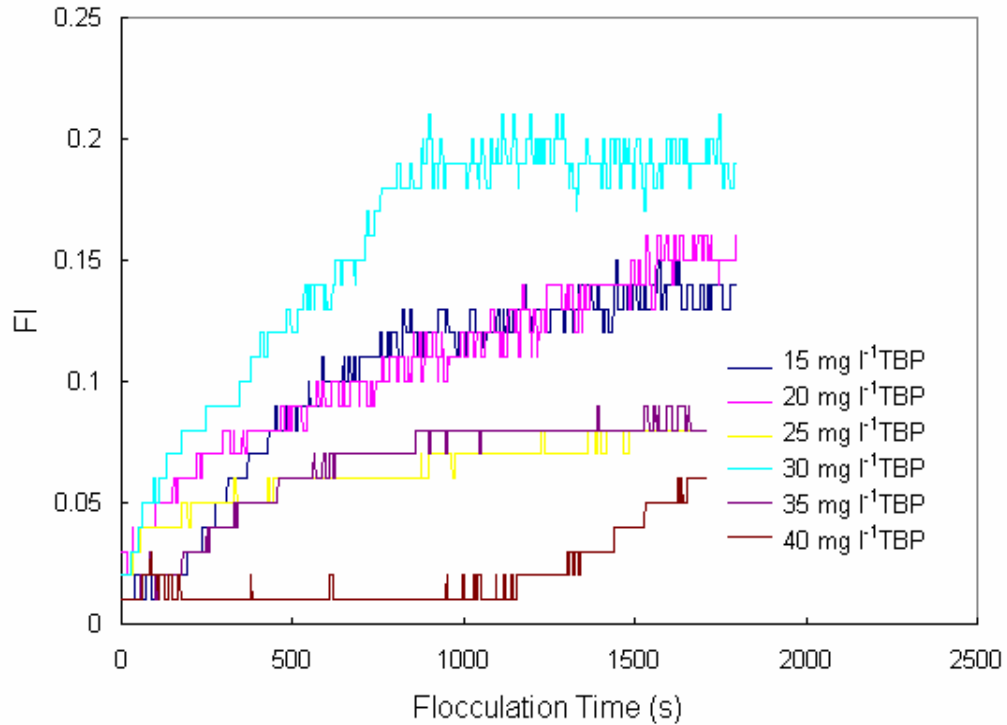


Figure 9.2 Dynamic monitoring of raw water (Bamford, UK) using different dosages of TBP without pH adjustment

TABLE 9.3 Variation of coagulation performance with TBP dosage for raw water (Bamford, UK) without pH adjustment

TBP dose (mg l ⁻¹)	Final pH	NPDOC (mg l ⁻¹)	Colour Hazen	UV 254nm	UV400nm	Floc Vol (ml)	FI
15	7.8	4.062	12.5	0.084	0.004	3.5	0.13
20	7.8	4.244	15	0.084	0.008	3.5	0.15
25	7.6	3.936	12.5	0.089	0.004	--	0.08
30	7.6	3.096	10	0.073	0.004	5	0.2
35	7.2	4.513	15	0.081	0.004	--	0.08
40	6.6	6.093	20	0.083	0.009	--	0.07

9.3.2 Coagulation Tests of Raw Water with pH Adjustment at pH 6

9.3.2.1 Coagulation Performance of Alum

In these laboratory tests, 0.1 mol l⁻¹ HCl solution was used to adjust the pH value to 6.0. The optimum dose of alum used as coagulant alone was measured by PDA and the results are shown in Figure 9.3. It is clear that 4.1 mg l⁻¹ as Al³⁺ gave the maximum FI as 0.17. The other water quality parameters were also measured and are summarised in Table 9.4. Clearly, the optimal results of final water qualities were in agreement with the PDA findings.

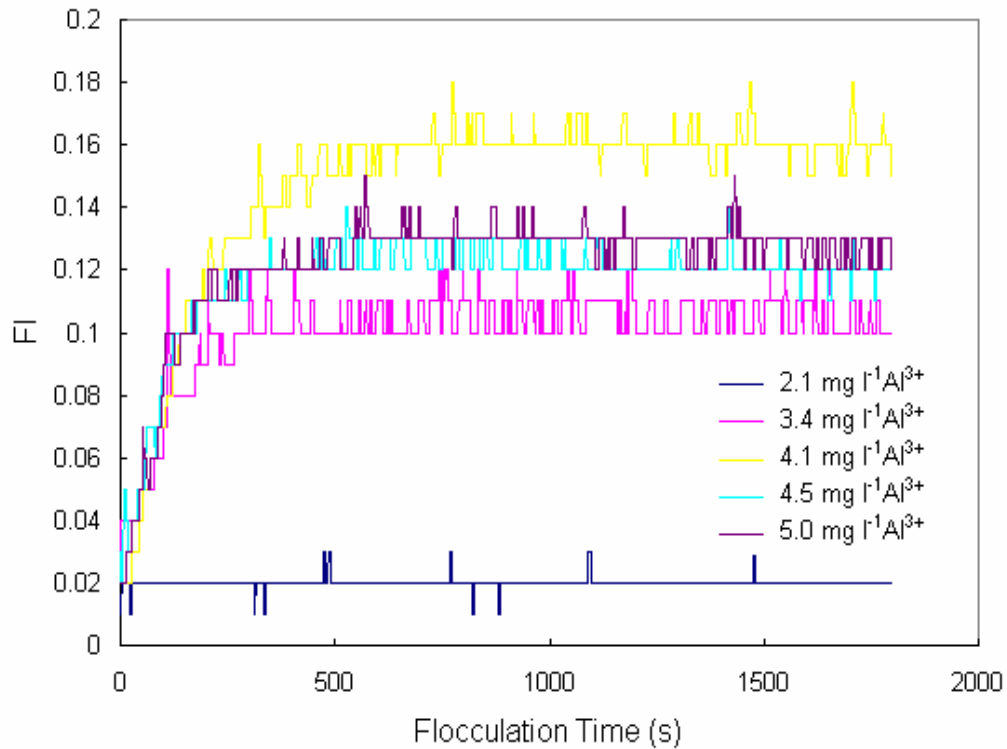


Figure 9.3 Dynamic monitoring of raw water at pH 6 using different doses of alum (Bamford raw water)

TABLE 9.4 Variation of coagulation performance with alum dosage at pH6 (Bamford raw water)

Al ³⁺ dosage (mg l ⁻¹)	NPDOC (mg l ⁻¹)	Colour Hazen	UV 254nm (cm ⁻¹)	UV400nm (cm ⁻¹)	Floc Vol (ml)	FI
3.4	1.090	10	0.022	0.002	3.5	0.11
4.1	1.003	5	0.019	0.001	4.5	0.17
4.5	1.026	7.5	0.024	0.002	3.5	0.13
5.0	1.052	15	0.024	0.003	2.0	0.14

9.3.2.2 Coagulation Performance of TBP

The optimum dose of TBP used as the sole coagulant was measured at pH 6. From Figure 9.4, it is clear that 25 mg l⁻¹ TBP gave a maximum FI value of around 0.35. This optimal dose was confirmed by the other water quality parameters shown in Table 9.5. However, the NPDOC value of the final water using 10 mg l⁻¹ TBP as the sole coagulant was smaller than that using 25 mg l⁻¹ TBP, owing to the lower dose of TBP added to the initial water.

Compared to the previous results with model water containing 15 mg l⁻¹ HA (NPDOC approximately 4.01 mg l⁻¹), the dosages of alum and TBP for real water (NPDOC approximately 3.662 mg l⁻¹) are higher. However, it is reasonable to expect significant differences between the real and model waters owing to the different water qualities.

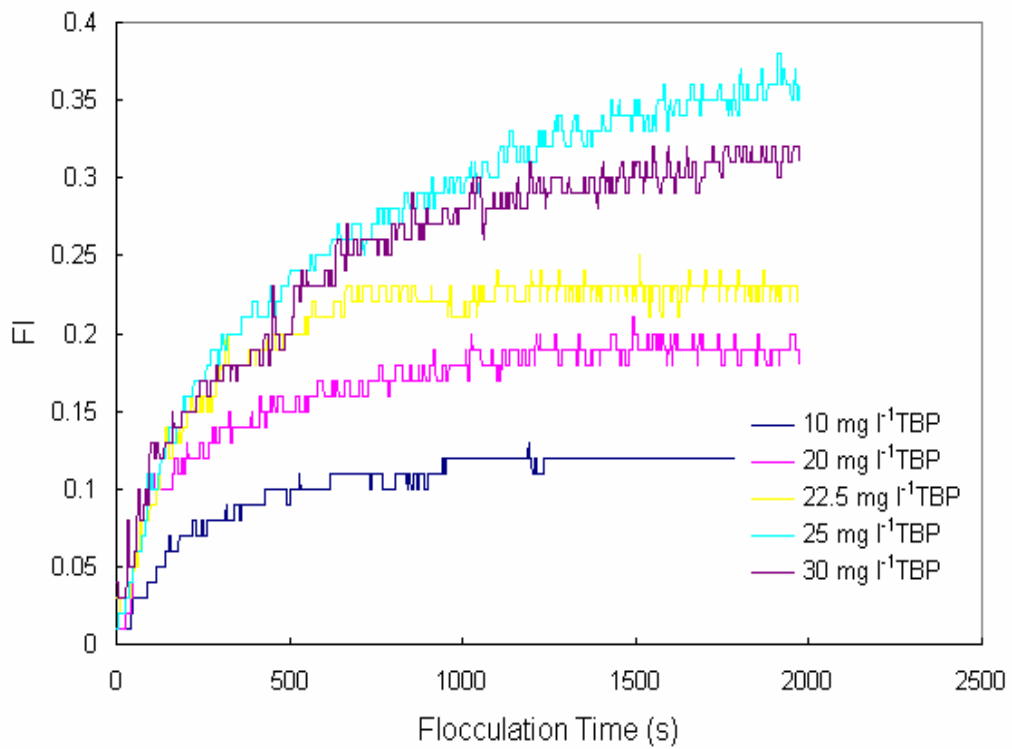


Figure 9.4 Dynamic monitoring of raw water at pH 6 using different doses of TBP (Bamford raw water)

TABLE 9.5 Variation of coagulation performance with TBP dosage at pH6 (Bamford raw water)

TBP dose (mg l ⁻¹)	NPDOC (mg l ⁻¹)	Colour Hazen	UV 254nm (cm ⁻¹)	UV400nm (cm ⁻¹)	Floc Vol (ml)	FI
10	2.064	15	0.046	0.007	3	0.12
20	2.927	15	0.060	0.004	5	0.20
22.5	2.858	7.5	0.057	0.004	8	0.23
25	2.809	5	0.049	0.003	10	0.35
30	3.240	10	0.056	0.003	8	0.31

9.3.2.3 Coagulation Performance of Alum/TBP Combination

A narrow matrix test of the TBP/Alum dose combination for real water at pH 6 was undertaken, based on the optimum dose of alum and TBP for real water and the combination of TBP/Alum with the model water. The PDA results are shown in Figures 9.5, 9.6 and 9.7 for different doses of TBP and alum.

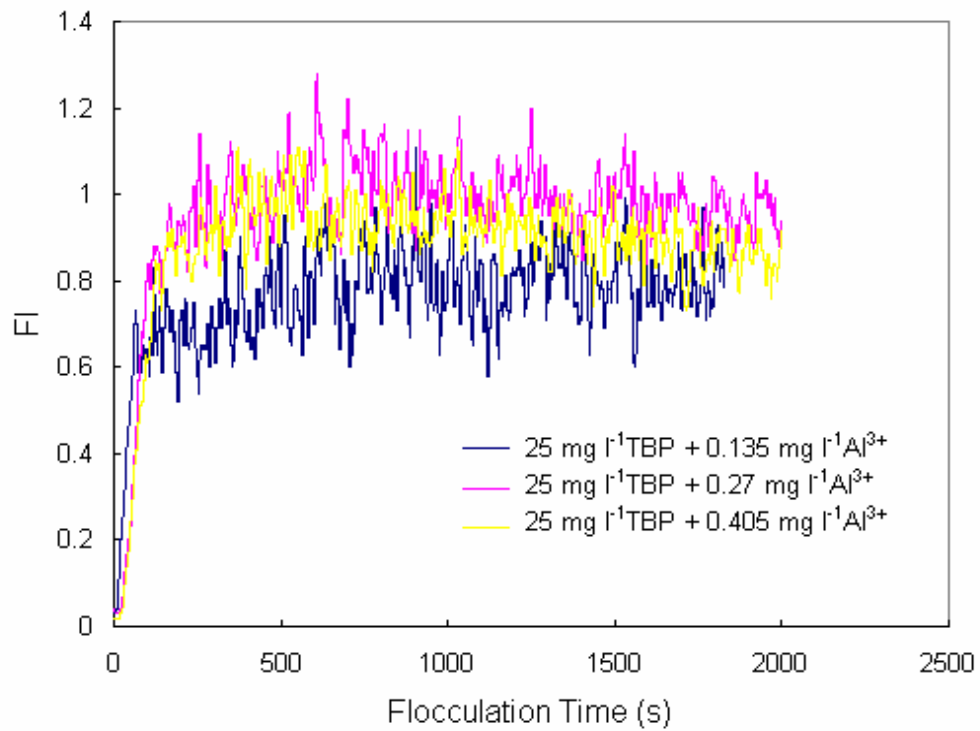


Figure 9.5 Flocculation index response with 25 mg l⁻¹ TBP and different Alum doses at pH6 (Bamford raw water)

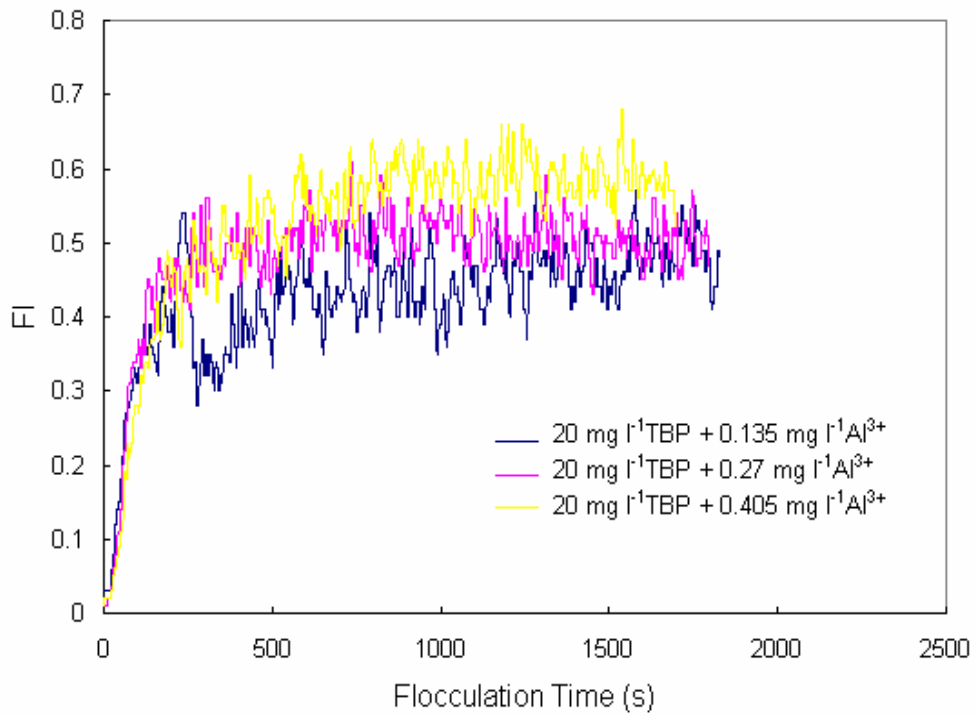


Figure 9.6 Flocculation index response with 20 mg l⁻¹ TBP and different Alum doses at pH6 (Bamford raw water)

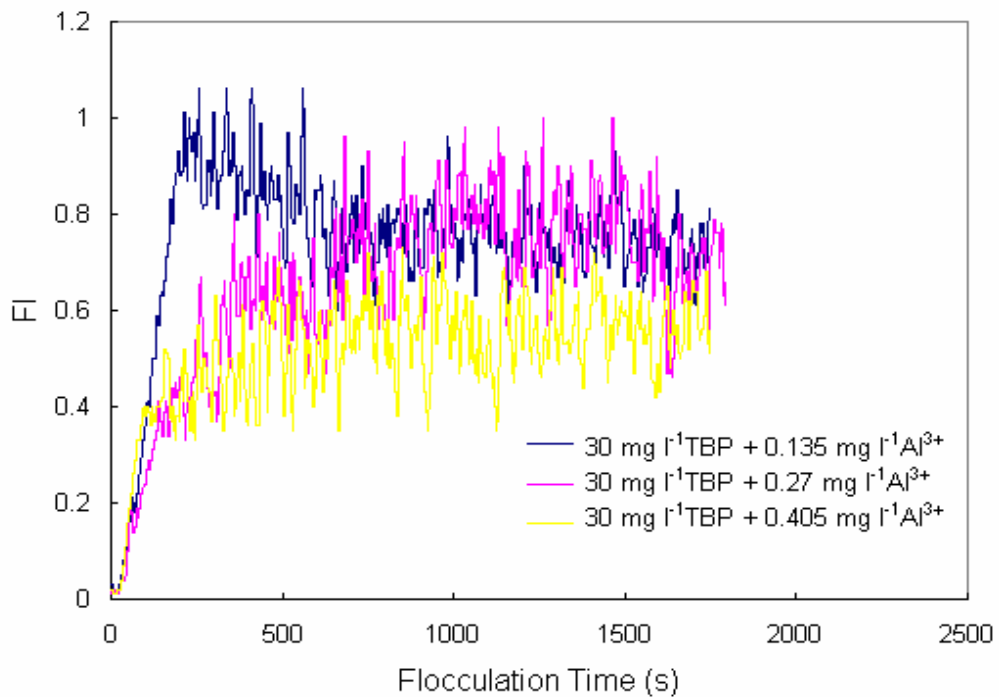


Figure 9.7 Flocculation index response with 30 mg l⁻¹ TBP and different Alum doses at pH6 (Bamford raw water)

It is clearly seen that the combination of TBP/Alum remarkably improved the coagulation performance (FI value). The optimal combination of TBP/Alum (25 mg l⁻¹ TBP and 0.27 mg l⁻¹ as Al³⁺) gave the maximum FI value of about 1.1. With an increase or decrease in the amount of TBP (30 mg l⁻¹ or 20 mg l⁻¹), the coagulation performances were inferior. However, the complementary relationship between TBP and alum was evident in this study. The locus of alum-TBP doses is shown in Figure 9.8.

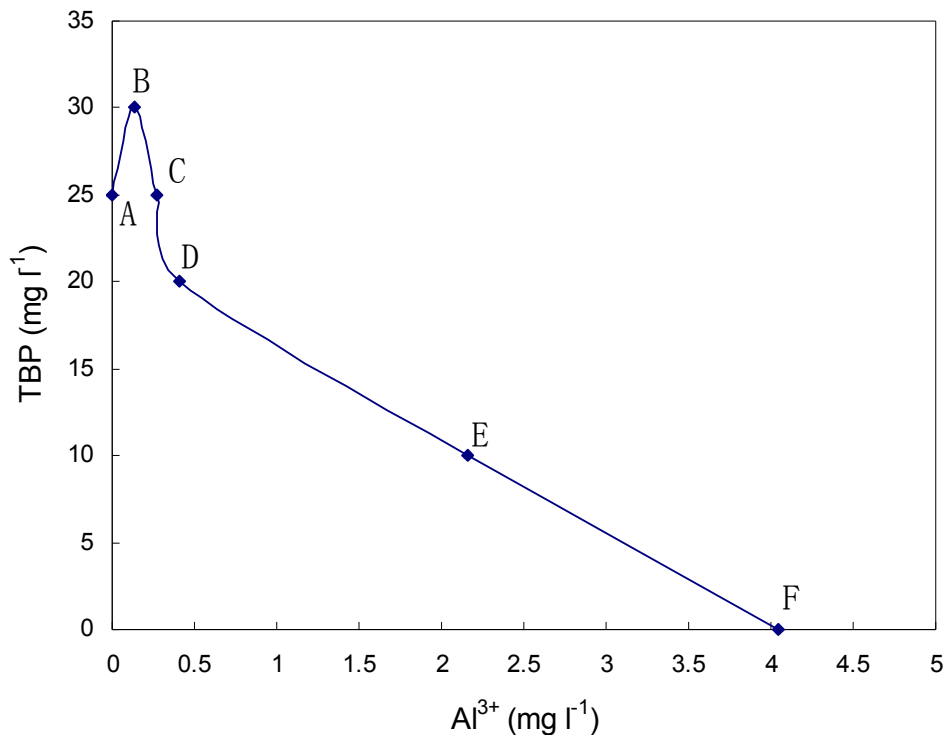


Figure 9.8 Locus of alum-TBP dosage combinations for optimal coagulation performance at pH6 (Bamford raw water)

The corresponding values for FI and colour removal at each point along the locus line are shown in Figure 9.9. The results showed that while colour removal is fairly insensitive to the alum-TBP dose combination over the full range considered, the FI is strongly influenced by the dose combination. Thus, point C is clearly the optimal dose combination.

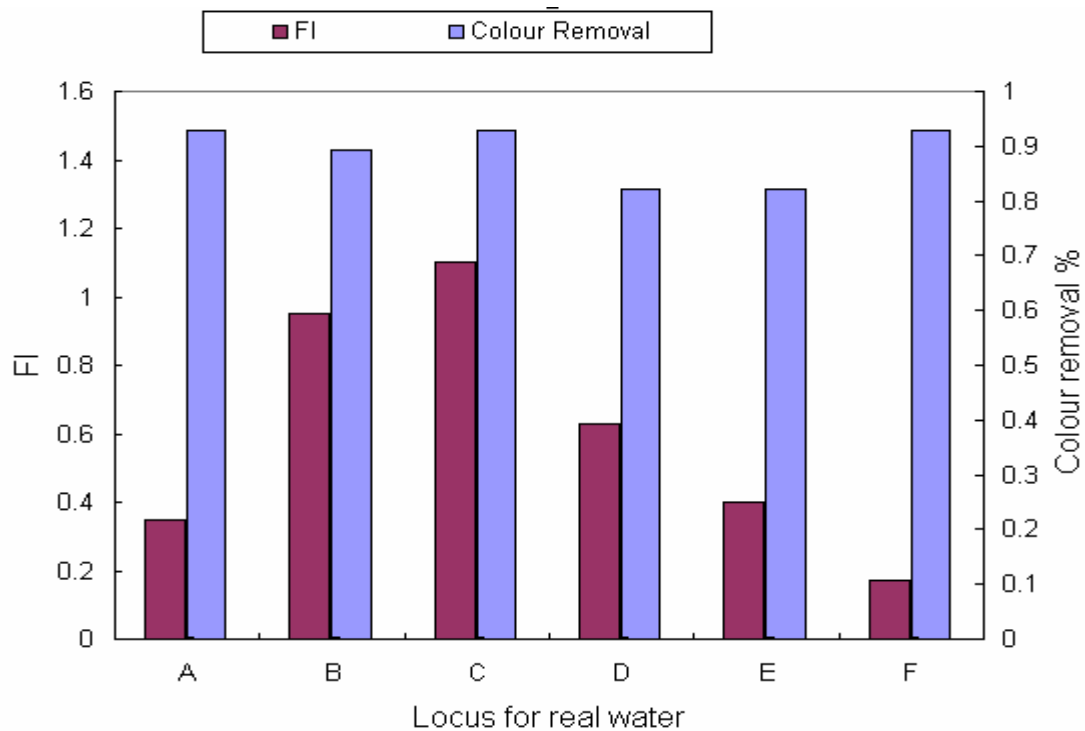


Figure 9.9 Variation of Flocculation Index and colour removal along locus line of coagulant dosage at pH6 (Bamford raw water)

In general, the locus line of doses for the real water is very close to that found for the model water with 15 mg l^{-1} HA. The coagulation performance in terms of other water quality parameters is summarized in Table 9.6. From Table 9.6, it is seen that 25 mg l^{-1} TBP with 0.27 mg l^{-1} as Al^{3+} significantly improved the coagulation performance and reduced the amount of alum compared to using alum alone. However, the addition of TBP as coagulant increased the value of final NPDOC, in comparison with alum as sole coagulant. It is also observed that the values of NPDOC in the final treated water are very close for the different TBP/alum combinations. It is likely that this was caused by the presence of residual TBP concentrations remaining in the final water, since the high removal of UV absorbance at 254nm indicated the absence of humic matter. Using the standard method for measurement of residual tannin, the absorbance at 700nm is about 0.132. From the calibration curve equation: $Y = 0.0943X - 0.0043$ (4.2), the corresponding residual TBP concentration in the final water is about 1.445 mg l^{-1} (the calibration curve is described in Section 4.5.3).

TABLE 9.6 Coagulation performance for the combination of TBP/Alum at pH6
(Bamford raw water)

TBP dose (mg l ⁻¹)	Al ³⁺ (mg l ⁻¹)	NPDOC (mg l ⁻¹)	Colour Hazen	UV 254nm (cm ⁻¹)	UV400nm (cm ⁻¹)	Floc Vol (ml)	FI
30	0.135	2.687	7.5	0.033	0.002	10	0.95
	0.27	2.791	10	0.038	0.002	8	0.85
	0.41	2.783	12.5	0.037	0.002	6	0.6
25	0.135	2.777	7.5	0.039	0.003	10	0.9
	0.27	2.432	5	0.031	0.002	14.5	1.1
	0.41	2.566	7.5	0.042	0.003	12	1.0
20	0.135	2.843	17.5	0.049	0.004	2	0.45
	0.27	2.828	15	0.046	0.004	4	0.55
	0.41	2.602	12.5	0.037	0.002	5.5	0.63
25	0	2.809	5	0.049	0.003	10	0.35
0	4.1	1.003	5	0.019	0.001	4.5	0.17

In the previous tests for model water with 15 mg l⁻¹ HA, the results indicated that a small amount of TBP with rather higher dose of alum improved the coagulation performance. In this case, 10 mg l⁻¹ TBP was chosen to combine with a range of alum (from 1.08 mg l⁻¹ to 3.24 mg l⁻¹ as Al³⁺) to see whether the coagulation performance is improved. The results are shown in Figure 9.10 and Table 9.7. It is clearly seen that in comparison with the performances using TBP or alum as coagulant alone, 10 mg l⁻¹ TBP with 2.16 mg l⁻¹ as Al³⁺ gave a modest performance.

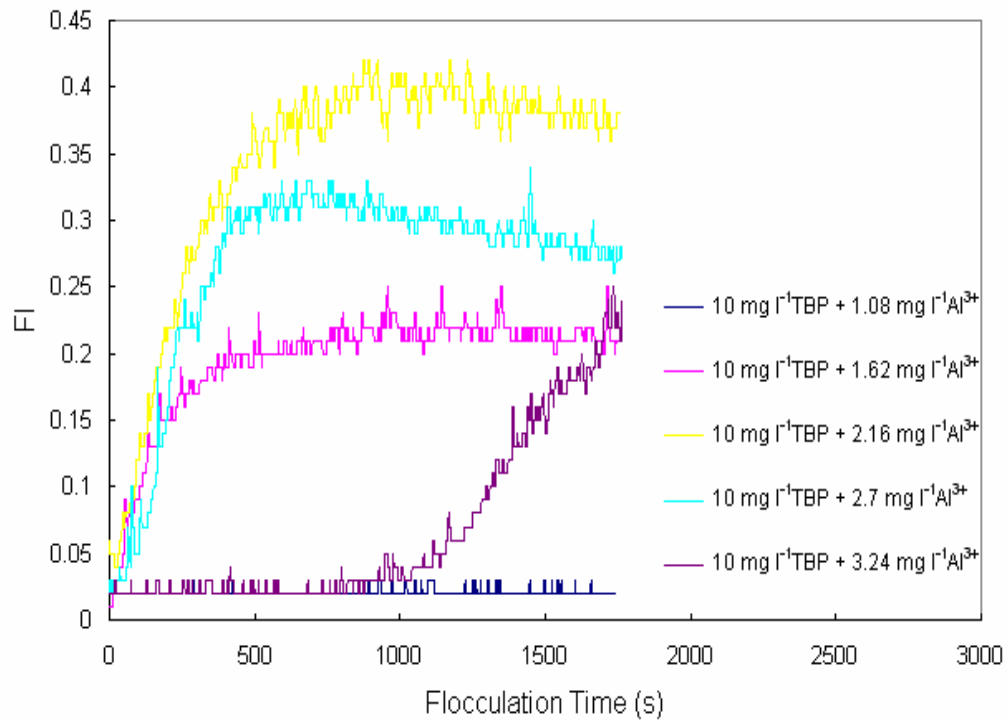


Figure 9.10 Flocculation index response with 10 mg l⁻¹ TBP and different Alum doses at pH6 (Bamford raw water)

TABLE 9.7 Variation of coagulation performance with TBP and alum doses at pH6 (Bamford raw water)

TBP dose (mg l ⁻¹)	Al ³⁺ (mg l ⁻¹)	NPDOC (mg l ⁻¹)	Colour Hazen	UV 254nm (cm ⁻¹)	UV400nm (cm ⁻¹)	Floc Vol (ml)	FI
10	1.62	1.834	15	0.045	0.005	1.5	0.22
	2.16	1.464	12.5	0.026	0.003	5.5	0.40
	2.7	1.474	15	0.030	0.008	1.5	0.32
	3.24	1.773	25	0.033	0.010	0.5	0.24
25	0	2.809	5	0.049	0.003	10	0.35
0	4.05	1.003	5	0.019	0.001	4.5	0.17

9.3.2.4 Floc Strength of Alum-TBP Combination

In this experiment, the optimum dose of alum, TBP and the combinations of TBP/alum were pipetted into real water at pH 6, and an initial period of 25 minutes for the slow stirring at 50 rpm (48 s^{-1}) was chosen since no significant changes were observed in the FI value after this. Floc breakage was brought about by suddenly increasing the stirring speed to 300 rpm (600 s^{-1}) after the initial period, and maintaining this for 60 seconds. Then, the stirring speed was reduced back to 50 rpm (48 s^{-1}). The PDA results are shown in Figure 9.11. The behaviour of the flocs during these hydrodynamic changes can be described by the following semi-quantitative parameters (Section 6.6.2) based on the FI response:

$$\text{Strength factor} = (FI_2 / FI_1) \cdot 100 \quad \text{----- (6.1)}$$

$$\text{Recovery factor} = [(FI_3 - FI_2) / (FI_1 - FI_2)] \cdot 100 \quad \text{----- (6.2)}$$

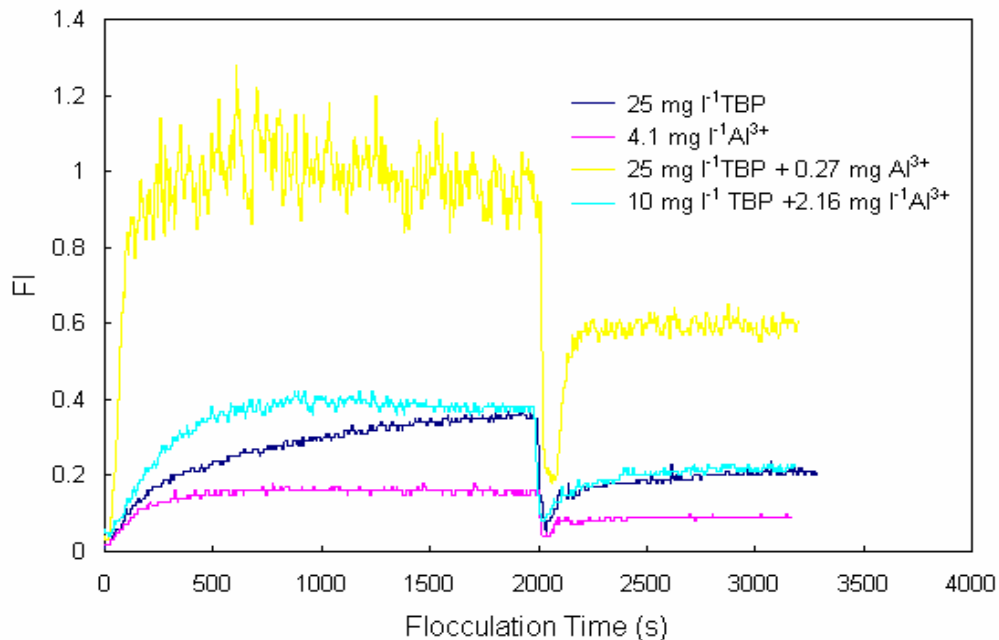


Figure 9.11 Monitoring of floc formation at 50 rpm, breakage at 300 rpm for 60s and re-formation at 50 rpm using different coagulants at pH6 (Bamford raw water)

TABLE 9.8 Strength and recovery factors obtained for different coagulants (floc breakage at 300rpm for 60s) at pH6 (Bamford raw water)

	Alum	TBP	10 mg l ⁻¹ TBP and 2.16 mg l ⁻¹ as Al ³⁺	25 mg l ⁻¹ TBP and 0.27 mg l ⁻¹ as Al ³⁺
Strength factor (%)	23.5	14.3	20.0	18.2
Recovery factor (%)	38.5	50	40.6	44.4

It is believed that the higher the value of the strength factor, the stronger the flocs, since they are less sensitive to breakage as a result of the increased shear rate. Compared with TBP, a stronger floc and lower recovery factor was found with alum for model waters containing kaolin suspensions at low pH in our previous studies (Section 6.6.2). In these experiments, from table 9.8 the strength and recovery factors of the TBP/alum combinations at the optimum ration (10/2.16 mg/mg) were similar to those with alum, and the strength factor was greater than TBP alone. However, with the increasing dose of TBP in the combination, the floc strength decreased slightly.

9.4 Discussion

The coagulation of a simulated river water showed that a relatively high dose (15 mg l⁻¹- 20 mg l⁻¹) of TBP gave a good performance of colour and turbidity removal, but less so with NPDOC removal. The results were consistent with those reported by WRc for real river water under equivalent conditions. Evidence that when particles are present, as would normally occur in natural waters, the coagulation performance is improved (31) was supported by the observed behaviour of a quaternary ammonium polymer with high CD and MW in the study of Bolto *et al.* (31). The examination of the addition of kaolinite when polyDADMAC was used as a primary coagulant suggests a 16% better removal of colour, but there was little change in the removal of NOM, as

measured by UV absorbance. In this case, at pH 7, comparing the “synthetic” water, in the presence of particles, with the HA model water, it is clearly observed that kaolinite has a great effect on coagulation performance. Although an adequate explanation is not possible, it seems likely that on addition of kaolinite to humic acid solutions, the organic material is partly adsorbed on to the clay surface, due to a strong affinity for humic acid (174). Therefore the enhanced polymer coagulation could be explained by bridging, probably by hydrophobic interaction between polymer molecules adsorbed onto adjacent particles (31).

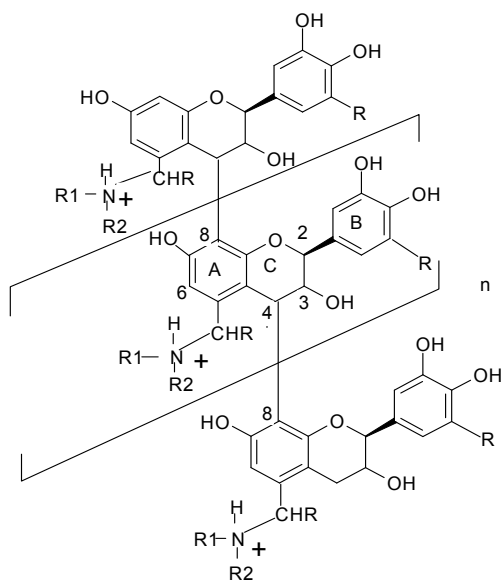
The observed locus line (Figure.9.8) of TBP-alum combination dose for the Bamford real water, an organic-rich river source, at pH 6 is totally consistent with the previous results for the model water with 15 mg l^{-1} HA at the same pH. The results of the Gator jar investigation showed that for the real water, at pH 6.0, the optimum Al/TBP dose ratio was identified as 0.27/25 mg/mg, suggesting that the addition of TBP at the same time as alum would enable a 93.25% reduction of aluminium coagulant (as sole coagulant) with an improvement of coagulation efficiency (FI is about 1.1), in comparison with the coagulation effectiveness by TBP or alum alone. A rather high dose of alum with a low dose of TBP at a Al/TBP ratio of 2.16mg/10mg also improved the coagulation performance and reduced the alum usage. The strong complementary relationship between TBP and alum favours the conclusion from the model water that at pH 6, the mechanism of the flocculation action of the combination is predominantly charge neutralization. The floc strength of the alum/TBP combination at the optimum ratio (0.27/25 mg/mg) was found to be clearly greater than the strength of TBP alone, and slightly lower than that of alum alone, as expressed in terms of strength factor. This trend is in agreement with the findings for model waters containing kaolin suspensions. There is still concern that as the amount of alum was reduced significantly by the use of the dual coagulant, the NPDOC value in the final treated water increases and is higher, compared to that with alum as a sole coagulant.

10. GENERAL DISCUSSION

Cationic polymers are used in water and wastewater treatment primarily as coagulants/flocculants to aid in solid-liquid separation. The majority of such applications are treated with synthetic polymers mainly due to their high charge densities and high molecular weights. However, synthetic products are likely to have toxicity problems and their long-term effects on human health are not well understood. To minimize these drawbacks, natural polymers and their derivatives have gained popularity in water and waste water treatment. The selection of natural polymers as primary coagulants is mainly on the basis of their cost, coagulation effectiveness, biodegradability and safety to human health. The exact coagulation mechanisms involved with these natural polymers are likely to vary with the nature of the coagulant chemical. To select a suitable natural polymer for a given application and evaluate its coagulation performance, it is necessary to fully understand its properties, particularly its molecular weight, charge density, chemical structure and functional groups. In general, naturally occurring products used for coagulation are medium or high molecular weight polymers with high cationic charge, such as chitosan. Although the relative importance of “charge neutralisation” and “polymer bridging” during the coagulation process is still unclear, it is evident from previous observations that highly positive CD polymers tend to adsorb in a rather flat configuration, thus there is more opportunity for neutralising the negative charges on the surface of particles (43); and the most effective polymers for bridging are linear chains with high molecular weight (55). For a high MW polymer with high CD, the ‘charge neutralisation’ is the dominant coagulation mechanism for humic acid removal, and the absence of any effect of molecular weight on the degree of removal indicated that a ‘bridging’ mechanism is unlikely to play a major part in the process (18). Whilst natural polymers, such as chitosan, have been used as primary coagulants to treat particles or organic matter, it is difficult to determine a predominant mechanism due to their complicated properties (175-177). Therefore, some workers (16) have strongly

proposed that a detailed knowledge of the character and properties of natural polymers would be a significant step toward developing the study of coagulation mechanisms and further polymer selection.

In agreement with the general information supplied by the TBP manufacturer, the characterisation results described in Section 5, indicate that the TBP is a moderate-to-high molecular weight polymer ($\sim 600,000 \text{ g mol}^{-1}$), with approximately 1000-2000 repeating units, and a reasonably narrow molecular weight distribution. Thus, the cationic tannin based polymer is assumed to be as shown in Figure 10.1; the condensation polymerization is believed to occur at the 4- and 8-positions of the "A" and "C" ring, respectively (129).



CHR: the remainder of the aldehyde compound after the carbonyl oxygen has left.

R₁ and **R₂**: hydrogen or other organic moieties that were part of the original amino compound.

Figure.10.1 Proposed model structure for TBP

According to this model, the molecular weight of a repeating TBP unit is estimated to be approximately 300, and the cationic charge is represented by the amino group of the TBP.

From the literature review, it is understood that condensed tannins comprise a group of polyhydroxyflavan-3-ol oligomers and polymers linked by carbon-carbon bonds between flavanol subunits. Analysis of TBP is complicated by the diversity of structures found within the group of condensed tannins. According to the accepted principles of colloid science, systems are considered to exhibit colloidal properties when the dimensions of the dissolved or dispersed components (in hydrophilic or hydrophobic colloids, respectively) are in the range of 1 to 1000nm (178). As we have measured the “radius of gyration” of TBP to be around 78.4 (\pm 19.3) nm, a colloidal system containing TBP could be formed, depending on the chemical composition of the dissolved or dispersed components and on the molecular interactions with the solvent molecules.

It is well understood that the dissociation of acidic HA functional groups, such as carboxyl and phenolic groups, in aqueous media leads to the spontaneous formation of an electric double layer. Therefore, electrostatic interactions play the determining role in the conformational changes of humic macroions as well as in the colloidal stability of humic solutions and in the aggregation of the individual humic macroions (178). At high pH the functional groups are fully ionized, resulting in the highly water-soluble anion. These chemically linked charges endeavour to situate themselves as far apart as possible. In contrast, at low pH, humic molecules can accumulate in interfacial layers, without any repulsion from the charges. However, the explanation of HA precipitation is likely to be different to the behavior of TBP, which also includes phenolic groups. In this case a macromolecular solution is formed if TBP is dissolved in water at low pH and precipitation occurred at higher pH (>6). It is assumed that the charges in the electric double layer, caused by cationic amino groups, are mutually repelling at low pH values. The dissociation of the cationic group with increasing pH leads to TBP molecule accumulation. Further study of the chemistry of natural tannin found that tannin may offer the potential to reconstruct by nucleophilic reactions (179, 180). This is certainly true under basic conditions in the presence of oxygen,

both the extender unit and terminal unit of tannin (dependent on R group in Figure 2.6) are subject to rearrangement (180), which can then possibly undergo cross-link reactions between TBP molecules. Therefore, a higher degree of polymerization corresponds to lower solubility and greater resistance to degradation (181). These aspects supply some possible explanation for TBP precipitation, but the precise mechanisms linking TBP precipitation to pH are still considered to be far from straightforward.

The explanation of the ‘ageing effect’ by Shyluk and Stow (182), who proposed that the diminishing flocculation ability of polymers with time was associated with the disentangling of polymer chains, do not support the observation of TBP precipitation with time in this study. A reasonable assumption is that with an increasing time of exposure, a slow deprotonation process of the phenolic hydroxyl group present on TBP might cause an increase in anionicity of TBP, giving an inferior coagulation performance only by charge neutralization. However, this effect may not contribute to the observed flocculation extent with polymer bridging or precipitation of TBP. In overall terms, it can be concluded that TBP is substantially affected by hydrolysis/hydration processes which lead to changes in its charge density and solubility with solution time and pH.

Strong evidence of a non-quaternized amine group, possibly a tertiary amine group, was found from different characterization tests (Section 5). The positive charge density of TBP at low pH is believed to be due to the N^+ ion of its amine groups. However, by the deprotonation effect, the cationic TBP loses its positive charge with increasing pH values. The results of the coagulation experiments using TBP as a sole primary coagulant in this study (section 6) have clearly illustrated that the variation in positive charge density with pH is the major reason for the difference in optimum dosages of TBP. The greater the positive charge density of TBP, the less the dose required to neutralize the negative charge of the colloid. In contrast, a considerably greater dose was found

for TBP at relatively high pH corresponding to the polymer having weak or non-positive charge, indicating flocculation caused by ‘bridging’(58) or other mechanisms. In addition, it is clear from this work (Section 5) that at $\text{pH} \geq 6$, the degree of insolubility of TBP increased dramatically with increasing pH values, possibly caused by a low dissociation constant value (pK_a) of its amino functions. A relatively fast precipitation process of TBP, observed at higher pH (≥ 7), appeared to influence the coagulation process and performance by the enmeshment of precipitation.

It is well known that electrostatic interaction gives strong adsorption between negatively charged particles and cationic polyelectrolytes. Coagulation could occur by “charge neutralization” simply as a result of the reduced surface charge of the particles and hence a decreased electrical repulsion between them (19). From the results of the optimum TBP dosages for different concentrations of kaolin, there seemed to be a simple one-to-one charge interaction between negatively charged particles and the cationic TBP with a charge density of around 3 meq g^{-1} to 0.7 meq g^{-1} at low pH values (4 ~ 7). This is consistent with the conclusions of Gregory (45) and Narkis and Rebhun (83), that if charge neutralization is not a significant contribution to coagulation process then the stoichiometric interaction between the anionic sites of particles/ humic substances and the cationic charge of the polyelectrolytes might not exist. In contrast, the theoretical optimum dosage for polymer bridging corresponds to “half-surface coverage” of particles (61). However, Gregory (45) proposed that for adsorbed polymers, it is difficult to precisely define “surface coverage” and optimum flocculation usually occurs at well below monolayer coverage. Runkana *et al.* (62) found that theories of bridging flocculation assuming equilibrium conditions were of limited use in practice. Therefore, bridging interactions are likely to present a non-equilibrium flocculation. The observed behaviour of non-stoichiometry by TBP at high pH indicated that ‘bridging’ or the precipitate enmeshment mechanism was only likely to play a major part in the process when the TBP has

a low positive charge or non-charge under higher pH conditions. Higher aggregation rates and relatively larger flocs were found to occur under conditions corresponding to ‘bridging’ or ‘sweep flocculation’ rather than charge neutralization in this case. These observations could be explained by the fact that the production of Al(OH)_3 precipitate increased the effective particle concentration and hence increased the collision rate; hydroxide precipitates are quickly formed from large numbers of colloidal particles, and the aggregation of these small particles gives low-density flocs, with a relatively large volume (145). By understanding the chemical properties and structure of TBP, the interrelationship between charge density, solution pH and polymer dosage with its mechanism/performance of coagulation can be hypothesized. The loss of cationic charge (amine de-protonation) and solubility with pH in the typical pH range for water treatment (ie. pH 6-9) makes the behaviour of TBP similar to that of conventional aluminium salt coagulants. A description of the aluminium hydrolysis species and the solid precipitate domain as a function of pH can be found from the well-established aluminium solubility diagram (134). At pH 5.0 - 6.0, the dominant Al species has been identified as doubly- and singly-charged cationic species, leading to aggregation of particles by charge neutralization. At pH 6 and above, due mainly to the uncharged (weakly charged) metal hydroxide, Al(OH)_3 , the dominant coagulation mechanism is believed to be adsorption of particles on, and enmeshment, by precipitates (“sweep flocculation”). In the same way, at low pH (≤ 6) TBP is present as a moderate-to-high molecular weight, soluble cationic polyelectrolyte with a charge density of approximately 3 meq g^{-1} , which is able to destabilise kaolin suspensions by charge neutralisation. Under higher pH conditions ($\text{pH} > 6$), increasing degrees of polymer precipitation occurs leading to a decrease in soluble polymer concentration, a loss of cationic charge and probable changes in polymer configuration. The impact of these changes on coagulation performance is complex and likely to involve the well-established mechanisms of charge interactions (including “electrostatic patch” effects), polymer bridging, and colloid adsorption/enmeshment by solid phase TBP

hydrolysis products. Of importance to the first two mechanisms is the dependence of the polymer configuration (ie. chain length, cross-linkage and chain stiffness) on the solution chemistry. A summary of the proposed mechanisms with solution pH is given in Table 10.1.

TABLE 10.1 Characteristics and coagulation behaviour of TBP with kaolin

pH	Charge Density (meq g ⁻¹)	Optimum Dosage (mg l ⁻¹)	Flocculation Index (FI)	Turbidity Removal	Possible Mechanism
4	3.072	0.15	0.25	63.7%	Charge Neutralisation
5	2.662	0.25	0.32	53.7%	Charge Neutralisation
6	2.048	0.25	0.35	57.5%	Charge Neutralisation
7	0.666	0.3	0.52	67.5%	Charge Neutralisation and/or Polymer Bridging
8	0.256	12.5	1.6-1.8	70%	Polymer Bridging and/or Precipitate Enmeshment
9	0.205	14	2.3-2.5	72.5%	Polymer Bridging and/or Precipitate Enmeshment

To study the optimal coagulation performances of individual coagulants, the maximum Flocculation Index (as a surrogate for floc size) and strength factor (as a surrogate for floc strength) at the optimum dose were compared by the results determined from a Photometric Dispersion Analyser (PDA). At pH9, using both model waters containing particles (kaolin) and soluble organic matter (HA), considerably increased values of FI and strength factor were found, for polymer bridging, in comparison with the lower values of these two parameters as expected, for charge neutralisation with TBP at pH4 and 7. In comparison with two alternative coagulant chemicals, alum and polyDADMAC, the performance of the TBP in treating a kaolin suspension was inferior at neutral pH. For

polyDADMAC this is because it is a larger ($1 \times 10^6 \text{ g mol}^{-1}$) and more highly charged (6 meq g^{-1}) polymer, and its solubility is unaffected by solution time and pH. Thus, it is capable of producing large flocs through efficient charge neutralisation and polymer bridging. For alum at pH 7, the coagulation is effective through rapid adsorption/enmeshment by aluminium hydrolysis species and $\text{Al}(\text{OH})_3$ precipitates. Although the slow precipitation of TBP occurred at pH 7, the small amount of optimum dose may not produce enough enmeshment to effectively “sweep” all the particles in the solution. Therefore, the main coagulation mechanism of TBP at pH 7 is believed to be charge neutralization and/or polymer bridging. However, in higher solution pH conditions the coagulation performance of TBP appears to improve substantially, albeit with a greater dose required, and at pH 9 it was arguably superior to the other coagulants.

It is clear that “polymer bridging” is dependent on the adsorption of polymer segments on to colloidal particles. When a long-chain polymer comes into contact with a colloid particle, some of its active groups adsorb on to the particle surface, while the rest of the segment of the macromolecule stretches out from the surface into the solution as “loops” and “tails” to adsorb the other particle. In general, the types of adsorption interaction between the polymer and particle include electrostatic interaction, hydrogen bonding, hydrophobic bonding and ion binding. In practice, the possibilities of these interactions are dependent on the properties of the polymer and particle. In this case, at pH 9, a fair proportion of TBP segments are believed to remain unattached and are available for adsorption on other kaolin or HA particles. These particles then aggregate to form flocs. “Bridging” will occur when the adsorbed chains interact with another floc in the same way. Since TBP has a very weak charge at pH 9, hydrophobic bonding and hydrogen bonding are believed to be important in considering the affinity of segments for particle surfaces. The observation of stronger flocs by the TBP at pH9 and by polyDADMAC in comparison with alum is matched by the

conclusion of Yukselen and Gregory (101), who proposed that the flocs produced by bridging flocculation can be much larger and stronger than those formed when particles are ionically destabilized by the charge neutralization of salts. Unlike polyDADMAC which is a quaternary ammonium polymer and produces destabilization of colloids as a result of charge neutralization and polymer bridging, the action of TBP partially relies on its relative insolubility at pH values higher than its isoelectric point (where the net charge on the polymer is close to zero), which causes TBP to self-flocculate and sweep up other suspended particles into the floc volume. This phenomenon is thought to be similar to the precipitate enmeshment or 'sweep flocculation' mechanism of hydroxide precipitate when alum is used as primary coagulant. The cross-linkage by TBP precipitate probably enhances the strength of bonds between particles.

The main advantage of combining polymers with inorganic coagulants is a consequent decrease in the inorganic coagulant dosage, leading to a decrease in the generation of dry sludge, while achieving either an equivalent coagulation performance or better performance. This has been clearly demonstrated by the works of Filho *et al.* (105) for ferric sulphate with a cationic polymer. The results from different model waters in this study (Section 6) have consistently shown a substantial reduction in the dose of alum with a significant improvement of coagulation effectiveness by the combination of alum/TBP. In mechanistic terms, charge neutralisation appears to be a more important factor than polymer bridging for the combination of coagulants at low pH for particle suspensions. This would be expected to lead to an inversely quantitative relationship between alum and TBP dosages (Figure 7.16). Notwithstanding a similar complementary relationship between alum and TBP dosages at $\text{pH} > 6$, the values in this case were found to be non proportional. This is not surprising, since the dominant flocculation mechanism of alum at $\text{pH} > 6$ was believed to be adsorption of particles on to and within precipitated $\text{Al}(\text{OH})_3$, known generally as 'sweep flocculation' (134). For model water with a turbidity of 70 NTU, Kawamura (3)

found that the addition of chitosan with alum would allow a 20% reduction of alum as a coagulant alone with a small improvement of turbidity removal. The optimum Al/chitosan dose ratio was suggested as 0.70/0.05mg (assumed the alum as $\text{Al}_2(\text{SO}_4)_3 \cdot 14\text{H}_2\text{O}$). In our study, for a turbidity water at 40 NTU, the optimum Al/TBP dose ratio was identified as 0.05/0.06 mg/mg, suggesting that the addition of TBP with alum allowed a 75% reduction of aluminium coagulant (as sole coagulant) with a small change of turbidity removal. It is seemed that TBP was more efficient to replace alum when used as dual coagulant, compared with chitosan. For HA solutions at pH 6, a superior performance and less dose were achieved with the dual coagulant (alum-TBP combination), compared to the commercial product TSL; however, both of them presented a higher floc volume compared with alum as coagulant alone. The findings from this investigation indicated that the precipitation of TBP at neutral and high pH produced a significant amount of sludge, which may remove the advantage of alum replacement by polymer in terms of sludge reduction.

In the results presented in this study, there is some doubt about the locus of optimal alum/TBP combinations (Figure 7.34) at a relatively high concentration of humic substances (30 mg l^{-1} HA). The precise reason for the constant trend of the TBP dose with increasing alum is not obvious. The most likely explanation for this trend was that for a high concentration of humic acids, a large dosage of TBP combined with a small dose of alum gave charge neutralisation and restabilisation at pH 6; further increasing the dose of alum only gave an opportunity to produce a large amount of hydroxide precipitate. Therefore, sweep flocculation played a predominant role in the flocculation process, and reduced the impact of charge neutralisation effects by TBP. Thus, the locus line levels off, and the TBP dose has a constant value (30 mg l^{-1}) as the alum dose increases. In practice, due to the precipitation of alum and/or TBP, a rather wide range of alum/TBP dose combinations gave a coagulation performance close to the optimum (indicated by the similar FI values). In Figure

10.2, the original Figure 7.34 has been modified to include the locii of dose combinations corresponding to 75% of FI_{max} , for the two levels of HA; this is taken to be a range of good coagulation. The purpose of this is to show the sensitivity of the peak coagulation performance to the coagulant dose combinations.

At the lower level of HA, the locii are consistent and cover a narrow range of dose variation corresponding to good coagulation. At the higher level of HA, there is a wide range of dose combinations between the “upper limit” and “lower limit” locii. It is interesting to note that while the optimum dose locus (FI_{max}) indicated a constant TBP dose for $Al > 0.5 \text{ mg l}^{-1}$, the upper limit and lower limit locii displayed an inverse trend, or dose complementarity, as might be expected for a coagulation mechanism based on charge neutralisation. The departure from a simple inverse dose trend for the optimum dose locus may be a consequence of the broad range of alum-TBP dose combinations giving good coagulation and the imprecision in defining the optimum dose.

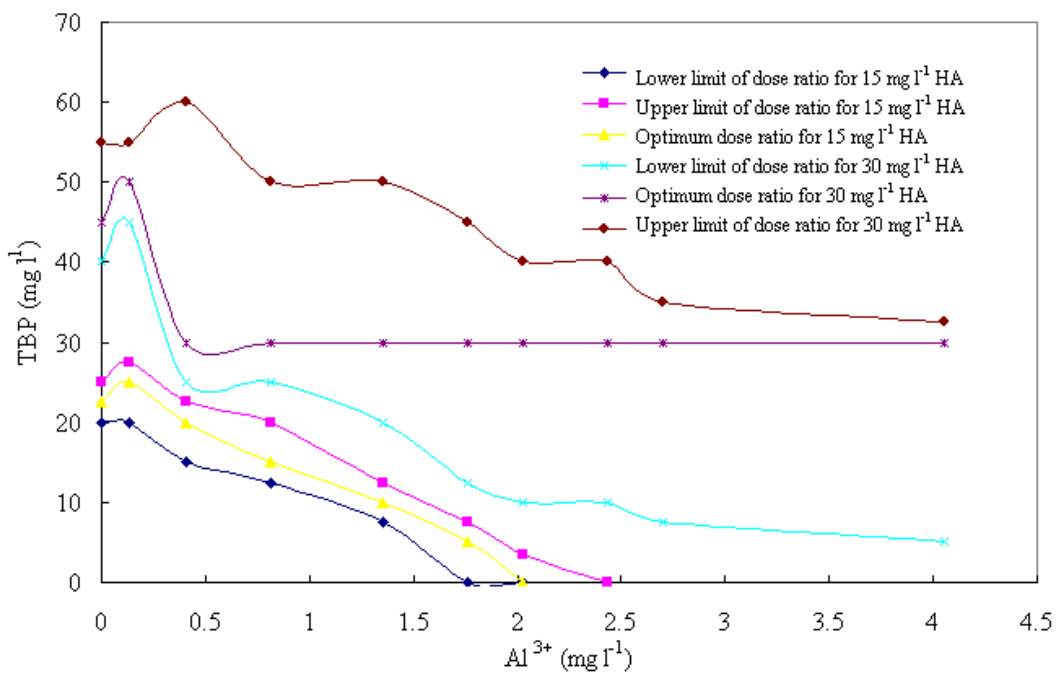


Figure 10.2 Locii of alum-TBP dose combinations for FI_{max} (optimum) and 0.75 FI_{max} with HA at two concentrations at pH 6

The distinct improvement of coagulation efficiency by the combination of alum and TBP using as the primary coagulant (Section 7) is consistent with that reported by Bolto *et al.* (6) and Edzwald *et al.* (7). Compared with a sole coagulant, the combination of coagulants gave the benefits of more rapid kinetics of floc growth and larger floc size (indicated by Flocculation Index) suggesting an advantage in the use of the two coagulants. However, the presence of residual polymer as a consequence of the use of TBP inevitably increases the value of the final NPDOC in treated water, which may not be desirable.

Polyelectrolytes are known to produce stronger flocs than inorganic coagulants (101). Some researchers (183) have indicated that polyelectrolytes of a medium charge density and very high molecular weight were the optimum for the production of strong flocs. Leentvaar and Rebhun (184) using ferric chloride for water treatment found that a coagulant aid lead to stronger floc than coagulation-flocculation without polymer addition. In this study, the combination of TBP with alum caused a considerable increase in floc strength as indicated by the calculated strength factor, compared to TBP as sole coagulant. The effect of addition sequence on TBP/alum performance was not investigated in this research. However, a previous study (185) using a cationic polymer with ferric inorganic coagulant to coagulate clay suspensions, indicated that simultaneous addition of coagulants produced higher flocculation index values, as well as higher strength of flocs than the flocs formed when other addition sequences were used. There have been previous reports of the irreversible nature of floc breakage in the case of hydrolyzing coagulants and polymeric flocculants, due to “sweep flocculation” and “bridging interactions”, respectively (101). For TBP and the TBP-alum combination used as coagulants at pH6 or 7, it was noticeable that only limited re-growth of flocs occurred indicating a significant irreversibility of the floc break-up process. It was supposed that high shear rates may cause scission of TBP cross-linkage chains, and adsorbed polymer could adopt a more flat configuration during the breakage phase, and the reformed flocs may have a more

compact structure than that before breakage (101).

Whilst in general agreement with the performance observed in model waters, the improvement of coagulation effectiveness of alum combined with cationic TBP appeared to be substantially greater in real water (Section 9). The real water test with an initial NPDOC of approximately 3.7 mg l⁻¹ (Section 9) presented a similar trend in the locus line of alum/TBP doses as the result from the model water containing an equivalent NPDOC concentration of approximately 4.0 mg l⁻¹ (Section 7). The strong complementary relationship between TBP and alum dose for the real water supports the conclusion from the model water that at pH6, the coagulation mechanism of the alum-TBP combination is predominantly charge neutralization. The results of the coagulation experiments using both waters with similar NPDOC content can be compared by considering the optimum dose of coagulants and the removal of NPDOC; these are summarized in Table 10.2.

TABLE 10.2 Optimum dose of coagulants and treatment effectiveness from real water and model water

	NPDOC (mg l ⁻¹)	TBP dose (mg l ⁻¹)	Al ³⁺ dosage (mg l ⁻¹)	Ratio of Al/TBP (mg l ⁻¹ /mg l ⁻¹)	Al Reduction %	Colour Removal %
Model water	4.0	22.5	2.03	0.14/25	93.35	96
Real water	3.7	25	4.1	0.27/25	93.41	93

Using the optimal combination of TBP and alum as coagulants, the good coagulation efficiency observed for the real water is in agreement with other reported findings. Lee *et al.* (106) and Filho (105) have all demonstrated that both cationic polyamine and polyDADMAC combined with metal salts were effective as coagulants to treat river water; and enabled a reduction of the consumption of

inorganic coagulants. In this study, the results of the model water tests agreed very well with the coagulation behaviour observed with the real water using the dual coagulant of alum/TBP. However, it is worth noting that the values of NPDOC in the final treated real water do not vary substantially for the different TBP/alum combinations. Thus the removal of natural organic matter (NOM) by coagulation alone was largely insensitive to the dose. Although total NOM is similar in the final water, there may be differences in NOM fractions, and some NOM fractions are probably unable to be coagulated by TBP. This is consistent with the observation by Bolto *et al.* (6) that high MW polymers were effective to remove NOM from water and the more hydrophobic NOM fractions were more easily removed.

A preliminary two-stage (sedimentation/filtration) pilot scale investigation of the performance of TBP has been undertaken by WRc (Swindon, UK) using a “hard” (high alkalinity), lowland surface water (River Thames) (186). The results of the pilot-scale tests were contradictory to the coagulation effectiveness at bench scale when the TBP was observed in comparison with PACl. The inferior performance of TBP in pilot scale tests, in contrast to that in bench-scale tests, was speculated to be due to a slower floc formation with TBP preventing a floc blanket to form in the clarifier during the plant run; this causes either the TBP-dosed water to be inadequately flocculated or small flocs to pass through the clarifier without separation. Thus, from a practical standpoint, TBP may not be an appropriate coagulant for floc blanket clarification (FBC). However, TBP may be effective for dissolved air flotation (DAF) or could be applied to direct filtration processes.

The use of a “solid bound TBP” method (in Section 8) permits the attachment of appropriate quantities of TBP on the surface of inert sands in order to minimize the residual soluble polymer in the final water, and may enhance the coagulation performance. Such a method which pre-determines the adsorption

ratio of cationic-charged TBP (at low pH) by negatively charged sand grains has been found in this study to be moderately successful for the coagulation of a given concentration of humic substances, and to the reduction of the residual TBP in the treated water. A significantly faster settlement within several seconds, as the other benefit of “solid bound TBP”, has been observed in the coagulation processes. However, more research effort is required for this application in order to avoid the breakage of forming flocs from a rather high mixing speed, which was applied to keep the “solid bound TBP” suspended in water. The mechanism of this method is based on the interaction between the polymer and particles whereby some of the polymer’s segments are attached to the sand surfaces and the “loops” and “tails” of the polymer are available to adsorb the particles in solution. In contrast, polyDADMAC, which has a high charge density at pH6, is believed to adsorb via a rather flat configuration which leads to little opportunity for bridging interaction with sand. It is hypothesized that a polymer with low or non charge density, such as TBP, is the optimum for this application.

In overall terms, as a primary coagulant for water treatment, TBP has been found to be capable of effectively removing turbidity, colour and DOC. The large flocs formed by this medium to high molecular weight polymer under optimal conditions could give an accelerated rate of floc sedimentation prior to the subsequent filtration process. Even though pre-adjustment of the pH is still required, it can be concluded that TBP can be used over a wide range of pH. Unlike synthetic polymers, the coagulation performance of TBP has been shown to improve with the pH, although greater optimal doses are required. In considering the usual range of natural water pH (say, 5-9), the TBP would be a workable substitute for synthetic polymer or metal coagulants in the pH 8-9 range, partly as a result of its diminishing solubility with pH. At $\text{pH} \leq 7$, the results suggested that the performance of TBP was inferior to other coagulants. To minimize these drawbacks, TBP combined with alum has been investigated extensively in this study. It is clear that the application of the dual coagulant

dramatically improves the coagulation performance at $\text{pH} \geq 6$ in both model water and real water. However, at pH 5, the coagulation performance is still similar to that of using alum as coagulant alone. There are still two aspects of concern, which will need to be evaluated further; these are any potential toxicity and increased sludge volumes, which may affect the practical application of this novel polymer. With the latter, it is generally recognised that alum forms rather weak flocs and produces significant amounts of sludge. However, the results from this study show that less strong and larger floc volumes were produced by TBP alone and TBP/alum combinations in real surface water at pH6, compared with alum as a sole coagulant. These effects may complicate the subsequent filtration (eg. more rapid clogging) and disposal procedures after coagulation. It is important to determine the residual TBP in the product water, and thus the presence of any impurities in the TBP (and chlorinated TBP) that may reach the consumers. To date, there is still no satisfactory method to effectively measure the amount of residual polymers in treated water. A toxicological evaluation of TBP and TBP coagulation sludge has been undertaken by São Paulo University (187). The results of an autopsy accomplished with a test animal did not reveal any signs of alteration in the viscera, and the tested sludge sample did not present acute toxicity for *Hialella azteca*. The toxicity of TBP needs to be studied further to meet the stringent limits of drinking water before it can be used as coagulant in the UK.

The UK is probably the largest user of coagulants for water treatment in the European Community because of the proportion of the supply that is derived from surface water (137). The increasing price and demand for inorganic coagulants and the growing interest in polymers presents a potential opportunity for TBP in the water and wastewater treatment field, particularly because of its value as a naturally-derived product. For example, the greater bio-degradability of the resultant sludge from TBP (187) could improve the acceptability of waste sludge for disposal to agriculture.

11. CONCLUSIONS

- (1) This study has investigated extensively the nature and performance of a new, natural cationic polymer for use in water treatment.
- (2) TBP (a tannin-based polymer), as a ‘Mannich’ polymer, can be classified as a medium-to high molecular weight polymer with a mean molecular weight of $5.7 (\pm 2.8) \times 10^5 \text{ g mol}^{-1}$, based on the light scattering method; the charge density of cationic TBP varied with pH and time (max $\sim 3.1 \text{ meq g}^{-1}$), based on colloid titration method.
- (3) A semi-quantitative identification of TBP predicted that the cationic function group of monomer was a non-quaternized amine, believed to be the tertiary amine group, R_3NH^+ , as suggested by infra-red and NMR spectra. The presence of the tertiary amine gave a variable charge density and possibly was a cause of precipitation in solution due to the deprotonation of amine groups, with pH.
- (4) A consistent trend of increased TBP optimum dose with increase of pH values was found for both model waters involving suspension particles and humic substances. This phenomenon was directly linked to the observation of the diminishing charge density with increasing pH.
- (5) The mechanism of coagulation by TBP is closely related to the chemistry of TBP in aqueous solution and depends strongly on pH values.

- (6) Two important coagulation mechanisms of cationic synthetic polymers, charge neutralisation and polymer bridging, were believed to be important in the coagulation actions of TBP. However, the precipitation of TBP was also proposed to cause “sweep coagulation”. The predominance of these different mechanisms was considered to be strongly dependent upon pH values. A dose stoichiometry can be appreciable at an acid or neutral pH, and hence the predominance of charge interaction as the mechanism of coagulation was proposed under these conditions. In contrast, there was no dose stoichiometry under alkali pH conditions, suggesting polymer bridging or precipitation enmeshment to be the dominant mechanism at this elevated pH value.
- (7) The comparative coagulation effectiveness of alum, polyDADMAC and TBP were measured in terms of Flocculation Index, the turbidity reduction for particle suspensions, the NPDOC removal in HA water and floc strength, under certain similar conditions. A larger and stronger floc was achieved by the effect of ‘polymer bridging’ or precipitation enmeshment of TBP at high pH value.
- (8) Evidence from coagulation experiments with kaolin suspensions suggested that the coagulation performance and kinetics at optimal TBP dosages were considerably influenced by factors such as the polymer age, mixing speed and reactor design, apart from pH and the concentration of particles. The apparent diminution of the peak flocculation index at low pH for ‘ageing’ TBP was thought to be the consequence of changes in the deprotonation of the charge group with time.

- (9) By studying the coagulation of kaolin suspension with combinations of alum and TBP at different pH values, the interrelationship between coagulation effectiveness and the ratio of optimum alum/TBP dosages represented different coagulation mechanisms (charge neutralization and/or sweep flocculation), which influence the amount of coagulants used. However, the reduction of alum and the improvement in coagulation performance through the combination of alum with TBP were consistently significant.
- (10) The locii of the alum-polymer dosages for optimal coagulation performance were achieved with two model waters at different concentrations of humic acid. A unique optimal dosage of combined alum and TBP that maximizes the coagulation performance can be easily determined by these locii with the colour removal. The results from these experiments validated the benefit of the dual coagulants in the reduction of alum requirement and the improvement of coagulation effectiveness.
- (11) A moderate adsorption was found by attaching the TBP to an inert solid (fine sand) at low pH. The optimal adsorption ratio was determined by determining the residual polymer indirectly by UV absorbance at the maximum absorption wavelength of TBP solution (210nm). Through this modified 'solid bound TBP' method, it was assumed to be possible to achieve a low residual TBP in final water. Experimental evidence suggested that some degree of coagulation performance (HA removal) was achieved, but this was significantly lower than that achieved with an optimal dose of solution phase TBP.
- (12) Good agreement was found in the coagulation performance of cationic TBP, for the simulated water and samples of lowland coloured real water under

equivalent conditions. A relatively high dose (15 mg l⁻¹-20 mg l⁻¹) of TBP gave a good performance of colour and turbidity removal, but less so in terms of NPDOC removal.

- (13) The use of the PDA instrument was found to be a sensitive and reliable method to monitor coagulation performance. The optimum dosage of alum for a wide range of pH values were determined by the PDA method, and found to be consistent with previous findings by other methods.
- (14) It is suggested that the observed locus line of the optimum TBP-alum dose combinations for real water from an organic-rich river source was broadly consistent with the experimental results for the model water with the similar concentration of NPDOC at the same pH. The results indicate that significant opportunities exist for making a substantial reduction of alum and the improvement of coagulation performance by using the combination of alum/TBP as a primary coagulant in real water.
- (15) The results of the tests indicated that the floc strength of TBP under “charge neutralization” conditions was weaker than under “bridging” conditions. The aggregates formed by the combined alum/TBP under “charge neutralization” conditions appeared to be more resistant to breakage than those formed by TBP alone.
- (16) The colorimetric method, 5550B (18th Edition 1992), was approved to be feasible for the determination of tannin acid in solution, but its suitability for determining residual TBP remains in doubt. With the (uncertain) assumption that it can be applied to the measurement of TBP, the results in this study

suggested that low concentrations of TBP ($<1.5 \text{ mg l}^{-1}$) remained in the final water using optimal doses of TBP or TBP/alum as coagulants for the model water and real water.

12. SUGGESTED FUTURE WORK

Topics for further investigation and development towards achieving a better understanding and the improved use of TBP are as follows:

1. It is the case that all the characterisation data obtained so far have not been able to provide an unambiguous description of the polymer, or monomer, structure. This remains an important objective and an opportunity arises in the future to apply new techniques to achieve this. A MALDI-TOF mass spectrum method could be considered to give valuable information about molecular weight distribution, end groups, and the oligomer repeating unit.
2. The nature of the coagulation mechanism of TBP (and cationic polymers in general) with humic substances is still uncertain; particularly, the effect of polymer molecular weight on the removal of NOM fractions. Further insight could be obtained by analysing the coagulation performance and fundamental behaviour of the hydrophobic and /or hydrophilic fractions of humic acid with TBP. To do this, NOM can be fractionated by resin adsorption and coagulation tests can be carried out using different fractions.
3. Attention has been given principally to the coagulation mechanism and behaviour of TBP as a primary coagulant in this study. Further investigation is necessary to evaluate in detail the nature of the flocs produced from the optimal coagulant combinations (eg. size, density, charge and settling velocity) to understand the fundamental mechanisms giving rise to good treatment performance and the specific contribution of the polymer.
4. There is still no adequate method to effectively measure accurately the concentration of residual polymer in treated water. In this work, the application of

a colorimetric method, which proved to be feasible for the determination of tannin acid in solution, is not suitable or accurate for the measurement of TBP. The possibility of chemically labeling the polymer (eg. by fluorescence) could be undertaken for determining residual TBP in the future. The potential formation of disinfection by-product (DBPs) from chlorine reactions with residual TBP would also be a valuable topic of further work.

5. One potential application for TBP is as a filter aid applied to direct filtration processes, due to a slow and less voluminous floc formation process, compared to inorganic metal salts. This remains an important objective and a future investigation might consider whether direct filtration could be improved by partially or totally replacing alum with cationic TBP. A full matrix of coagulant doses could be examined in order to identify optimal combinations of coagulant doses giving the best filter performance and least volume of sludge solids in both bench-and pilot-scale filter tests.

6. The role and use of TBP for sewage or waste water treatment have not been studied adequately elsewhere in applications where it can be compared with traditional metal coagulant and synthetic polymeric coagulant. For example, TBP might be effective in the removal of phosphorus – this is an important subject worthy of future investigation.

13. REFERENCES

1. Bolto, B. (1995) Soluble polymers in water purification. *Progress in Polymer Science*. Vol. 20, 987-1041.
2. Amirtharajah, A. and C. R. O'Melia. (1990) Coagulation Processes: Destabilization, Mixing and Flocculation. in *Water Quality and Treatment*, 4th ed., F. W. Pontius, ed., McGrawHill, Toronto, pp. 269-365.
3. Kawamura, S. (1991) Effectiveness of natural polyelectrolytes in water treatment. *Journal of American Water Works Association*. Vol.83, 88-91.
4. Huang, C.P. and Chen, Y. (1996) Coagulation of colloidal particles in water by chitosan. *J. Chemical Technology and Biotechnology*. Vol. 66, 227-232.
5. Tang, H. and Shi, B. (2002) The characteristics of composite flocculants synthesized with inorganic polyaluminum and organic polymers. *Chemical Water and Wastewater Treatment VII*, H.H.Hahn, E.Hoffmann, H.ØDEGAARD (Eds.) IWA Publishing, London. 17-28.
6. Bolto, B., Abbt-Braun, G., Dixon, D., Eldridge, R., Frimmel, F., Hesse, S., King, S.J. and Toifl, M. (1999) Experimental evaluation of cationic polyelectrolytes for removing natural organic matter from water. *Water Science and Technology*. Vol.40, 71-79.
7. Edzwald, J.K., Haff, J. D. and Boak, J. W. (1977) Polymer coagulation of humic-acid waters. *J. Environmental Engineering DIV ASCE* Vol.103, 989-1000.
8. Reed, P.E. and Finck, M.R. (1997) Modified tannin mannich polymers.

United States Patent No.5,659,002. 19 August.

9. Mallevalle, J., Bruchet, A. and Fiessinger, F. (1984) How safe are organic polymers in water treatment? Journal of American Water Works Association. Vol.76, 87-93.
10. Hutchison, P.R. and Healy, T.W. (1990) Surface and Colloid Chemistry in Natural Water and Water Treatment. Plenum Press, New York.
11. Lee, J. F., Liao, P.M., Tseng, D.H. and Wen, P.T. (1998) Behavior of organic polymers in drinking water purification. Chemosphere. Vol.37, 1045-1061.
12. Schwoyer, W.L.K. (1981) Polyelectrolytes for Water and Wastewater Treatment. CRC Press Inc, Florida.
13. Napper, D.H. (1983) Polymeric Stabilization of Colloidal Dispersions. Academic Press, London.
14. Hiemenz, P.C. and Rajagopalan, R. (1997) Principles of Colloid and Surface Chemistry. Dekker, NewYork
15. Dentel, S.K., Abu-Orf, M. M. and Griskowitz, N.J. (1993) Guidance Manual for Polymer Selection in Wastewater Treatment Plants. Water Evt. Research Foundation, Alexandria, Va.
16. Ghosh, M.M., Cox, C.D. and Prakash, T.M. (1985) Polyelectrolyte selection for water treatment. Journal of American Water Works Association. Vol.77,67-73.

17. Wakeman, R.J. and Tarleton, E.S.(1999) FILTRATION: equipment selection, modelling, and process simulation. Elsevier Science Ltd, New York.
18. Kam, S.K. and Gregory, J. (2001) The interaction of humic substances with cationic polyelectrolytes. *Water Research*, Vol.35, 3357-3566.
19. Bolto, B. and Gregory, J. (2007) Review: organic polyelectrolytes in water treatment. *Water Research*, Vol.41, 2301-2324.
20. Ebeling, J.M., Rishel, K. L. and Sibrell, P.L. (2003) Screening and evaluation of polymers as flocculation aids for the treatment of aquacultural effluents. *Aquacultural Engineering*. Vol.29, 23-42.
21. Graham, N.J.D. (1982) Significance of Filter Pore Particle Flocculation in Direct Filtration. PhD Thesis. Imperial College London.
22. Dentel, S.K., Gucciardi, B. M., Griskowitz, N. J., Chang, L.L., Raudenbush, D.L. and Arican, B. (2000) Chemistry, Function, and Fate of Acrylamide-Based Polymers. 9th Gothenburg Symposium, Istanbul.
23. Chio, J.H., Shin, W.S., Lee, S.H., Joo, D.J., Lee, J.D., Choi, S.J. and Park, L.S. (2001) Application of synthetic polyamine flocculations for dye wastewater treatment. *Separation Science and Technology* Vol.36, 2945-2958.
24. Bailey, K.J. and Jackson, P. J. (1992) Determination of residual polyelectrolyte in water. WRC Report number UM 1370 December.
25. Mangravite, F.J. (1983) Synthesis and properties of polymers in water

treatment. WRc Report Number 83-08.

26. Kawamura, S. (1959) Effectiveness of various types of flocculation aids on alum flocculation, parts 1,2 and 3. J. Japan Water Works Association, 299:6 (Aug.1959), 302:10 (Nov.1959), and 303:34 (Dec.1959).
27. Rinaudo, M. (2006) Chitin and chitosan: properties and applications. Progress in Polymer Science. Vol.31,603-632.
28. Huang, C.P., Chen, S. H. and Pan, J.R. (2000) Technical Note: Optimal condition for modification of chitosan: a biopolymer for coagulation of colloidal particles. Water Research. Vol.34, 1057-1062.
29. Guibal, E. and Roussy, J. (2007) Coagulation and flocculation of dye-containing solutions using a biopolymer (chitosan). Reactive & Functional Polymer. Vol.67, 33-42
30. Kvinnesland, T. and Odegaard, H. (2004) The effects of polymer characteristics on nano particle separation in humic substances removal by cationic polymer coagulation. Water Science and Technology. Vol.50, 185-191.
31. Bolto, B., Dixon, D., Eldridge, R. and King, S. (2001) Cationic polymer and clay or metal oxide combinations for natural organic matter removal. Water Research. Vol.35, 2669-2676.
32. Divakaran, R. and Pillai, V. N. S. (2004) Mechanism of kaolinite and titanium dioxide flocculation using chitosan-assistance by fulvic acids. Water Research. Vol.38, 2135-2143.

33. Fanta, G. C., Burr, R.C., Doane, M.M. and Russell, C.R. (1972) Graft copolymers of starch with mixtures of acrylamide and the nitric acid salt of dimethylaminoethyl methacrylate. *J. Applied Polymer Science*.Vol.16, 2835-2845.
34. Jarnstrom, L., Lason, L. and Rigdahl, M. (1995) Flocculation in Kaolin Suspensions Induced by Modified Starches .1. Cationically Modified Starch - Effects of Temperature and Ionic-Strength. *Colloids and Surface A: Physicochem. Eng. Aspects*. Vol.10, 191-205.
35. Nystrom.,R., Backfolk, K., Rosenholm, J.B. and Nurmi. K. (2003) Flocculation of calcite dispersions induced by the adsorption of highly cationic starch. *Colloids and Surfaces A: Physicochem. Eng. Aspects* Vol .219, 55-66.
36. Sableviciene, D., Klimaviciute, R., Bendoraitiene, J. and Zemaitaitis, A. (2005) Flocculation properties of high-substituted cationic starches. *Colloids and Surface A: Physicochem. Eng. Aspects* Vol. 259, 23-30.
37. Pal, S. Mal, D. and Singh, R. P. (2006) Synthesis, characterization and flocculation characteristics of cationic glycogen: a novel polymeric flocculant. *Colloids and Surface A: Physicochem. Eng. Aspects* Vol. 289, 193-199.
38. McKague, A.B. (1974) Flocculating agents derived from Kraft lignin. *J. Applied Chemical Biotechnology*. Vol.24, 607-615.
39. Ndabigengesere, A., Narasiah, K.S. and Talbot, B.G. (1995) Active agents and mechanism of coagulation of turbid water using moringa oleifera. *Water Research*, Vol.29, 703-710.

40. Deryagin, B.V. and Landau, L.D. (1941) Theory of the stability of strongly charged lyophobic sols and of the adhesion of strongly charged particles in solutions of electrolytes. *Acta Physicochim, URSS*, Vol.14, 633.
41. Verwey, E.J.W. and Overbeek, J.Th. G. (1948) Theory of the stability of lyophobic colloids. Elsevier, Amsterdam.
42. Ravina, L. (1993) Everything you want to know about coagulation and flocculation. Zeta-Meter, Inc. USA.
43. Gregory, J. (1975) The effect of cationic polymers on the colloidal stability of latex particles. *J. Colloid and Interface Science*. Vol.55, 35-44.
44. Higgins, J.M. (1999) Monitoring of polyelectrolytes in waters, process streams and the environment. PhD Thesis. Imperial College London.
45. Gregory, J. (1978) Effects of polymers on colloid stability, *The Scientific Basis of Flocculation* (Edited by Ives, K.J) NATO ASI Series. Sijthoff&Noordhoff, Alphen a/d Rijn, Netherlands.
46. Krozel, J.W. (1993) Electrokinetic interactions between two spheres: the role of surface charge transport in coagulation. *J. Colloid and Interface Science*. Vol.163, 437-453.
47. Zhang, J, W. and Buffle, J. (1995) Kinetics of hematite aggregation by polyacrylic acid: importance of charge neutralization. *J. Colloid and Interface Science*. Vol.174, 500-509.
48. Jiang, J.Q. (1995) Development and performance of polyferric sulphate as a coagulant in water treatment. PhD thesis. Imperial College London.

49. Sezaki, T., Hubbe, M.A., Heitmann, J.A., Argyropoulos, D.S. and Wang, X.W. (2006) Colloidal effects of acrylamide polyampholytes Part 1. Electrokinetic behaviour. *Colloids and Surface A: Physicochem Eng. Aspects* 281, 74-81.
50. Gregory, J., and Nelson, D.W.(1986) Monitoring of aggregates in flowing suspensions. *Colloids and Surface*. Vol.18, 175-188.
51. Gregory, J. (1973) Rates of flocculation of latex particles by cationic Polymers. *J. Colloid Interface Science*. Vol.42, 448-456.
52. Gregory, J. (1978) *Chemistry and Technology of water soluble polymer*.; Edited by Finch, C.A. Publisher Plenum Press. Chapter 18. polymeric Flocculants.pp.307-313.
53. Kozlova, N. and Santore, M.M. (2006) Manipulation of micrometer-scale adhesion by tuning nanometer-scale features. *Langmuir*, Vol.22,1135-1142.
54. Ruehrwein, R.A. and Ward, D.W. (1952) Mechanism of clay aggregation by polyelectrolytes. *Soil Science*. Vol.73, 485-492.
55. Caskey, J. A. and Primus, R. J. (1986) The effect of anionic polyacrylamide molecular-conformation and configuration on flocculation effectiveness. *Environmental Progress*. Vol. 5, 98-103.
56. Williams, P.A. (1982) The relationship between polyelectrolyte configuration and colloid stability. The effect of polymer on dispersion properties (Th.F.Tadros, editor).Academic Press, London.

57. Yu, J.F., Wang, D.S., Ge, X.P., Yan, M.Q. and Yang, M. (2006) Flocculation of kaolin particles by two typical polyelectrolytes: A comparative study on the kinetics and floc structures. *Colloids and Surface A: Physicochem.Eng.Aspects*. Vol.290, 288-294.
58. Ferretti, R., Zhang, J.W. and Buffle, J. (1997) Kinetics of hematite aggregation by polyacrylic acid: effect of polymer molecular weights. *Colloids and surface A: Physicochem.Eng. Aspects* Vol.121, 203-215.
59. Chen, L., Chen, D. and Wu, C. (2003) A new approach for the flocculation mechanism of chitosan. *J. Polymers and Environment*. Vol.11, 87-92.
60. Roussy, J., Vooren, M.V., Dempsey, B. A, and Guibal, E. (2005) Influence of chitosan characteristics on the coagulation and the flocculation of bentonite suspensions. *Water Research*. Vol.39, 3247-3258.
61. La Mer, V.K. and Healy, T. W. (1963) Adsorption flocculation reactions of macromolecules at the solid-liquid interface. *Pure and Applied Chemistry*. Vol.13,122.
62. Runkana,V., Somasundaran, P. and Kapur, P. C. (2006) A population balance model for flocculation of colloidal suspensions by polymer bridging. *Chemical Engineering Science*. Vol. 61,182-191.
63. Bolto, B., Dixon, D., Eldridge, R. and King, S. j. (1998) The use of cationic polymers as primary coagulants in water treatment. In:Hahn,H.H.,Hoffmann,E., Odegaard,H. (Eds.), *Proceedings of the Fifth Gothenburg Symposium. Chemical Water and Wastewater Treatment*.

Berlin, Springer, pp.173-182.

64. Graham, N. (1980) Orthokinetic flocculation rates for amorphous silica microspheres with cationic polyelectrolytes. *Colloids and Surface*, Vol.3, 61-77.
65. Crompton, T.R. (1993) *Practical polymer analysis*. Plenum Press, New York.
66. Fler, G. J. (1971) *Polymer adsorption and its effect on colloidal stability*. PhD Thesis. Agricultural University, Wageningen, The Netherlands.
67. Gregory, J. (1982) Polymer flocculation in flowing dispersions, in *The Effect of Polymers on Dispersion Properties* (Edited by Tadros, T.F.). Academic Press, London.
68. Von Smoluchowski, M. (1917) Versuch Einer Mathematischen Theorie der Koagulations Kinetic Kolloider Losungen. *Phys. Chem.* Vol.92, 129.
69. Gregory, J. (1988) Polymer adsorption and flocculation in sheared suspensions. *Colloids and Surface*. Vol.31, 231-253.
70. Pelssers, E.G.M., Stuart, M.A.C. and Fler, G.J. (1990) Kinetics of bridging flocculation-role of relaxations in the polymer layer. *J.Chem.Soc.—Faraday Trans.* Vol.86, 1355-1361.
71. Gill, R.I.S., and Herrington, T.M. (1989) The effect of colloid concentration and pH on kaolin suspensions flocculated with cationic polyacrylamides of high molar mass. *Colloids and Surfaces*. Vol.42,

23-37.

72. Morrow, J.J. and Rausch, E.G. (1974) Colloid destabilization with cationic polyelectrolytes as affected by velocity gradients. *Journal American Water Works Association*. Vol.66, 646.
73. Li, T., Zhu, Z., Wang, D.S., Yao, C.H. and Tang, H.X. (2006) Characterization of floc size, strength and structure under various coagulation mechanisms. *Powder Technology*. Vol.168, 104-110.
74. Ray, D.T. and Hogg, R. (1987) Agglomerate breakage in polymer-flocculated suspensions. *Journal of colloid and interface science*. Vol.116, 256-268.
75. Boller, M. and Blaser, S. (1998) Particles under stress. *Water Science and Technology*. Vol.37, 9–29.
76. Parker, D. S., Kaufman, W. J. and Jerkins, D. (1972) Floc break up in turbulent flocculation processes. *J.Sanit. Eng.Div.: Proc.Am.Soc. Civ. Eng. SA1*, 79-99.
77. Gregory, J. and Yukselen, M. A. (2002) Break-up and re-formation of flocs formed by hydrolyzing coagulants and polymeric flocculants. In: *Chemical Water and Wastewater Treatment –VII*, IWA Publishing, UK, pp29-38.
78. Jarvis, P., Jefferson, B., Gregory, J. and Parsons, S. A. (2005) A review of floc strength and breakage. *Water Research*. Vol.39, 3121-3137.

79. Pan, J.R., Huang, C., Chen, S and Chung, Y.C. (1999) Evaluation of a modified chitosan biopolymer for coagulation of colloidal particles. *Colloids and Surfaces A: Physicochemical and Engineering Aspects*. Vol.147, 359-364.
80. Thurman, E.M. and Morgan, R. L. (1981) Preparative isolation of humic substances. *Environmental Science and Technology*. Vol.15, 463.
81. Newcombe, G. (1994) Activated carbon and soluble humic substances: adsorption, desorption, and surface charge effects. *J. Colloid and Interface Science*. Vol.164, 452-462.
82. Sutton, R. and Sposito, G. (2005) Molecular structure in soil humic substances : the new view. *Environmental Science and Technology*. Vol.39, 9009-9015.
83. Narkis, N. and Rebhun, M. (1977) Stoichiometric relationship between humic and fulvic acids and flocculants. *Journal American Water Works Association*. Vol.69, 325-328.
84. Bratskaya, S.Y, Avramenko, V.A., Sukhoverkhov, S.V. and Schwarz, S. (2002) Flocculation of humic substances and their derivatives with chitosan. *Colloid Journal*. Vol.64, 681-685.
85. O'Melia, C.R., Becker, W. C. and Au, K. (1999) Removal of humic substances by coagulation. *Water Science and Technology*. Vol.40, 47-54.
86. Chang, E. E., Chiang, P.C., Tang, W.Y., Chao, S.H. and Hsing, H.J. (2005) Effects of polyelectrolytes on reduction of model compounds via coagulation. *Chemosphere*. Vol.58, 1141-1150.

87. Hall, T. and Hyde, R. A. (1992) *Water Treatment Processes and Practices*. Water Research Centre, Swindon.
88. Yeh, H.-H. and Ghosh, M.M. (1981) Selecting polymers for direct filtration. *Journal American Water Works Association*. Vol.73, 211
89. Duan, J.M., Wang, J. H., Graham, N. and Wilson, F. (2002) Coagulation of humic acid by aluminium sulphate in saline water conditions. *Desalination*. Vol.150, 1-14.
90. Riddick, T.M. (1961) Zeta potential: new tool for water treatment. *Chemical Engineering*. Vol.68, 121.
91. Ratnaweera, H., Hiller, N. and Bunse, U. (1999) Comparison of the coagulation behaviour of different Norwegian aquatic NOM sources. *Environment International*. Vol.25, 347-355.
92. Bob, M.M. and Walker, H.W. (2001) Effect of natural organic coatings on the polymer-induced coagulation of colloidal particles. *Colloids and surface A: Physicochemical and Engineering Aspects*. Vol.177, 215-222.
93. Mikkelsen, L.H. (2003) Applications and limitations of the colloid titration method for measuring activated sludge surface charges. *Water Research*. Vol.37, 2458-2466.
94. Dentel, S.K., Wehnes, K. M. and Abu-Orf, M.M. (1994) Use of streaming current and other parameters for polymer dose control in sludge conditioning, In: Klute, R., Hahn, H.H. (Eds.) *Proceedings of the Sixth Gothenburg Symposium. Chemical Water and Wastewater Treatment III*. Berlin, Springer, pp.373-381.

95. Barron, W., Murray, B.S., Scales, P.J., Healy, T.W., Dixon, D.R. and Pascoe, M. (1994) The streaming current detector: A comparison with conventional electrokinetic techniques. *Colloids and surface A: Physicochemical and Engineering Aspects*. Vol.88, 129-139.
96. Negro, C., Sanchez, L.M., Fuente, E., Blanco, A. and Tijero, J. (2006) Polyacrylamide induced flocculation of a cement suspension. *Chemical Engineering Science*. Vol.61, 2522-2532.
97. Lartiges, B.S., Bottero, J. Y., Democrate, C. and Coupel, J. f. (1995) Optimizing flocculant demand by following floc size distribution. *J. Water Supply: Research and Technology—Aqua*. Vol.44, 219-223.
98. Huang, C. P. and Liu, C. B. (1996) Technical note: Automatic control for chemical dosing in laboratory-scale coagulation process by using an optical monitor. *Water Research*. Vol. 30, 1924-1929.
99. Francois, R.J. (1987) Strength of aluminium hydroxide flocs. *Water Research*. Vol. 21, 1023-1030.
100. Govoreanu, R., Seghers, D. and Nopens, I. (2000) Linking floc structure and settling properties to activated sludge population dynamics in an SBR. *Water Science and Technology*. Vol. 47, 9-18.
101. Yukselen, M.A. and Gregory, J. (2004) The reversibility of floc breakage. *International Journal of Mineral Processing*. Vol.73, 251-259.
102. Rout, D., Verma, R. and Agarwal, S.K. (1999) Polyelectrolyte

treatment--an approach for water quality improvement. *Water Science and Technology*. Vol. 40, 137-141.

103. Lindqvist, N., Jokela, J. and Tuhkanen, T. (2004) "Enhancement of coagulation by using polyelectrolytes as coagulant or flocculant aids." In *Chemical Water and Wastewater Treatment VIII* edited by H.H.Hahn, E.Hoffmann, H.Odegarrd IWA Publishing London, pp161-169.
104. Chang, E. E., Chiang, P. C., Chao, S. H. and Liang, C. H. (1999) Effects of polydiallyldimethyl ammonium chloride coagulant on formation of chlorinated by products in drinking water. *Chemosphere*. Vol.39, 1333-1346.
105. Filho, S.S.F, Fernandez, A. N., Mendes, R.L., Sinelli, P.A. and Cipriani, M.J.I. (2004) Drinking water treatment of highly eutrophic waters: coagulation process control by means of cationic polymers associated with inorganic coagulants *Chemical Water and Wastewater Treatment VIII* edited by H.H.Hahn, E.Hoffmann, H.Odegarrd IWA Publishing London, p.233-242.
106. Lee, S.H., Shin, M. C., Choi, S. J., Shin, J. H. and Park, L.S. (1997) Improvement of flocculation efficiency of water treatment by using polymer flocculants. *Environmental Technology*. Vol. 19, 431-436.
107. Shultz, C. R. and Okun, D. A. (1982) Practical water treatment for communities in developing countries. *AWWA Ann. Conf.*, Miami, Fla.
108. Divakaran, R. and Sivasankara, P. V. N. (2001) Flocculation of kaolinite suspensions in water by chitosan. *Water Research*. Vol.35, 3904-3908.

109. Vogelsang, C., Andersen, D.O., Hey, A., Hakonsen, T., Jantsch, T.G., Muller, E.D., Pedersen, M.A. and Varum, K.M. (2004) Removal of humic substances by chitosan. *Water Science and Technology: Water Supply*. Vol. 4, 121-129.
110. Scheuch, L.E. and Edzwald, J.K. (1981) Removing color and chloroform precursors from low-turbidity waters by direct filtration. *Journal of American Water Works Association*. Vol.73, 497.
111. Edzwald, J.K., Becker, W.C., and Tambini, S.J. (1987) Organics, polymer and performance in direct filtration. *Jour. Engrg. Div,—ASCE*. Vol.113, 167.
112. Graham, N. J. D., Brandao, C. C. S. and Luckham, P. F. (1992) Evaluating the Removal of Color from Water Using Direct-Filtration and Dual Coagulants. *Journal of American Water Works Association*. Vol.84, 105-113.
113. Department of the Environment. *Water, England and Wales: The Water Supply (Water Quality) Regulations 2001*. Statutory Instruments 3911. HMSO, London 2002.
114. Lee, J.F., Liao,P.M., Tseng, D.H, and Wen, P. T. (1998) Behavior of organic polymers in drinking water purification. *Chemosphere*. Vol.37, 1045-1061.
115. National Sanitation Foundation. Standard ANSI/NSF 60 1988 Drinking-water treatment chemicals-health effects. Standard NSF International Brussels, Belgium.

116. NSF International, Drinking-water treatment chemicals-health effects; 2001 Certified product listings. ANSI/NSF Standard 60. Washington, NSF.
117. Criddle, J. (1990) A review of the mammalian and aquatic toxicity of polyelectrolytes. NR 2545, Medmenham, Foundation for Water Research.
118. BSI Standards (1998) Chemicals used for treatment of water intended for human consumption-poly(diallyldimethylammonium chloride). BS EN 1408.1998, British Standards Institute, London.
119. Lettermen, R.D. and Pero, R.W. (1990) Contaminants in polyelectrolytes used in water treatment. Journal of American Water Works Association. Vol.82, 87-97.
120. Parazak, D. P., Burkhardt, C.W. and McCarthy, K. J. (1987) Determination of low-levels of cationic polyelectrolytes in water. Analytical Chemistry. Vol.59, 1444-1445.
121. Howes, N.J. and Harper, G. (1998) Review of analytical methodology for cationic polyacrylamides at levels of environmental significance. R&D Technical Report No.E47, Environment Agency, Bristol, UK, pp.34.
122. Soponkanaporn, T. and Gehr, R. (1987) Quantitative determination and peak molecular weight analysis of acrylamide-based polyelectrolytes by size-exclusion chromatography. International Journal of Analytical Chemistry. Vol.29, 1-8.
123. Martin, J., Thomas, S., Bellen, G.E., King, L.W. and Hylko, J.M. (1990)

Carbon-14 tracer study of polyacrylate polymer in a wastewater plant. *Applied Radiation and Isotopes*. Vol.41, 1165-1173.

124. Chang, L. L., Bruch, M.D., Griskowitz, N.J. and Dentel, S.K. (2001) NMR spectroscopy for determination of cationic polymer concentrations. *Water Research*. Vol.36, 2255-2264.
125. Becker, N. S .C., Bennett, D.M., Bolto, B. A., Dixon, D.R., Eldridge, R. E., Le, N. P. and Rye, C.S. (2004) Detection of polyelectrolytes at trace levels in water by fluorescent tagging. *Reactive & Functional Polymers*.Vol.60, 183-193.
126. Fielding, M, Hutchison, J., Hughes, D. M., Glaze, W. H. and Weinberg, H.S. (1999) Analytical methods for polymers and their oxidative by-products. Americal Water Works Association Research Foundation, Denver.
127. Nozaic, D. J., Freese, S. D. and Thompson, P. (2001) Long term experience in the use of polymeric coagulants at Umgeni Water. *Water Science and Technology: Water Supply*. Vol.1, 43-50.
128. Roux, D.G. (1972) Review article: Recent advances in the chemistry and chemical utilization of the natural condensed tannins. *Phytochemistry*. Vol.11,1219-1230.
129. Quamme, J.E. and Kemp, A.H. (1985) Stable tannin based polymer compound. United States Patent. No.4,558,080.
130. Hemingway, R. W. (1989) Structural variations in proanthocyanidins and their derivatives. In: Hemingway, R.W., Karchesy, J. J., Branham, S. J.,

(Eds.), Chemistry and Significance of Condensed Tannins. Plenum Press, New York, pp.83-107.

131. Ozacar, M. and Sengil, I. A. (2003) Evaluation of tannin biopolymer as a coagulant aid for coagulation of colloidal particles. *Colloids and Surfaces*. Vol. 229, 85-96.
132. Fife, J.G. (1962) Process for flocculating suspensions. British Patent. No.899, 721, 27.
133. Pefferkorn, E. (2006) Clay and oxide destabilization induced by mixed alum/macromolecular flocculation aids. *Advances in Colloid and Interface Science*. Vol.120, 33-45.
134. Duan, J.M. and Gregory, J. (2003) Coagulation by hydrolyzing metal salts. *Advances in Colloid and Interface Science*. Vol.100, 475-502.
135. Greenbery, A.E., Clesceri, L.S. and Eaton, A.D. (1992) Standard Methods for the examination of water and wastewater, 4500-Cl⁻ CHLORIDE B. Argentometric titration .18th edition. APHA AWWA. Washington.
136. Duan, J.M. and Gregory, J. (1996) Influence of soluble silica on coagulation by aluminium sulphate. *Colloids and Surfaces A: Physicochemical and Engineering Aspects*. Vol.107, 309-319.
137. Watts, M. (2002) Evaluation and approval of tannin products for potable water treatment - preliminary laboratory evaluation. WRc Report number: UC 4081.

138. Greenbery, A.E., Clesceri, L.S. and Eaton, A.D. (1992) Standard Methods for the examination of water and wastewater, 4500-N_{org} NITROGEN (organic).18th edition. APHA AWWA. Washington.
139. Karaca, F., Islas, C.A., Millan, M., Behrouzi, M., Morgan, T.J., Herod, A.A. and Kandiyoti, R. (2004) The calibration of size exclusion chromatography columns: molecular mass distributions of heavy hydrocarbon liquids. Energy and Fuels. Vol.18, 778-788.
140. Zimm, B. H. (1948) Apparatus and methods for measuring and interpolation of the angular variation of light scattering preliminary results on polystyrene solutions. J. Chemical Physics. Vol.16,1099.
141. Gregory, J., and Chung, H.J. (1995) Continuous monitoring of flocculation properties in stirred suspensions. Water SRT – Aqua. Vol.44, 125-131.
142. Gregory, J. (1985) Turbidity fluctuations in flowing suspensions. J. Colloid and Interface Science. Vol.105, 357.
143. AWWA. (2000) Operational Control of Coagulation and Filtration Processes. Manual of Water Supply Practices-M37. 2nd Edition, American Water Works Association, Denver, USA.
144. Greenbery, A.E., Clesceri, L.S. and Eaton, A.D. (1992) Standard Methods for the examination of water and wastewater, 5550. TANNIN AND LIGNIN.18th edition. APHA AWWA. Washington.
145. Gregory, J. (2007) Particles in water (properties and processes). CRC

Press Taylor & Francis Group. USA.

146. Prashanth, K.V.H. and Tharanathan, R.N. (2006) Crosslinked chitosan—preparation and characterization. *Carbohydrate Research*. Vol. 341, 169-173.
147. Payne GF, Chaubal MV, Barbari T. Enzyme-catalyzed polymer modification: reaction of phenolic compounds with chitosan films. *Polymer*. 1996;37:4643-4648.
148. Williams, D. H. and Fleming, I. (1996) *Spectroscopic methods in organic chemistry*. Mc Graw-Hill Publishing Company Limited, London.
149. Huglin, M. B. (1972) *Light scattering from polymer solutions*. Academic Press Inc Ltd, London.
150. Payne, G. F., Chaubal M. V. and Barbari, T. (1996) Enzyme-catalyzed polymer modification: reaction of phenolic compounds with chitosan films. *Polymer*. Vol.37, 4643-4648.
151. Nielsen, A.B., Frydenvang, K. and Liljefors, T. (2005) Assessment of the combined approach of N-alkylation and salt formation to enhance aqueous solubility of tertiary amines using bupivacaine as a model drug. *Eur.J.Pharm. Sci*. Vol.24, 85-93.
152. Mitchell ,D.B., Minnis, R. L., Curran, T. P., Deboo, S.M., Kelly, J. A., Patwardhan, R. and Tai, W.T. (1998) Treatment of aqueous systems using a chemically modified tannin. U.S. Patent No.5, 830, 315
153. Michaels, A. S. (1954) *Aggregation of suspensions by polyelectrolytes*,

Industrial and Engineering Chemistry. Vol. 46, 1485.

154. Dixon, J. K., La Mer, V. K., Messinger, S. and Linford, H.B. (1976) Effect of the structure of cationic polymers on the flocculation and the electrophoretic mobility of crystalline silica. *J. Colloid and Interface Science*. Vol.23, 465.
155. Owen, A. T., Fawell, P. D., Swift, J.D. and Farrow, J.B.(2002) The impact of polyacrylamide flocculant solution age on flocculation performance. *International Journal of Mineral Processing*. Vol.67, 123-144.
156. Gregory, J. (2003) Monitoring floc formation and breakage. In; *Proceedings of the Nano and Micro Particles in Water and Wastewater Treatment Conference*. International Water Association, Zurich, September.
157. Gregory, J. (1997) The density of particle aggregates. *Water Science Technology*. Vol.36, 1-13.
158. Gregory, J. and Yukselen, M. A. (2004) The effect of rapid mixing on the break-up and re-formation of flocs. *Journal of Chemical Technology and Biotechnology*. Vol.79, 782-788.
159. Black, A. P., Birkner, F. B. and Morgan, J. J. (1966) The effect of polymer adsorption on the electrokinetic stability of dilute clay suspensions. *J.Colloid and Interface Science*. Vol.21, 626.
160. Gregory, J. (1978) "Flocculation by inorganic salts." The scientific basis

of flocculation. Edited by Kenneth J.Ives. Sijthoff & Noordhoff International Publishers, The Netherlands.

161. Stumm, W. and O'Melia, C. R. (1986) Chemical aspects of coagulation II Stoichiometry of coagulation. Journal of American Water Works association. Vol.60,514.
162. Yu, J., Sun, D. D. and Tay, J. H. (2003) Characteristics of coagulation-flocculation of humic acid with effective performance of polymeric flocculant and inorganic coagulant. Water Science and Technology. Vol.47, 89-95.
163. Jackson, P.J. (1988) Studies of colour removal by coagulation. Rept.734-S. Water Research Center, Stevenage, UK.
164. Amirtharajah, A. and Mills, K. M. (1982) Rapid-mix design for mechanisms of alum coagulation. Journal of American Water Works association. Vol.74, 210-216.
165. Holt, P. K., Barton, G. W., Wark, M. and Mitchell, C. A. (2002) A quantitative comparison between chemical dosing and electrocoagulation. Colloids and Surfaces A: Physicochem.Eng. Vol.211, 233-248.
166. Stol, R.J., Van Helden, A. K. and Debruyn, P. L. (1976) Hydrolysis-precipitation studies of aluminium solution. 2. A kinetic study and model. J.Colloid and Interface Science. Vol.57,115.
167. McCOOK, N. J. and West, J.R. (1978) The coagulation of a kaolinite

- suspension with aluminium sulphate. *Water Research*. Vol. 12, 793-798.
168. Hanna, G. P. and Rubin, A. J. (1970) Effect of sulphate and other ions in coagulation with aluminium. *Journal of American Water Works association*. Vol. 54, 315-321.
169. Gupta, V. S., Bhattacharjya, S. K. and Dutta, B. K. (1975) Zeta-potential control for alum coagulation. *Journal of American Water Works Association*. Vol.63, 21-23.
170. Hall, E.S. and Packham, R.F. (1965) Coagulation of organic color with hydrolyzing coagulants. *Journal of American Water Works Association*. Vol.57,1149-1166.
171. DWI (2007) List of approved products and processes. *Drinking Water Inspectorate Regulation January 2007; The UK*.
172. Semmens, M.J. and Field, T. K. (1980) Coagulation: experiences in organics removal, *Journal of American Water Works Association*. Vol.72, 476-485.
173. Desjardins, C., Koudjonou, B. and Desjardins, R. (2002) Laboratory study of ballasted flocculation. *Water Research*. Vol.36,744-754.
174. Parazak, D. P., Burkhardt, C.W., McCarthy, K. J. and Stehlin, M.P.(1988) Hydrophobic flocculation. *J.Colloid and surface Science*.Vol.123,59-72.
175. Divakaran, R. and Pillai, V.N.S. (2002) Flocculation of river silt using

chitosan. *Water Research*. Vol.36, 2414-2418.

176. Magdassi, S., Kamyshny, A. and Baszkin, A. (2001) Interfacial properties of hydrophobically modified biomolecules: fundamental aspects and applications. *J. Dispersion Science and Technology*. Vol.22, 313–322.
177. Roussy, J., Van Vooren, M. and Guibal, E. (2004) Chitosan for the coagulation and flocculation of mineral colloids. *J. Dispersion Science and Technology*. Vol.25, 663–677.
178. Ghabbour, E.A. and Davies, G. (1999) *Understanding Humic Substances: advanced methods, properties and applications*. Published by the Royal Society of Chemistry. UK.
179. Schofield. P., Mbugua, D.M and Pell, A.N (2001) Review: Analysis of condensed tannins: a review. *Animal feed science and technology*. Vol 91, 21-40.
180. Hernes.J.P., Benner. R., Cowie. G.L., Goni. M.A., Bergamaschi. B.A. and Hedges, J.I. (2001) Tannin diagenesis in mangrove leaves from a tropical estuary: A novel molecular approach. *Pergamon*. Vol.65, 3109-3122.
181. Ferreira D., Steynberg. J.P., Burger. J.F.W. and Bequidenhoudt. B.C.B.(1992) Oxidation and rearrangement reactions of condensed tannins. In *Plant Polyphenols: Synthesis, Properties, Significance*, PP.349-384., Plenum Press, New York.
182. Shyluk, W. P. and Stow, F. S.(1969) Aging and loss of flocculation activity of aqueous polyacrylamide solution. *Journal of Applied Polymer*

Science. Vol.13, 1023.

183. Gray, S.R. and Ritchie, C.B. (2006) Effect of organic polyelectrolyte characteristics on floc strength. Colloids and Surfaces A: Physicochem.Eng. Vol.273, 184-188.
184. Leentvaar, J. and Rebhun, M. (1982) Strength of ferric hydroxide flocs. Water Research. Vol.17, 895-902.
185. Ammary, B. Y. and Cleasby, J.L. (2004) Effect of addition sequence on dual coagulant performance. Journal of American Water Works association. Vol. 96, 90-101.
186. Watts, M. (2004) Personal Communication.
187. Lamb, L.H. (2005) Personal Communication.

14. APPENDIX

APPENDIX I: Laboratory G Curve for Flat Paddle in 2L Gator Jar (143)

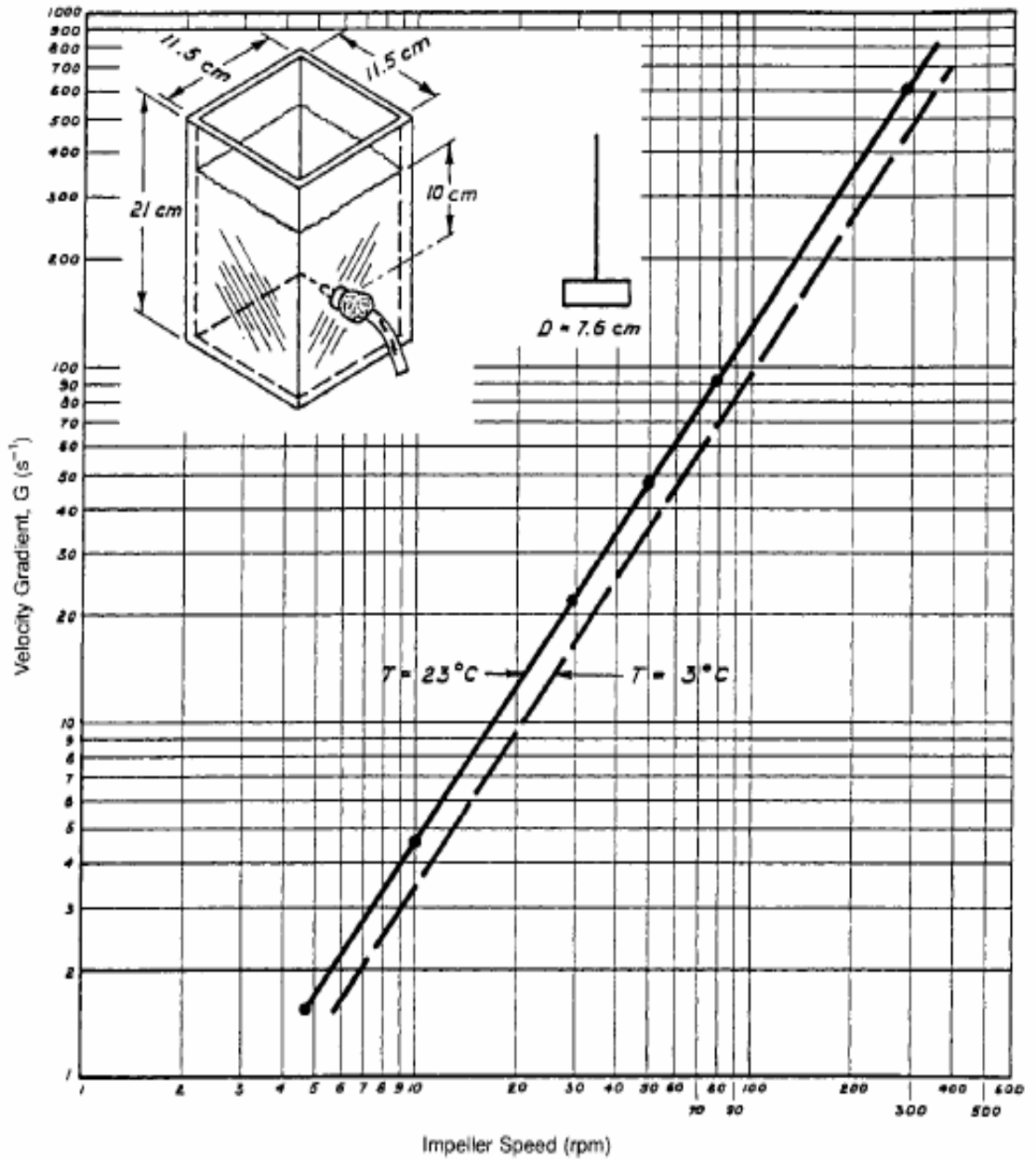


Figure 1. Laboratory G Curve for Flat Paddle in 2 Liter Gator Jar

APPENDIX II: The specific refractive index increment (dn/dc) of TBP



Report 201024

Background

A samples of Tannin based polymer was submitted for a determination of the specific refractive index increment (dn/dc).

Experimental

Instrumentation

Pump:	Agilent 1100
Injector:	Wyatt dn/dc kit (1.5ml loop)
Flow Rate:	0.3 ml/minute
Eluent:	Water (Filtered to 0.1 micrometer)
RI Dectetor:	Optilab rEX (633 nm, 25 °C)

Data was collected using ASTRA V software, the data was processed using the same program.

A stock solution was made up by dissolving 161mg of sample in 50ml water (volumetric flask). This solution was left overnight to ensure complete solubility of the sample and then subsequent dilutions were made from this stock solution.

Concetrations used (g/ml):

1. 3.220e-3
2. 2.415e-3
3. 1.610e-3
4. 8.050e-4
5. 4.680e-4

Results

Sample	dn/dc results		
	dn/dc	error	Linearity
Tannin Polymer	0.1846	+/-0.0006	+/-2.13%

Discussion

The dn/dc determination was relatively straight forward with no concentration based trend. i.e. dn/dc value was linear with respect to concentration over the ranged used.

Conclusions

The result above can be relied on as an accurate dn/dc value for this polymer at 633nm and at 25 °C.

APPENDIX III: Laser Scattering Zimm Plot for TBP

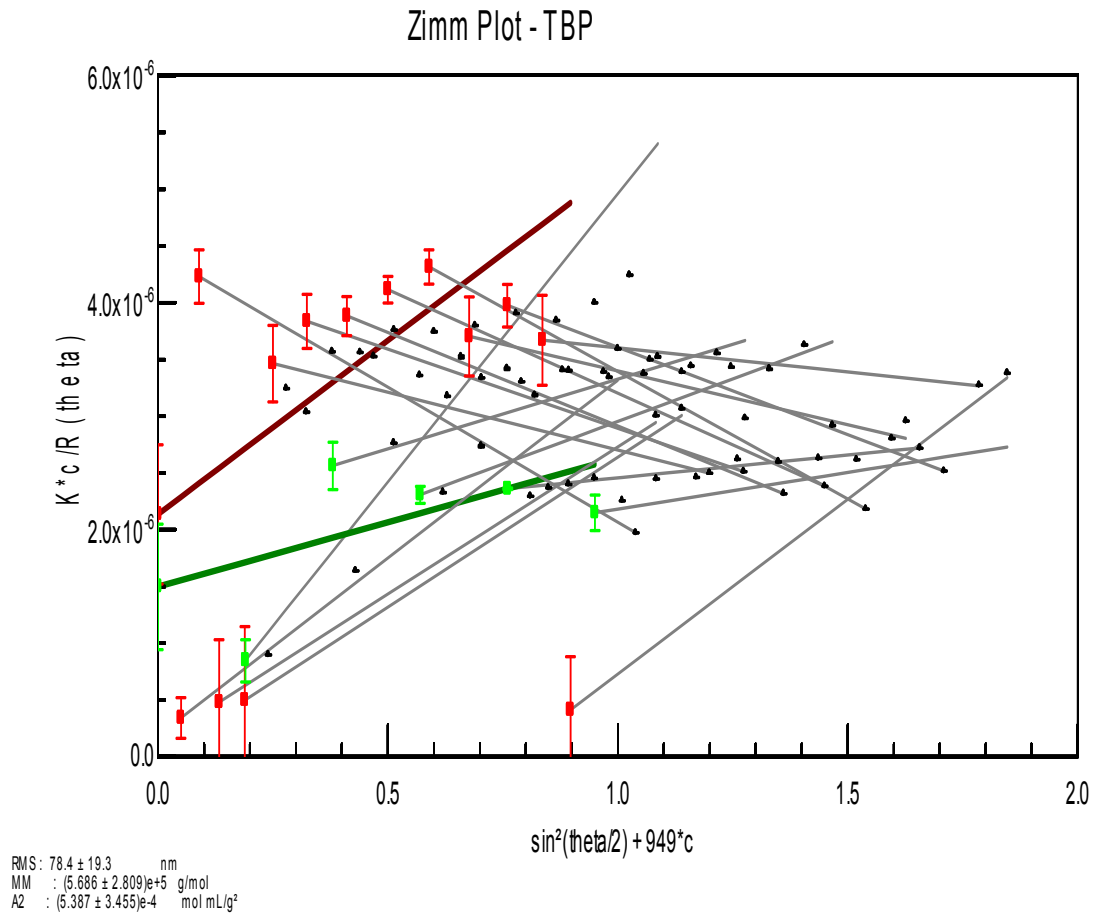


Figure Zimm Plot of TBP solution

Basic light scattering equation (Rayleigh-Gans-Debye equation):

$$R(\theta) = K^* MCP(\theta)[1 - 2A_2 MCP(\theta)]$$

The Rayleigh-Gans-Debye (RGD) approximation is a powerful generalization of light scattering theory that is applicable for particles much smaller than the wavelength of the light. The Rayleigh-Gans-Debye (RGD) equations can be recast to facilitate data analysis using the Zimm formalism:

$$\frac{K^* C}{R(\theta)} = \frac{1}{MP(\theta)} + 2A_2 C$$

In their new form, the light scattering equations offer a simple means to retrieve the quantities of interest from linear relationships at low angle and concentration limits (140).